

NASA Technical Memorandum 4368

NASA Aerodynamics Program Annual Report 1991

Louis J. Williams, Kristin A. Hessenius,
Victor R. Corsiglia, Gary Hicks, Pamela F. Richardson,
George Unger, Benjamin Neumann, and Jim Moss
*NASA Office of Aeronautics and Space Technology
Washington, D.C.*

This document has been approved
for public release and sale; its
distribution is unlimited.



National Aeronautics and
Space Administration
Office of Management
Scientific and Technical
Information Program

1992

Accession For	
NTIS	CRA&I <input checked="" type="checkbox"/>
DTIC	TAB <input type="checkbox"/>
Unannounced <input type="checkbox"/>	
Justification	
By	
Distribution /	
Availability Codes	
Dist	Avail and/or Special
A-1	

92 515 124

92-1315



NASA Technical Memorandum 4368

NASA Aerodynamics Program Annual Report 1991

Louis J. Williams, Kristin A. Hessenius,
Victor R. Corsiglia, Gary Hicks, Pamela F. Richardson,
George Unger, Benjamin Neumann, and Jim Moss
*NASA Office of Aeronautics and Space Technology
Washington, D.C.*

Accession For	
NTIS CRA&I	<input checked="" type="checkbox"/>
DTIC TAB	<input type="checkbox"/>
Unannounced	<input type="checkbox"/>
Justification	
By	
Distribution /	
Availability Codes	
Dist	Avail and/or Special
A-1	



National Aeronautics and
Space Administration

Office of Management

Scientific and Technical
Information Program

1992



Preface

This annual report contains information describing highlighted accomplishments for the past year from NASA's Aerodynamics Research and Technology Program.

The Aerodynamics Research and Technology Program is conducted as part of the response to NASA's charter to: (1) Preserve the role of the United States as a leader in aeronautical science and technology, and the application thereof; (2) Improve the usefulness, performance, speed, safety, and efficiency of aeronautical vehicles; (3) Supervise and direct the scientific study of the problems of flight with a view to their practical solution; and (4) Ensure the timely provision of a proven technology base for a safe, efficient, and environmentally compatible air transportation system.

The Aerodynamic Research and Technology Program includes both fundamental and applied research directed at the full spectrum of aerospace vehicles, from rotorcraft to planetary entry probes. The program encompasses analytical, computational, and experimental efforts conducted using the world's best wind tunnel, computational, and flight research facilities at NASA's Ames and Langley Research Centers.

It is impossible to do justice to the breadth and depth of this comprehensive research program in a single document. The intent of this report is to render a balanced view of NASA's Aerodynamics Program by presenting accomplishment highlights from fiscal year 1991. Other documents and conferences provide a more extensive forum for detailed coverage of a given area. For brevity, we have not included all of the highlights that were submitted for consideration, and we apologize to those whose submissions were not incorporated.

This report is arranged in chapters which outline the applied research and technology programs by vehicle type and the fundamental research by subject area. Each chapter includes an introduction by the appropriate Aerodynamics Division program manager, and each accomplishment highlight identifies the responsible researcher at the field centers. To facilitate communication, the address and phone numbers are also listed.

During this year, the Aerodynamics Research and Technology Program was managed by the Aerodynamics Division, one of five divisions in the Office of Aeronautics and Space Technology (OAST) at NASA Headquarters. At the close of 1991 OAST was reorganized, and the five discipline divisions were replaced by separate aeronautics and space divisions in specific thrust areas. In line with this new organization, this will be the last report of this type covering the entire Aerodynamics Research and Technology Program.

Mr. Louis J. Williams
Director

Dr. Kristin A. Hessenius
Deputy Director

Aerodynamics Division, Code RF
National Aeronautics and Space Administration
Washington, DC 20546

Table of Contents

Chapter One Subsonic Aerodynamics	1
Hybrid Laminar Flow Control Flight Research	3
Vortex Generators for High-Lift Airfoils	5
Porous Transonic Airfoils for Multipoint Design	7
Subsonic Transport High-Lift Flight Research - Phase I	9
Chapter Two Test Techniques and Instrumentation	11
Luminescent Paint Sensor Development	13
Temperature and Density Measurements in Air Using Laser-Induced Fluorescence	15
Phosphor Thermography Technique	17
Density Field Measurements in a Nonequilibrium Expanding Flow Using Holographic Interferometry	19
Measurement Techniques for Hypersonic Flows	21
Chapter Three Transition and Turbulence Physics	23
Compressible Boundary Layer Transition Using PSE	25
Compressible Large-Eddy Simulation of Isotropic Turbulence	27
Compressible Turbulence Modeling for High-Speed Shear Layers	29
Development of a Mach 18 Quiet Helium Tunnel	31
Direct Simulation of Compressible Homogeneous Shear Flow	33
Dynamic Subgrid Scale Modeling and the New LES Program	35
Efficient Supersonic Wind Tunnel Drive System for Transition Research at Mach 2.5	37
Numerical Simulation of Laminar Breakdown in Supersonic Transition	39
Receptivity of Low-Speed Boundary Layers	41
Simulation of Homogeneous Turbulence on the Intel i860 Hypercube	43
Compressible Turbulence: Modeling Rapid Compression	45
Separating Boundary Layer Experiment for Turbulence Modeling	47
Chapter Four Computational Methods and Validation	49
Direct Numerical Simulation of Transition and Turbulence in a Spatially Evolving Boundary Layer	51
Multigrid Algorithm for Hypersonic Viscous Flows	53
Unstructured and Adaptive Multigrid for the Three-Dimensional Euler Equations	55
S3D - An Interactive Surface Grid Generation Tool	57
Accelerated Preparation of Grid Generation Input Data	59
Numerical Simulation of the YAV-8B Harrier VSRA in Ground Effect	61
High-Speed Civil Transport Navier-Stokes Computations	63
CFD-Based Aerodynamics Design of Hypersonic Wind Tunnel Nozzles	65
Turbulent Flow Over a Backward Facing Step	67
Near-Wall Laser Velocimeter Measurements	69

Chapter Five Numerical Aerodynamics Simulation (NAS)	71
Parallel Computers in the NAS Program	73
NAS Parallel Benchmarks	75
Virtual Wind Tunnel	77
Vector Field Topology Visualization Software	79
Distributed and Cooperative Processing of Unsteady Fluid Flows	81
Chapter Six Rotorcraft	83
Large-Scale Tiltrotor Performance Program	85
Tiltrotor Aeroelastic Stability Control	87
Tiltrotor Download Reduction	89
Tiltrotor Hover Acoustics	91
Civil Tiltrotor Technology	93
Theoretical Determination of Noise Reduction With Increasing Blade Number for the XV-15 Tiltrotor Aircraft	95
XV-15/ATB Flight Investigations: Advanced Technology Blades Loads, Stability, and Performance	97
Analysis of Tiltrotor Phenomena Utilizing CAMRAD/JA	99
Blade-Vortex Interaction Noise Prediction Validation	101
High Resolution Rotor Blade Loads for Blade-Vortex Interaction Noise Prediction	103
Ray-Acoustics Approach to Fuselage Scattering of Rotor Noise	105
Rotor Impulsive Noise Reduction Using Higher Harmonic Control	107
Cooperative Army/NASA/Boeing Pressure-Instrumented Rotor Program	109
Rotor/Fuselage Aerodynamic Interactions Program	111
Rotor-Wake-Fuselage Code Development	113
Five-Bladed Bearingless Rotor Program	115
Rotor Airloads Correlation Using CFD/Lifting-Line Methods	117
Rotor Flow Field Investigation	119
Chapter Seven Fighter/Attack Aircraft	121
Full-Scale Test of F/A-18 at High Angles-of-Attack	123
Tail Buffet Research	125
Development of High-Angle-of-Attack Nose-Down Pitch Control Requirements for Relaxed Static Stability Combat Aircraft	127
Investigation of the Tumbling Phenomenon in Aerodynamic Configurations	129
F-106 Vortex Flap Flight Experiment	131
Wing Camber Effects on Flap Effectiveness at Supersonic Speeds	133
Outdoor Static Tests of the Full-Scale Ejector-Lift/Vectored-Thrust STOVL E-7A Configuration	135
Validation of Out of Ground Effect Prediction Capability for Powered Lift Aircraft	137
Comparison of Shaved and Beveled Fins for Rolling Missile Applications	139
STOL/STOVL Concepts for High-Performance Aircraft	141
Effect of a Close-Coupled Canard on Wing-Body Aerodynamics	143
Fundamental Research in Vortex Interactions	145

Chapter Eight Hypersonic Aerodynamics..... 147

Experimental Study of Hypersonic Shock-Wave/Turbulent-Boundary Layer Interaction Flows	149
Numerical Performance Estimates for a Generic Hypersonic Forebody	151
Calculation of Forebody Flow Field for a Candidate Aero-Space Plane Configuration	153
Computational/Experimental Parametric Study of 3-D Scramjet Inlets at Mach 10	155
Technique for Hypersonic Powered Tests of Airbreathing Configurations.....	157
Effect of Inlet Representation on Powered Hypersonic Aftbody Flows	159
Generic Scramjet Nozzle/Aftbody Studies	161
Advanced Aero-Propulsion Performance Design Tool (PEMACH)	163
Wing Glove for Pegasus Crossflow Transition Experiment	165

Chapter Nine Aeroacoustics Research and Technology 167

Jet Noise Predictions for Reduced Thrust Takeoff Study	169
ASTOVL Acoustic Loads Test	171
Aeroacoustic Loads on F-18 High Alpha Research Vehicle (HARV)	173
Direct Computation of Aerodynamic Sound Generation.....	175
Computational Model for Long-Range Acoustic Propagation	177
Quiet Struts and Sensors for Wind Tunnel Acoustic Studies	179

Chapter Ten High Speed Research..... 181

Effect of Fuselage Forebody Fineness Ratio on HSCT High-Lift Directional Stability	183
High-Lift Systems Research for HSCT Application.....	185
Integration of Flight Simulation With Aircraft Noise Prediction	187
Design System for Low Sonic Boom Configurations	189
Sonic Boom Shaping For Reduced Loudness	191
Prediction of Subjective Response to Sonic Booms	193
Indoor/Outdoor Sonic Boom Simulation Facility	195
Preliminary Sonic Boom Survey	197
Minimum Sonic Boom Rise Time Determined by Absorption	199
Supersonic Laminar Flow Control Program	201
Flow Quality Study in the Unitary Plan Wind Tunnel.....	203

Chapter Eleven Aerothermodynamics Research and Technology 205

Advancements in Radiation Transport	207
Energetics of Gas-Surface Interactions in Transitional Flows at Entry Velocities.....	209
Asynchronous Macrotasked Relaxation Strategies for the Solution of Viscous Hypersonic Flows	211
Particle Simulation in a Multiprocessor Environment	213
Numerical and Experimental Analyses of Small Rocket Flows	215
Hypersonic Rarefied Flow About a Compression Corner	217
Advancement in Developing an Efficient 3-D DSMC Code	219

Flow-Field Computations for Shuttle Orbiter	221
Approximate Heating Analysis	223
Comparison of Heating Rate Calculations with Experimental Data on a Modified Shuttle Orbiter at MACH 6	225
Numerical Simulation of Unsteady Shock-Induced Combustion	227
Aerodynamic/Aerothermodynamic Characteristics of HL-20/HL-20 A/B Lifting Body Configurations	229
Chapter Twelve Aerobraking	231
Effect of Atmospheric and Aerodynamic Uncertainties on Manned-Mars Aerobrake Feasibility	233
Heat Shield Erosion in a Dusty Martian Atmosphere	235
Aerobraked Lunar Transfer Vehicle Cost and Operations Study	237
Aerobrake Design Studies for Manned Mars Missions	239
Heating Rates for Aeroassist Flight Experiment	241
Wake Flows for Aerobrakes	243
Aeroassist Flight Experiment Ground-Based Testing	245

List of Figures

Chapter One Subsonic Aerodynamics	1
Figure 1-1. Hybrid Laminar Flow Control Flight Research	2
Figure 1-2. Separation Control for High-Lift Airfoils; Three Element Landing Configuration; Counter Rotating Low-Profile Vortex Generators	4
Figure 1-3. Porosity for Transonic Airfoils With a View Toward Multipoint Design	6
Figure 1-4. Flight Results on a Subsonic Transport Flap System	8
Chapter Two Test Techniques and Instrumentation	11
Figure 2-1. Luminescent Paint Sensor Development	12
Figure 2-2. Laser-Induced Fluorescence Instrumentation in the Ames 3.5-Foot Hypersonic Wind Tunnel	14
Figure 2-3. Application of Thermographic Phosphor Technique	16
Figure 2-4. Holographic Interferometry Layout at EAST Reflected Shock Tunnel	18
Figure 2-5. Infrared Map of Wakes Behind Vortex Generators in Hypersonic Flow	20
Chapter Three Transition and Turbulence Physics	23
Figure 3-1. Evolution of Linear and Nonlinear Disturbances in Mach 1.6 Boundary Layer Flow at the Given Nondimensional Frequency $F(R = \sqrt{Re_\tau})$	24
Figure 3-2. Large-Eddy Simulation of Compressible Isotropic Turbulence	26
Figure 3-3. Effect of Compressibility Corrections on Vorticity Thickness Growth Rate	28
Figure 3-4. Mach 18 Quiet Helium Tunnel	30
Figure 3-5. Direct Simulation of Compressible Homogeneous Shear Flow	32
Figure 3-6. Dynamic Subgrid Scale Modeling and the New LES Program	34
Figure 3-7. Efficient Supersonic Wind Tunnel Drive System for Transition Research at Mach 2.5	36
Figure 3-8. Precursor Effect in Hypersonic Transition	38
Figure 3-9. Receptivity of Low-Speed Boundary Layers	40
Figure 3-10. Simulation of Homogeneous Turbulence on the Intel i860 Hypercube	42
Figure 3-11. (A) Pressure Dilatation During 1D Rapid Compression (B) Response of Turbulent Energy to the Normal Shock	44
Figure 3-12. An Experiment to Guide Turbulence Modeling for Separated Flows	46
Chapter Four Computational Methods and Validation	49
Figure 4-1. Direct Numerical Simulation of Transition and Turbulence in a Spatially Evolving Boundary Layer	50
Figure 4-2. Multigrid Algorithm for Hypersonic Viscous Flows	52
Figure 4-3. Unstructured and Adaptive Multigrid for the Three-Dimensional Euler Equations	54
Figure 4-4. S3D - An Interactive Surface Grid Generation Tool	56

Figure 4-5.	Accelerated Preparation of Grid Generation Input Data	58
Figure 4-6.	Numerical Simulation of the YAV-8B Harrier VSRA in Ground Effect	60
Figure 4-7.	High-Speed Civil Transport Navier-Stokes Configuration	62
Figure 4-8.	CFD-Based Hypersonic Wind Tunnel Nozzle Design	64
Figure 4-9.	Turbulent Flow Over a Backward Facing Step	66
Figure 4-10.	Near-Wall Laser Velocimeter	68

Chapter Five Numerical Aerodynamics Simulation (NAS) 71

Figure 5-1.	Parallel Computers in the NAS Program	72
Figure 5-2.	Performance of NAS Pseudo CFD Applications	74
Figure 5-3.	Virtual Wind Tunnel	76
Figure 5-4.	Harrier Topological Vortex Cores	78
Figure 5-5.	Distributed and Cooperative Visualization of Unsteady Fluid Flow	80

Chapter Six Rotorcraft 83

Figure 6-1.	Large-Scale Tiltrotor Performance Program	84
Figure 6-2.	Tiltrotor Aeroelastic Stability Control	86
Figure 6-3.	Wing Surface Pressure Distributions Within Wake	88
Figure 6-4.	Directivity Characteristics of the XV-15 in Hover	90
Figure 6-5.	Civil Tiltrotor Technology	92
Figure 6-6.	Measured Contours of the 65 Day-Night Noise Level (DNL) for the XV-15 Tiltrotor Aircraft With 3 Blades, Corrected for 4 Blades, for Takeoff and Approach Conditions	94
Figure 6-7.	XV-15/ATB Flight Investigations: Advanced Technology Blades Loads, Stability, and Performance	96
Figure 6-8.	Analysis of Tiltrotor Phenomena Utilizing CANRAD/JA	98
Figure 6-9.	Comparison of Measured and Predicted Acoustic Signal for a Model Helicopter at a Strong Blade-Vortex Interaction Noise Condition	100
Figure 6-10.	Comparison of Predicted Rotor Blade Loading for 10° Azimuthal Resolution and 1° Resolution	102
Figure 6-11.	Predicted Effects of Fuselage Scattering of an Impulsive Rotor Noise Signal	104
Figure 6-12.	Comparison of Mid-Frequency Noise Contours for the BO-105 Rotor in Normal Flight and With Higher Harmonic Control	106
Figure 6-13.	Joint Army/Boeing Research Program	108
Figure 6-14.	Effect of Rotor on Upper Surface Pressures	110
Figure 6-15.	Rotor-Wake-Fuselage Code Development	112
Figure 6-16.	University of Maryland/Ames Research Center Bearingless Rotor Aeroelastic Analysis	114
Figure 6-17.	Rotor Airloads Correlation Using CFD/Lifting-Line Methods	116
Figure 6-18.	Roto Flow Field Investigation	118

Chapter Seven Fighter/Attack Aircraft 121

Figure 7-1.	Tail Buffet Frequency vs Angle-of-Attack	122
Figure 7-2.	Tail Buffet Research	124
Figure 7-3.	Typical Nose-Down Control Capability Characteristics for Relaxed Stability Combat Aircraft	126
Figure 7-4.	Investigation of the Tumbling Phenomenon in Aerodynamic Configurations	128
Figure 7-5.	F-106 Vortex Flap Flight Experiment	130
Figure 7-6.	Generic Fighter Models Installed in the Unitary Plan Wind Tunnel	132
Figure 7-7.	Outdoor Static Tests of the Full-Scale Ejector-Lift/Vectored-Thrust STOVL E-7A Configuration	134
Figure 7-8.	Validation of Out-of-Ground Effect Prediction Capability for Powered Lift Aircraft ...	136
Figure 7-9.	Effect of Tail Fin Shaving	138
Figure 7-10.	STOL/STOVL Concepts for High-Performance Aircraft	140
Figure 7-11.	Effect of Canard on Wing-Body Aerodynamics	142
Figure 7-12.	Fundamental Research in Vortex Interactions	144

Chapter Eight Hypersonic Aerodynamics 147

Figure 8-1.	Hypersonic Shock-Wave Boundary Layer Interaction	148
Figure 8-2.	Generic Option II -- Flow Field at the Inlet Plane ($X/L = 0.75$)	150
Figure 8-3.	Forebody Pressure Contours	152
Figure 8-4.	Computational/Experimental Parametric Study of 3-D Scramjet Inlets at Mach 10	154
Figure 8-5.	Technique for Hypersonic Powered Tests of Airbreathing Configurations	156
Figure 8-6.	Aftbody Effect of Inlet Representation	158
Figure 8-7.	2-D GASP PNS Turbulent Solution vs Experiment	160
Figure 8-8.	PEMACH - Computed Pressure Distributions and Experimental Data Comparisons	162
Figure 8-9.	Wing Glove for Pegasus Crossflow Transition Experiment	164

Chapter Nine Aeroacoustics Research and Technology 167

Figure 9-1.	Contours of Effective Perceived Noise Levels (EPNdB) for Standard Takeoff and Reduced Thrust/Increased Lift Takeoff for a Jet Aircraft	168
Figure 9-2.	ASTOVL Acoustic Loads Test	170
Figure 9-3.	Aeroacoustic Loads on Thrust Vectoring Vanes of a Model F-18 High Alpha Research Vehicle (HARV)	172
Figure 9-4.	Scattering of Plane Sound Waves by a Compressible Vortex	174
Figure 9-5.	Comparison of Boundary Element Method with Experimental Results	176
Figure 9-6.	Quiet Struts and Sensors for Wind Tunnel Acoustic Studies	178

Chapter Ten High Speed Research 181

Figure 10-1. Effect of Forebody Length on Directional Stability	182
Figure 10-2. Computed Streamlines for Various Fence Heights on a NACA 4412 Airfoil	184
Figure 10-3. Integration of the VMS and ANOPP for High-Speed Civil Transport (HSCT) Community Noise Prediction	186
Figure 10-4. Computed Signature Results for Low Boom Configuration	188
Figure 10-5. Benefit of Boom Shaping	190
Figure 10-6. (1) Sonic Boom Simulator. (L-90-5755) (2) Subjective Loudness of Sonic Booms as a Function of Perceived Level (PL)	192
Figure 10-7. Indoor/Outdoor Sonic Boom Simulation Facility	194
Figure 10-8. Preliminary Sonic Boom Survey	196
Figure 10-9. Sonic Boom Propagation - Effect of Atmosphere on Boom Shape	198
Figure 10-10. Supersonic Laminar Flow Control Program	200
Figure 10-11. The AEDC 10-Degree Transition Cone	202

Chapter Eleven Aerothermodynamics Research and Technology 205

Figure 11-1. Advancement in Radiative Transport	206
Figure 11-2. Energetics of Gas-Surface Interactions in Transitional Flows at Entry Velocities	208
Figure 11-3. Convergence History: Six Tasks Adapting Partition Boundaries	210
Figure 11-4. Particle Simulation in a Multiprocessor Environment	212
Figure 11-5. Experimental and Numerical Analyses of Small Rockets (Transverse Pitot Pressure Profiles at Nozzle Exit)	214
Figure 11-6. Hypersonic Rarefied Flow About a Compression Corner	216
Figure 11-7. Rarefied Flow Regime Hypersonic Waverider Configuration, Mach No. 25	218
Figure 11-8. Shuttle Orbiter Pressure	220
Figure 11-9. Approximate Flow Field and Heating Analysis	222
Figure 11-10. Heating on Modified Shuttle Orbiter	224
Figure 11-11. Computed Meridional Pressure Contours from Mach 5.04 Flow of Premixed Hydrogen-Air Over a Blunt Body Using a 181x127 Grid (4 Frames of an Oscillation Cycle).	226
Figure 11-12. Subsonic L/D Improvements of HL-20	228

Chapter Twelve Aerobraking 231

Figure 12-1. Additional Post-Aerocapture DV Requirements Resulting Form Multiple Off-Nominal Effects	232
Figure 12-2. Heat Shield Erosion in a Dusty Martian Atmosphere	234
Figure 12-3. Aerobraked Lunar Transfer Vehicle (LTV) Cost and Operations Study	236
Figure 12-4. Mass Fraction of Aerobrakes for Manned Mars Mission	238
Figure 12-5. Stagnation Point Heating Rate on AFE	240
Figure 12-6. Wake Flows for Aerobrakes Shear-Layer Deflection Angles	242
Figure 12-7. Aeroassist Flight Experiment Ground-Based Testing	244

Chapter 1

Subsonic Aerodynamics

The objective of the Subsonic Aerodynamics Program is to provide the technology to improve the performance, efficiency, and economics of future transport aircraft. To accomplish this objective, the program is currently focusing on the areas of hybrid laminar flow control technology and high lift.

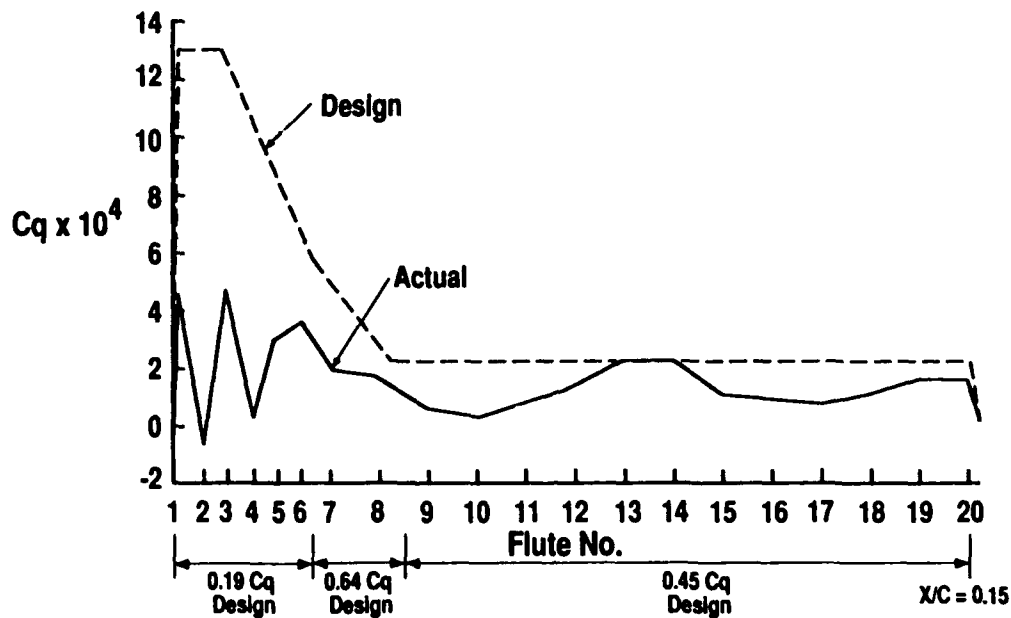
A hybrid laminar flow control system has been installed on the wings of a Boeing 757 transport aircraft to investigate the effectiveness, maintainability, and cost of applying this technology to subsonic transports.

High-lift studies include both wind tunnel tests and computational fluid dynamics (CFD) calculations. Two-dimensional wind tunnel tests that focused on three element airfoils have been conducted. Three-dimensional tests at high Reynolds Number and large scale are planned. CFD calculations are guiding the activity for both the two- and three-dimensional tests.

Program Manager: Victor R. Corsiglia
OAST/RF
Washington, D.C. 20546
(202) 453-2261

HLFC DESIGN SUCTION vs. ACTUAL SUCTION

$M = 0.8$ $C_L = 0.5$ $H = 39,000$ ft.



HLFC WAKE RAKE RESULTS

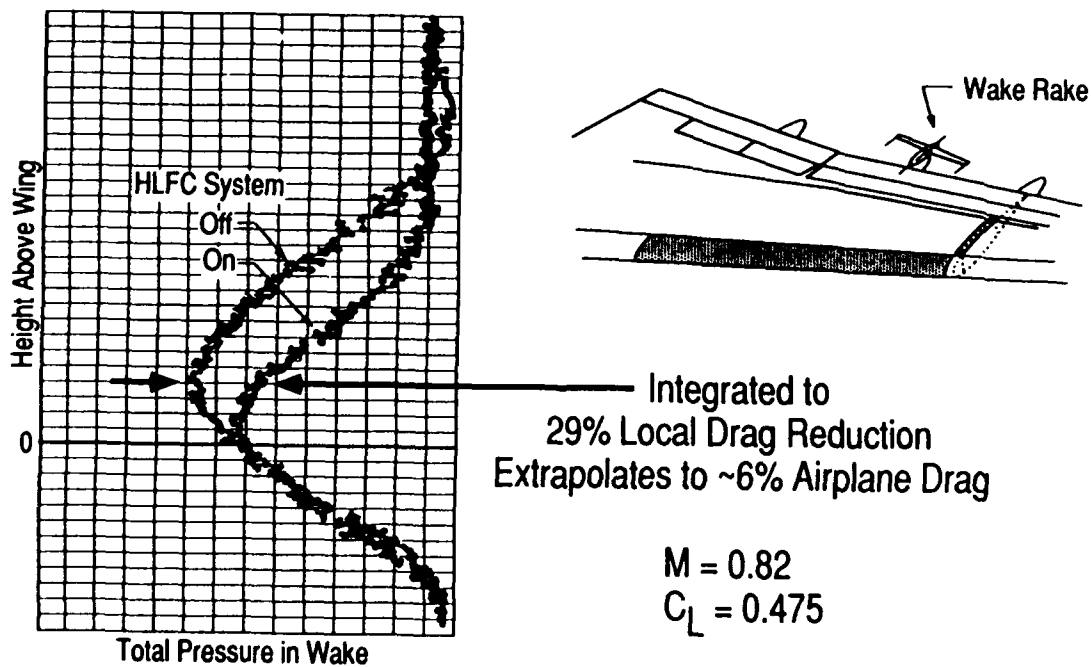


Figure 1-1. Hybrid Laminar Flow Control Flight Research

1-1 Hybrid Laminar Flow Control Flight Research

Objective. To conduct flight research experiments with the Hybrid Laminar Flow Control (HLFC) system installed in the Boeing 757 flight research aircraft.

Approach. The program is jointly funded by the NASA, the U.S. Air Force, and Boeing Commercial Airplane Co. An HLFC system provides suction boundary layer control in the leading edge (to the front spar) to control the highly three-dimensional laminar boundary layer. Downstream of the front spar, the surface pressure distribution is used to stabilize the boundary layer flow and maintain laminar flow to the wing shock or aft pressure rise. The suction surface in the leading edge is a microperforated titanium skin with over 19 million tiny, laser-drilled, closely spaced holes.

Accomplishments. Last year the flight test experiments yielded momentous results that could advance significantly the application of this technology into the commercial transport fleet. The research showed that the suction system flow capacity, power requirements, weight, and complexity had been overestimated by more than 200%.

Significance. The experiments of the past year have demonstrated that the suction required to obtain large amounts of laminar flow over the wing chord (as much as 65% chord) is much less than had been previously believed, and amounts to one-third of that indicated by the early design calculations (shown in Figure A). In addition, pressure measurements made in the wake behind the trailing edge of the wing in the center of the 17-foot test span (shown in Figure B) confirmed a major reduction in wing drag over a wide variety of test conditions and showed that large amounts of laminar flow over the aircraft's wing box area had been achieved as indicated by the early hot-film data.

Status/Plans. Flight testing is continuing. Detailed experiments will be made to estimate the tolerance of extensive laminar flow to relaxation of the stringent laminar flow design requirements.

Dal V. Maddalon
Flight Applications Division
Langley Research Center
(804) 864-1909

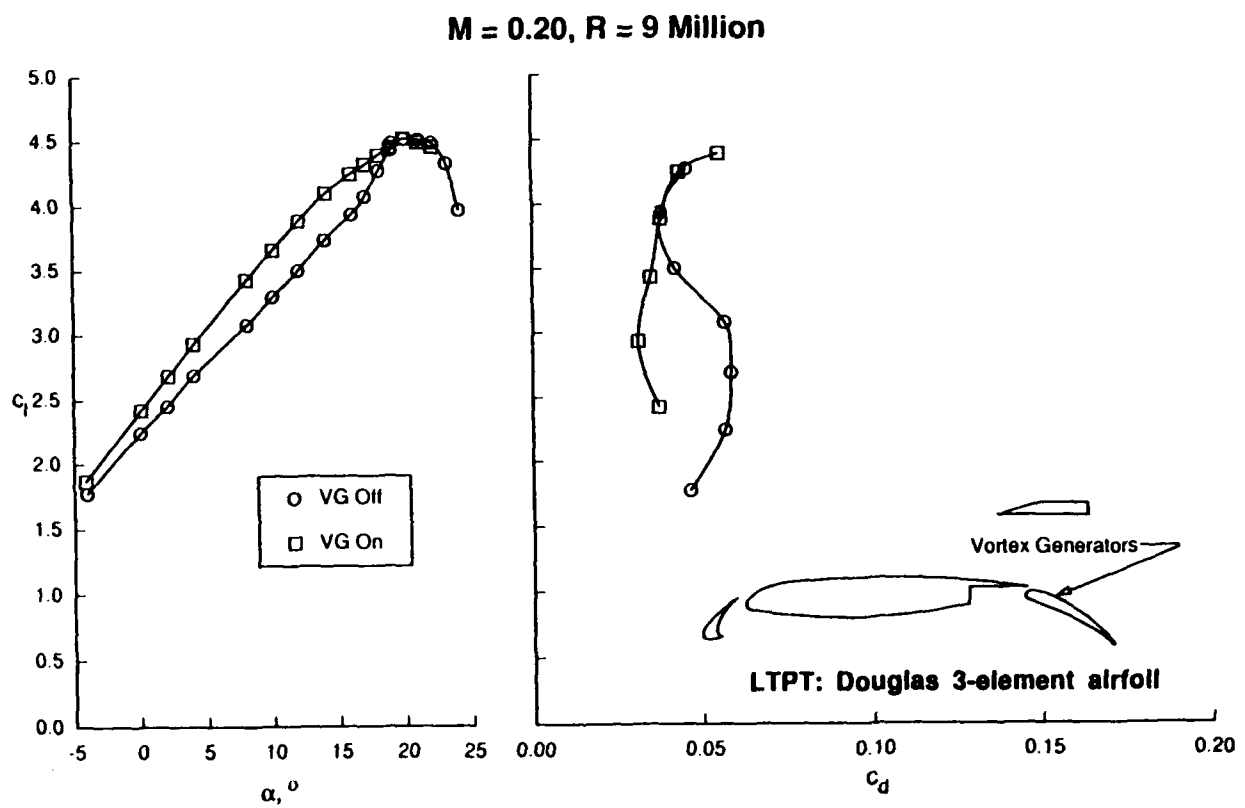


Figure 1-2. Separation Control for High-Lift Airfoils; Three Element Landing Configuration; Counter Rotating Low-Profile Vortex Generators

1-2 Vortex Generators for High-Lift Airfoils

Objective. To evaluate the effectiveness of very small vortex generators for controlling boundary layer separation over three-element high-lift airfoils.

Approach. Small, vane-type vortex generators were mounted on a Douglas three-element, two-dimensional model in landing configurations as part of a cooperative test program between NASA and Douglas Aircraft Company conducted in the Langley Low-Turbulence Pressure Tunnel (LTPT). The investigation was conducted at near-flight conditions with chord Reynolds numbers of 5 million and 9 million and a Mach number of 0.2.

Accomplishments. Separation control with vortex generators was investigated during the second and third quarter of FY 1991 on the Douglas high-lift model. Measurements include lift, drag, surface pressure, wake profiles, and fluctuating shear stress. Low-profile vortex generators mounted at 25% of the flap chord, and with a device height of only 0.2 inches at full scale, were effective in alleviating flap separation. The resulting wake of the three-element airfoil was significantly narrowed, providing measured drag reductions of up to 50%, (see figure). In addition, lift coefficients at approach angles-of-attack (i.e., 8° to 12°) were increased by up to 10%.

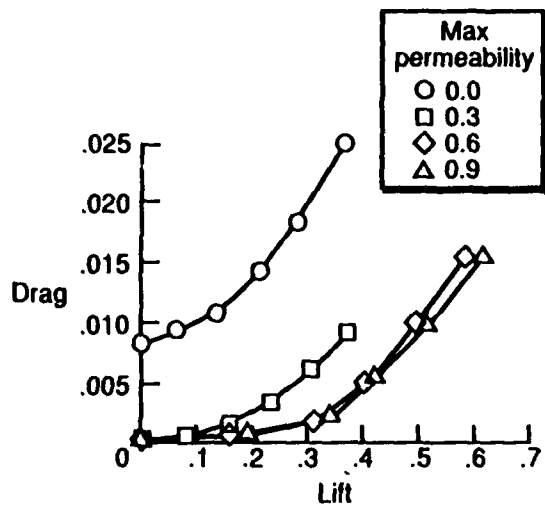
Significance. The results of this investigation have indicated: (1) Separation alleviation on the flap can significantly improve the performance of the entire high-lift system. (2) A practical vortex-generator system that not only can produce effective separation alleviation but also produce low drag when deployed, no drag when retracted in cruise (stow inside the flap well), and simplicity and ease of maintenance. (3) Low-profile, flap mounted vortex generators can be integrated into a modern transport to maximize performance and eliminate buffeting.

Status/Plans. More vortex generator tests are planned for 1992, as well as a vortex generator jet test on a NASA high-lift model.

John C. Lin
Fluid Mechanics Division
Langley Research Center
(804) 864-5556

DRAG POLARS FOR SOLID AND POROUS NACA 0012 AIRFOILS

$M_\infty = 0.80$



SELF-ADAPTIVE AIRFOIL THROUGH POROSITY

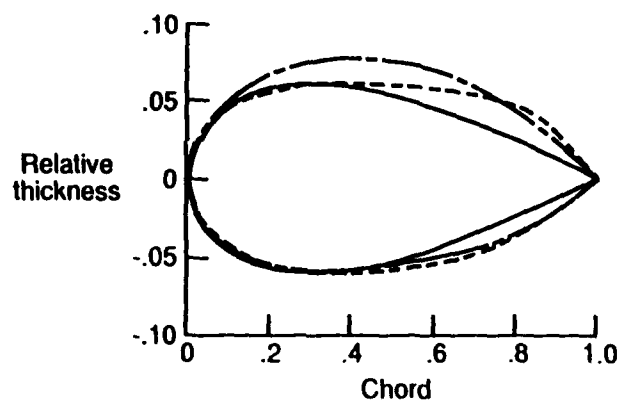
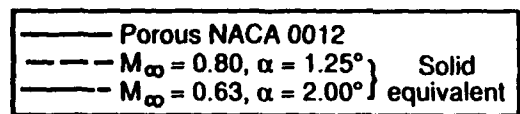


Figure 1-3. Porosity for Transonic Airfoils With a View Toward Multipoint Design

1-3 Porous Transonic Airfoils for Multipoint Design

Objective. To determine the feasibility of using porosity to achieve multipoint design for transonic airfoils.

Approach. A computational pilot study was conducted with an in-house developed time-implicit upwind method for the nonconservative Euler equations using floating shock fitting for accurate representations of shocks. The computational approach allowed for a faster and less-expensive assessment of influencing parameters, such as profile geometry, arrangement of porous surface patches, and degree of porosity, than an experimental study.

Accomplishments. Solutions were computed for steady transonic flow over NACA 0012 and supercritical airfoils with solid as well as porous surfaces. The porous surfaces were applied to both upper and lower profile surfaces, and they extended over the nominal chord. Either connected or separated cavities were assumed to lie beneath the upper and lower surfaces. The porosity distribution is described by a modified sine wave with several amplitudes. The sinusoidal porosity distribution was chosen to facilitate the numerical approximation of flow through permeable surfaces.

Applied to a NACA 0012 airfoil, porosity generally increases lift for a given angle-of-attack, in some instances by up to 65%. As indicated by the accompanying figure, the wave drag taken at constant lift for supercritical flow past a porous NACA 0012 airfoil with separated cavities is up to one order of magnitude lower than for its solid counterpart.

The accompanying figure also illustrates the new quality of a porous NACA 0012 airfoil being self-adaptive to dissimilar flow conditions. Using the calculated porous surface pressure distributions as target pressures, equivalent solid airfoil shapes were con-

structed using a computational design tool. While the subcritical equivalent airfoil basically retains the teardrop shape of the NACA 0012 profile, the supercritical companion piece reveals a distinct flattening of the upper surface combined with hump-shaped closure toward the trailing edge.

Making the surfaces of an already optimized supercritical airfoil permeable also broadens its operational speed and incidence range.

Significance. Euler analyses indicated a potential of using passive venting techniques for restructuring the flow past airfoils such that they become self-adaptive to very dissimilar flow conditions. This property could open an alternate route for achieving multipoint design, that is, the design of airfoils which satisfies several, oftentimes conflicting constraints.

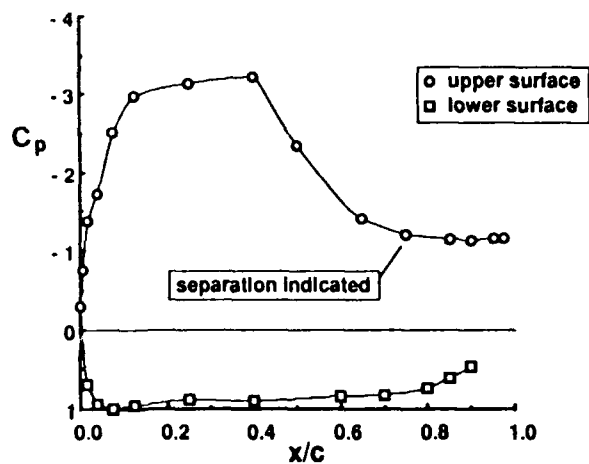
Status/Plans. The proposed concept will be experimentally verified in the 8-Foot Transonic Pressure Tunnel at Langley Research Center.

Peter M. Hartwich (ViGYAN Inc.)
Applied Aerodynamics Division
Langley Research Center
(804) 864-2881

Flight Results on a Subsonic Transport Flap System

Pressure Distributions on 1st Flap Element

Flap deflection = 40 deg
 $C_L = 2.46$ Airspeed = 101 kts (Indicated)
 Angle of attack = 10.21° $RN, \bar{c} = 9.96 \times 10^6$



Tuft Flow Visualization of the Flap System

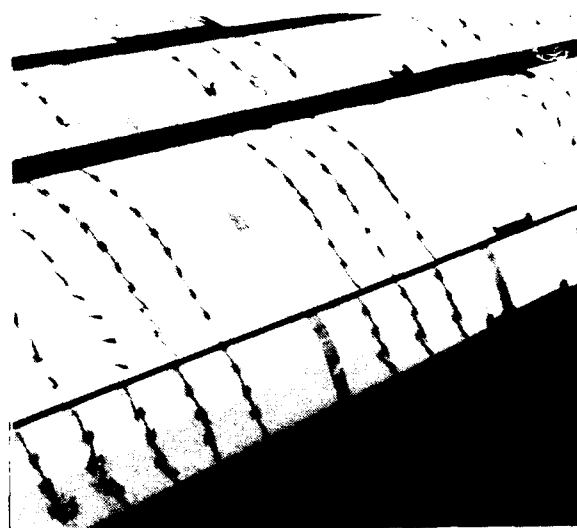


Figure 1-4. Flight Results on a Subsonic Transport Flap System

1-4 Subsonic Transport High-Lift Flight Research - Phase I

Objective. To obtain in-flight aerodynamic flow measurements on subsonic transport high-lift systems for correlation with wind-tunnel data and validation of CFD results to improve high-lift design methodology.

Approach. As part of a multiphase research activity, Phase I flight experiments were conducted on a B737-100 (NASA 515) research aircraft to measure pressure distributions on the high-lift flap system of a transport configuration. Phase I activities included measuring pressure distributions at select spanwise locations of the aircraft flap system. Pressure data were obtained in flight using belts of thin plastic tubing wrapped around the upper and lower surfaces of each of the trailing-edge flap elements at two spanwise locations. In addition, surface tufts were used to document flow-separation characteristics, and Preston tubes were used to measure surface shear-stress characteristics at selected locations.

Accomplishments. Phase I flight tests on the NASA 515 research aircraft were completed in May 1991. Steady-state test points (about 250 test conditions) were obtained for a range of altitudes up to 20,000 feet and airspeeds as low as the stick shaker speed. Chord Reynolds numbers ranged from 10 to 20 million and Mach numbers ranged from 0.16 to 0.40. Pressure data was obtained on each flap element of the triple-slotted flap system for deflections from 15° to 40°. Flow-separation characteristics on the flap system were documented with surface tufts, and surface shear-stress measurements were determined from Preston tube readings.

Significance. An aerodynamic database including pressure distributions and documentation of flow separation was established on a complex high-lift flap system in flight over a range of Reynolds and Mach numbers and angle-of-attack conditions. These data will

contribute to the improved understanding of high-lift flow physics and will provide a good test case for correlation of wind tunnel data and validation of computational fluid dynamic results.

Status/Plans. Additional flight tests (Phase IA) are planned for winter 1991/1992 to obtain full-chord pressure distributions along the wing and slat elements as well as the flap elements. Analysis of flight data will be made using two and three-dimensional computational methods to help plan a follow-on Phase II flow physics flight experiment. Phase II activities will incorporate the use of replacement 737 slat and flap spare parts to house instrumentation for detailed surface pressure distributions, boundary layer, and wake flow measurements.

Long Yip, Paul Vijgen
Flight Research Branch
Langley Research Center
(804) 864-3866

Chapter 2

Test Techniques and Instrumentation

Technology is being provided for critical experimental research required to improve the measurement of the fundamental flow properties of fluids and the overall aerodynamic performance of aircraft components and configurations. The development of instrumentation and measurement techniques for real-time, flow diagnosis is being performed with emphasis on nonintrusive methods. These developments occur across the range of conditions from cryogenic to high temperature and from low subsonic to hypersonic speeds.

One of the more exciting instrumentation developments underway is the use of pressure sensitive luminescent paint on aerodynamic models. This will provide nonintrusive, inexpensive sensing of pressure in real time for wind tunnel and flight testing.

Other research areas being addressed are (1) heavy gas wind tunnel testing to operate at high Reynolds numbers; (2) solid-state camera/optical image correction techniques to correlate flight test data of aircraft encounters with wing tip vortices generated by large aircraft; (3) nonintrusive Rayleigh-Raman multipoint measurements of gas density in hypersonic flow; (4) liquid crystal skin friction sensors capable of high-frequency response in high-speed flows; and (5) nonintrusive infrared thermography of global heat transfer rates on wind tunnel models in hypersonic flow.

Program Manager: Gary Hicks
OAST/RF
Washington, DC 20546
(202) 453-2830

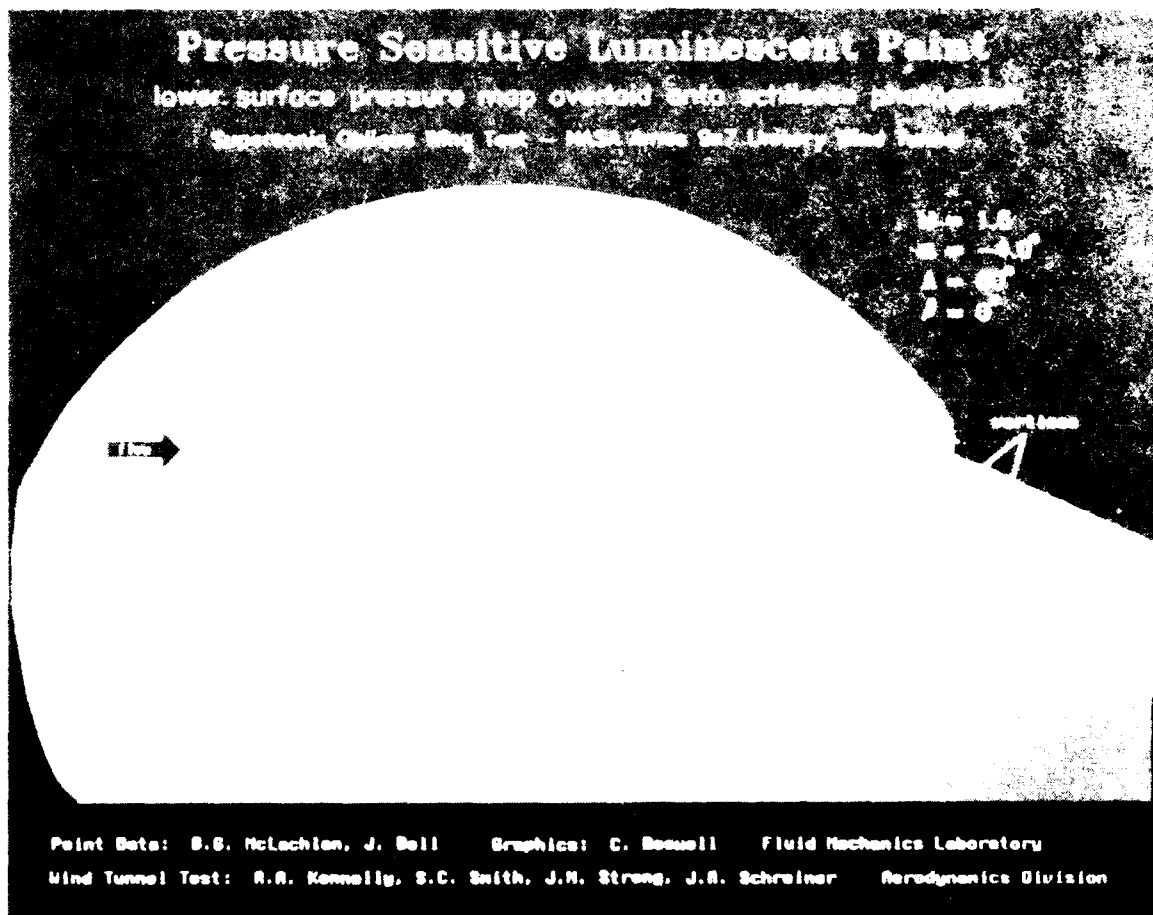
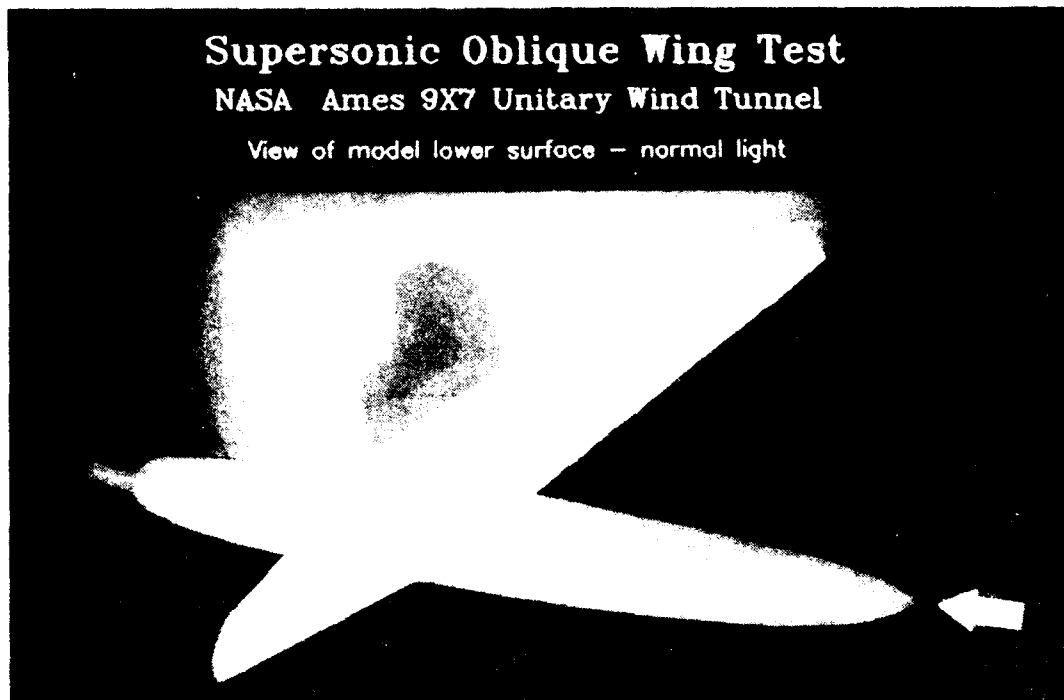


Figure 2-1. Luminescent Paint Sensor Development

2-1 Luminescent Paint Sensor Development

Objective. To develop luminescent "paints" for the measurement of surface pressure and temperature fields in aerodynamic testing. Our ultimate goal is to develop this methodology into a practical tool such that it can replace conventional methods.

Approach. This work is a cooperative research program between the Ames Fluid Mechanics Laboratory and the University of Washington Chemistry Department. Candidate luminescent molecule/coating formulations were identified, and trial coatings were made. The suitability of these trial coatings was assessed through static and wind tunnel tests.

Accomplishments. In May 1991 the supersonic oblique wing test was being conducted in the Ames 9 by 7-foot Unitary Plan Wind Tunnel. The pressure sensitive luminescent paint test was piggybacked onto the larger experiment, whose objective was to evaluate the performance and surface flow characteristics of a generic oblique wing model for Mach 1.6 to 2.0. Figure A is a photo of the model in the test section showing the model's lower surface. The lower surface of the wing was coated with the pressure sensitive paint. Because of the extreme test conditions, a low test section static pressure and a high total temperature, it was not possible to determine the absolute pressure level using the paint. Relative pressure change, however, could be seen.

Figure B is a representative example of the data acquired. Shown is a map of the lower surface pressure field over the forward swept portion of the oblique wing. Conditions are noted in the figure. The unique field measurement capability of the paint method is evident: the paint capturing the passage of the fuselage bow shock over the outboard portion of the wing and the passage over the wing inboard portion of a shock arising from reflec-

tion of the wing tip shock off the fuselage. More subtle features such as the formation of streamwise vortices over the wing surface from the cross-flow and the subsequent separation can also be seen.

Significance. The oblique wing test represents the first use of the pressure paint under supersonic flow conditions. The flow conditions for this test were outside the previous operational experience with the pressure paint and were considered marginal at best. However, the paint did provide qualitative information. From this experience we now have more information on the practical operating range of the pressure paint and the experimental methodology associated with its use in a large-scale supersonic facility.

Status/Plans. Further development of the pressure sensitive paint to improve its characteristics continues. Near-term work is focusing on the development of a temperature sensitive luminescent paint and a dual sensor paint that will allow simultaneous measurement of pressure and temperature. We are also pursuing the development of luminescent sensor coatings for unsteady aerodynamic applications.

B.G. McLachlan, J. Bell,
J. Schreiner
Fluid Dynamics Research Branch
Advanced Aerodynamic Concepts Branch
Ames Research Center
(415) 604-4142

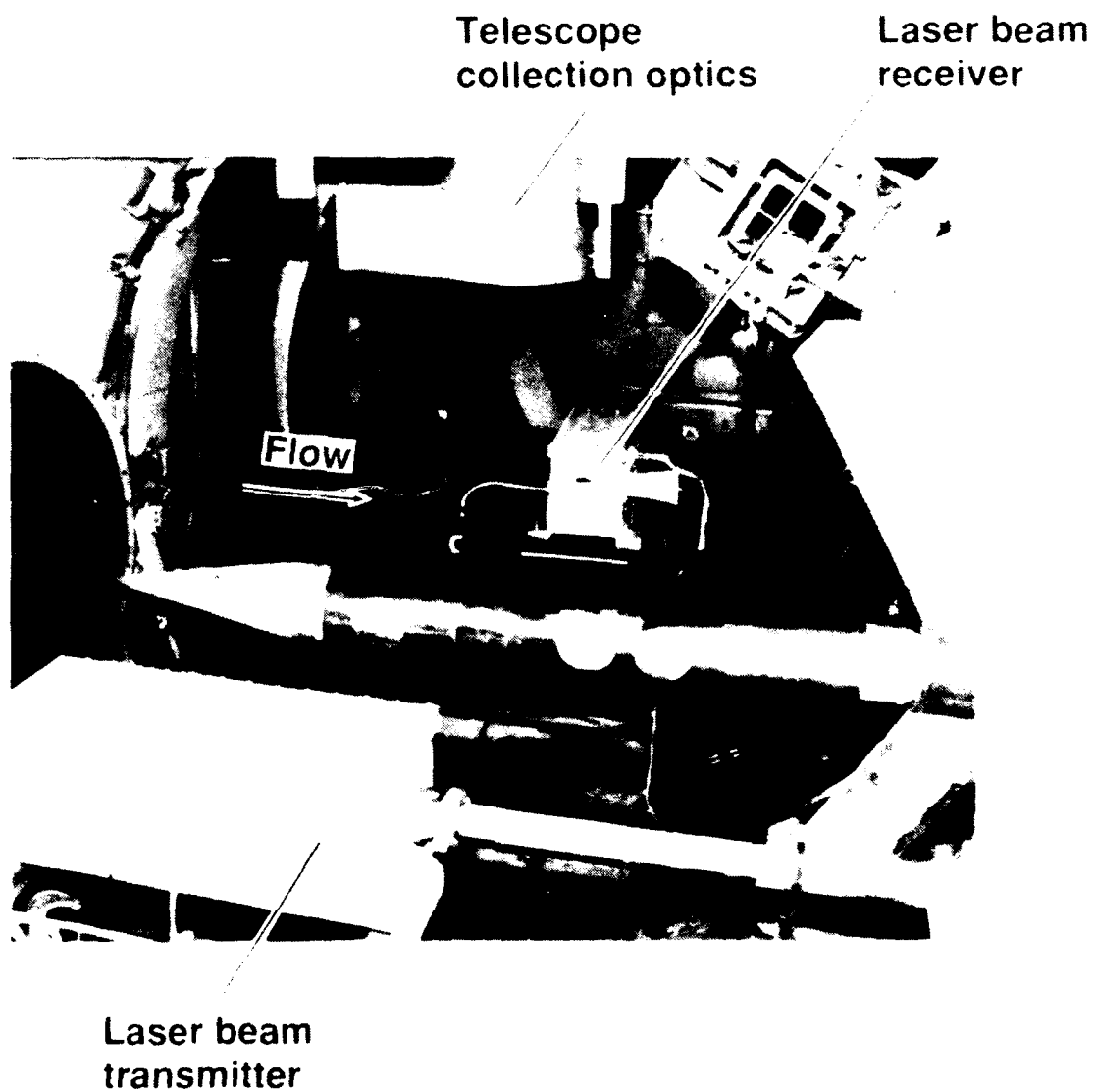


Figure 2-2. Laser-Induced Fluorescence Instrumentation in the Ames 3.5-Foot Hypersonic Wind Tunnel

2-2 Temperature and Density Measurements in Air Using Laser-Induced Fluorescence

Objective. To provide nonintrusive measurements of flow-field temperature, density, and their fluctuations owing to turbulence with application capability in all air flows including hypersonic wind tunnel flows.

Approach. Laser-induced fluorescence of oxygen is used in combination with Raleigh scattering from the same laser beam to provide instantaneous and simultaneous measurements of temperature and density from each laser pulse.

Accomplishments. Bench-top experiments have demonstrated that measurements can be made at the free-stream conditions of the Ames 3.5-foot hypersonic wind tunnel at Mach 10 with uncertainties of less than 2%. Initial measurements have been made in the 3.5-ft Wind Tunnel at Mach 7.

Significance. Nonintrusive measurements of flow-field properties and their fluctuations in hypersonic flows will provide significant new information for turbulent model development and the validation of 3-D numerical simulation codes that is not obtainable by other means.

Status/Plans. The instrumentation has been installed in the Ames 3.5-foot hypersonic wind tunnel and preliminary measurements have been demonstrated. Further refinement of the instrumentation is in progress.

Robert L. McKenzie
(415) 604-4749
Douglas Fletcher
(415) 604-5244
Experimental Fluid Dynamics Branch
Ames Research Center

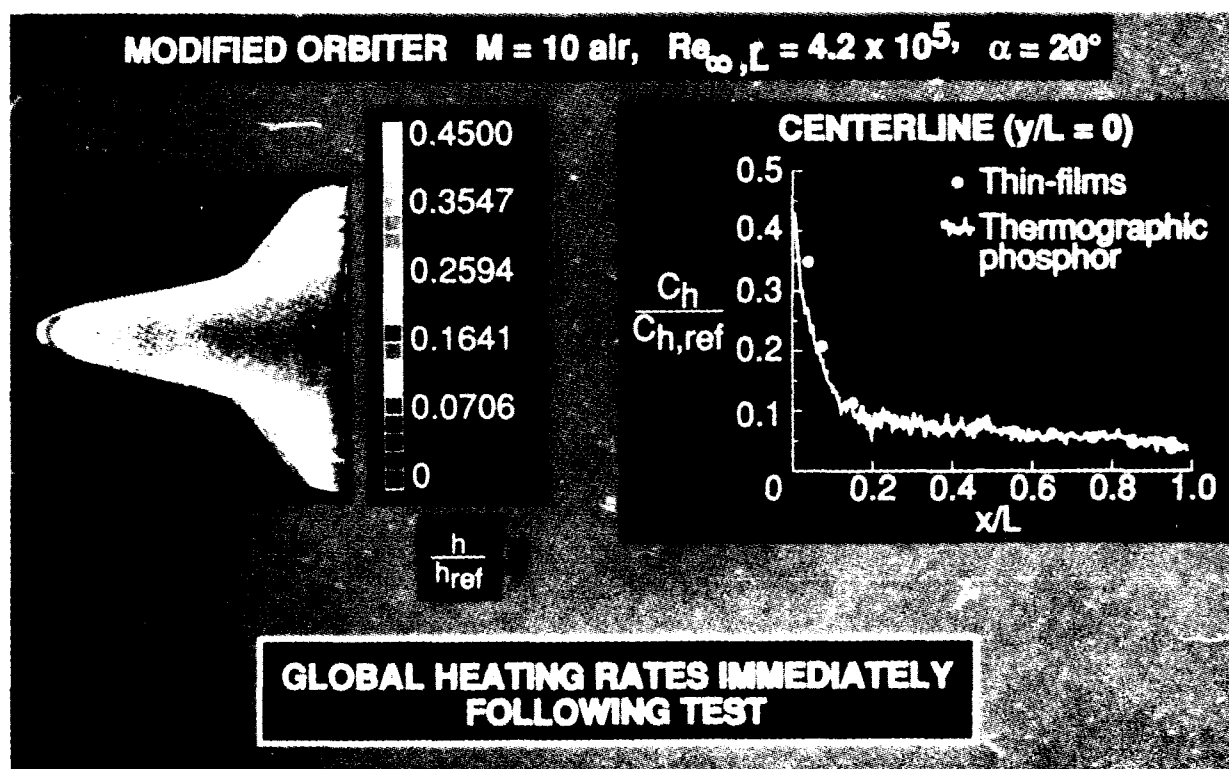


Figure 2-3. Application of Thermographic Phosphor Technique

2-3 Phosphor Thermography Technique

Objective. To extend the capability of the relative-intensity, two-color thermographic phosphor technique to provide global, quantitative heat transfer data on models in hypersonic wind tunnels.

Approach. Model surface temperature time history was accurately measured, pixel by pixel, prior to and during injection of the model through the nozzle boundary layer into the test core and following flow establishment of freestream flow about the model. One-dimensional conduction heat transfer equations were used for each pixel on the model within the field-of-view of the camera (maximum of 262,000 pixels for each time) to determine the quantitative value of heat transfer rate. These values of heating were compared with benchmark values obtained with thin-film resistance gages for the same model geometry at the same flow conditions and attitude.

Accomplishments. Global heat transfer rates were measured on a ceramic "modified orbiter" model at Mach 10 in air using the relative-intensity, thermographic phosphor technique. Surface temperature time histories were determined during the model injection process, and newly developed software was used to reduce data to values of heat transfer rate. These results were compared with heating distributions measured with thin film gages on the same configuration at the same flow conditions (referred to as HALIS orbiter CFD code calibration study). Data from these two techniques along the model centerline and several spanwise cuts showed good to excellent agreement.

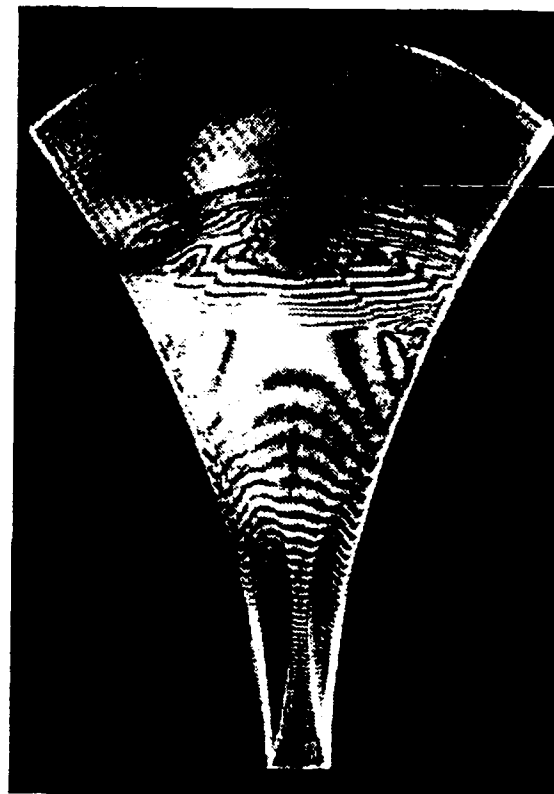
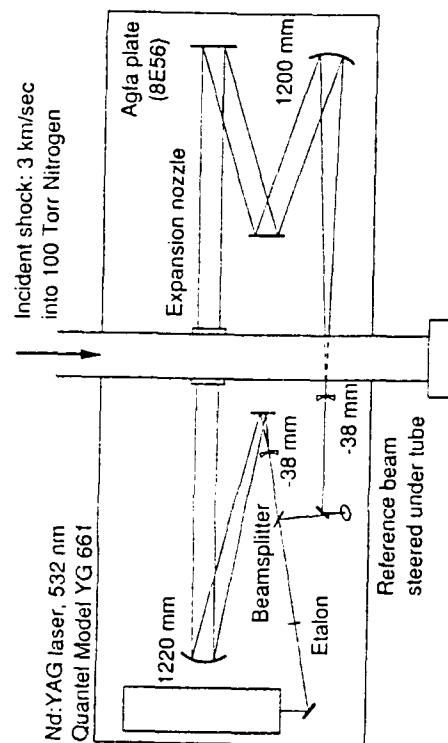
Significance. Phosphor thermography has evolved from a thermal mapping technique to a viable quantitative heat transfer measure-

ment technique. Global heating distributions can be obtained minutes after a wind tunnel run, allowing researchers to optimize (i.e., tailor) investigation run by run. Compared with the thin-film gage technique (recognized as the most accurate method for measurement of heat transfer rate), phosphor thermography provides invaluable global information, and the time and cost to construct ceramic models are an order of magnitude less than the time and cost for thin-film models. This phosphor technique has revolutionized aerothermodynamic testing at LaRC and has generated considerable interest in the national/international hypersonic-testing community.

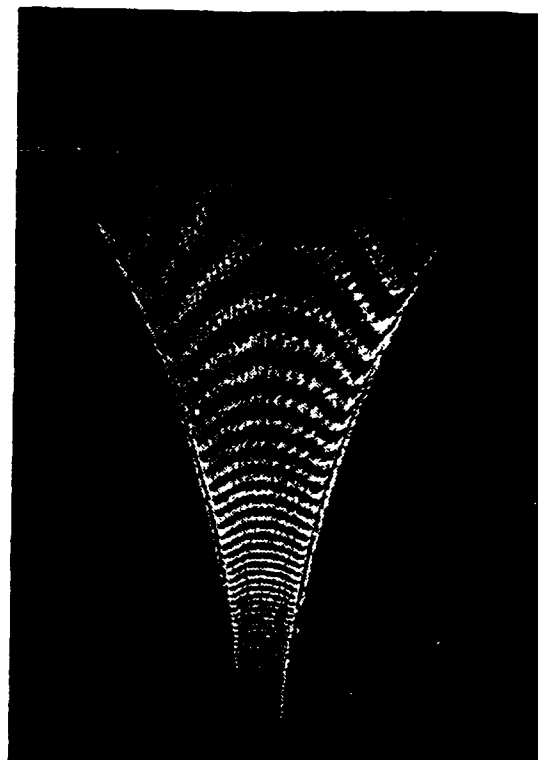
Status/Plans. A next-generation phosphor system, which will provide tracking during the model injection process and accurate spatial definition including regions of high surface curvature, has been specified and is being acquired. Advanced methods of applying phosphors are being examined and improved data reduction techniques are under development. Potential application to impulse facilities having run times less than 50 msec will be investigated.

N. Ronald Merski
Experimental Hypersonics Branch
Langley Research Center
(804) 864-7539

Holographic Interferometry Layout at EAST Reflected Shock Tunnel



$T_0=7000$ K, $P_0=1500$ psi, startup,
 $t=9$ μ sec after shock arrival.



$T_0=7000$ K, $P_0=1500$ psi, steadystate,
 $t=40$ μ sec after shock arrival.

Figure 2-4. Density Field Measurements in a Nonequilibrium Expanding Flow Using Holographic Interferometry

2-4 Density Field Measurements in a Nonequilibrium Expanding Flow Using Holographic Interferometry

Objective. To characterize the flow field of a two-dimensional nozzle using holographic interferometry as a first step towards the investigation of nonequilibrium expanding flows.

Approach. The 10-cm drive section of the Ames's electric arc-driven shock tube facility was converted into a reflected shock tunnel facility by installing a 2-D nozzle insert in the tube. A 3.2 km/sec shock in 100 Torr nitrogen reflected off the nozzle insert, providing a reservoir of compressed test gas with P5=1500 psi and T5=7000 K. A Nd:YAG laser doubled to 532 nm was used to produce holograms of the nonequilibrium expanding flow.

Accomplishments. A diagnostics system capable of producing a snapshot (6-ns exposure time) single-plate, double-exposure hologram has been developed. Holograms of the expanding flow, including startup flow, at intervals of 9, 17, 20, 40, and 60 μ s from the time of shock arrival have been recorded. Static pressures at 10 points in the wall of the nozzle have also been recorded.

Significance. The relaxation time scale in expanding flows can be 1-2 orders of magnitude lower than the time behind a normal shock. To develop a better understanding of this nonequilibrium in expanding flows, the vibrational populations during the relaxation will be measured. However, to accomplish this, the bulk density in the flow field must be known. The holograms provide the bulk density data.

Status/Plans. In addition to these holograms, synthetic holograms using the computed flow-field data will be generated. The experimentally obtained holograms then will be compared with the synthetic ones. Such an exercise will enable us to test our ability to compute the expanding flows. Also, the density flow-field data from the holograms will be used in the next stage of the experimental program on the investigation of nonequilibrium expanding flows.

Surendra P. Sharma, Scott A. Meyer,
Walter D. Gillespie
Aerothermodynamics Branch
Ames Research Center
(415) 604-3432

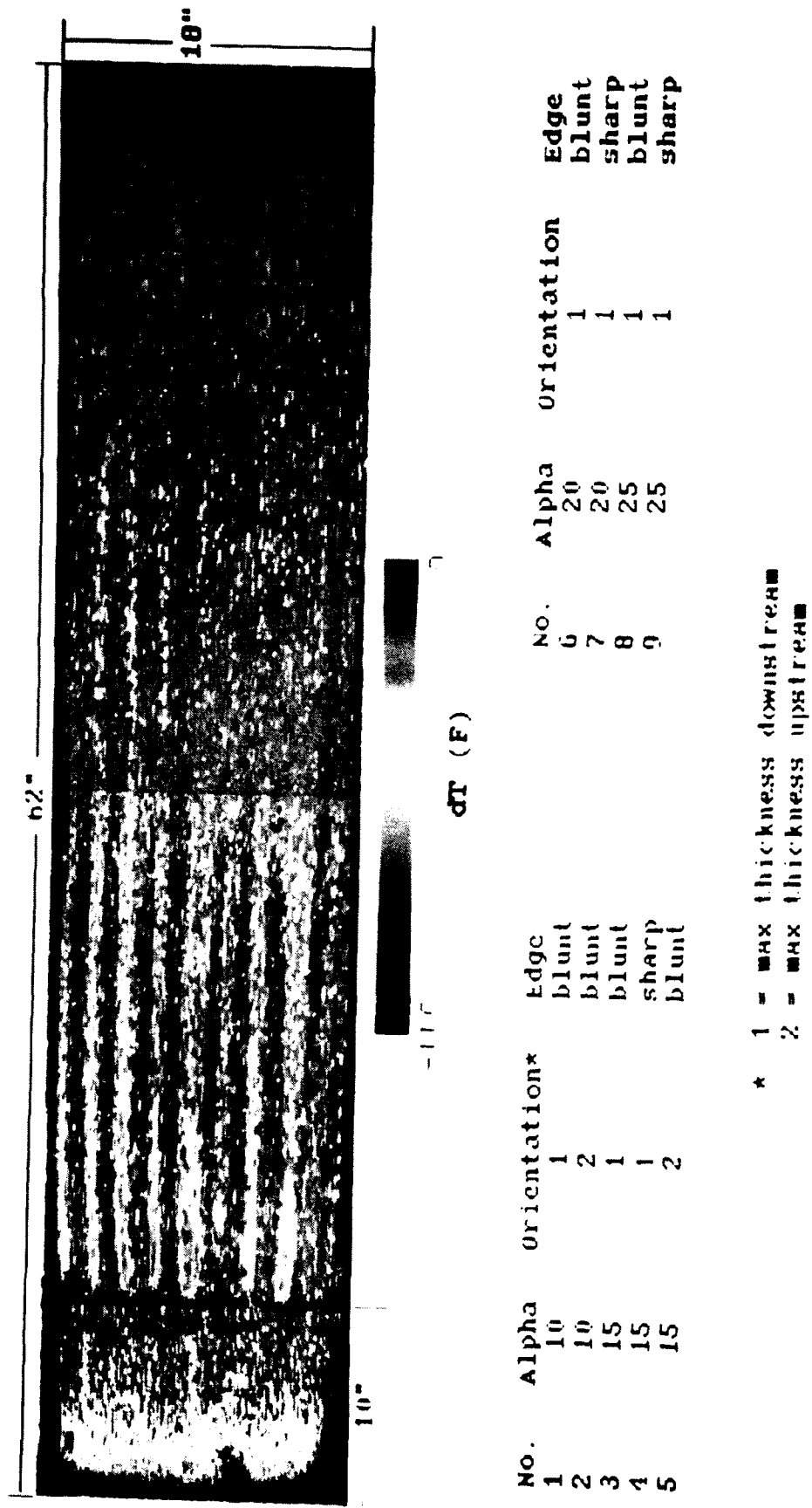


Figure 2-5. Infrared Map of Wakes Behind Vortex Generators in Hypersonic Flow

2-5 Measurement Techniques for Hypersonic Flows

Objective. To evaluate and develop experimental methods for use in scheduled Generic Hypersonics and NASP-related programs.

Approach. Two experimental techniques for hypersonic flows in helium were examined: (1) An exploratory test was made to determine if infrared measurements could be used to map the two-dimensional temperature field on the surface behind a series of vortex generators. Prior to the test, it was not known if the infrared imaging system would be sensitive enough to accurately determine the location of vortex-induced surface heating behind vortex generators. (2) Measurement of the constant-temperature hot-wire anemometer characteristics was made, and examination of hot-wire data reduction techniques in hypersonic flow was begun by a summer research associate, Professor Eric Spina of Syracuse University in collaboration with Catherine McGinley of Experimental Flow Physics Branch, Fluid Mechanics Division.

Accomplishments. Despite the very low heat transfer rates on the surface of the base model in the High Reynolds Number Helium Tunnel, the wakes behind a series of vortex generators were visible, allowing the assessment of wake strength as a function of generator angle and orientation. A frequency response of the hot-wire system was found to be adequate for measuring turbulence quantities at Mach 11.

Significance. Infrared measurements will enable a relatively simple determination of the geometry, size, and spacing of vortex generators needed to trip a hypersonic boundary layer with minimum drag penalty. With a constant-temperature anemometer system, measuring mass-flow fluctuations in hypersonic boundary layers with adequate frequency response will be possible. These tests showed that a constant current system is not necessary.

Status/Plans. Infrared tests will be continued, and a parametric study of vortex generator geometry will be made to determine the most effective configuration for hypersonic flow. Measurements of mass flux fluctuations in a hypersonic boundary layer will be made. Efforts to improve data reduction methods will continue.

Ralph Watson
Experimental Flow Physics Branch
Langley Research Center
(804) 864-5723

Chapter 3

Transition and Turbulence Physics

The objective of the Transition and Turbulence Physics Program is to develop a fundamental understanding of flow structures relating to transition and turbulence and to incorporate these flow structures into sophisticated flow models for use with computational methods. Extensive efforts are being developed within the program to solve the full Navier-Stokes equations, which include transitioning and turbulent flows. However, the realities of today's supercomputer limitations in terms of memory and speed make it impractical to consider full Navier-Stokes solutions for all but the simplest problems. Practically speaking, research in transition and turbulence modeling with various levels of approximation is providing the bridge for the gap until the computer power is available. The understanding of the physical flow structures of transitioning and turbulence flows is being examined from two directions, computational and experimental. Extensive advancements in test instrumentation being developed within other discipline programs is enhancing transitional and turbulence experimental research. The development of quiet supersonic wind tunnels will provide an experimental tool for investigating supersonic viscous flows. Exciting advances are occurring in compressible boundary layer transition with the use of parabolized stability equations derived from the complete Navier-Stokes equations. The program supports the Center for Turbulence Research which assembles world renowned experts in the field to generate new concepts regarding turbulence. A similar effort is being established for fluid mechanics research emphasizing transition.

Program Manager: Gary Hicks
OAST/RF
Washington, DC 20546
(202) 453-2830

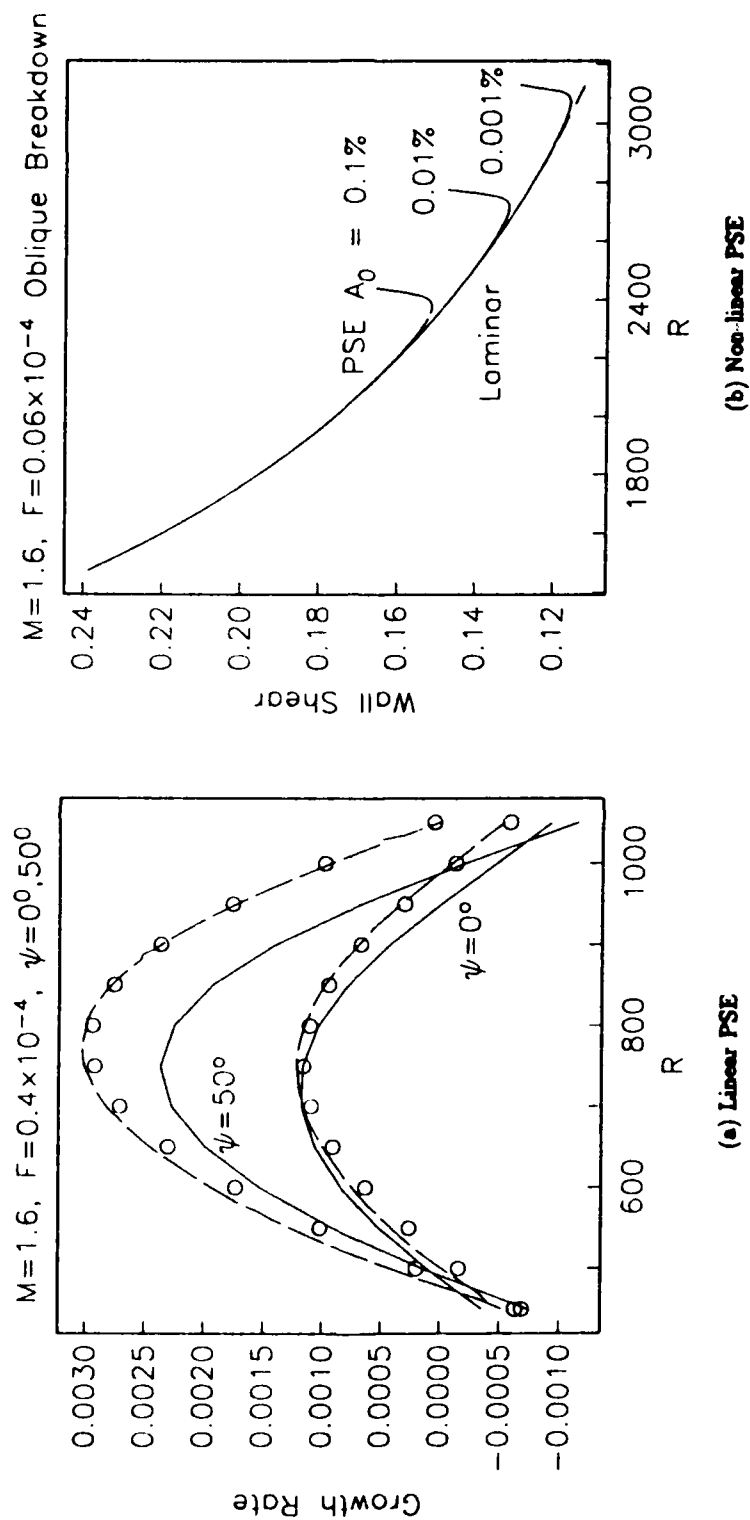


Figure 3-1. Evolution of Linear and Nonlinear Disturbances in Mach 1.6 Boundary Layer Flow at the Given Nondimensional Frequency $F(R = \sqrt{Re_t})$

3-1 Compressible Boundary Layer Transition Using PSE

Objective. To understand the mechanisms involved in compressible boundary layer transition, specifically to provide a capability for boundary layer transition prediction in both "quiet" and "disturbed" environments.

Approach. For convective instabilities such as T-S waves in boundary layers, the governing PDEs are only weakly elliptic along the dominant flow direction. The original PDEs are reduced to a set of parabolized stability equations (PSE), which is parabolic along the dominant flow direction, allowing solution by single-sweep marching. Both nonparallel and nonlinear effects of growing boundary layers are studied up to the transition stage using this new PSE approach.

Accomplishments. The PSE code for three-dimensional linear and nonlinear disturbances was developed for flat-plate geometry. Linear PSE calculations were performed for Mach numbers 0 to 4.5. The effect of boundary layer growth was shown to be important for both the first- and second-mode disturbances in supersonic boundary layers. Nonlinear PSE calculations show very good agreement with earlier temporal direct numerical simulations (DNS) at Mach 4.5 for the nonlinear evolution of a second-mode disturbance. The computational time required is an order of magnitude less than that for DNS.

Part (a) of the figure compares the growth rates of a linear disturbance as computed by the parallel PSE (solid line), the nonparallel PSE (dashed line), and the multiscale DNS methods. The results indicate that nonparallel effects are more important for oblique ($y = 50^\circ$) waves than for 2-D ($y = 0^\circ$) waves. A likely route to transition may consist of two oblique primary waves interacting with each other. Part (b) of the figure shows the oblique breakdown procedure for three different initial amplitudes at the given frequency. Transition is clearly located at the abrupt rise of

wall shear. The results indicate that rapid growth of the secondary disturbance is triggered when the primary amplitude is sufficiently high.

Significance. The PSE method can be used to study the nonparallel and nonlinear evolutions of disturbances in compressible boundary layers starting from the linear stage up to transition. Coupled with receptivity phenomena this approach offers a computationally viable means for studying and predicting the complex and intricate phenomenon of compressible boundary layer transition.

Status/Plans. An axisymmetric version of the PSE will be developed and used for transition studies in conical flows. The PSE theory will be extended to 3-D boundary layers. Work is also under way on formulating the leading edge receptivity problem using the PSE approach.

C. L. Chang
Fluid Mechanics Division
Langley Research Center
(804) 864-5563

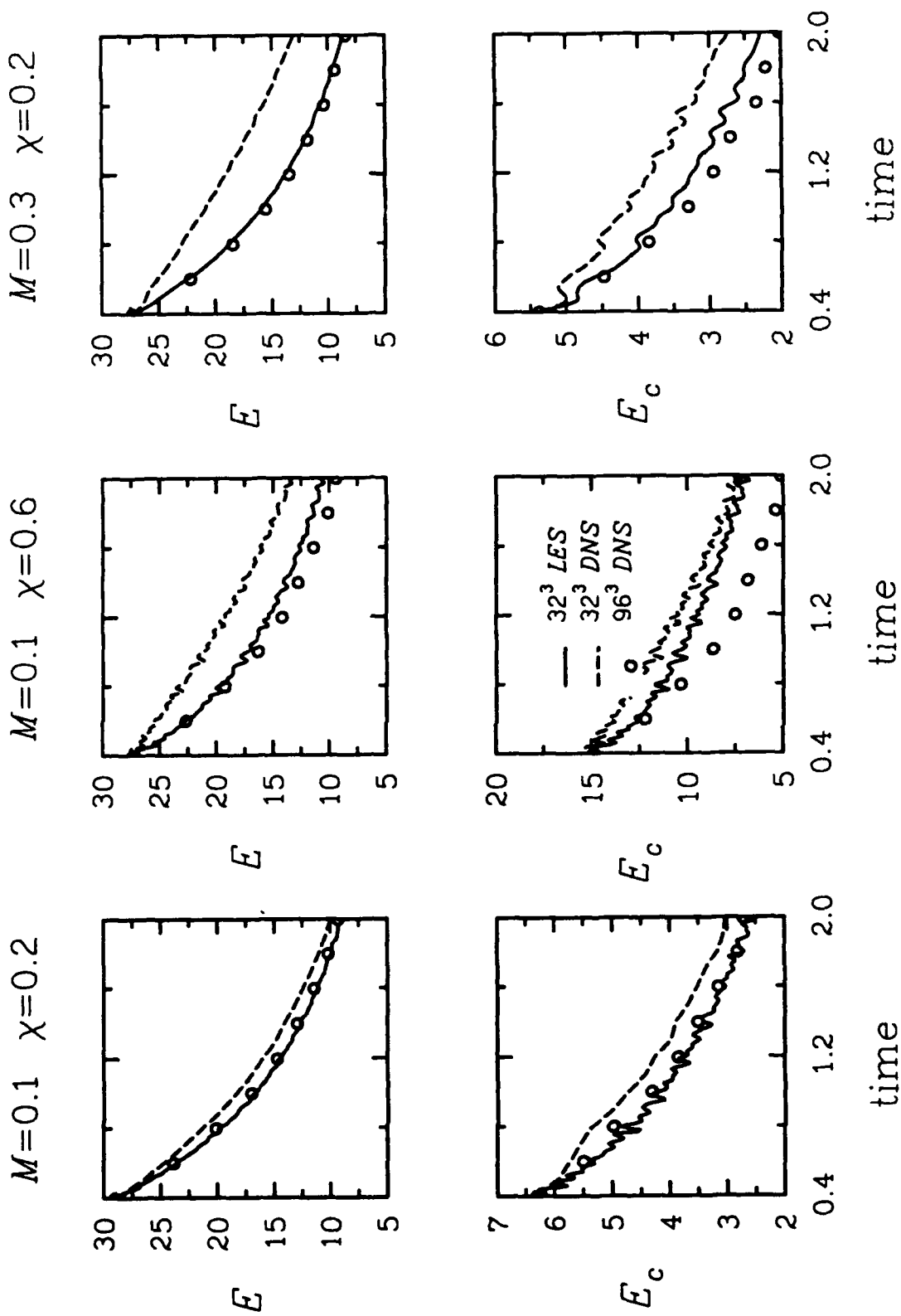


Figure 3-2. Large-Eddy Simulation of Compressible Isotropic Turbulence

3-2 Compressible Large-Eddy Simulation of Isotropic Turbulence

Objective. To assess the subgrid-scale (SGS) model proposed for compressible large-eddy simulation (LES) by Speziale, Erlebacher, Zang, and Hussaini.

Approach. The assessment was performed by conducting actual large-eddy simulations of compressible, isotropic turbulence and comparing the results with direct numerical simulation (DNS) data.

Accomplishments. An extensive new set of DNS data on 96^3 grids was generated. These data covered a range of fluctuating Mach numbers (M) and fraction of compressible energy (χ), the key parameters in compressible turbulence, according to a recent theory developed at ICASE. The proposed SGS model was utilized in LES for all of these cases. The figure compares the time evolution of the kinetic energy of decaying, isotropic turbulence from three different runs - a fine-grid (96^3) DNS, a coarse-grid (32^3) DNS, and a coarse-grid (32^3) LES. As shown in the figure, coarse-grid LES is quite accurate on the total kinetic energy (E), but is somewhat less accurate for the compressible component of the kinetic energy (E_c). Moreover, the coarse-grid LES does substantially better than a coarse-grid DNS. Surprisingly, the model predictions for the compressible component sometime improve as the flow becomes more compressible. Some of the problems can be ameliorated by refining the constants in the SGS model. However, subtle changes in the model itself appear necessary to obtain more consistent predictions in the compressible regime.

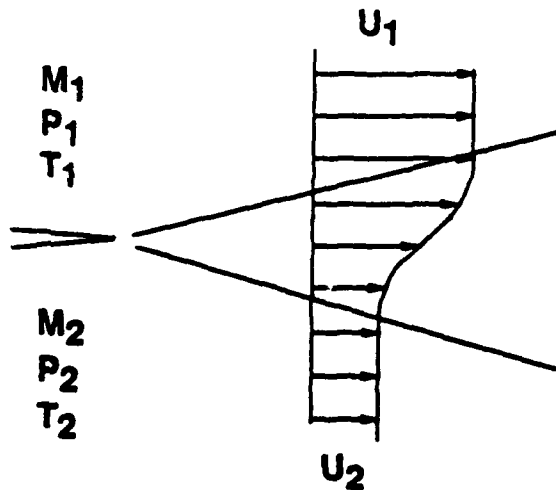
Significance. These were the first systematic, compressible LES calculations that have been performed. Previous tests of the SGS model were based solely on DNS data and did

not include actual large-eddy simulations. The results show that this first-cut SGS model for compressible turbulence performs better than anticipated.

Status/Plans. The results of these first compressible LES calculations have sparked considerable interest within the Langley group. Several improvements to the compressible part of the SGS model have already been suggested. The improved model will be applied to more challenging flows, such as compressible turbulence containing eddy shocklets, homogeneous turbulence in uniform shear flow, and wall-bounded shear flows.

Thomas A. Zang
Fluid Mechanics Division
Langley Research Center
(804) 864-2307

Shear layer



Vorticity thickness

$$\delta_\omega = (U_1 - U_2) / (\partial U / \partial y)_{\max}$$

$$\delta'_\omega = C_\omega(M_c) \frac{1 - U_2/U_1}{1 + U_2/U_1}$$

$$C_\omega(M_c) / C_\omega(0)$$

$$M_c = \frac{M_1 \sqrt{\frac{\rho_2}{\rho_1}} - M_2}{\sqrt{\frac{\rho_2}{\rho_1}} + 1.0}$$

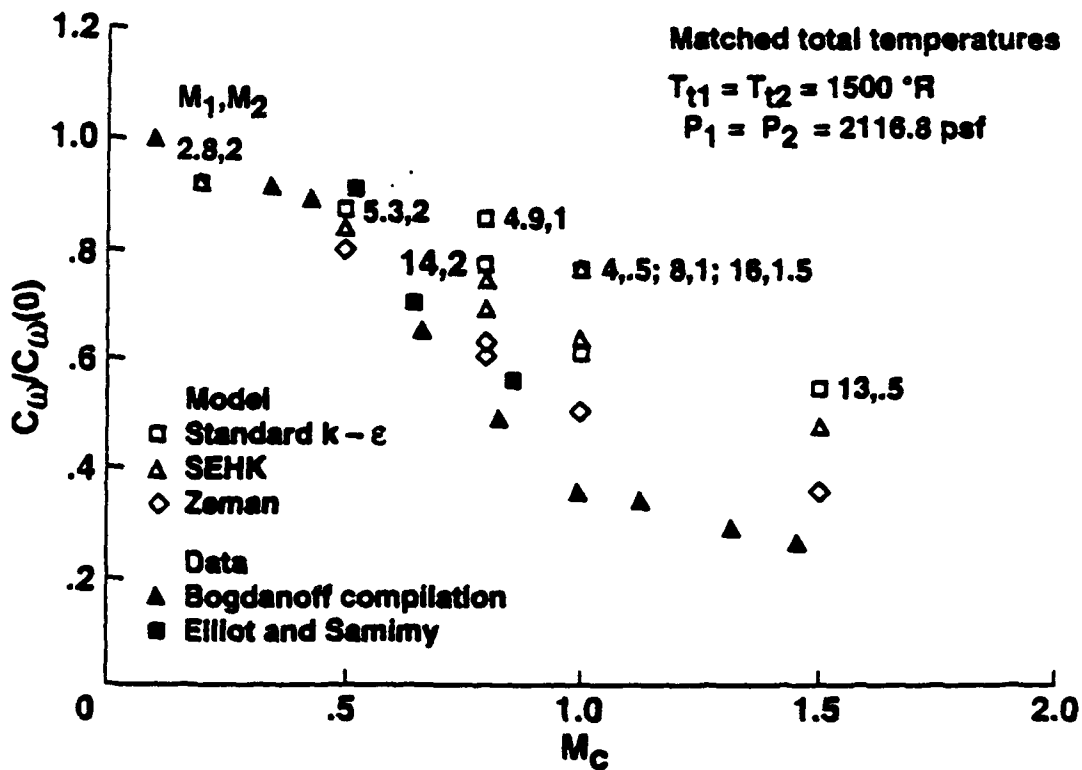


Figure 3-3. Effect of Compressibility Corrections on Vorticity Thickness Growth Rate

3-3 Compressible Turbulence Modeling for High-Speed Shear Layers

Objective. To assess the performance of several compressibility corrections to turbulence models applied to high-speed shear layers.

Approach. The compressible Navier-Stokes equations were numerically solved using a two-equation turbulence model with and without compressibility corrections. Numerical results were compared with available experimental data to determine the most appropriate model.

Accomplishments. Each of the compressibility corrections studied was developed to increase the dissipation in the kinetic energy of the turbulence in a shear layer. By lowering the eddy viscosity through a reduction in the turbulence energy, these models reduced the spread rate of free-shear layers for a wide variety of flow conditions as the convective Mach number increased.

Significance. The vorticity thickness growth rate comparisons between computation and experiment indicate that the application compressibility corrections can significantly improve predictions of high-speed shear layer mixing.

Status/Plans. This study is ongoing. Recent results were reported in June 1991 at the AIAA 22nd Fluid Dynamics, Plasma Dynamics and Lasers Conference. Further studies will include testing of additional compressibility corrections and detailed comparisons with shear layer experiments.

John R. Viegas
Fluid Dynamics Division
Ames Research Center
(415) 604-5950

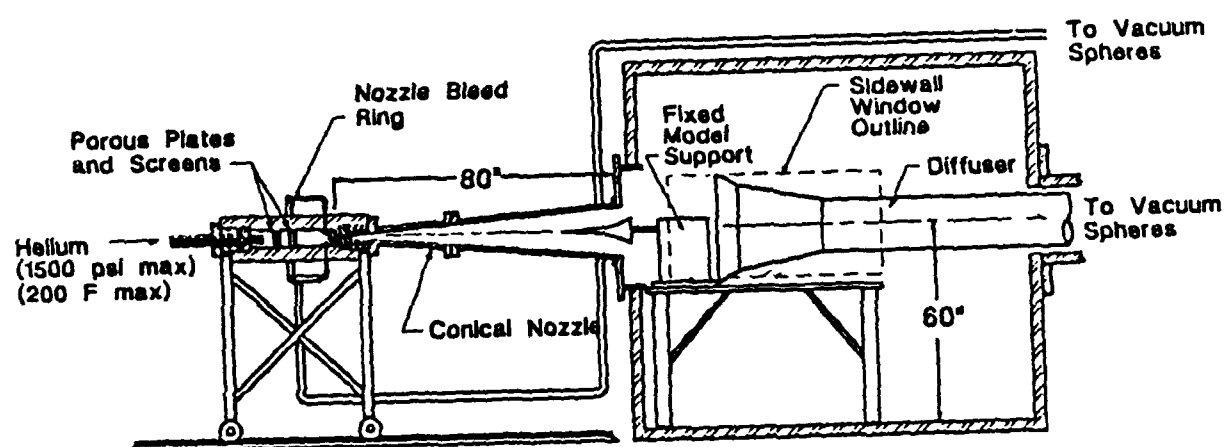


Figure 3-4. Mach 18 Quiet Helium Tunnel

3-4 Development of a Mach 18 Quiet Helium Tunnel

Objective. To modify the Mach 20/40 Open Jet Helium Tunnel to operate as a Mach 18 Quiet Helium Tunnel.

Approach. Only the minimum essential modifications required to convert the existing conventional facility to a quiet flow tunnel were made. The settling chamber was outfitted with freestream turbulence and noise control devices. These consisted of a new inlet diffuser, two high-density woven wire porous plates, and two high open-area screens. The existing settling chamber was modified to accept a slotted nozzle and associated boundary layer bleed system piping. The downstream portion of the existing Mach 20 conical nozzle was retained to eliminate the possibility of nozzle wall transition due to the Gortler instability mode. The throat section, however, was replaced with a highly polished unit with an annular sonic orifice upstream of the throat for removal of the settling chamber boundary layer.

Accomplishments. Engineering design of the tunnel modifications was completed in FY 1989. Manufacture and acquisition of the new hardware was completed during FY 1990. Installation of the new components and associated piping has occupied most of FY 1991.

Significance. Because of the high radiated noise environment of conventional high-speed wind tunnels, transition experiments with known noise sensitivity or experiments where the noise sensitivity has not been established must be conducted under quiet flow conditions. Virtually all hypersonic transition tests fall in the latter category. If the modifications prove to be successful, this facility will offer the first hypersonic, quiet transition testing capability above Mach 6.

Status/Plans. At the present time, certification of the new high-pressure piping is 90% complete. Start-up and shake-down runs are

projected for October 1991. Initial runs will use an existing, unpolished nozzle throat section and will focus on ensuring that the system helium flow is free of particles that may damage the highly polished nozzle finish. In the event that particles are found to be present, plans to install a filter upstream of the settling chamber are in preparation.

Stephen P. Wilkinson
Fluid Mechanics Division
Langley Research Center
(804) 864-5733

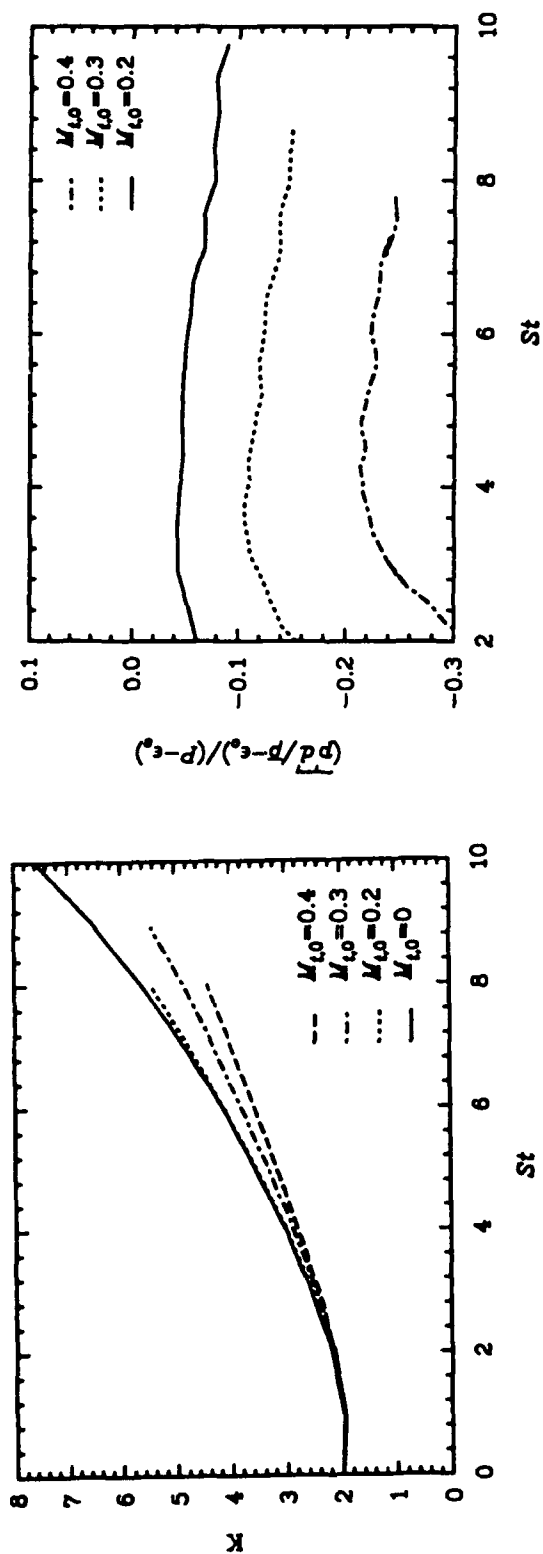


Figure B

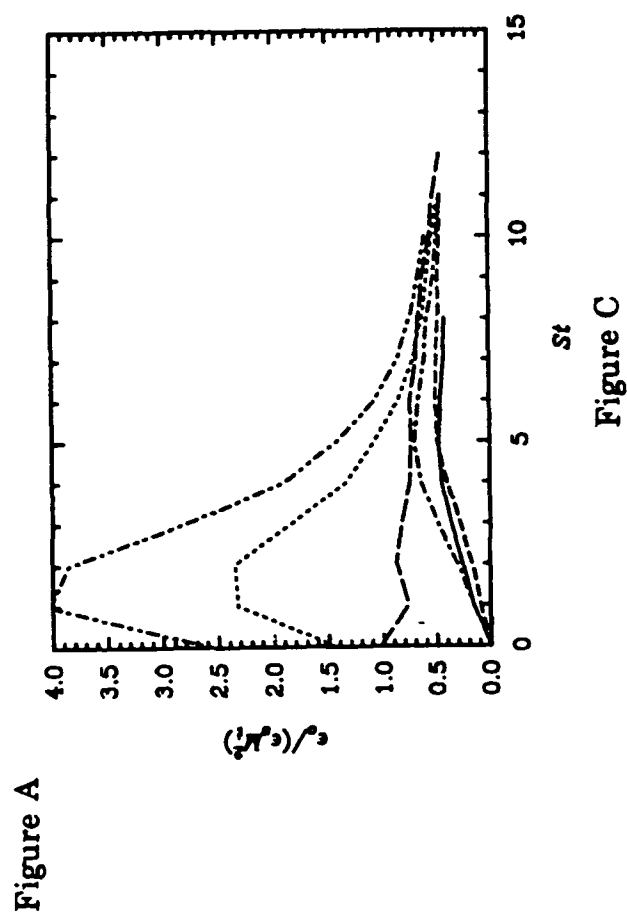


Figure C

Figure 3-5. Direct Simulation of Compressible Homogeneous Shear Flow

3-5 Direct Simulation of Compressible Homogeneous Shear Flow

Objective. To increase the physical understanding of the effects of compressibility on flow turbulence so that these effects can be modeled in flow computations.

Approach. Homogeneous compressible turbulence was considered wherein a linear mean velocity field sustains the random turbulence field. A spectral collocation method, along with a third-order Runge-Kutta time advancement, was used to perform direct numerical simulations (DNS), which are highly resolved in space and time. The resulting database was analyzed for statistical and structural features of the flow.

Accomplishments. Figure A shows the evolution of turbulent kinetic energy, K , as a function of time, t , nondimensionalized by the shear rate, S , for several values of $M_{t,0}$, the Mach number of the turbulent velocity fluctuations. The figure shows that the level of turbulent kinetic energy decreases with increasing values of initial turbulent Mach number, $M_{t,0}$. Thus, compressibility decreases the growth rate of the turbulence intensities. The exact equation for the evolution of turbulent kinetic energy in homogeneous flows is $d(\rho K) / dt = \rho P - \rho \epsilon_s - \rho \epsilon_c + p'd'$, where the production, ρP , and solenoidal dissipation, ϵ_s , are supplemented by two compressibility terms: compressible dissipation, $\rho \epsilon_c$, and pressure-dilatation, $p'd'$. Figure B shows that these compressibility terms alter the balance between production and dissipation by as much as 25% for the case with $M_{t,0} = 0.4$, suggesting that incompressible turbulence models are inappropriate. Physically, the augmented dissipation that is due to compressibility and the transfer of energy from the velocity field to the pressure field via the pressure-dilatation term contribute to the reduced growth of K . A previous theoretical study had shown that the compressible dissipation obeys the scaling $\epsilon_s/\epsilon_c = M_{t,0}^2$. Figure C shows that for a variety of DNS cases, the

ratio $\epsilon_c/(\epsilon_s M_{t,0}^2)$ approaches an equilibrium value of approximately 0.5 for large St .

Significance. Simulations of homogeneous shear flow show that the growth of turbulent kinetic energy decreases with increasing Mach number - a phenomenon that is similar to the experimentally observed reduction of turbulent intensities in the supersonic shear layer. The numerically generated databases have exhibited great potential for developing models for terms (e.g., the compressible dissipation) important in high-speed flows.

Status/Plans. Further analysis of the database will be carried out to improve the understanding of compressibility effects and augment our present turbulence modeling capabilities.

Sutanu Sarkar
ICASE
Langley Research Center
(804) 864-2194

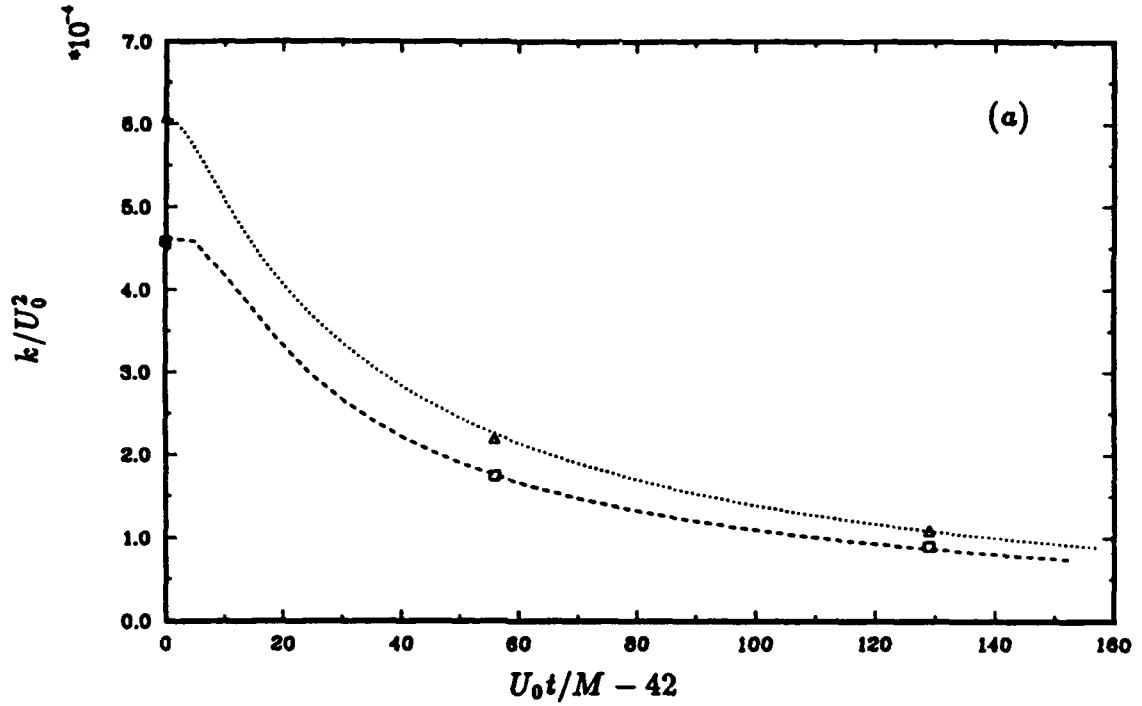


FIGURE 1 . Time development of resolved-scale turbulence kinetic energy from LES of isotropic turbulence. \square , filtered data of Comte-Bellot and Corrsin (32^3); ----, LES (32^3); \triangle , filtered data of Comte-Bellot and Corrsin (64^3); , LES (64^3).

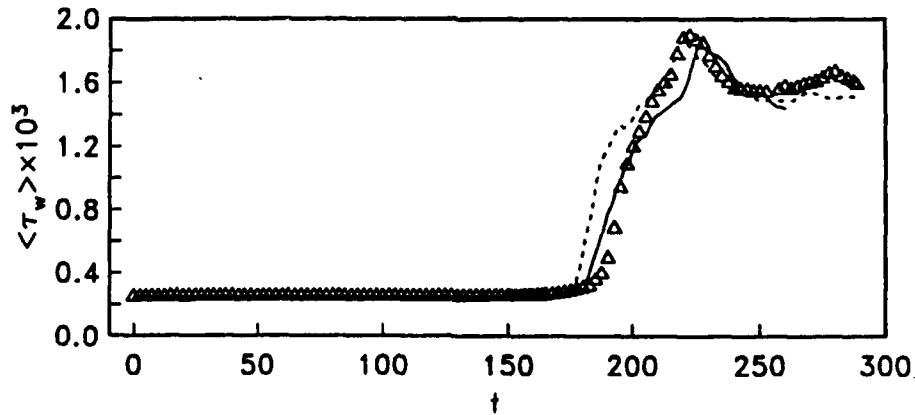


FIGURE 2. Time development of the plane-averaged wall shear stress $\langle \tau_w \rangle$ in $Re = 8000$ transitional channel flow. \triangle DNS (Zang *et al.* 1990); — present results; LES (Piomelli & Zang 1990b).

Figure 3-6. Dynamic Subgrid Scale Modeling and the New LES Program

3-6 Dynamic Subgrid Scale Modeling and the New LES Program

Objective. Subgrid scale models used in large eddy simulations of turbulent flows have had several drawbacks: the inability to correctly represent, with a single universal constant, different turbulent fields in rotating or sheared flows, the requiring of ad hoc damping functions near solid walls, and the requiring of ad hoc intermittency functions to predict the transition from laminar to turbulent flow. A new eddy viscosity model has been developed that alleviates many of these drawbacks. At present, our objective is to evaluate this model in a variety of incompressible, compressible, transitional, and fully developed turbulent flows.

Approach. In large eddy simulations (LES) the large-scale field is directly computed and the effects of small scales are modeled. In the dynamic mode approach, the coefficient of the subgrid scale eddy viscosity is a function of space and time, and hence varies in the different flows and flow regimes. The coefficient is computed dynamically during the computation rather than input a priori. This model was used in large eddy simulations of transitional and turbulent channel flow with heat transfer and in compressible homogeneous turbulence.

Accomplishments. The concept of dynamic modeling was used to derive expressions of the subgrid scale eddy viscosity and turbulent Prandtl number. The results were in good agreement with the experimental data and direct numerical simulations, and were better than those of LES using conventional models that include ad hoc intermittence and damping functions. The model has performed remarkably well without any adjustments in very different flow situations.

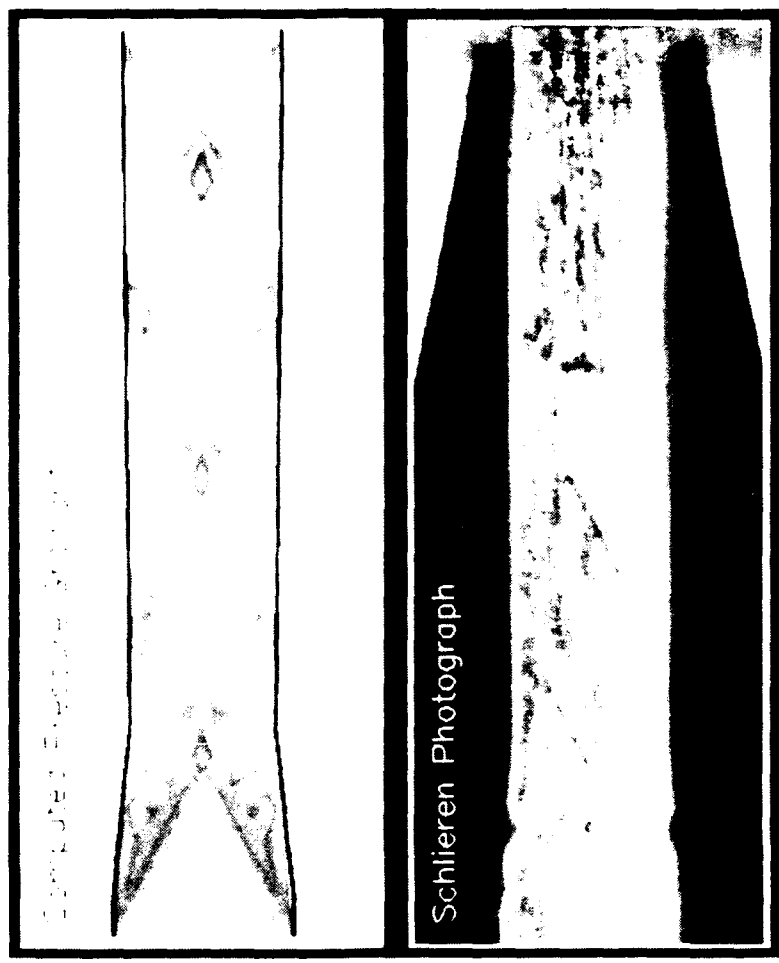
Significance. The idea of dynamic modeling is an altogether new approach in turbulence modeling. It has led to physically sound models for momentum and energy transport.

Its inherent versatility should facilitate its use in applied CFD.

Status/Plans. The dynamic model will be applied to complex flow configurations. These include flow over a cylinder, backward facing step, separated flat plate boundary layer, compressible flow transition on a flat plate, and flow over a concave wall.

Parviz Moin
Center for Turbulence Research
Ames Research Center and Stanford University
(415) 723-9713 or 604-5127

Comparison of Mach 2.5 Wind Tunnel Pressure Distributions
 and Schlieren Photographs



Comparison of Mach 2.5 Wind Tunnel Pressure Distributions
 and Schlieren Photographs

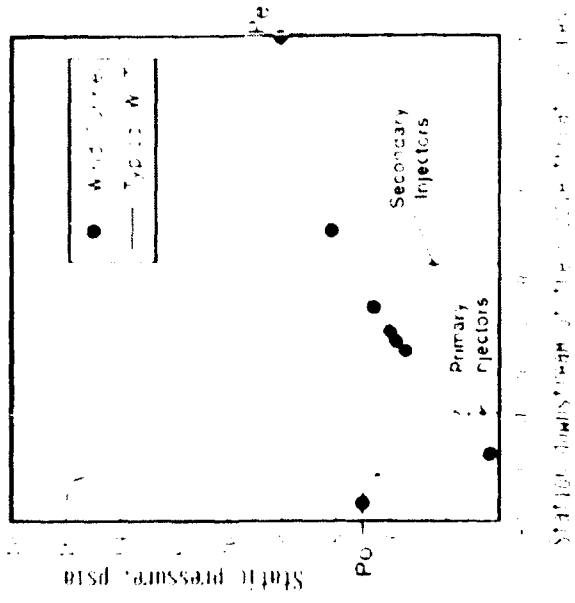


Figure 3-7. Efficient Supersonic Wind Tunnel Drive System for Transition Research at Mach 2.5

3-7 Efficient Supersonic Wind Tunnel Drive System for Transition Research at Mach 2.5

Objective. To validate design principles for a new generation of low-cost Laminar Flow Supersonic Wind Tunnels (LFSWTs) using "Quiet" technology. The LFSWT is essential for boundary layer receptivity studies at high-speed civil transport (HSCT) Mach numbers.

Approach. A 1/8 scale Proof of Concept (PoC) model of the LFSWT was built to research unknowns for the full-scale design. The primary purpose of PoC was to establish that the Fluid Mechanics Laboratory (FML) indraft compressor could support the desired LFSWT test envelope of $M = 2.5$ @ $Re = 1.3$ million per foot. The low compression ratio ($\sim 1.8:1$) of the compressor precluded the use of any conventional tunnel drive system. For the past 19 months, there has been an experimental research effort, supported by CFD studies, to develop a unique drive system for the LFSWT. In parallel, innovative design techniques for the "Quiet" settling chamber and supersonic nozzle are being investigated.

Accomplishments. In February 1991, we achieved $M = 2.5$ in the PoC test section over the desired Re range. To achieve the lowest Re of 1 million per foot, a stagnation pressure (P_o) of 5 psia, is required. A P_o of 5 is less than the exit pressure (P_e) of 8 psia, which makes the compression ratio across the test section 0.625:1, which is a major and unique accomplishment. By comparison, a conventional supersonic tunnel requires a compression ratio greater than 2:1 to run and an overpressure to start. The PoC has an advantage in that the starting and running test conditions are the same. Operation at such a low compression ratio is achieved through the use of a supersonic diffuser (optimized by CFD support) at the end of the test section and dual ambient injector system. The primary injector is designed for an $M = 2.4$ exit flow and the second-

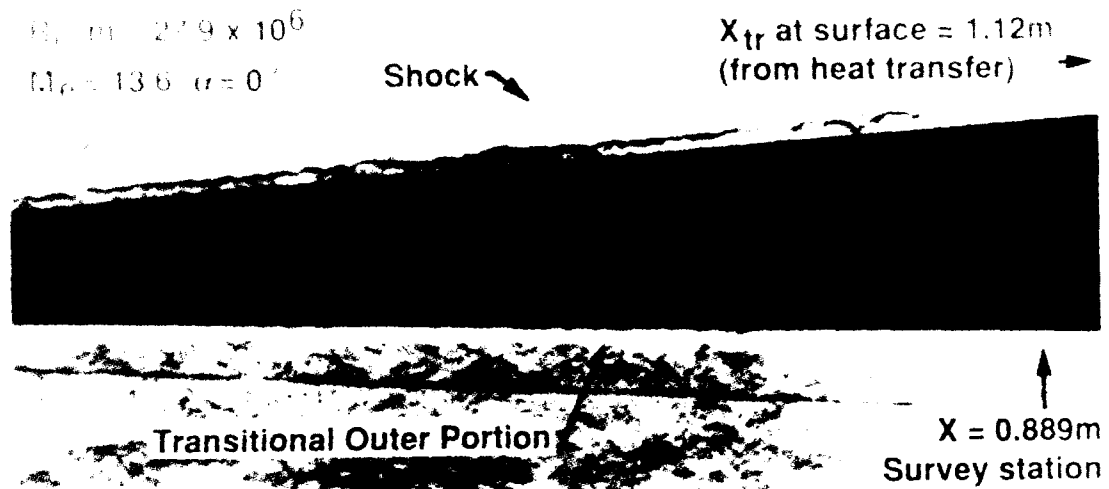
ary for $M = 2.0$. The injectors pull conditioned air through the test section. The ratio of mass flow through the primary injector over that of the test section is an unprecedented 9.17:1.

Significance. This low-budget project has demonstrated that we can operate a supersonic wind tunnel with a nonspecialized indraft compressor. We now have the technology to design a drive system for the full-scale LFSWT. The LFSWT will enhance supersonic nozzle and transition research progress within NASA while impacting HSCT.

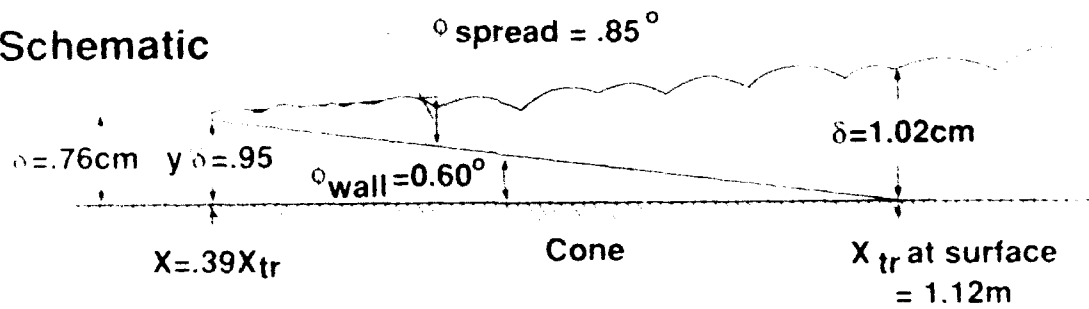
Status/Plans. The LFSWT drive system is being designed, and the LFSWT design principles are being studied for the settling chamber and supersonic nozzle, which are critical to establishing quiet flow.

J. Laub, S. Wolf, L. King, D. Reda
Fluid Dynamics Research Branch
Ames Research Center
(415) 604-4136

Fischer-Weinstein(1972) Experiment



Schematic



Direct Numerical Simulation

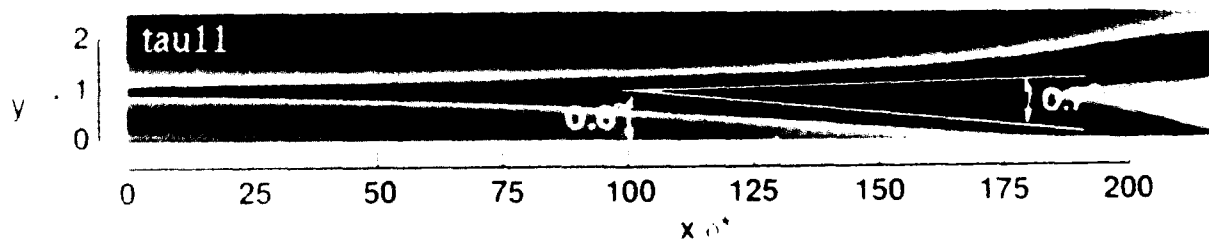


Figure 3-8. Precursor Effect in Hypersonic Transition

3-8 Numerical Simulation of Laminar Breakdown in Supersonic Transition

Objective. To explain theoretically, the “rope-like structures” and the “precursor transition effect” that have been observed in supersonic transition experiments since the 1960s. The rope-like structures refer to the braided patterns that are visible near the boundary layer edge in schlieren photographs. The precursor transition effect refers to the origination of transitional disturbances near the boundary layer edge a considerable distance upstream of the first detection of transition by surface measurements.

Approach. The approach was to conduct high-resolution direct numerical simulations (DNS) of laminar breakdown in supersonic boundary layers on cylinders and cones, utilizing linear stability theory (LST) and secondary instability theory (SIT) to select cases that represent the most likely paths to transition.

Accomplishments. Two high-resolution temporal DNS of the strongly nonlinear, laminar breakdown stage of supersonic transition to turbulence were conducted: for Mach 4.5 flow past a cylinder and for Mach 6.8 flow past a cone. The top frame of the accompanying figure shows a schlieren photograph that is typical of experimental results for transition on a cone in hypersonic flow. The essential features are displayed in the cartoon in the middle of the figure. The spatially reconstructed turbulence intensities extracted from the DNS of the Mach 6.8 cone case (bottom frame) display these key features. In particular, the “precursor transition effect” has been captured, with even the spreading angles of the disturbance regions in good agreement with the experimental range: between 0.5° and 1° . Moreover, numerical schlieren flow-field visualizations from the DNS display “rope-like” structures are remarkably similar to those that have been observed experimentally.

Significance. A comparison of LST, SIT, and DNS results for the spreading angle of the disturbances indicates that the spreading rate cannot be attributed to linear instability alone (as has long been believed), nor even to secondary instability, but is, indeed, a strongly nonlinear effect.

Status/Plans. The numerical databases already generated will be analyzed in detail, with particular emphasis given to their implications for transition modeling.

C.D. Pruett
Fluid Mechanics Division
Langley Research Center
(804) 864-6788

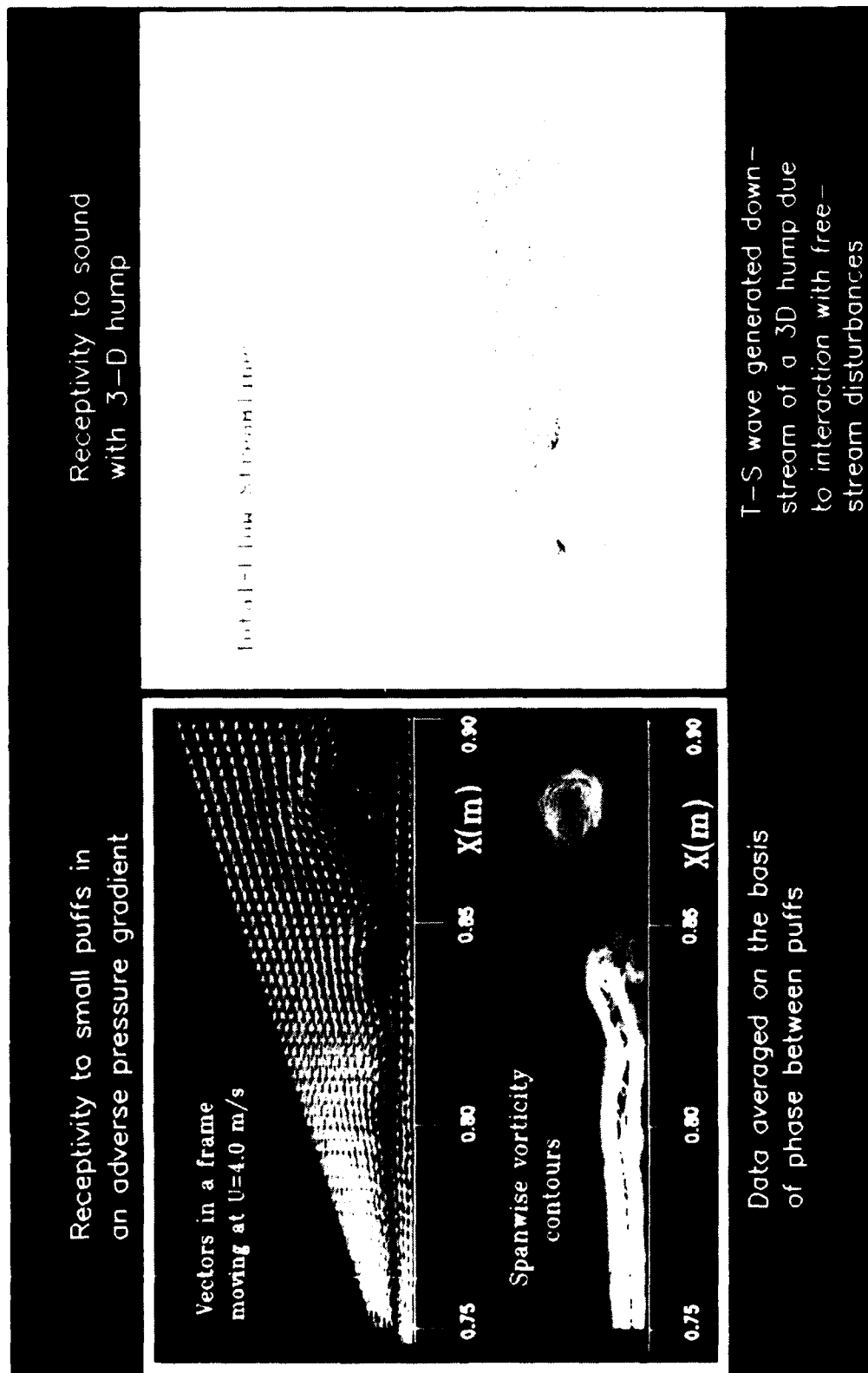


Figure 3-9. Receptivity of Low-Speed Boundary Layers

3-9 Receptivity of Low-Speed Boundary Layers

Objective. To develop a research program to understand the essential issues underlying the receptivity process and to use this knowledge in developing new approaches to transition prediction. Transition can be considered a three-stage process consisting of receptivity, instability, and breakdown to turbulence. While most previous work has been concerned with the issue of flow stability, receptivity is now considered a critical first-order parameter.

Approach. A combined experimental/computational effort is under way to develop a receptivity database. Following previous work on receptivity to suction surfaces (see FY 1990 Research Accomplishments), two new experiments are now under way. One experiment concerns the transition of a laminar, low-speed boundary layer in an adverse pressure gradient. The disturbance created by a puff periodically introduced through a small hole in the test surface is tracked with an automated data acquisition system using phase-lock-averaging software. Pattern formation in the boundary layer – expressed as velocity vectors and vorticity contours – is examined using video animations. The second experiment concerns the receptivity to a roughness element and follows a theoretical treatment using triple deck theory. This experiment will study the nature of roughness-induced receptivity resulting from freestream acoustic disturbances.

Accomplishments. The response of a low-speed boundary layer to a periodic jet at one phase interval is shown in the left panel of the accompanying figure. The minimum local boundary layer thickness is approximately 6 mm. Animated flow sequences clearly show the generation of vortical flow structures and their downstream convection. The second experiment is currently being designed based on results of the computational visualization. The right panel in the figure shows the

analytical streamlines induced by the “roughness element” and the down wind extent of this disturbance.

Significance. This integrated computational/experimental project is designed to understand the essential features of boundary layer receptivity. By collecting a detailed database concerning the receptivity process, enough knowledge will be gained to incorporate these effects in transition prediction schemes. The final result will be amplitude- and scale-dependent criteria for transition.

Status/Plans. Current work is focused on low-speed, incompressible boundary layers. Further receptivity studies on suction holes are also planned. Once the basic physical processes are understood, emphasis will shift to high-speed flows. A special interest is in receptivity of supersonic boundary layer ($1.5 \leq M \leq 2.5$) to suction surfaces as are envisioned for the next-generation supersonic transport.

S. Davis, J. Watmuff, M. Tadjfa,
D. Reda
Fluid Dynamics Research Branch
Ames Research Center
(415) 604-4197

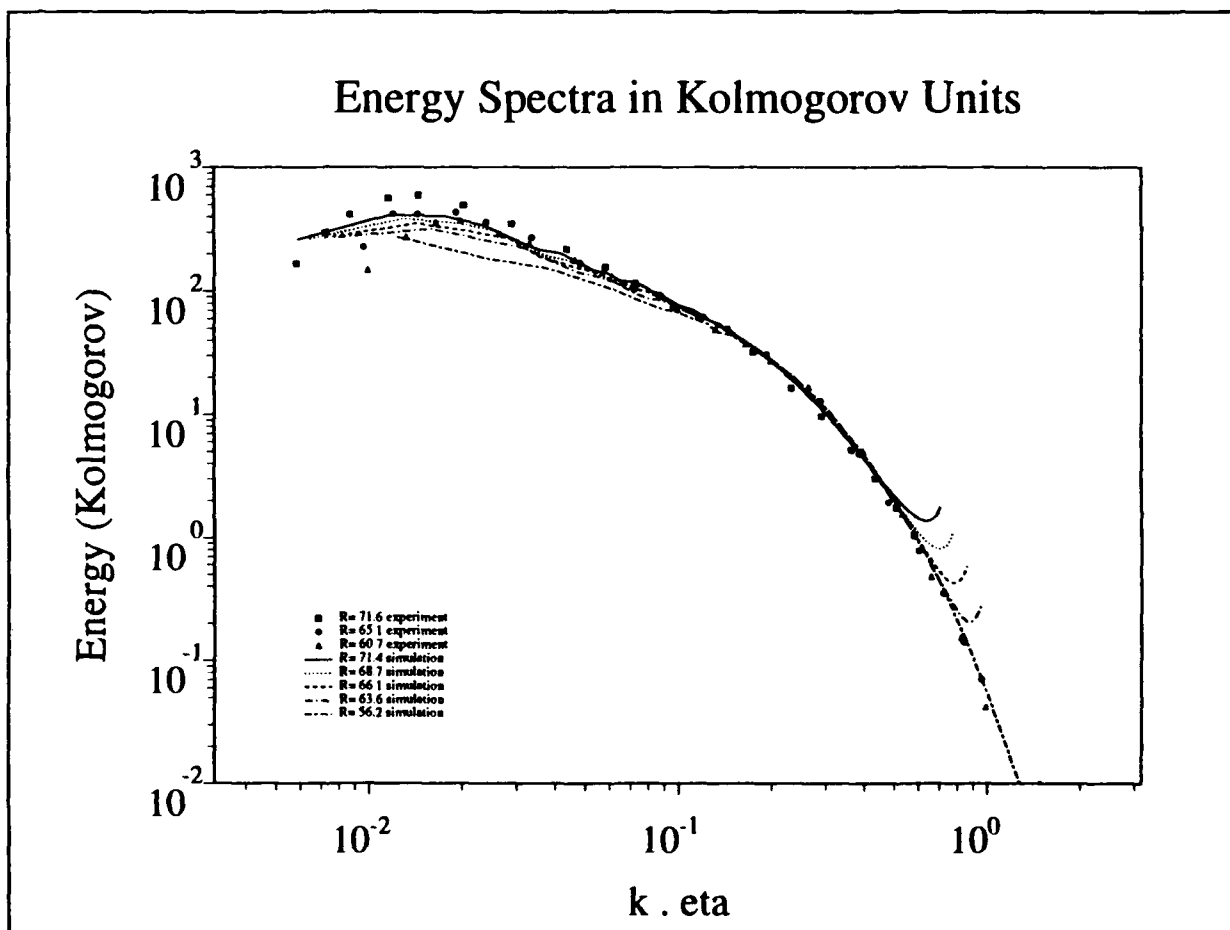


Figure 3-10. Simulation of Homogeneous Turbulence on the Intel i860 Hypercube

3-10 Simulation of Homogeneous Turbulence on the Intel i860 Hypercube

Objective. To develop programming and compiler techniques to exploit highly parallel computers for turbulence research.

Approach. The three-phase approach was first to construct a highly optimizing compiler for the i860 microprocessor, then to develop and implement efficient inter-processor communication procedures, and finally to apply these to a program and compile an existing homogeneous turbulence algorithm.

Accomplishments. First, the vectoral compiler was ported to the i860 microprocessor and the hypercube multiprocessor environment. A number of new compiler techniques were developed to exploit the high level of internal concurrency available in the i860. Techniques were also developed to alleviate the problem of inadequate raw memory bandwidth. The homogeneous turbulence code of Rogallo was then ported from the Cray Y-MP to the 128 processor NAS iPSC/860 Gamma Prototype. A highly efficient implementation of interprocessor communication was added to the code. A wall-clock speed of 1.64 Gigafllops was obtained for the largest mesh size (256^3). Excellent agreement with experimental results was obtained (see accompanying figure) at Reynolds numbers obtainable only at great expense on Cray computers. The code has also been ported to the 528 processor Caltech Delta Machine, which has a mesh rather than a hypercube architecture.

Significance. It is recognized in the industry that highly parallel, distributed-memory computers are the future of supercomputing, and it is therefore crucial to begin learning how to implement our most computationally intensive applications on these machines. This project has shown that a typical turbulence simulation code can run on such a machine at

a very high-performance level; in the case of 128 40MHz i860's, at a speed exceeding that of 10 Y-MP processors. Within the next 2-years, machines of the iPSC/860 type will have performance in the 50-Gigaflop range, far exceeding that of current supercomputers.

Status/Plans. We will continue to refine the i860 Vectoral compiler, since this processor and its successors will be used in important new multiprocessors, port other turbulence codes to the i860 machines to be used as true production supercomputers, and port the compiler and turbulence codes to other new multiprocessor computers, such as the Stanford DASH machine.

Alan Wray
Computational Fluid Dynamics Branch
NASA Ames Research Center
(415) 604-6066

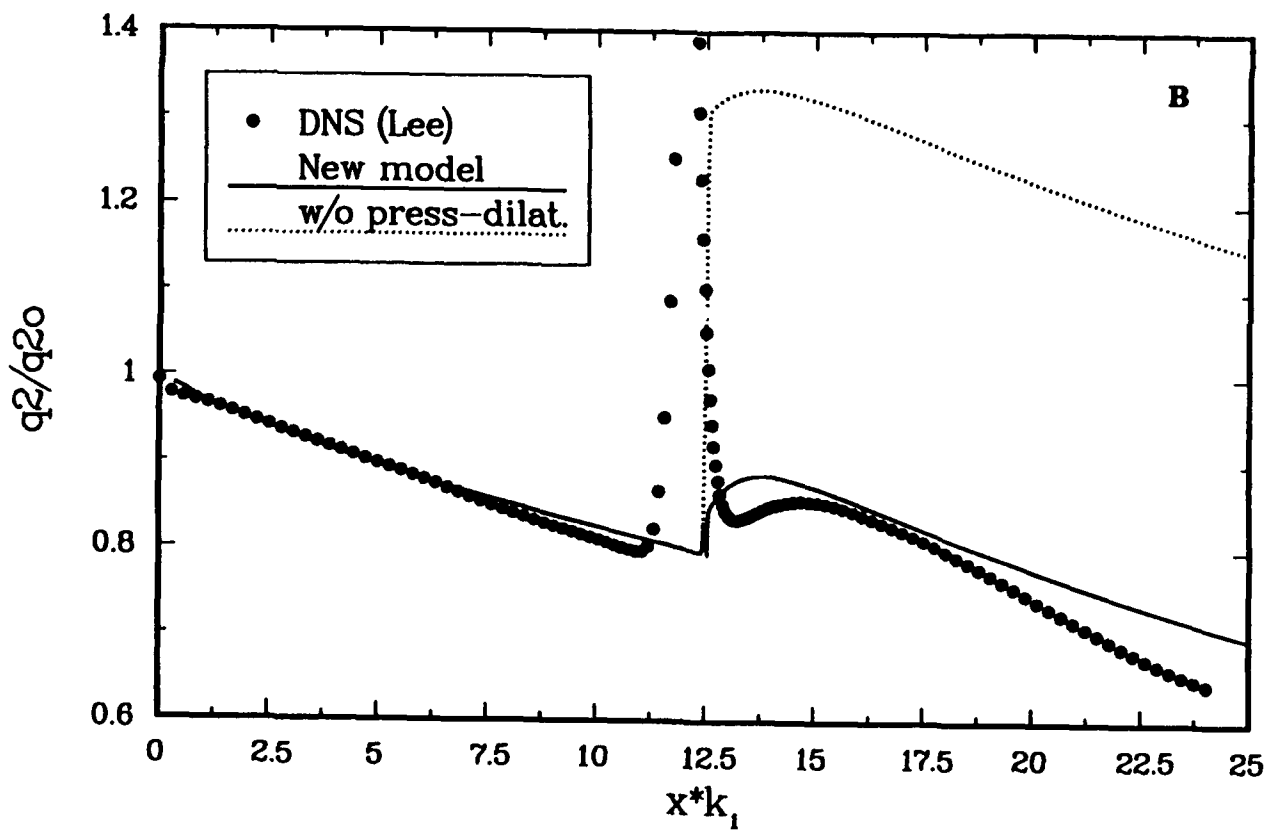
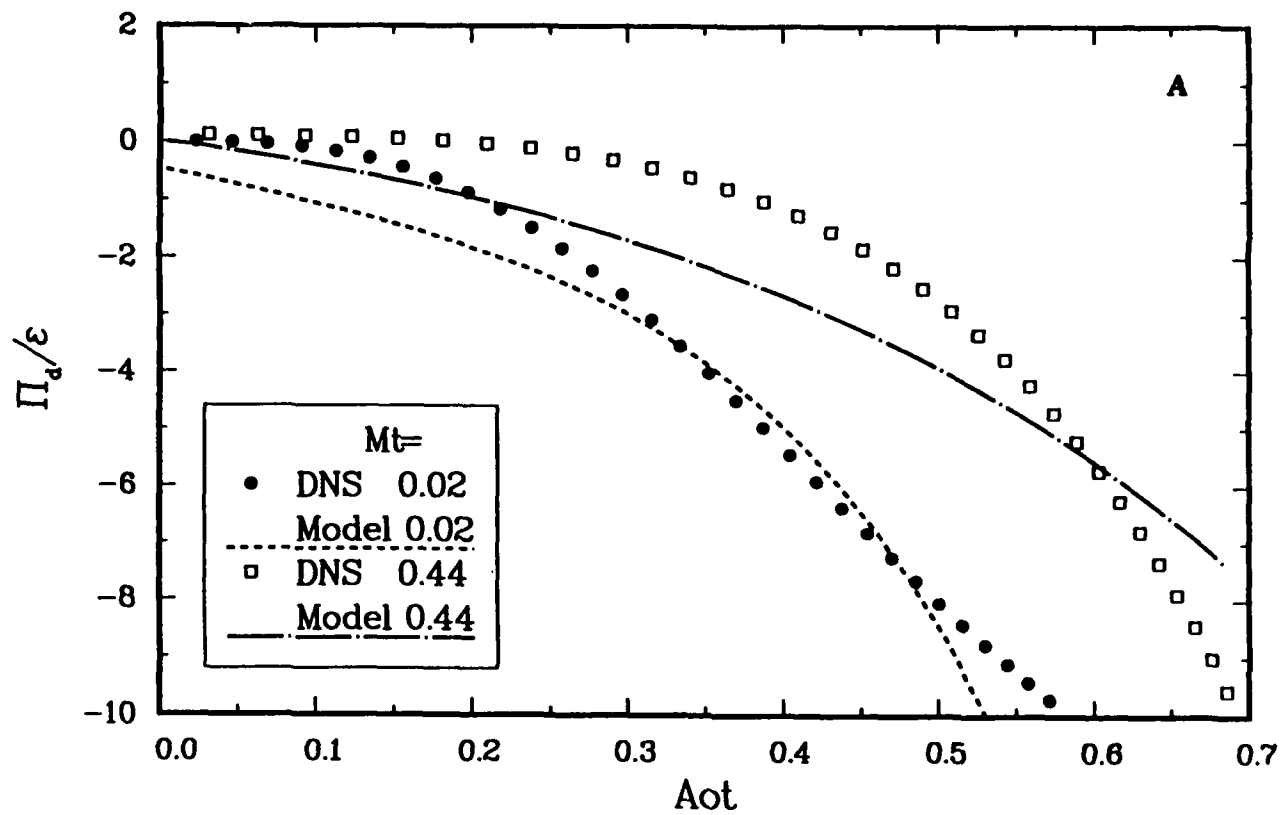


Figure 3-11. (A) Pressure Dilatation During 1D Rapid Compression (B) Response of Turbulent Energy to the Normal Shock

3-11 Compressible Turbulence: Modeling Rapid Compression

Objective. To develop new, and improve the old, models for compressible turbulent flows. A specific goal reported here is investigation of the rapid compression effect on turbulence. This effect is present in flows with turbulence/shock interactions.

Approach. In real flows, the individual mechanisms and processes of turbulence dynamics cannot be studied in isolation. Therefore, the basis for the investigation of the rapid compression effect on turbulence has been the direct numerical simulations (DNS) of compression of *homogeneous* turbulence (Coleman and Mansour, 1991). The study led to a development of new turbulence closure models that represent the physics of rapid compression.

Accomplishments. The study of the DNS of compressed turbulence yielded the following important findings: it was established that when nearly incompressible turbulence (with r.m.s. Mach numbers $M_t \ll 1$) is rapidly compressed in one direction (1D), unexpectedly high levels of negative pressure-dilatation correlation are generated. The pressure-dilatation term (Π_d) appears in the turbulence kinetic energy and its magnitude during the 1D compression can become by $O(10)$ larger than the total dissipation (ϵ_t); hence, Π_d can represent a significant loss of turbulent kinetic energy (to pressure fluctuations). The striking aspect of this rapid compression mechanism is that it is most effective when $M_t \ll 1$, and that it is inefficient when the compression is more isotropic, i.e., acting in all three directions. All these aspects have been included in the new model for pressure dilatation. The model-DNS comparison of the ratio Π_d/ϵ_t for two values of $M_t = 0.02$ and 0.44 are shown in Figure A. Here, the abscissa A_{ot} represents the compression time with $1/(1-A_{ot})$ being the total compression. The difference in kinetic energy q_2 -levels (solely due to the pressure dilatation effect) is also predicted by the model.

Significance. In the flows of practical interest, the condition of directional rapid compression arises in flow configurations where turbulence passes through a shock. A typical example of this kind is a compression corner flow. The discussed mechanisms of the rapid compression effect on the pressure dilatation has so far not been considered in turbulence modeling. Its significance is apparent in a real flow configuration represented by a uniform turbulent flow passing through a normal shock wave and shown in Figure B. Here, the DNS data (Lee 1991) of the turbulent kinetic energy (q_2) response to the shock passage are compared with a turbulence model results, with and without the rapid contribution to the pressure-dilatation term; the abscissa xk_1 represents the distance normal to the shock.

Status/Plans. The new model is being tested in the compression corner flow configuration; rapid compression theory has been developed; and modeling of turbulence subjected to rapid expansion is also being studied.

Otto Zeman
Center for Turbulence Research
Stanford U/NASA Ames Research Center
(415) 723-9596; (415) 604-4726

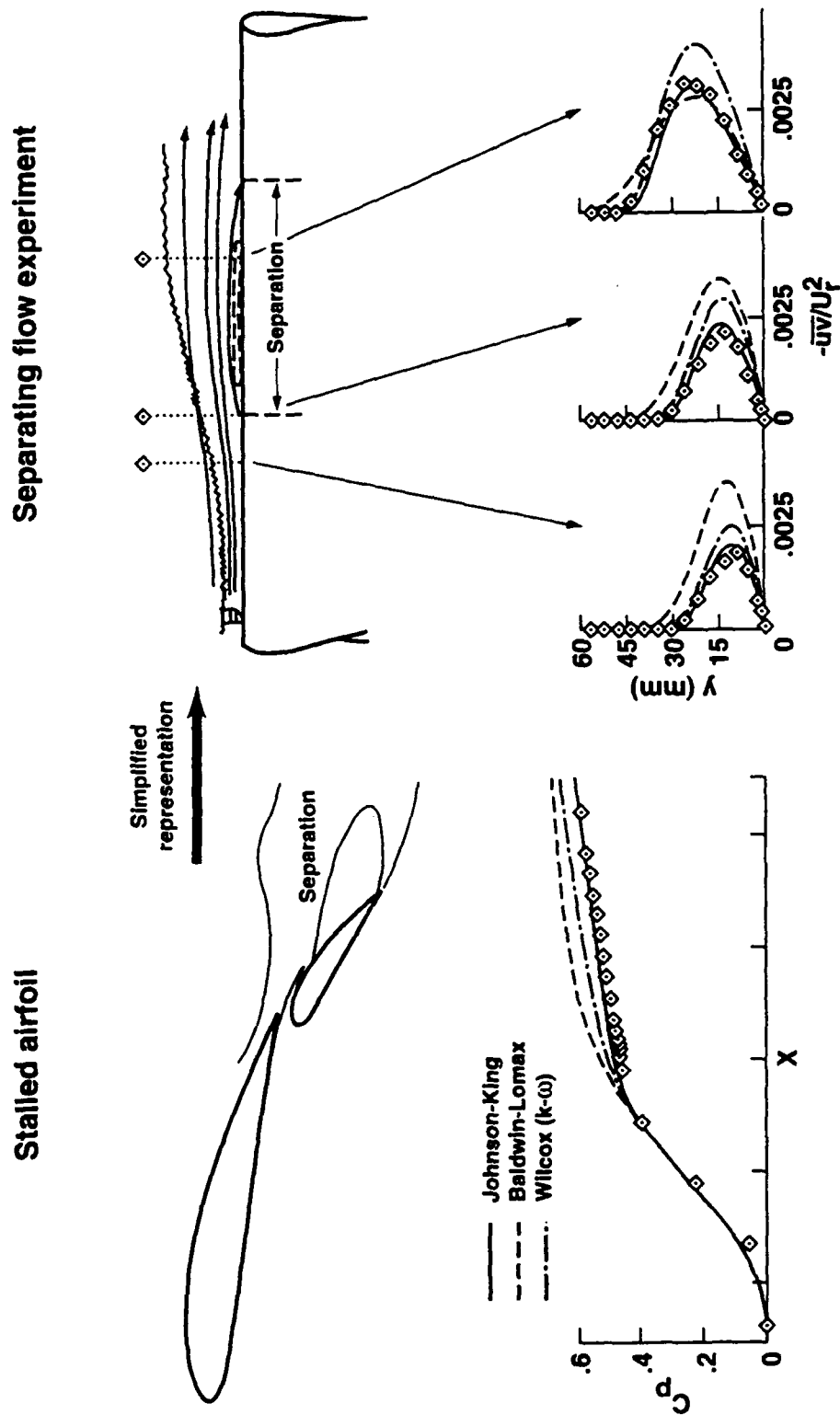


Figure 3-12. An Experiment to Guide Turbulence Modeling for Separated Flows

3-12 Separating Boundary Layer Experiment for Turbulence Modeling

Objective. To evaluate turbulence models used in the prediction of separating flows in such applications as high lift airfoils.

Approach. A computational study was undertaken to numerically calculate two cases of adverse pressure gradient: one with flow separation and the other attached. Solutions to the incompressible Navier-Stokes equations were obtained with INS3D and various different turbulence models. Comparisons between numerical results and previously measured velocities and turbulent Reynolds stresses were performed to determine which is the most appropriate model to use in adverse pressure gradients

Accomplishments. Various turbulence models such as the Baldwin-Lomax model, the Johnson-King model, the Wilcox(k-omega) model, and the Baldwin-Barth model were incorporated into INS3D. Solutions were obtained with each of the models for both the separating case and the attached case of adverse pressure gradient. These solutions revealed that only those models that accurately predicted the Reynolds shear stress would accurately predict the pressure distribution. The numerical results as well as the experimental measurements of velocities and Reynolds stresses were reported at the June 1991 AIAA meeting.

Significance. Accuracy of flow calculations involving strong adverse pressure gradient is inextricably linked to the accuracy of the turbulence model that is employed. Computational Fluid Dynamics is being significantly advanced by the advent of the Johnson-King turbulence model, which was developed at NASA Ames Research Center and has been further validated in this study. Boeing Commercial Aircraft Company is actively and successfully using the Johnson-King model in the design of future aircraft.

Status/Plans. The experimental database will be distributed to other researchers in the turbulence modeling community for use in model development.

David M. Driver, Florian Menter
Experimental Fluid Dynamics Branch
Ames Research Center
(415) 604-5396

Chapter 4

Computational Methods and Validation

The objective of the Computational Methods and Validation Program is to develop and apply advanced analysis and computational methods for solving complex, fluid dynamics problems and to perform detailed, benchmark experiments using redundant facilities and instrumentation to produce high-quality archival data sets to which computational fluid dynamics (CFD) solutions can be compared. Areas of interest include modeling turbulence and transition and computing complex flows (steady and unsteady, inviscid and viscous) over two- and three-dimensional geometries ranging in speed from zero to hypersonic and including such effects as mass injection and withdrawal. Additional objectives are to (1) demonstrate proof-of-concept computations for pioneering applications, (2) disseminate validated computer codes to the aerospace community and provide maintenance and consultation on their use, (3) develop innovative techniques for scientific visualization of flow-field solutions, and (4) provide an experimental database that is taken in the form and detail consistent with CFD modeling requirements and that has documented accuracy and limitations of the experimental data.

The Computational Methods Program is focused on the present and future technology needs of the aerospace community. These needs include (1) developing faster and more efficient numerical algorithms to facilitate solutions of the full Navier-Stokes equations by large-eddy, simulations/small-scale turbulence modeling; (2) developing advanced geometric modeling and grid generation techniques for complex, three-dimensional configurations; (3) improving understanding of the effects of grid characteristics on solutions accuracy, convergence, and stability; (4) enhancing computational capabilities through development and use of advanced computer architectures and expert systems concepts; and (5) developing improved methods for numerical simulation of aerothermodynamic flow phenomena associated with hypersonic cruise and maneuver vehicles, including real-gas chemistry.

Experiments are designed for comparison with numerical CFD results in order to (1) understand flow physics, (2) develop physical models for CFD codes, (3) calibrate CFD codes, and (4) validate CFD codes. The experiments range in speed from subsonic to hypersonic and include a variety of configurations including generic, fighter/attack, subsonic transport, rotorcraft, ASTOVL, and propulsion systems. Work continues in developing high-quality data bases for several classes of flows, including (1) high- and low-aspect ratio wings in subsonic and transonic flows; (2) simple 3-D turbulent flows, including time histories; (3) flow fields about aircraft components; (4) propulsive lift flow interactions in ground effect; and (5) unsteady flow interaction in rotor flow fields.

Program Manager: Pamela F. Richardson
OAST/RF
Washington, DC 20546
(202) 453-9857

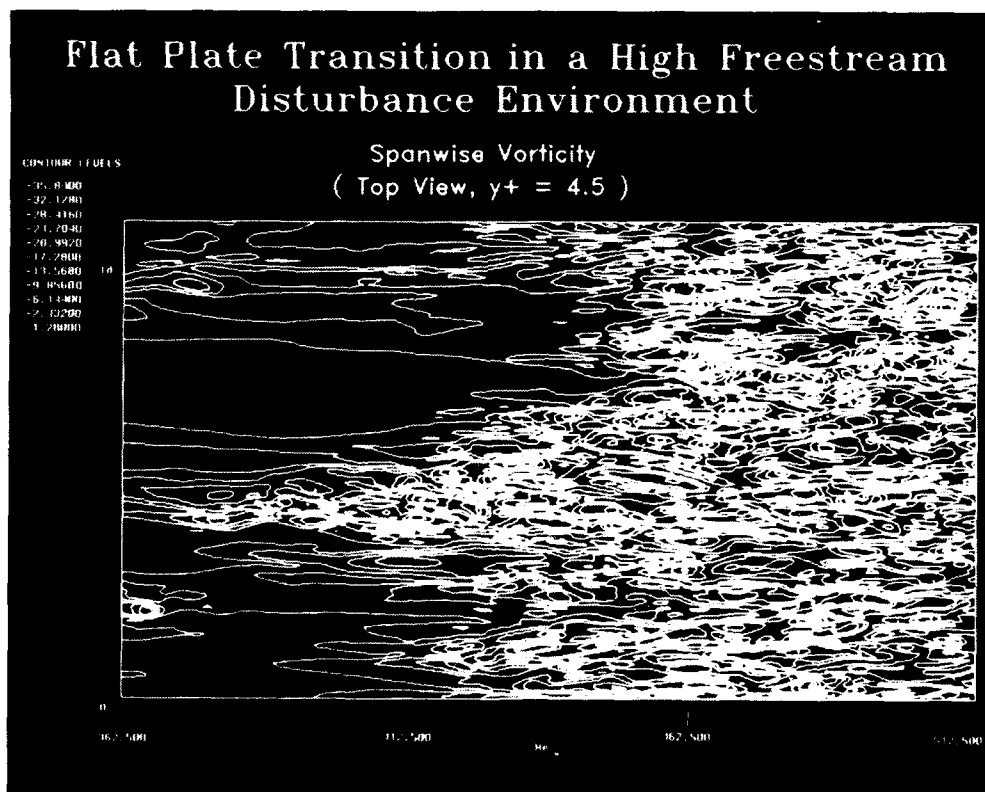
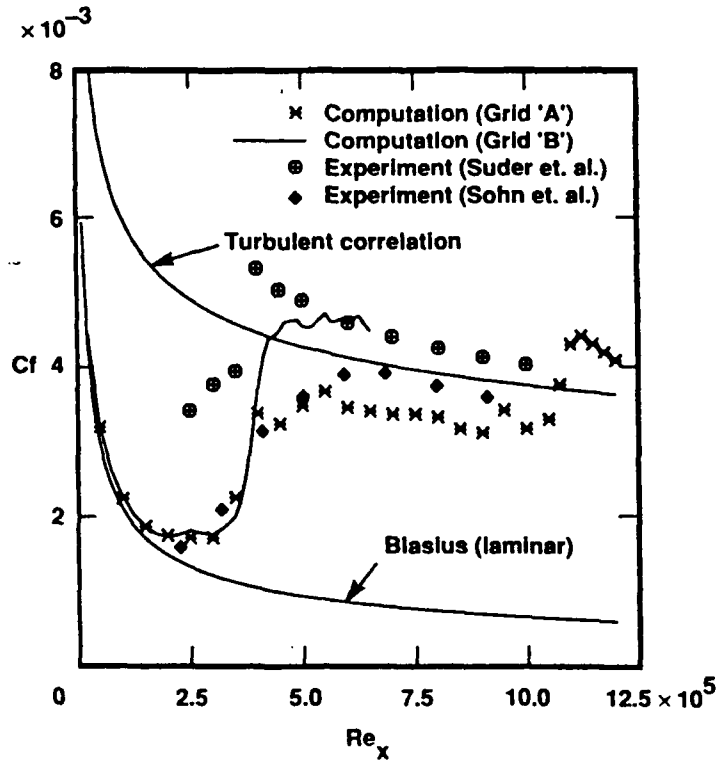


Figure 4-1. Direct Numerical Simulation of Transition and Turbulence in a Spatially Evolving Boundary Layer

4-1 Direct Numerical Simulation of Transition and Turbulence in a Spatially Evolving Boundary Layer

Objective. To develop a high-order-accurate, finite-difference method to compute compressible, transitional, and turbulent flow and to demonstrate the capability of the method by computing transition to turbulence on a flat plate. A study of the physics of transition and the creation of a data base for turbulence and transition modeling are an integral part of this effort.

Approach. The unsteady, compressible formulation of the Navier-Stokes equations are solved using a high-order-accurate, upwind-biased, finite-difference method. This method is an extension of an earlier high-order-accurate method developed to compute incompressible, turbulent flows. The new code that has been developed uses a zonal methodology to efficiently process the number of grid points used for the computation.

Accomplishments. The high-order-accurate method was successfully used to compute transition to turbulence on a flat plate in a high freestream disturbance environment. The numerical results agree qualitatively with the available experimental data. Flow visualization of the computed flow indicated that the transition region was characterized by detached shear layers and pairs of counter-rotating streamwise vortices. The results indicate that the essential features of the transition process have been captured in the computation. Figure A shows instantaneous spanwise vorticity contours just above the flat plate and Figure B shows the computed skin friction along the plate compared with experimental data.

Significance. This computation is the first "transition to turbulence" simulation. It indicates that computing transition to turbulence in certain spatially evolving boundary layers to a reasonable degree of accuracy is possible on currently available supercomputers (provided there is judicious use of zonal methods

and high-order-accurate schemes). The finite-difference method developed in this study can be extended in a straightforward manner to curvilinear grids and thus enable direct simulations of transitional and turbulent flow over general geometries.

Status/Plans. The method has been extended to curvilinear grids. A new code to compute compressible, turbulent/transitional flow over a turbine airfoil is being developed.

Man Mohan Rai
Fluid Dynamics Division
Ames Research Center
(415) 604-4499

INRIA II CASE 3.4

Mach Contours



Detail of Separation Zone

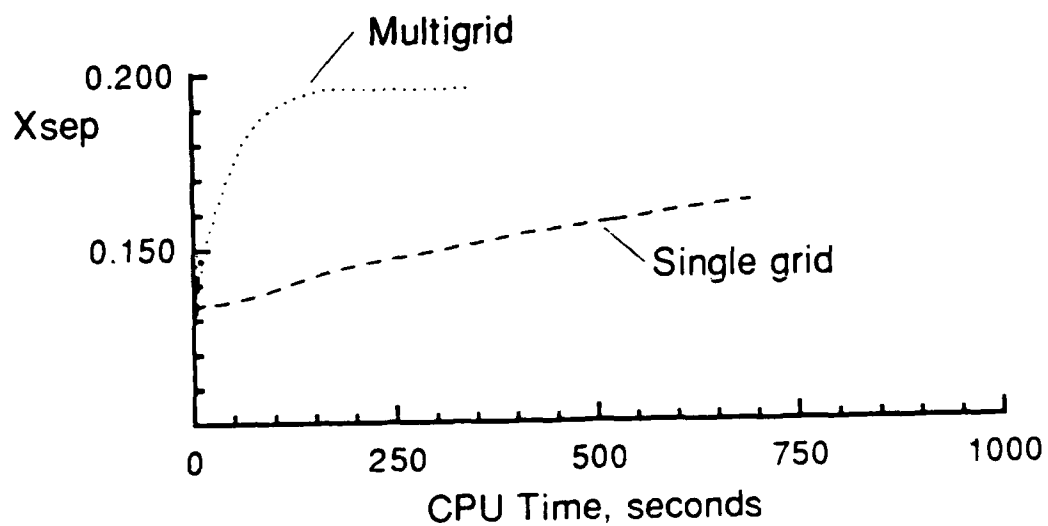


Figure 4-2. Multigrid Algorithm for Hypersonic Viscous Flows

4-2 Multigrid Algorithm for Hypersonic Viscous Flows

Objective. To develop a multigrid algorithm for the efficient solution of viscous flows at hypersonic Mach numbers.

Approach. A Full Approximation Scheme (FAS) multigrid was developed based on an implicit upwind-biased algorithm for the compressible Navier-Stokes equations. The algorithm uses upwind differencing for the convective and pressure terms and central differencing for the viscous terms. The implicit equations were modified so that the primitive variables, instead of the conserved variables, were updated during the iteration. The time advancement and correction stages of the FAS algorithm were modified to maintain positivity of the thermodynamic variables, density and pressure. The FAS algorithm was modified to include multiple iterations on coarser meshes in order to speed up the upstream transfer of information through the subsonic part of the boundary layer.

Accomplishments. The convergence rates for a number of hypersonic strong-interaction viscous flows were improved with the multigrid scheme. The test cases were those of the second Institut National de Recherche en Informatique et en Automatique (INRIA) Workshop on Hypersonic Flows for Reentry Problems. An application to case 3.4, corresponding to a laminar strong-interaction flow over a compression ramp at a Mach number of 11.68, is shown in the accompanying figure. The Mach contours show the leading-edge shock and separation-induced shock at the compression; the enlarged view shows the separated flow in the region of the compression corner. The variation of separation extent with computer time is shown for the multigrid and single grid schemes. An order-of-magnitude improvement in efficiency occurs with the multigrid scheme.

Significance. The multigrid method, previously shown to be highly successful for subsonic and low supersonic flows, has been extended to viscous hypersonic flow. An order-of-magnitude increase in efficiency obtained with the scheme allowed grid refinement studies to be completed for all test cases of the INRIA code-validation workshop.

Status/Plans. Further applications of the algorithm are continuing, including blunt bodies and three-dimensional configurations.

James L. Thomas, David H. Rudy
Fluid Mechanics Division
Langley Research Center
(804) 864-2146

4-3 Unstructured and Adaptive Multigrid for the Three-Dimensional Euler Equations

Objective. To develop an accurate and efficient method for computing steady-state compressible flow about complex three-dimensional configurations.

Approach. The steady-state 3-D Euler equations are solved on an unstructured tetrahedral mesh by a Galerkin finite-element scheme. The flow variables are stored at the vertices of the mesh, and an edge-based data-structure is employed to minimize memory requirements. An unstructured multigrid technique is used to accelerate convergence to steady-state. This procedure operates on a sequence of non-nested coarse and fine meshes, and the patterns for interpolation between the various meshes of the sequence are determined in a preprocessing step, using an efficient search algorithm. This strategy is combined with an adaptive meshing approach, where new, finer meshes are automatically generated as the solution evolves.

Accomplishments. The present methodology is capable of providing accurate and efficient solutions for steady-state inviscid 3-D flows without incurring large memory overheads. The figure illustrates the computation of transonic flow over an ONERA M6 wing. A multigrid sequence of four meshes has been employed, with the last two being adaptive meshes. The final solution was obtained in 100 multigrid cycles on the finest grid, which required 35 minutes of CPU time on a single Cray Y-MP processor, and 22 million words of memory.

Significance. The ability to accurately and efficiently predict compressible flows over complex 3-D geometries is of particular importance to the aircraft industry. The use of adaptive meshing enables unprecedented resolution of highly localized phenomena, while the multigrid strategy maintains the overall efficiency of the scheme.

Status/Plans. Future work will center on the inclusion of more adequate surface modeling and grid generation techniques, as well as the extension of the present work to viscous turbulent flow cases in three dimensions. This will require the implementation of a multiple field-equation turbulence model.

Dimitri J. Mavriplis
Institute for Computer Applications in
Science and Engineering (ICASE)
Langley Research Center
(804) 864-2213

1. Select the type of surface to be generated.
 2. Select the type of grid to be generated.
 3. Select the type of mesh to be generated.

View

left	front	top
right	back	bottom
center	isometric	perspective
zoom	pan	rotate
border width	border height	border color

Pick

View Mode
Input Mode
File Mode
Help

Unsave

Grid Name
Grid Color
Grid Size
Grid Type

Options

Grid Name
Grid Color
Grid Size
Grid Type

Main Menu

Grid	Grid
Grid	Grid
Grid	Grid

SGG Menu

Grid Name
Grid Color
Grid Size
Grid Type

Point Menu

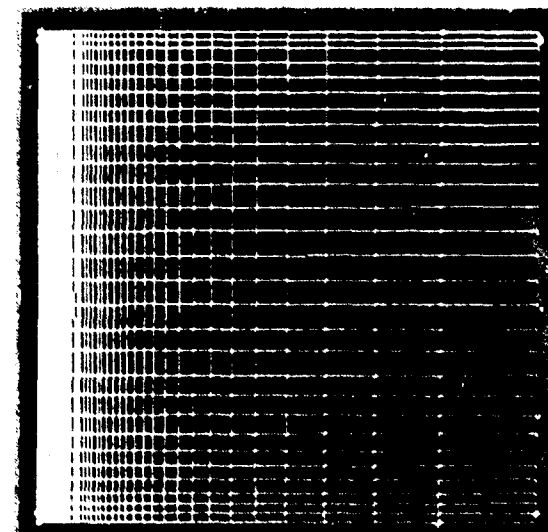
Grid Name
Grid Color
Grid Size
Grid Type

Point Specs

Edge	1
1	20
2	1
3	0.000000
4	0

DEF	US
SCF	US
Actual	0.000000
Delta	0.000000
Req.	0.000000

Grid	Grid
Grid	Grid
Grid	Grid



Dimensions

Grid
Grid
Grid

Cluster Point

Grid
Grid
Grid

Edge Dist.

Grid
Grid
Grid

Figure 4-4. S3D - An Interactive Surface Grid Generation Tool

4-4 S3D - An Interactive Surface Grid Generation Tool

Objective. To develop a surface grid generator with geometry modeling and surface gridding capabilities in an integrated, interactive environment, with the goal of vastly reducing turnaround time.

Approach. The scope of surface grid generation requirements were defined, and areas that have not been adequately addressed or treated by existing software were identified. The initial development effort of S3D has been directed at filling or enhancing those areas. A prototype S3D with primitive interface was developed and applied on a variety of complex geometries. These applications were helpful in identifying problem areas and permitted a greater focus on such issues as user-friendliness and ease of operation. The S3D code has since been expanded and enhanced with a user interface incorporating the latest in workstation technology. The code is now ready for hands-on application by CFD analysts.

Accomplishments. S3D can start from a geometry definition based either on a discretized curve set or a rectangular point set. Prominent geometric features such as discontinuities and high curvatures are easily preserved and deficiencies in geometry data easily removed in transforming from geometry definition to surface definition. At the heart of S3D is the analysis of curves and surfaces by robust and widely applicable piecewise cubic and bi-cubic interpolation techniques made possible by highly reliable curve and surface fitting schemes. Point redistributions are accomplished, through smart and user-friendly interfaces, by the use of hyperbolic function-based, two-sided stretching functions which have been shown to reduce the spacing-induced truncation error. Some of the more advanced features of S3D include surface-surface intersections, optimized surface domain decomposition and recomposition, and automated propagation of

edge distributions to surrounding patches. In the area of database management, S3D permits a variety of data formats including that of PLOT3D for ease of data transfer.

Significance. The efficiency and ease with which S3D can be used to handle commonly encountered tasks in surface grid generation will help CFD analysts drastically reduce the time required in gridding complex surface geometries.

Status/Plans. A workshop on S3D is planned for this October. Future plans include adding options to handle some of the common data exchange formats under Interim Graphics Exchange Standard (IGES) and capabilities to design and analyze geometries based on non-uniform rational B-spline (NURBS).

Raymond Luh
Fluid Dynamics Branch
Ames Research Center
(415) 604-4494

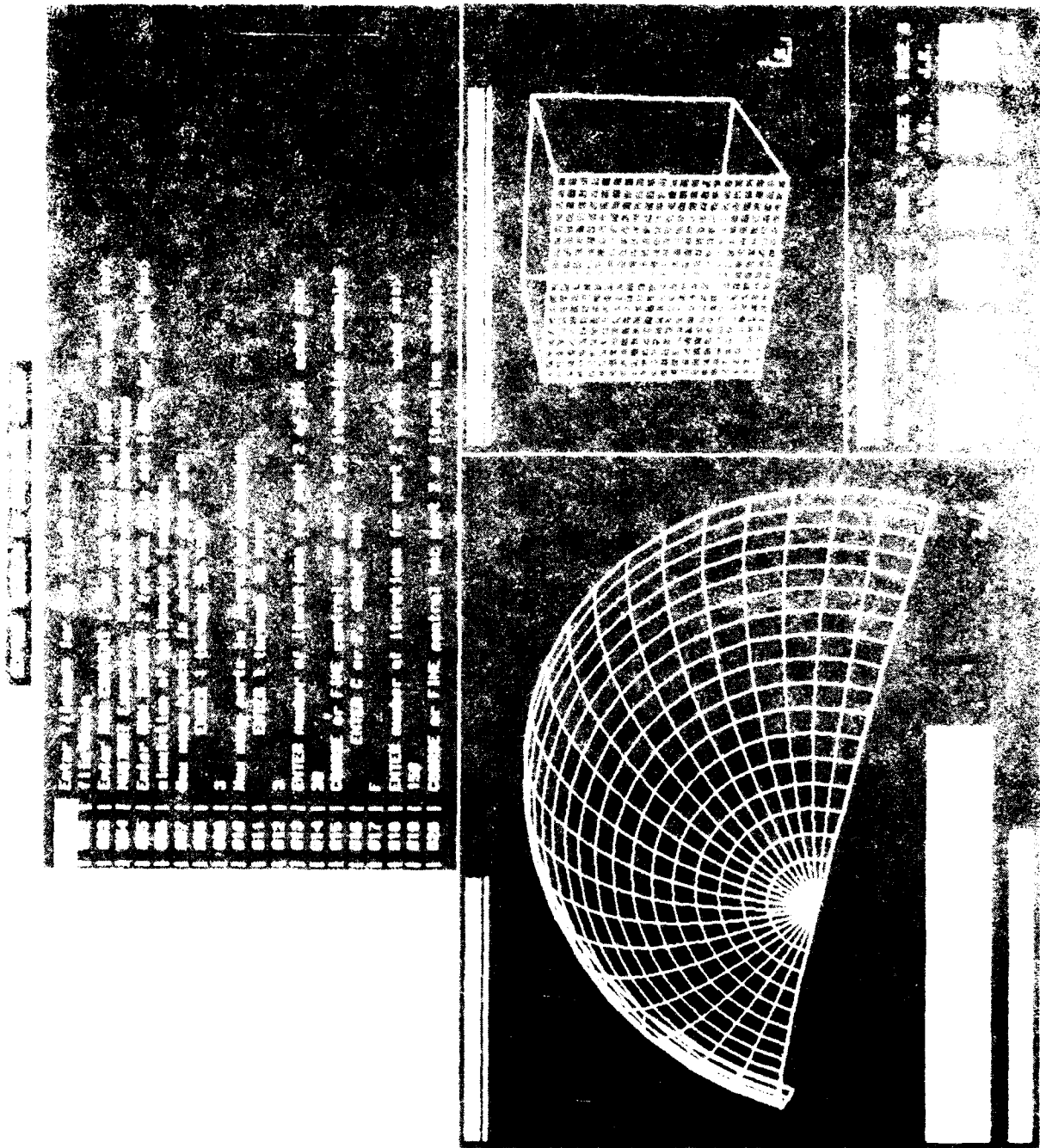


Figure 4-5. Accelerated Preparation of Grid Generation Input Data

4-5 Accelerated Preparation of Grid Generation Input Data

Objective. To greatly reduce the user time required to generate three-dimensional multiple-block computational volume grids.

Approach. The approach is to use the graphical capabilities of a powerful scientific workstation to accelerate the process of collecting and formatting the input data required by a grid generation program. This new software tool leads the user through the process of specifying input data by asking questions in sequence, error-trapping the responses, and then formatting those data for the grid generator. Users having more experience can view all the input data in a random-access fashion, enter or modify it, and then format it with automatic error-trapping. A suite of useful utilities completes the software system.

Accomplishments. Preliminary tests indicate that a reduction by a factor of ten has been achieved in the number of man-hours required to generate 3-D volume grids.

Significance. The generation of a suitable grid for computational analysis of a realistic aerodynamic configuration can take as long as 6 months, frequently dwarfing all other aspects of the computational fluid dynamics (CFD) process combined. This problem becomes even worse when the physical system to be modeled undergoes change requiring modification to the grid, such as deflecting control surfaces, rotating nozzles, or aeroelastic effects. Thus, any tool that greatly reduces the user time required to generate grids is a very significant advance.

Status/Plans. The software system to effect the above, called 3DPREP, is complete. An improved program to view 3-D computational grids, called 3DECANT, is complete. The elliptic volume grid generator, called 3DGRAPE, is also complete.

The next step is to combine the three modules to produce a truly integrated interactive 3-D volume grid generator. But this integration task is more significant than one might expect. The graphical user interface must run on a workstation, but the elliptic grid generator must run on a supercomputer. Thus, the integrated system must run over a network-connecting workstation and supercomputer running concurrently. This formidable program design and coding task is now well under way.

The integrated system will further accelerate the process by enabling the user to view the iterative grid generation process as it is taking place. This will give the user a better understanding of the grid generation process, and the ability to improve a grid generation effort that is working or to abort one that is not.

Reese L. Sorenson
Fluid Dynamics Division
Ames Research Center
(415) 604-4471

YAV-8B Harrier

Vertical/Shortly After Landing Approach

Figure 4-6

Flight Conditions

- 1000 ft
- 1000 ft/sec
- 1000 ft/sec
- 1000 ft/sec

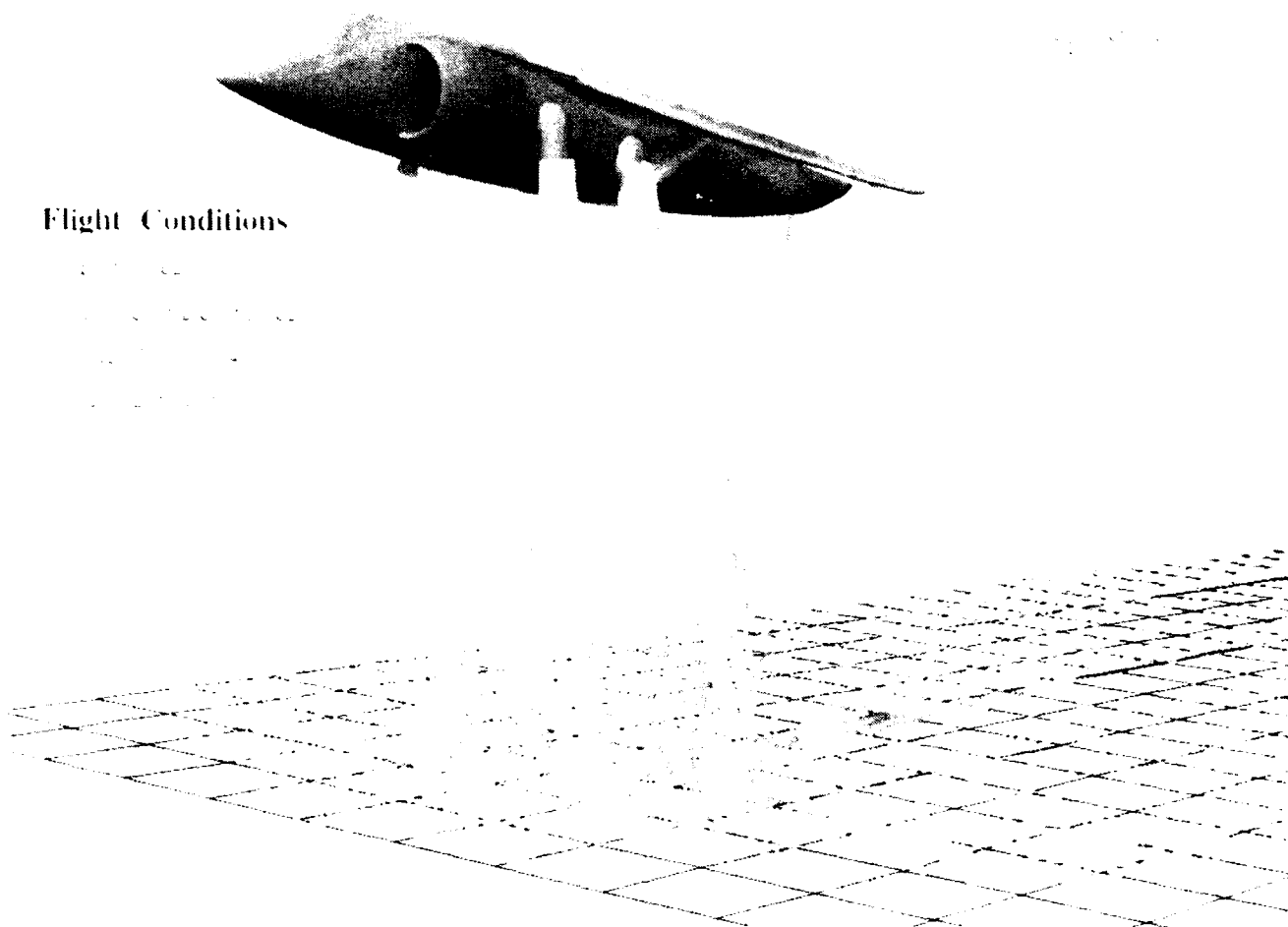


Figure 4-6. Numerical Simulation of the YAV-8B Harrier VSRA in Ground Effect

4-6 Numerical Simulation of the YAV-8B Harrier VSRA in Ground Effect

Objective. To develop a validated powered-lift flow-field analysis capability useful in the design of advanced powered-lift aircraft.

Approach. The flow field surrounding the YAV-8B Harrier in low-velocity jet-borne flight has been simulated through the numerical solution of the Reynolds-Averaged Navier-Stokes equations. This simulation also uses an engine model to specify inlet and nozzle mass flows and nozzle temperatures based on throttle inputs and inlet temperature and pressure. Over 2.8 million grid points in 18 grids are used to resolve the flow field using a diagonalized approximately factored algorithm and the chimera overset grid method.

Accomplishments. Simulation conditions of 30 knots forward speed at 30 feet above ground level with exhaust nozzles rotated 81° below horizontal have been modeled. This computation was performed on a Cray Y-MP 8/128 using 70 single processor CPU hours and running at a rate of 130 MFLOPS (million floating point operations per second). Improved, spatially varying time step methods for powered-lift flow fields have allowed a factor of six increase in the global time step and a corresponding decrease in the cost of computation. Software has also been developed for the analysis of infrared visualizations which will be used in the validation of the aircraft simulation capability.

Significance. Ground effect flow fields about powered-lift aircraft, such as the Harrier, are highly complex. Analysis is generally resistant to small-scale wind tunnel techniques due to a wide variety of scaling effects. This leads to expensive full-scale powered wind tunnel tests to quantify the effects of ground proximity on vehicle performance. Some of the hazards of operating in the ground environment include hot-gas ingestion, foreign object damage, and the "suckdown" effect. This simulation demonstrates a promising

and potentially money saving new technique for performance prediction of powered-lift designs in the ground environment.

Status/Plans. As a High-Performance Computing and Communications Program (HPCCP) Computational Aero Sciences (CAS) Grand Challenge, the powered-lift project is developing numerical analysis tools for complete powered-lift aircraft on massively parallel computers. Simulation methods for aerodynamics, propulsion, and controls will be combined. Additional flight tests are scheduled for the collection of infrared imaging validation data. Following validation, it is expected that an accurate and necessary design and analysis tool for powered-lift aircraft will result.

William R. Van Dalsem,
Fluid Dynamics Division
Ames Research Center
(415) 604-4469

HSCT Configuration

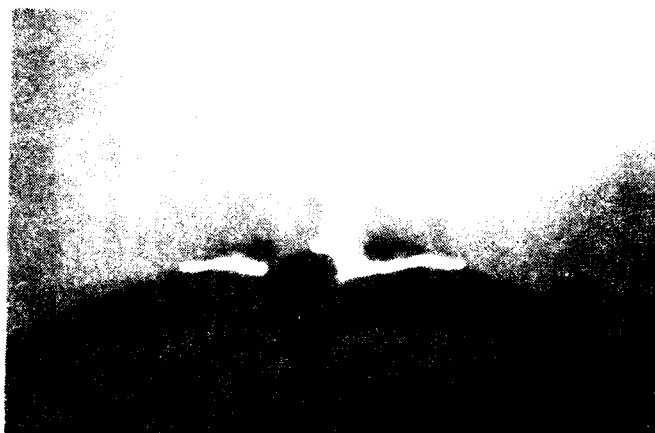
Mach = 3.

$\alpha = 5^\circ$

$Re_l = 6.0E+06$

Experiment

Computation



$x = 171$

laser sheet

density

$(M_\infty = 3.0, Re_l = 6.3 \times 10^6)$

(a) Lift coefficient

(b) Drag coefficient

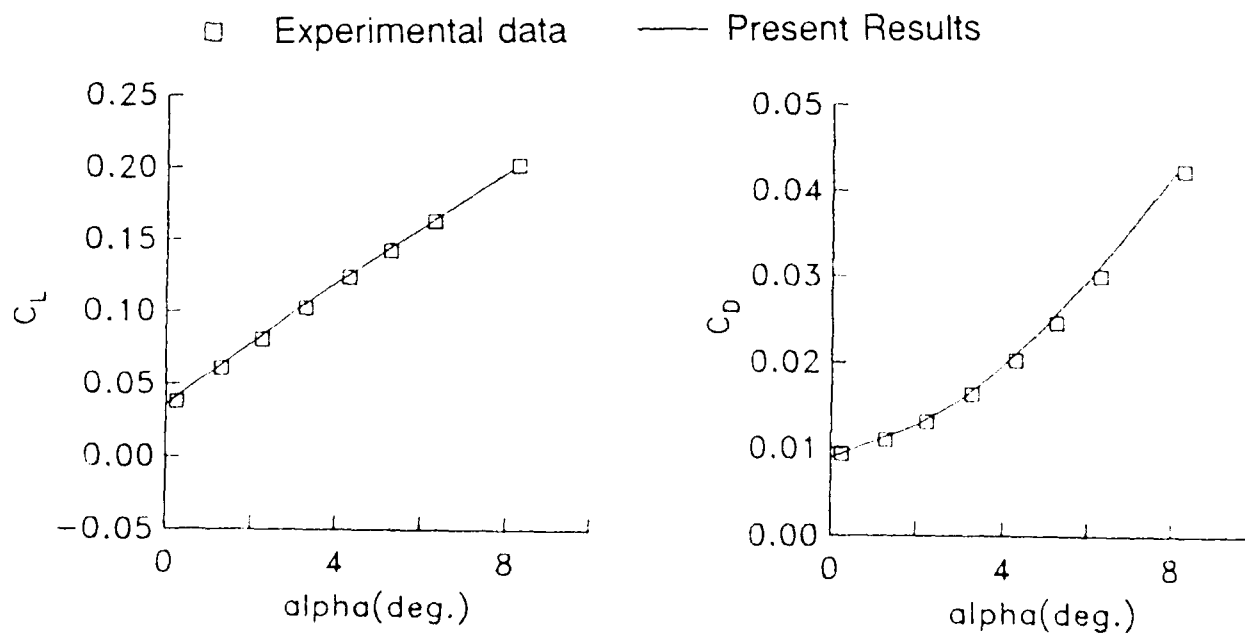


Figure 4-7. High-Speed Civil Transport Navier-Stokes Configuration

4-7 High-Speed Civil Transport Navier-Stokes Computations

Objective. To develop an efficient numerical procedure for computing viscous flow over a high-speed civil transport configuration.

Approach. A multistage Runge-Kutta time-stepping scheme with multigrid acceleration technique was employed for computing the steady-state solutions of the thin-layer Navier-Stokes equations. The accuracy of the numerical solutions was enhanced by the use of a matrix dissipation model.

Accomplishments. A multigrid-based finite volume numerical scheme developed for computing high Reynolds number viscous flows over aircraft components at transonic speeds has been extended to accommodate supersonic flows. The resulting numerical code, known as TLNS3D, has been applied to compute viscous flow over a generic high-speed civil transport model at the design cruise Mach number $M = 3$. The angle-of-attack varied from 0° to 8° in these computations to correspond to an in-house experimental investigation, and each test condition required approximately 2.5 hours on a Cray-2 computer. The computed lift and drag coefficients are compared with the experimental data in the adjoining figure. The computed solutions are in excellent agreement with the data over the entire angle-of-attack range, even for the drag coefficient, which is dominated by the viscous component at lower lift values.

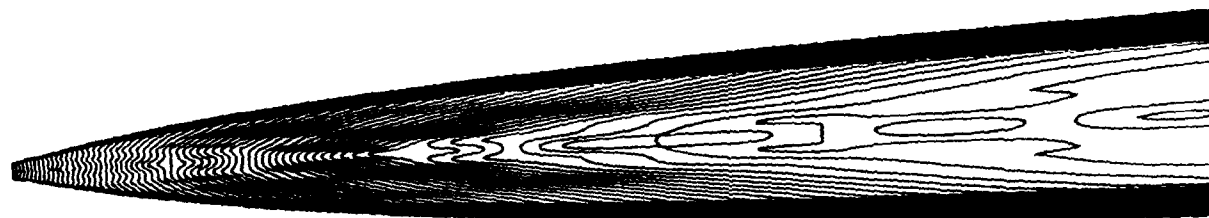
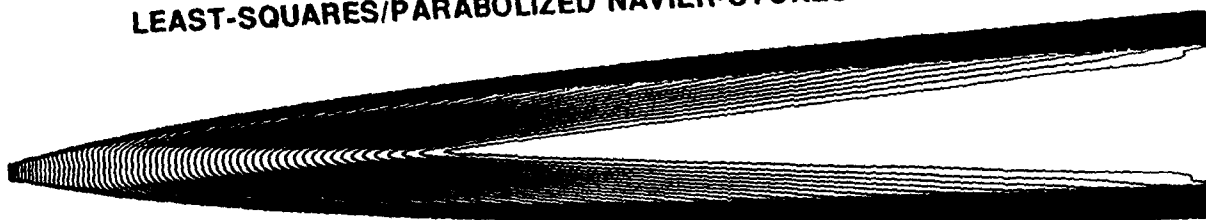
Significance. Navier-Stokes solutions for the flow over configurations of practical interest can be obtained routinely using the multigrid-based TLNS3D code. Because of the improved efficiency of this code, parametric studies to examine the performance of different configurations are feasible without resorting to wind tunnel testing in early phases of vehicle development.

Status/Plans. The method described here will be generalized to accommodate block-structured grids so that flow over complex aircraft can be calculated.

Veer N. Vatsa
Fluid Mechanics Division
Langley Research Center
(804) 864-2236

MACH 15 HELIUM NOZZLE, MACH NUMBER CONTOURS

LEAST-SQUARES/PARABOLIZED NAVIER-STOKES DESIGN



METHOD-OF-CHARACTERISTICS/BOUNDARY LAYER DESIGN

Figure 4-8. CFD-Based Hypersonic Wind Tunnel Nozzle Design

4-8 CFD-Based Aerodynamics Design of Hypersonic Wind Tunnel Nozzles

Objective. There was an immediate need for a new design procedure for high Mach number hypersonic wind-tunnel nozzles, for which the classical design procedures (using method-of-characteristics with boundary layer correction) have failed to produce the high-quality flow fields necessary for fundamental flow experiments and computational fluid dynamics (CFD) validation studies. The classical design procedure for hypersonic nozzles has been shown to break down at Mach numbers greater than 8 and when the boundary layer covers a large percentage of the test section diameter.

Approach. To develop a procedure that unifies the best of classical design practices, CFD, and optimization procedures, an efficient CFD code, which solves the parabolized Navier-Stokes (PNS) equations using an explicit upwind algorithm, was coupled to a nonlinear least-squares (LS) optimization procedure. A LS problem was formulated to minimize the difference between the computed flow field and the objective function, and consisted of the centerline Mach number distribution and the exit Mach number and crossflow velocity profiles. The aerodynamic lines of the nozzle were defined using cubic splines, the slopes of which are optimized with the design procedure. The thick boundary layer typical of hypersonic nozzles is accounted for by incorporating the solution of the PNS equations in the design procedure.

Accomplishments. Initial programming and validation have been completed on a computer code that exercises a LS/PNS optimization procedure for designing hypersonic wind tunnel nozzles. The program couples an optimum design procedure based on the LS minimization problem to an explicit upwind PNS CFD code. In the accompanying figure, a Mach 15 helium nozzle designed using the new CFD-based procedure is compared with a nozzle designed with the method-of-charac-

teristics with boundary layer (MOC/BL) correction methods. The CFD-based nozzle design reduced the fluctuations of static pressure to less than $\pm 2\%$ for the uniform core region. This is a significant improvement over the classically designed nozzle, which had fluctuations of static pressure greater than $\pm 30\%$ for the core region.

Significance. The new procedure for designing hypersonic wind-tunnel nozzle contours demonstrates that a CFD computer code can be efficiently coupled to an optimization algorithm. The effect of changes in the nozzle wall parameters is evaluated by computing the nozzle flow field using the PNS equations. This new procedure provides a method for designing hypersonic nozzles of high Mach numbers in which classical procedures break down.

Status/Plans. Work is under way to apply the new procedure to design other wind-tunnel nozzles and to extend it for use in the design of hypersonic inlets.

John J. Korte
Fluid Mechanics Division
Langley Research Center
(804) 864-6920



Figure 4-9. Turbulent Flow Over a Backward Facing Step

4-9 Turbulent Flow Over a Backward Facing Step

Objective. To develop a detailed database of the turbulent flow over a backward facing step for the validation of direct simulations, large-eddy simulations, and turbulence models.

Approach. State-of-the-art instrumentation was used to acquire the mean velocities and turbulence quantities in the turbulent flow. The primary instrumentation was a three-component laser velocimeter, which allowed the measurement of all three velocity components and the full Reynolds stress tensor. Test conditions and geometries were defined through interaction with the computational fluid dynamics (CFD) developers.

Accomplishments. During FY 1990, the initial investigation of the flow over the step was performed. The test conditions for that experiment were chosen to be suitable for direct simulations. The detail and quality of the data generated interest in the turbulence modeling community, which requested a higher Reynolds number case. A new facility has been constructed that allows a wide range of Reynolds numbers and expansion ratios. Currently, the flow at a Reynolds number of 47,000 based on step height with an expansion ratio of 1:2 is being investigated.

Significance. The data being acquired in this investigation are unique in that they document the full Reynolds stress tensor. Upon completion of the experiment, this database will represent the most complete statistical database for the validation of CFD methods.

Status/Plans. The acquisition of the flow-field data is currently under way and will continue throughout the next fiscal year.

Scott O. Kjølgaard
Fluid Mechanics Division
Langley Research Center
(804) 864-2160

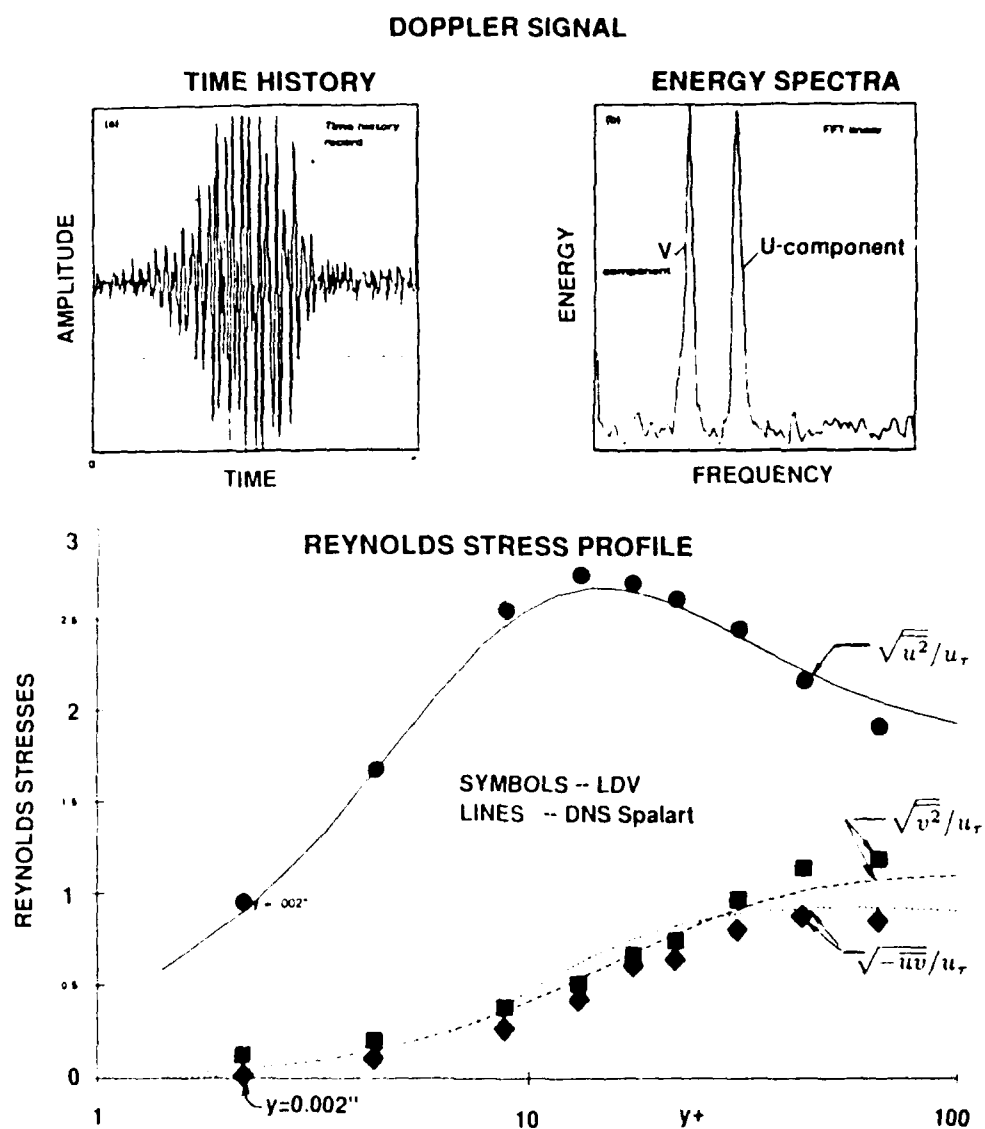


Figure 4-10. Near-Wall Laser Velocimeter

4-10 Near-Wall Laser Velocimeter Measurements

Objective. To increase near-wall Reynolds stress database for three-dimensional turbulent boundary layer flows with significant turning and separation.

Approach. A new Laser Doppler Velocimeter (LDV) instrument was developed capable of obtaining near-wall measurements in a three-dimensional boundary layer. Measurements were performed in a 3-D turbulent boundary layer flow apparatus, located at Stanford University for which previous measurements of the Reynolds stresses were obtained with a hot-wire anemometer.

Accomplishments. Turbulence measurements were acquired in a 3-D boundary layer at a distance of 0.02 mm (0.001 in.) from the surface. Conventional LDV approaches are limited to a distance of about 1 mm from the surface. The technique has undergone further improvements, such as the development of a single channel multifrequency signal processing method for measuring the cross correlations. 3-D Navier-Stokes calculations (on a coarse grid) have been performed for the 3-D wedge flow experiment.

Significance. The accurate prediction of skin friction and heat transfer is critically dependent on the modeling of the Reynolds stresses within the viscous sublayer. The present LDV development will allow the measurement of these stresses within the sublayers even under highly 3-D conditions. Such data will aid in the development and validation of improved turbulence closure models.

Status/Plans. Further develop the multifrequency signal processing system to obtain velocity components -vw and -uv Reynolds shear stresses. Fiber-optics are being developed to facilitate 3-D measurements.

Dennis A. Johnson
Fluid Dynamics Division
Ames Research Center
(415) 604-5399

Chapter 5

Numerical Aerodynamics Simulation (NAS)

The Numerical Aerodynamic Simulation (NAS) program provides readily accessible supercomputing capability to the United States' top aeronautical researchers in Government, industry, and academia. The NAS program also includes research and technology development to ensure application of emerging technologies to computational fluid dynamic and other computational sciences. Specifically, the current research involves the enhancement of user interfaces and software and hardware technology for parallel computer architectures.

The objectives of NAS are (1) to maintain a pathfinding role in providing leading-edge supercomputing capabilities to NASA, DoD, and other Government agencies, industry, and universities as a critical element for continued leadership in computational aeronautics and related fields; (2) to stimulate the development of state-of-the-art, large-scale, computer systems and advanced computational tools for pioneering research and development; and (3) to provide a strong research tool for OAST.

To maintain the lead in large-scale computing capability, NAS is implementing a strategy of installing, at the earliest possible opportunity, the most powerful high-speed processor (HSP) available. NAS maintains at least two HSPs, one of which is fully operational and represents more mature technology, and the other, which is a higher performance prototype or early production model. The current HSPs are a Cray-2 installed in January 1988 and a Cray Y-MP installed in November 1988. The Cray Y-MP is the first computer to sustain a computation rate of a billion floating point operations per second (GFLOP). Current plans are to replace the Cray-2 with a new processor (HSP-3) in 1992.

NAS was the first supercomputing facility to install a standard operating system (UNIX) and communication software on all systems. UNIX offers the flexibility of both batch and interactive computing and provides a common user interface on all user-visible subsystems. NAS is currently upgrading its remote network nationwide from NASnet, a switch-based, high-performance communication network, to Aeronet, a router-based system, allowing researchers at remote locations to have similar interactive capability as local users at the NAS facility.

The vision for the NAS program is to provide by the year 2000 an operational computing system capable of simulating an entire aerospace vehicle system within a computing time range from one to several hours. It is estimated that a computing time rate of one trillion floating point operations per second (TFLOPS) is required to accomplish this goal.

Program Manager: Pamela F. Richardson
OAST/RF
Washington, DC 20546
(202) 453-9857

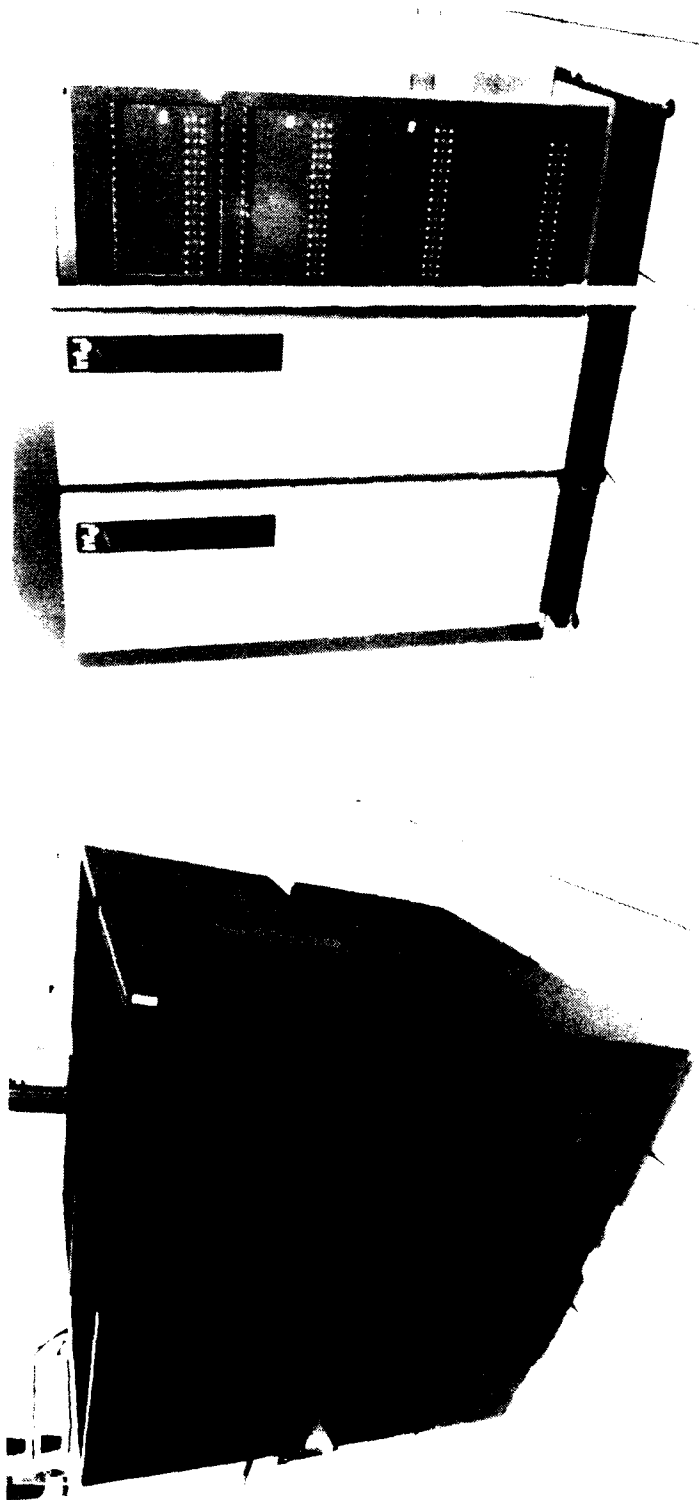


Figure 5-1. Parallel Computers in the NAS Program

5-1 Parallel Computers in the NAS Program

Objective. To evaluate the performance capabilities of parallel computers running computational fluid dynamics (CFD) codes.

Approach. A base level of performance statistics was established and algorithms that increase the performance of parallel computers were developed.

Accomplishments. The NAS Program has acquired two parallel computers, a Connection Machine-2 (CM-2) from Thinking Machines, Inc. (TMI) and an iPSC/860 system from Intel. The CM-2 has 32,000 1-bit serial processors and 1000 64-bit Weitek floating point processors with a SIMD (single instruction, multiple data) architecture. The peak speed is 14 GFLOPS (giga [billion] floating point operations per second). Scalar code is executed on either Sun or VAX front-end computers, which broadcast instructions to the CM-2 processors. Interprocessor communication occurs three ways: general router, compiled, and NEWS (North, East, West, South, that is, nearest neighbor). The CM-2 has 4 gigabytes of memory, and a 25 gigabyte Datavault for on-line storage as well as a high-performance parallel interface (HiPPI) to UltraNet. The CM-2 was upgraded in January 1991 to take advantage of TMI's new slice-wise architecture, which presents a programming model of the CM-2 based on 1000 floating point processors, instead of the 32,000 bit serial processors. Such a model is more relevant to the CFD work done at NAS. TMI has recently provided a time-sharing operating system and network queuing system.

The iPSC/860 system was installed in January 1990 as part of Intel's gamma prototype project with DARPA. This system has 128 nodes, each with an Intel i860 64-bit microprocessor and 8 megabytes of memory. It has a 40 megahertz RISC chip rated at 60 MFLOPS (M=mega [million]). Peak performance is thus 7.5 GFLOPS. Total memory

available is 1 gigabyte. The iPSC/860 is a MIMD (multiple instruction, multiple data) architecture. Interprocessor communication is through message passing. The interconnect network is a hypercube. The iPSC/860 has a concurrent file system of 10 gigabytes supporting a peak transfer rate of 10 megabytes/second. At present, all communication is done through a small (PC 80386) front-end computer, which also handles partitioning of the nodes and loading of jobs for execution.

Significance. The highest performance at NAS for CFD-related applications on parallel computers is 1.6 GFLOPS using a 32-bit isotropic turbulence code. This code used an assembly language FFT (Fast Fourier Transform) and a special compiler, Vectoral. The problem size was 256^3 nodes. A similar code runs at about 160 MFLOPS on a single Cray Y-MP processor. This code is achieving a 10-fold performance-to-price increase on the Intel compared to the Cray Y-MP.

Status/Plans. NAS will continue to explore the potentials of both parallel systems.

T. A. Lasinski
NAS Systems Division
Ames Research Center
(415) 604-4405

Performance of NAS Pseudo CFD Applications (7/24/91)

Algorithm 64 ³ grid	Computer	Number of Processors	Time/Iter (sec)	MFLOPS (YMP)	Efficiency (actual/peak)
LU	BBN	62	12.13	36	1/17
	CM2	32K	2.84	150	1/86
	iPSC	128	2.34	182	1/42
	YMP	1	2.10	203	3/5
	YMP	8	0.35	1218	<1/2
SP	BBN	62	3.71	95	1/7
	CM2	32K	11.63	25	1/521
	iPSC	64	2.42	122	1/31
	YMP	1	1.49	198	>1/2
	YMP	8	0.26	1335	1/2
BT	BBN	62	11.83	77	1/8
	CM2	32K	24.25	37	1/352
	iPSC	64	4.54	199	1/19
	YMP	1	4.22	214	3/5
	YMP	8	0.64	1411	>1/2

LU: Lower Upper Triangular Solve

SP: Scalar Pentadiagonal

BT: Block Tridiagonal

Figure 5-2. Performance of NAS Pseudo CFD Applications

5-2 NAS Parallel Benchmarks

Objective. To develop a new methodology for the performance evaluation of highly parallel computers running computational fluid dynamics (CFD) applications.

Approach. The principal distinguishing feature of the new benchmarks is their "pencil and paper" specification—all details of these benchmarks are specified only algorithmically. In this way many of the difficulties associated with conventional benchmarking approaches on highly parallel systems are avoided. The benchmarks consist of a set of kernels, the "parallel kernels," and a simulated application benchmark. Together they mimic the computation and data movement characteristics of large-scale CFD applications.

Accomplishments. A set of benchmark kernels and pseudo applications has been selected and completely specified. Sample serial implementations for the benchmarks have been developed. Parallel versions of the benchmarks have been implemented on the 8-processor Cray Y-MP, the 128-processor Intel iPSC/860, and the 32,000-processor Connection Machine CM-2 (from Thinking Machines). The benchmarks have been distributed to a large number of computer vendors and academic researchers interested in performance evaluation.

Significance. The NAS Parallel Benchmarks represent the first comprehensive effort to assess the performance of highly parallel computers. They present a new methodology that allows the suitability of parallel supercomputers for aerosciences applications to be evaluated. In addition, the benchmarks are an invaluable tool for selecting computers for the High Performance Computing and Communication Program (HPCCP) testbeds and will ensure the selection of computers suitable for the HPCCP "Grand Challenge" problems.

Status/Plans. Implementation on other parallel computers will continue in the next year. The inclusion of additional kernels/applications into future releases of the benchmarks is under investigation.

Horst D. Simon
Computer Sciences Corporation
NAS Systems Division
Ames Research Center
(415) 604-4322



Figure 5-3. Virtual Wind Tunnel

5-3 Virtual Wind Tunnel

Objective. To explore the effectiveness of virtual environment technology for flow visualization.

Approach. Virtual environment technology provides a new approach to user interfaces in computer software. This approach involved integrating a variety of input and display devices to give the user the illusion of being immersed in an interactive computer-generated environment. The computer-generated scene was displayed in stereo creating the illusion of depth, and was rendered from a point of view that tracks the user's head movements. The user had an input device, typically an instrumented glove, through which objects appeared to be directly manipulated in the computer-generated environment.

Accomplishments. A virtual environment was implemented for exploring numerically generated three-dimensional unsteady flow fields. A variety of interesting techniques were used for visualization and for navigation through the flow. A boom-mounted six degree-of-freedom head position-sensitive stereo CRT system was used for viewing. A VPL Dataglove™ Model II, which incorporates a Polhemus 3 Space™ tracker, was used to sense the user's hand position, orientation, and finger joint angles. The user's gestural movements were interpreted as commands for injecting various tracers (e.g., "smoke") into the virtual flow field. An eight-processor Silicon Graphics computer system was used for computation and rendering.

Significance. We have shown that a high-performance graphics workstation can be used to visualize three-dimensional flow fields in a virtual environment at acceptable frame rates; virtual environments are an effective tool for the rapid exploration of three-dimensional flow fields, both steady and unsteady; and the system may be applicable to the visualization of other vector fields.

Status/Plans. Future plans include distributing the software so that computation and data management is done on a supercomputer and upgrading to a higher resolution head-tracking display system.

Creon Levit
NAS Systems Division
Ames Research Center
(415) 604-4403



Figure 5-4. Harrier Topological Vortex Cores

5-4 Vector Field Topology Visualization Software

Objective. To create simple visualizations that capture the important properties of vector fields.

Approach. A new module, called Topology, has been created for the Flow Analysis Software Toolkit (FAST) graphics software package to find and display a portion of the topology of vector fields. FAST is a multiprocess software environment that consists of a collection of separate modules that can be run simultaneously, sharing data and allowing the user to create, load, analyze, visualize, animate, and record computational fluid dynamics (CFD) data. FAST was created at Ames Research Center, and beta versions of it are currently being tested at various U.S. sites.

Accomplishments. Topology, the new FAST graphics software module, finds, classifies, and displays critical points, i.e., where a vector field vanishes. The software integrates curves through the field from initial positions near critical points on the invariant manifolds of the linearized field near the points. By carefully choosing the curves to integrate, the user can find the vortex cores of all vortices containing critical points and/or examine the skin friction surface topology to determine the location of separation lines and other features of interest. The software has very flexible mechanisms for exploring other topological features as well.

Significance. Users of Topology can quickly find and display some of the important features of vector fields. In particular, separation lines and most vortex cores may be found quickly, easily, and, in many cases, automatically. Since the software functions properly on the large, multi-zoned, blanked (masked) grids typical of state-of-the-art CFD, scientists can gain additional insight into the results of their computations.

Status/Plans. We plan to extend the software to improve visualization of vortices and to integrate topological surfaces from the neighborhood of critical points. We will investigate implementing Topology in other visualization environments, particularly the FLORA (FLOW Real-Time Analysis) software, also developed at Ames, which enables a user to interactively generate particle traces and surfaces, and EXPLORER, developed by Silicon Graphics, Inc.

Al Globus
Computer Sciences Corporation
NAS Systems Division
Ames Research Center
(415) 604-4404

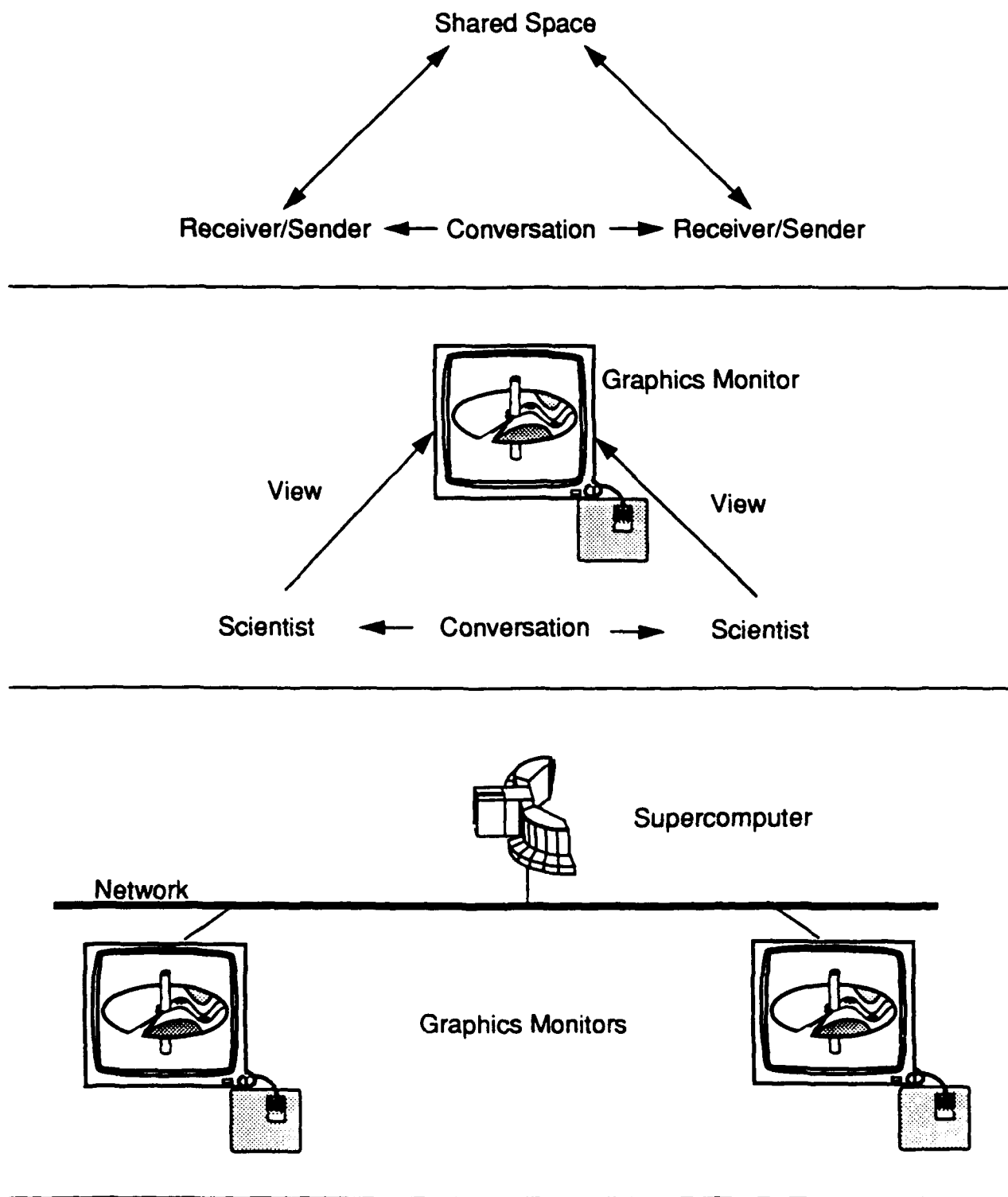


Figure 5-5. Distributed and Cooperative Visualization of Unsteady Fluid Flow

5-5 Distributed and Cooperative Processing of Unsteady Fluid Flows

Objective. To utilize distributed processing and cooperative processing to provide a powerful tool for visualizing computational fluid dynamics (CFD) data.

Approach. Distributed processing provides the user with the combined capabilities of a graphics workstation and a supercomputer, under a single application. The supercomputer's capabilities of high performance, large memory, large disk storage, and fast disk access are necessary to contain, access, and calculate the large data sets endemic to unsteady flow analyses. The high-speed graphics capability of the workstation presents high-resolution animations of features extracted from large data sets. In addition, the human interface environment provided by the workstation allows for controlling the analytical tools of the visualization system.

With cooperative processing, visualization is used as a communication medium. The paradigm is illustrated by the analogy of one scientist outlining ideas on a chalkboard for another scientist. Equal accessibility to the chalkboard by both scientists provides a platform for the exchange of ideas. The images produced on graphics workstations can be the platform. In combination with distributed processing, scientists may use this platform at geographically distant locations.

Accomplishments. Tempus Fugit/Interview is a CFD visualization application. Tempus Fugit ("time flies") interactively creates images animated over time from large data sets representing unsteady fluid flows. The companion program, Interview, presents simultaneously, identical and animated images to another workstation in a shared environment with Tempus Fugit. Interview attaches to the supercomputer process created by Tempus Fugit and transforms the process to a shared environment. Identical images are presented to both workstations simultaneously. Thus, a

cooperative environment is created via a network connection to the supercomputer and is uninhibited by geographical proximity.

Significance. The initial implementation of Tempus Fugit/Interview is a proof-of-the-concept capability providing interactive visualization of unsteady fluid flows by using distributed processing. Interview's prototype WYSIWIS ("what you see is what I see") interface provides a base for further research into group communication via a visualization medium.

Status/Plans. A prototype of Tempus Fugit/Interview has been completed. Additional visualization techniques and cooperative interaction methods will be added as operational experience is gained.

Michael J. Gerald-Yamasaki
NAS Systems Division
Ames Research Center
(415) 604-4412

Chapter 6

Rotorcraft

The objective of the Rotorcraft Program is to provide the technologies for helicopters and other rotorborne aircraft to achieve quiet, low-vibration operation with increased performance, agility, maneuverability, and stability, all with acceptable handling qualities. Much of the work is done in conjunction with the U.S. Army and the FAA and in cooperative programs with industry.

Improved analysis can now handle many local aerodynamic phenomena, but the transonic, unsteady, complex wake interaction flow requires another generation of codes. Therefore, much of the rotorcraft program still is empirically based, with validation of analysis as a goal. This approach requires new test techniques, upgraded test facilities, carefully instrumented models, sophisticated simulations, and increased use of the latest generation of computers. New ideas also are part of the program, since the complexity of rotorcraft makes it a fertile area for innovative approaches.

The heart of the aerodynamic portion of the program is airloads research. Small scale, pressure-tapped blade data have become available with the full-scale results due in 1992. Complementary efforts are under way in component, interference, and wake testing and prediction. These databases are used in acoustic and vibration research, which constitutes more than half of the program resources. The airload models also will be used for rotor state control and higher harmonic control to suppress noise or vibration or to enhance maneuverability.

Flight dynamics research in the Aerodynamics Division is based on unsteady rotor dynamics, with emphasis on simulation and eventually flight tests using a variable stability UH-60. New flight test capability is planned, with research challenges in higher-frequency control for rotor state control to achieve high agility.

Higher-speed rotorcraft activities are now focused on commercial tiltrotor technology. Certification issues are being addressed on the simulator and in noise testing and prediction. Also under way are improvements in performance, interior noise, vibration, and stability. The importance of these research opportunities for civil applications have been reported under contract to Boeing Commercial Airplane Company.

Program Manager: Mr. George Unger
OAST/RF
Washington, DC 20546
(202) 453-5420



Figure 6. *Continued*

6-1 Large-Scale Tiltrotor Performance Program

Objective. To acquire rotor performance and loads data with and without the wing installed to determine the influence of the wing on rotor operation, provide rotor performance data up to and beyond the aircraft operating envelope, and evaluate acoustics for terminal area operations.

Approach. A large-scale test program was developed for the 40- by 80 foot wind tunnel. The Prop Test Rig (PTR) was used to evaluate the forward flight performance for three different large-scale rotor blade sets including the V-22, XV-15 Metal, and XV-15 ATB (Advanced Technology Blades). The required measurements include acoustic as well as dynamic and performance data. Measurements made with and without the wing would be used to quantify effects of the wing on the rotor performance and acoustics.

Accomplishments. Testing was initiated, and isolated rotor data up to 240 knots was acquired on the 0.658-scale V-22 rotor prior to incident. The PTR recovery plan was initiated to rebuild/strengthen hardware to provide full test envelopes in both 40 by 80 and 80 by 120 test configurations.

Significance. The data obtained during testing will be used to provide experimental validation of the V-22 tiltrotor aircraft cruise performance. Future acoustic data will provide critical information into the feasibility of tiltrotor terminal air operations.

Status/Plans. The Ames Prop Test Rig will be rebuilt for both 40 by 80 cruise performance testing and 80 by 120 transition testing for performance and acoustics. The testing will use existing government-owned 25 ft diameter XV-15 rotor hardware.

Jeffrey Light
Rotorcraft Aeromechanics Branch
Ames Research Center
(415) 604-4881

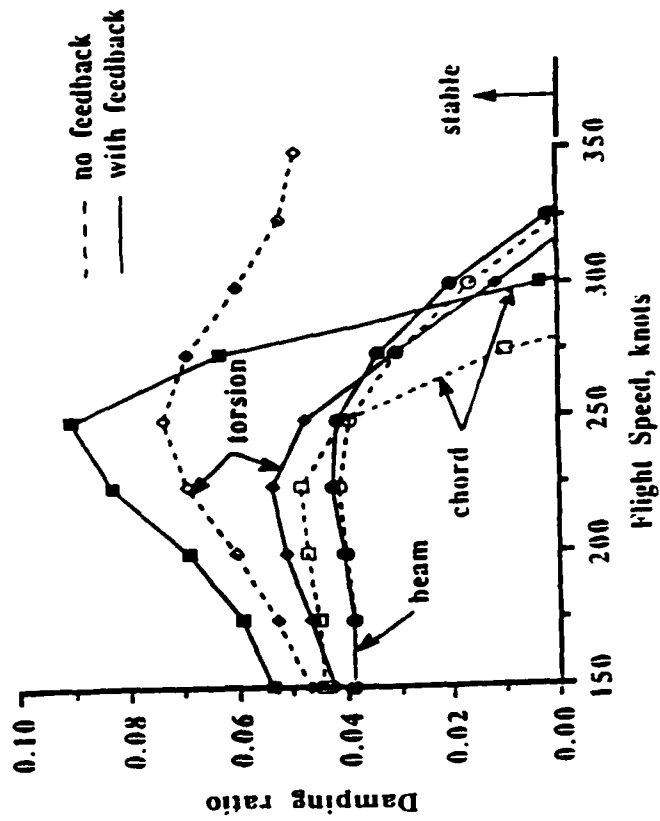
SYMMETRIC FLIGHT MODE

SENSORS AT LOCATION P4

WING HORIZONTAL ACC. TO LONG. CYCLIC PITCH, GAIN=+0.005 RAD/G

WING VERTICAL ACC. TO LONG. CYCLIC PITCH, GAIN=+0.005 RAD/G

DAMPING RATIO



LOCATION OF WING SENSORS

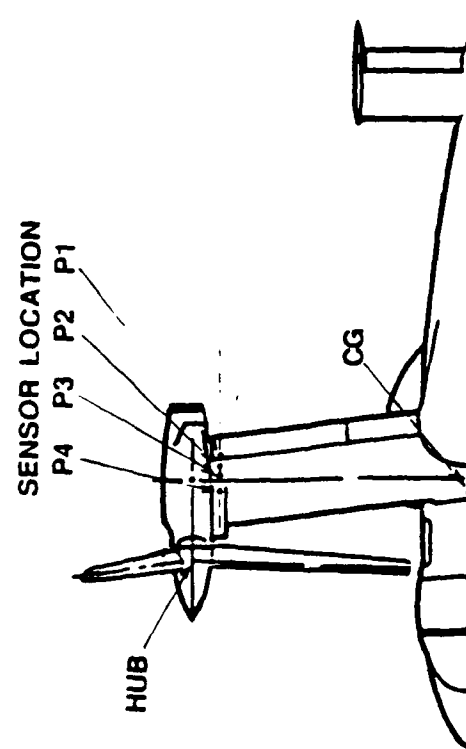


Figure 6-2. Tiltrotor Aeroelastic Stability Control

6-2 Tiltrotor Aeroelastic Stability Control

Objective. To investigate the use of active controls to delay tiltrotor whirl-flutter type instability.

Approach. The comprehensive rotorcraft analysis code CAMRAD/JA was used to obtain a set of linear differential equations, which describe the motion of a tiltrotor aircraft at various speeds. The hub motions from wing/body vibration are a standard input to CAMRAD/JA. The hub-motion is calculated using a separate structural analysis program. The CAMRAD/JA output consists of the open-loop system matrices which describe the aircraft motion in the state-variable domain. The matrices formed an input to a separate program, which performed the closed-loop, active control calculations. Additional input consists of the sensor model and the active controls feedback gain factors. The program performed an eigen-value analysis to determine the flutter stability for both the open and closed-loop systems. Time response calculation can be performed to estimate the magnitude of the required active control input for closed-loop stability. A separate utility was used to combine aircraft trim information from CAMRAD/JA with wing vibration data from the structural analysis program to define a sensor model, which is based upon physically measurable signals.

Accomplishments. The use of active controls to alleviate whirl-flutter was investigated for a cantilevered, high-wing tiltrotor model and an advanced joined-wing tiltrotor aircraft. Sensor models, defining the feedback of either pure state-variables or physically measurable wing accelerations to the rotor cyclic pitch were evaluated. The analysis showed that for both tiltrotor aircraft configurations, the feedback of accelerations, representing the wing torsion and chordwise motions, to the longitudinal cyclic pitch could increase the flutter velocity for the symmetric flight mode. The figure shows that for the

cantilevered-wing tiltrotor configuration the wing-chord instability could be increased from 280 knots to above 300 knots by feeding back vertical and horizontal accelerations measured near the wing tip to the longitudinal cyclic pitch.

Significance. The results of the investigation have shown that (1) active controls, using the rotor cyclic pitch can be used to delay the occurrence of whirl flutter instability; (2) an active cyclic pitch control level of 0.010° - 0.012° , which equates to a 10-15 pound active control force applied at the hub, was required to stabilize the tiltrotor; and (3) contamination of the sensor output signal with a 25% noise level did not adversely affect the closed-loop stability.

Status/Plans. The whirl-flutter alleviation investigation will be extended to include the anti-symmetric flight mode and for the complete aircraft in which the symmetric and anti-symmetric flight modes are coupled through the active control system. Optimization of the feedback system for a given sensor model will also be studied.

Johannes M. van Aken
Rotorcraft Aeromechanics Branch
Ames Research Center
(415) 604-6668

0.7-SCALE V-22 SEMI-SPAN
67 DEG WING FLAP ANGLE

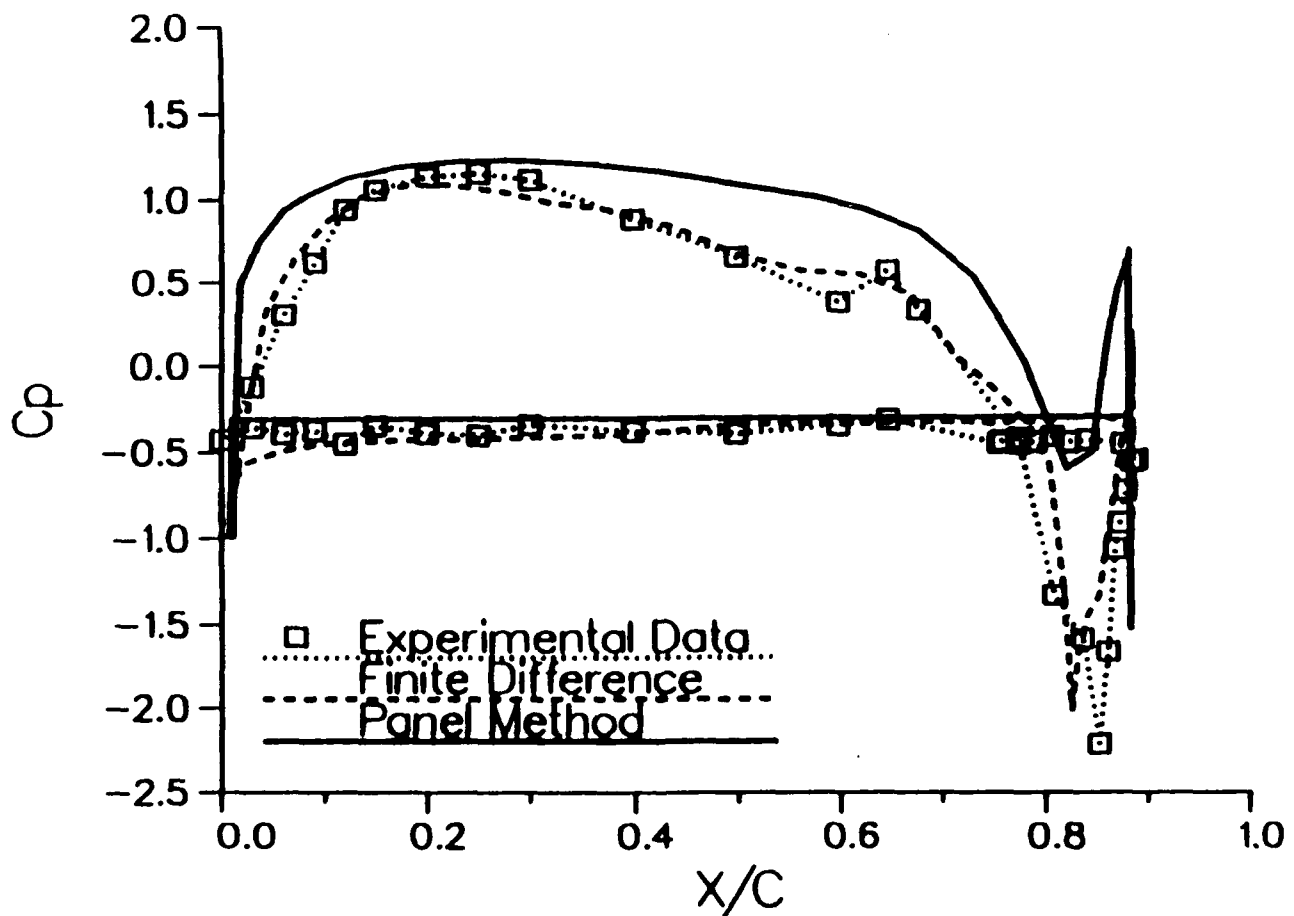


Figure 6-3. Wing Surface Pressure Distributions Within Wake

6-3 Tiltrotor Download Reduction

Objective. To understand the physics of tiltrotor download and develop download reduction concepts to minimize the adverse performance impact of the tiltrotor's wake on the aircraft's wing in hovering, vertical, and transition flight.

Approach. An experimental and analytical program has been pursued to quantify and demonstrate download reduction concepts. A model 7-foot diameter V-22 rotor system was used in hover at the Outdoor Aerodynamic Research Facility (OARF). Full potential and Navier Stokes models of tiltrotor hovering flow fields have been successfully developed to characterize and analyze the physics of the unsteady, vortical flow fields.

Accomplishments. A successful hover test was conducted at the OARF in FY 1991. Results included a demonstration of download reduction with upper surface wing blowing. Shadowgraphs of the wake/wing interaction were also acquired. Several papers were presented on three tiltrotor wake analysis codes. Two steady codes, a full-span potential flow code and a semi-span Navier-Stokes code, were developed. Wing pressures within the rotor's wake as well as outside the wake along the wing were predicted and compared. A new two-dimensional vortical wake interaction code using a velocity/vorticity formulation on a staggered grid was reported.

Significance. Results from the experimental program are directly applicable to aircraft configurations and result in a 10 to 20% reduction in download on current generation tiltrotor designs. The shadowgraph wake flows quantify the unsteady flow field, and the wing pressure database will be used to validate new 3-D analysis codes. The computational methods are the first successful analyses of tiltrotor flow fields in hover, and are available to industry for wing design on the next generation of tiltrotor aircraft.

The 2-D velocity/vorticity formulation results are the first-ever calculations to accurately predict the distributed airfoil pressures on both the upper and lower wing surfaces. The staggered grid method provides for the direct solution of the incompressible Navier-Stokes equations by means of a fully coupled implicit technique. This unique method was demonstrated to accurately predict the mean lift and drag and the periodic loading for several 2-D bodies including an NACA 0012 airfoil with and without a deflected flap at -90° incidence.

Status/Plans. Plans are to report the results of the experimental download program and to conduct a second test evaluation of other download reduction concepts. The prediction methodology will be expanded to include 3-D steady and unsteady analysis, turbulent flow, and rotor/fuselage interaction.

Paul M. Stremel
Rotorcraft Aeromechanics Branch
Ames Research Center
(415) 604-4563

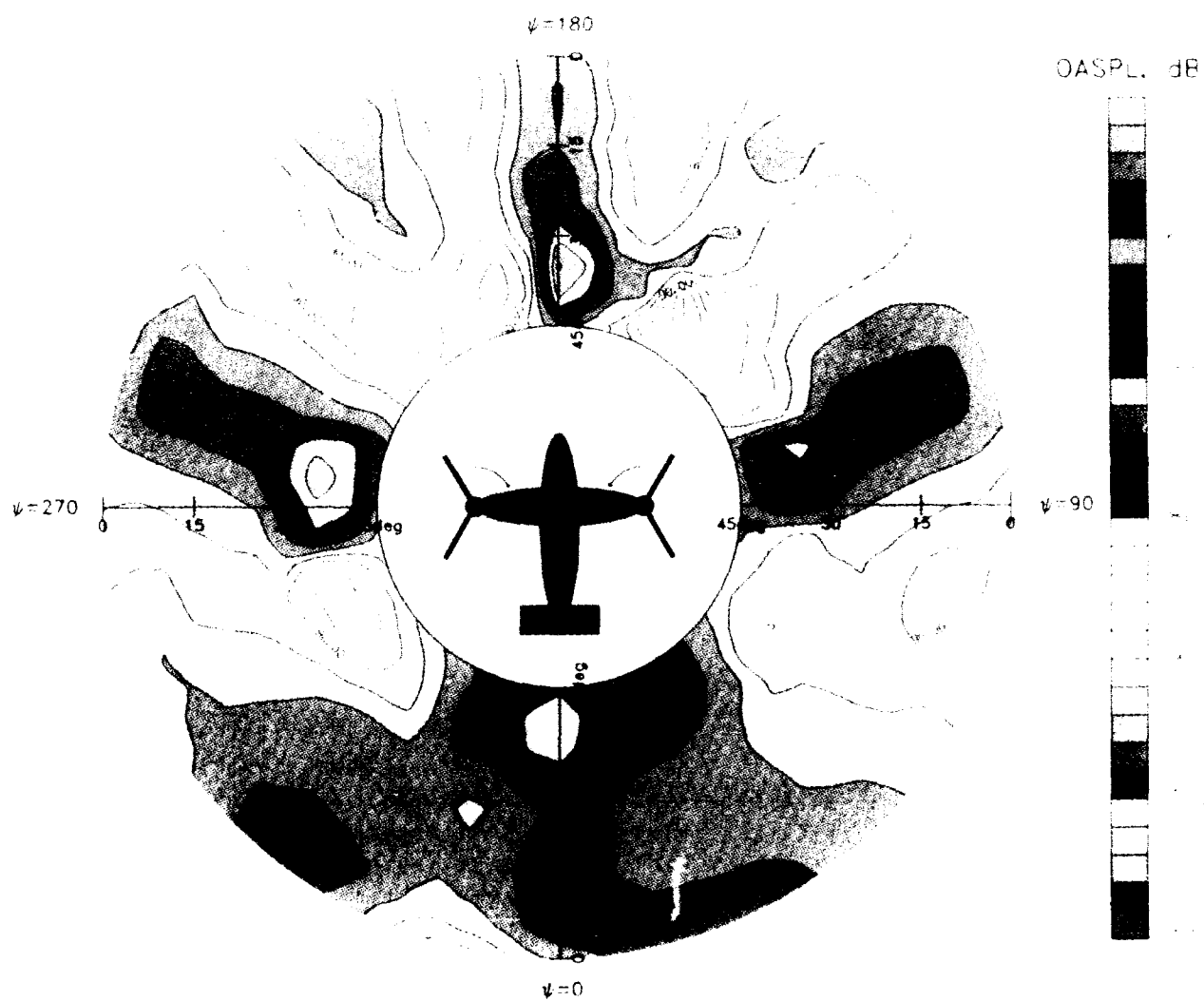


Figure 6-4. Directivity Characteristics of the XV-15 in Hover

6-4 Tiltrotor Hover Acoustics

Objective. To perform full-scale flight tests for validation of ROTONET and to determine methods of minimizing rotorcraft noise.

Approach. A cooperative program with Ames Research Center has been defined to evaluate the acoustic impact in hover of the Advanced Technology Blade system on the XV-15 tiltrotor aircraft. A database for validation of ROTONET is an objective of this program.

Accomplishments. A hover test evaluation of the XV-15 tiltrotor aircraft was conducted at Ames Research Center. The hover test program was conducted in December 1990.

Significance. The results of the hover test program have shown that: (1) A significant reduction of in-plane noise was achieved by reduced rotational speed, as expected. (2) The longitudinal directivity measurements identified a strong impulsive character propagating aft of the vehicle. This character has been identified before and related to the "fountain effect." Triangulation is currently in progress to identify the location of the impulsive source (see figure).

Status/Plans. The acoustic data from the hover test program is being prepared as two articles for publication. AHS Technical Specialist Meeting Rotorcraft Acoustics and Fluid Dynamics. Follow-on test programs are planned for level flight and terminal area descent/ascent conditions: a quick program scheduled for August 1991 and a more comprehensive program scheduled for early 1993.

Danny R. Hoad
Applied Acoustics Branch
Langley Research Center
(804) 864-5060

Brent Wellman, Martin Maisel
Flight Experiments Branch
Ames Research Center
(415) 604-6573/6372

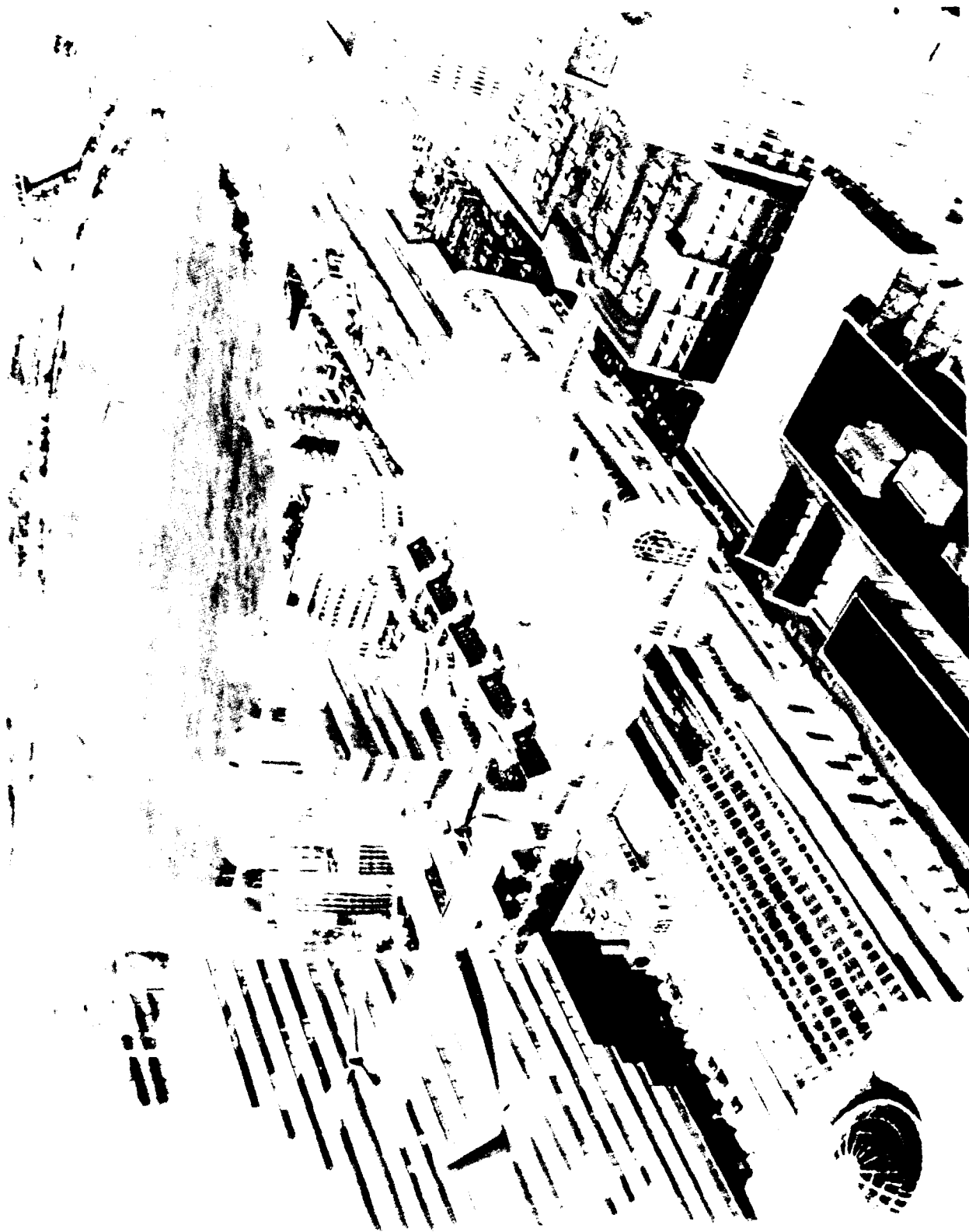


Figure 6-5. Civil Tiltrotor Technology

6-5 Civil Tiltrotor Technology

Objective. To determine the technical, economic, and environmental factors that are critical to the success of commercial, passenger-carrying tiltrotor aircraft in the national transportation system.

Approach. A follow-on study was performed with Boeing Commercial Airplane Group teamed with Bell Helicopter Textron and Boeing Helicopter to identify highest payoff technologies, economic evaluations, market size and "cost/price/ market" loop closure, civil requirements, and the potential changes needed to the V-22 for civil application. Operational analyses were conducted for steep approaches to vertiports, and actions required to achieve a national civil tiltrotor transportation system were defined.

Accomplishments. The study found anticipated demand for a fully designed commercial passenger carrying tiltrotor is forecast to be 2625 vehicles by the year 2000, growing to 4925 in the year 2010. The market value of 2625 aircraft is \$32 to \$42 billion, with half this being a domestic market and the remainder a potential worldwide export market. The study found that the tiltrotor has promise as a means to relieve airport congestion significantly. A projected airline schedule of airline service in the northeast corridor indicated that as replacement commuter aircraft a tiltrotor network could open up 1000 airport slots per day (1/3 of 1989 daily slots).

The study found that the cost/price/market loop can be closed. A fully designed commercial passenger-carrying tiltrotor was found to be different from the V-22 and must overcome three barrier technology challenges: (1) low external noise, (2) human factors-based pilot controls for commercial flight, and (3) terminal area low-speed control and navigation, allowing safe, precise, steep approaches. The study recommends increased research to over-

come the technology barriers and to develop enhancing technology to encourage civil applications.

Significance. The United States holds a commanding lead in tiltrotor technology. This study identified the opportunities, challenges, and actions required to develop a civil tiltrotor aircraft that is both market responsive and effectively integrated in the national transportation system utilizing its unique capability. The development of the recommended actions will reduce the risk to industry.

Status/Plans. The Phase II Study is complete and a final report was released in February. NASA is working with FAA to help determine Pre-Terminal Operating Procedure Criteria for safe, steep approaches to urban vertiports. Barrier technologies and other high payoff technologies are being assessed by NASA for future R & T consideration and the Advanced Tiltrotor Transport Technology new initiative.

John Zuk
Civil Technology Office
Ames Research Center
(415) 604-6568

XV-15 APPROACH

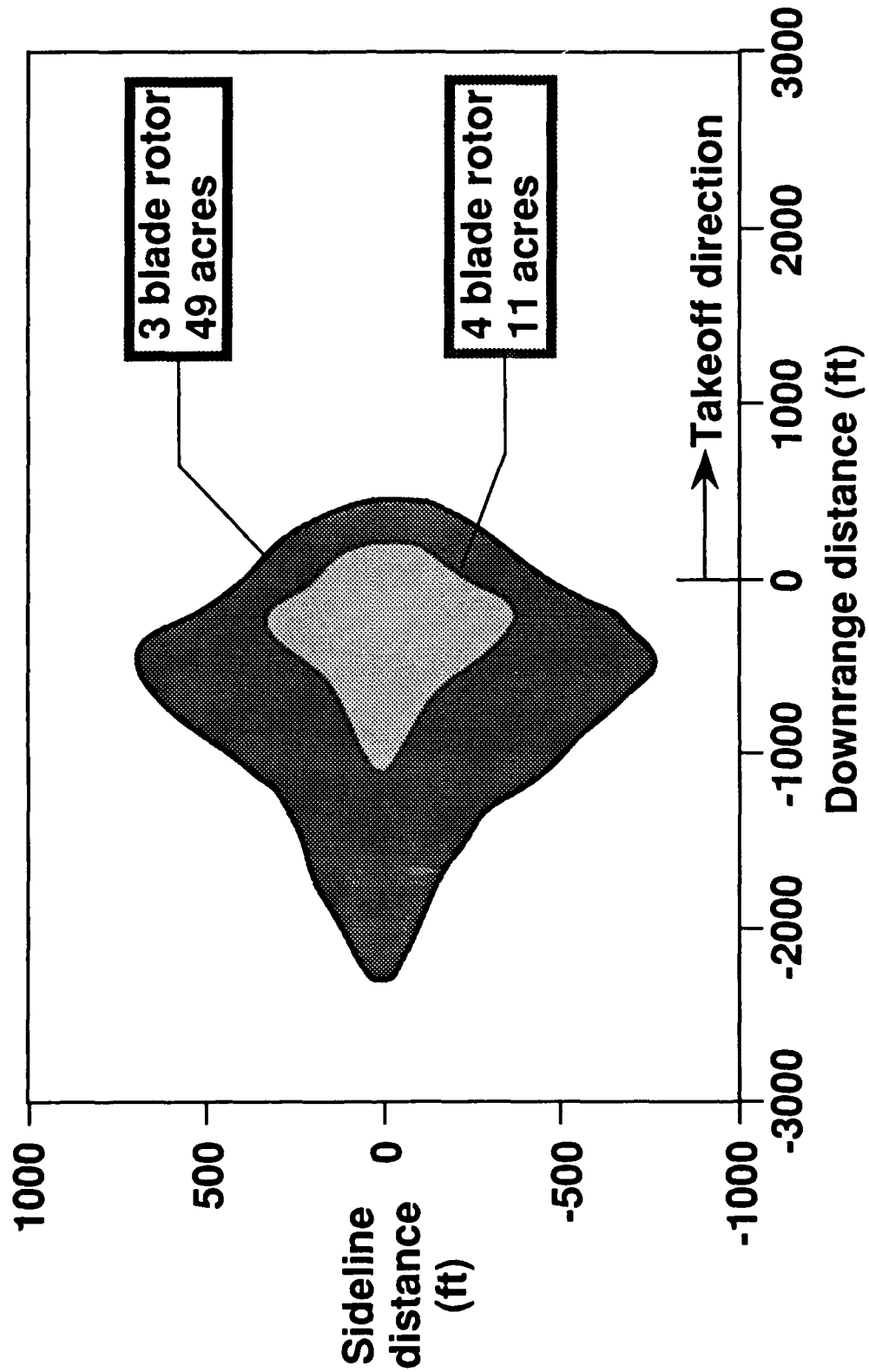


Figure 6-6. Measured Contours of the 65 Day-Night Noise Level (DNL) for the XV-15 Tiltrotor Aircraft With 3 Blades, Corrected for 4 Blades, for Takeoff and Approach Conditions

6-6 Theoretical Determination of Noise Reduction With Increasing Blade Number for the XV-15 Tiltrotor Aircraft

Objective. To predict the change in the 65 day-night noise level (DNL) contour area for a tiltrotor type aircraft as a result of increasing the number of rotor blades per rotor. The flight conditions of particular interest were takeoff and approach.

Approach. Contour corrections were obtained theoretically by comparing ROTONET acoustic predictions made for the baseline XV-15 tiltrotor system (three blades per rotor) with predictions made for the XV-15 modified to four blades per rotor. The resultant correction factor was applied to modify a measured XV-15 ground contour.

The predictions were calculated using ROTONET Phase I and included propagated tone and broadband noise. Effective perceived noise level (EPNL) values were calculated at five rows under the ground track: 63° and 45° port of the ground track; on the ground track; and 63° and 45° starboard of the ground track. All predictions were made for the XV-15 in a level flyover at 90 knots airspeed, 85° nacelle tilt, 95 knots groundspeed, 250 feet altitude, and gross weight of 13,000 pounds. Wing off-loading of rotor thrust was accounted for. Noise values from the port and starboard rotors in isolation were summed to give the combined rotor noise signature. The difference between the predicted baseline EPNL and extra blade EPNL was averaged over the five observer locations. This average was assumed to be a noise reduction attributed to a unit increase in the number of blades per rotor.

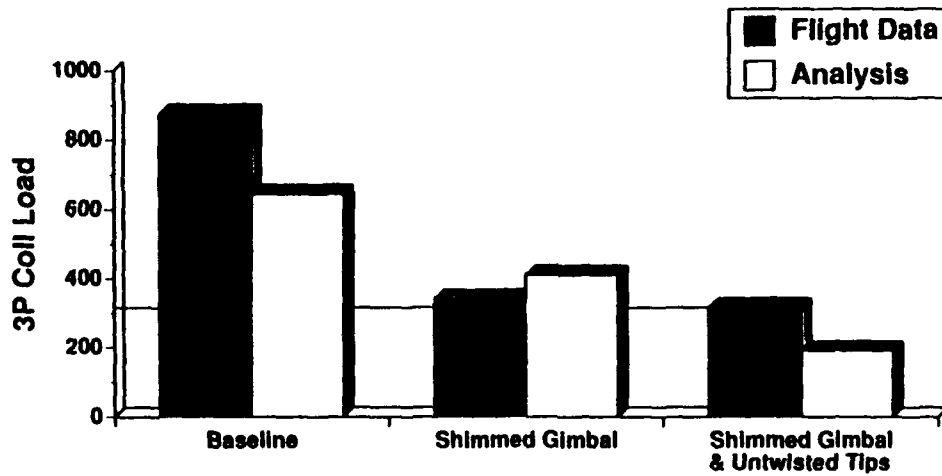
Accomplishments. The resultant noise reduction due to one additional blade per rotor was 6.2 EPNdB. This correction, when applied to the measured XV-15 ground contours (see figures), corresponds to a shrinking of the 65 DNL contour surface area by a factor of 0.23 for both takeoff and approach conditions.

Significance. This study has demonstrated a capability to use the ROTONET system noise prediction code to predict trends and magnitudes of resulting noise reduction from changing rotor system design parameters.

Status/Plans. Future plans will examine the predicted noise results to explain the differences in relative magnitudes of the noise corrections and to apply the approach to other combinations of rotor head design and operating parameters.

Robert A. Golub
Acoustics Division
Langley Research Center
(804) 864-5281

LOW SPEED (35-40 KTS)



Configurations

Figure 1. XV-15 collective actuator loads trends with configuration modifications - comparison of predicted and measured loads at low speed.

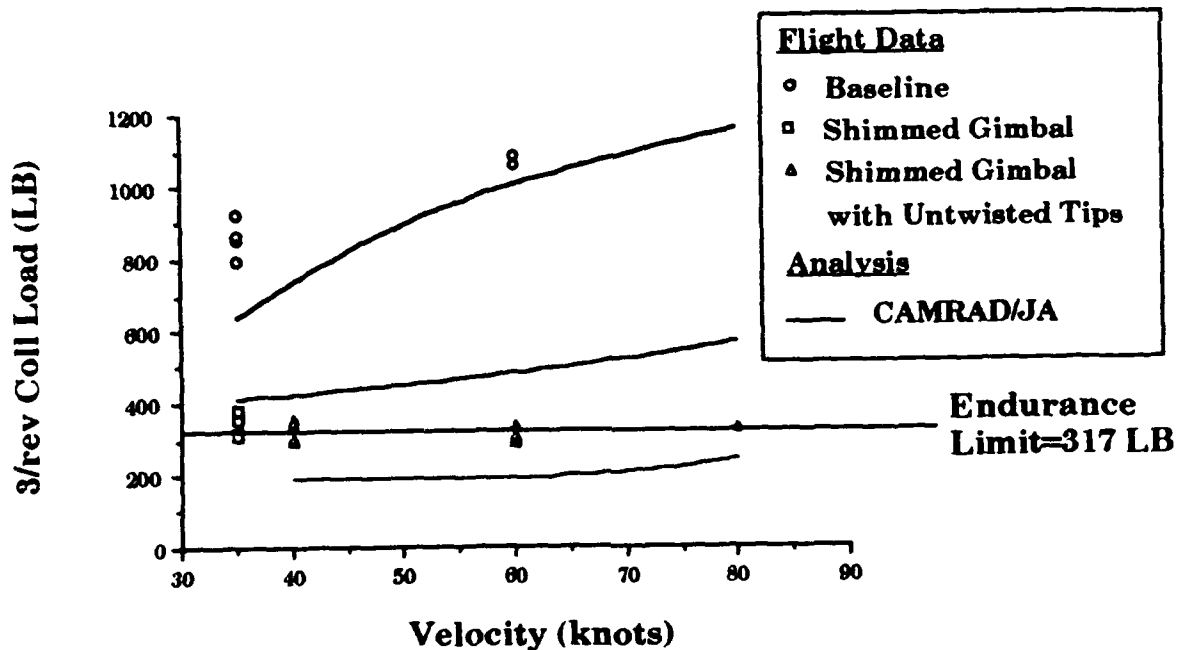


Figure 2. XV-15 collective actuator loads correlation using a modified version of CAMRAD/JA -Helicopter Mode, MSL, 35 to 80 KTS

Figure 6-7. XV-15/ATB Flight Investigations: Advanced Technology Blades Loads, Stability, and Performance

6-7 XV-15/ATB Flight Investigations: Advanced Technology Blades Loads, Stability, and Performance

Objective. To investigate advanced technology applied to tiltrotor blades for its impact on the performance, dynamics, loads, and aeroelastic stability of the advanced Technology Blades. These data provide a configuration perturbation for the development and validation of analytical prediction codes.

Approach. Advanced aerodynamics and mixed matrix composite materials are combined in the design of the Advanced Technology Blades (ATB) for XV-15 Tiltrotor Research Aircraft. The highly twisted blades are configured with a compound planform, thin tips, and an increased solidity to improve hover lift capability without degrading performance at high speeds in the airplane mode. Flight tests of the ATB will support the development of a broad range of analytical methodologies.

Accomplishments. Initial flight testing revealed unanticipated high oscillatory loads in the XV-15 rotor control system. Subsequent analyses identified potential control system and blade modifications to reduce loads and improve structural dynamic stability. To validate the analyses, variations of tip twist, blade chordwise, e.g., control stiffness, and blade sweep have been examined in flight. The most significant factor in the reduction of loads tested to date is the increase of the cyclic swashplate stiffness, accomplished by a temporary modification, which displaced the natural frequency of the system sufficiently far from the rotor 3-per-rev excitation to enable evaluation of the ATB's performance and loads in all operational modes. Also, improvements to the Stability and Control Augmentation System (SCAS) have been installed for flight evaluations.

Significance. The measured XV-15/ATB control loads flight investigation revealed limitations and deficiencies in current analytical and design methods. The flight data provides

an important configuration perturbation (from the original XV-15 metal blades) to develop and validate predictive codes.

Status/Plans. A scheduled 200-hour major transmission inspection and overhaul will follow the completion of the FY 1991 XV-15/ATB flight tests. A vibration survey will be conducted immediately following the flight activity to document the airframe resonant frequencies in support of the dynamics and load analyses. Control system and blade modifications to increase stability and reduce loads will be performed during the inspection period. A full spectrum of tiltrotor flight experiments in support of the advanced tiltrotor transport technology activity will commence in late FY 1992 after the inspection/overhaul effort is completed.

Brent Wellman, Martin Maisel
Flight Experiments Branch
Ames Research Center
(415) 604-6573/6372

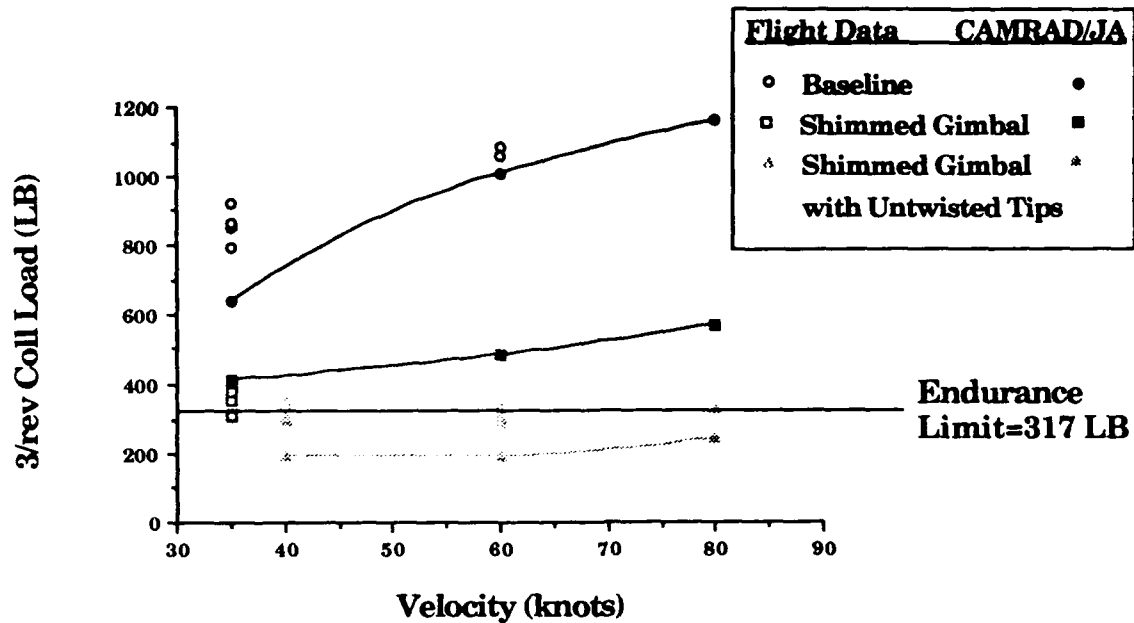


Figure A XV-15/ATB collective actuator loads correlation using a modified version of CAMRAD/JA - Helicopter Mode, 35 to 80 KTS

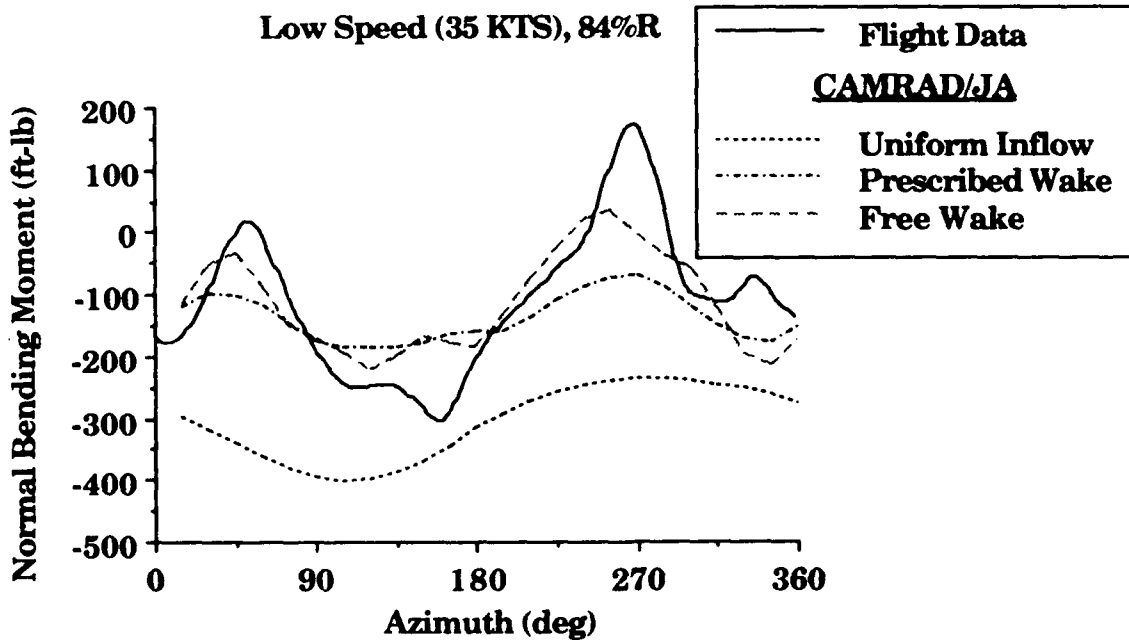


Figure B XV-15/ATB Normal bending moment correlation using a modified version of CAMRAD/JA showing variation in correlation for different wake models - Helicopter Mode, MSL, 35 KTS.

Figure 6-8. Analysis of Tiltrotor Phenomena Utilizing CANRAD/JA

6-8 Analysis of Tiltrotor Phenomena Utilizing CAMRAD/JA

Objective. To evaluate the accuracies of the state-of-the-art comprehensive rotorcraft analysis codes, such as CAMRAD/JA (Comprehensive Analytical Model of Rotorcraft Aerodynamics and Dynamics/Johnson Aeronautics), in the prediction of rotor system performance, loads, and stability and to identify and address sources of inaccuracies to enhance the analysis and design of advanced rotor systems.

Approach. Extensive correlation efforts identified the limitations of the current state-of-the-art in comprehensive rotorcraft analysis codes. Improvements in the comprehensive codes will be judged by respective improvements in correlation. Advanced high-speed tiltrotor blade optimization efforts also have been initiated using a rigorous two-point optimization of the XV-15/ATB (Advanced Technology Blades) rotor system. The validity of the results of the optimization effort will be strengthened by improvements in correlation of the current state-of-the-art comprehensive codes.

Accomplishments. Extensive correlation efforts have been performed and reported using predictions generated from a modified version of CAMRAD/JA and XV-15/ATB rotor correlated with control system loads flight data, as shown in Figure A. This effort identified the importance of accounting for control system flexibility. The modified version of CAMRAD/JA reflected the flexibility, and this resulted in improved correlation. This modified version of CAMRAD/JA is currently being used to generate results for the advanced high-speed tiltrotor blade optimization effort. The predicted performance and stability gains resulting from this effort will reflect the improved accuracies obtained with the modified version of CAMRAD/JA.

Extensive correlation results have been obtained utilizing CAMRAD to predict airloads for the AH-1G and correlating them with AH-1G airload measurements.

A major effort was also undertaken to upgrade the UH-60 CAMRAD model through improved input and input source documentation as requested by UH-60 PEER Review.

Significance. Improvements in correlation will strengthen the validity of the optimization work and lead to a realistic rotor blade design for advanced helicopters and high-speed tiltrotor configurations. Improvements in performance and aeroelastic stability must be achieved to enhance the feasibility and various measures of aircraft efficiency for rotorcraft at high speeds.

Status/Plans. Further aeroelastic stability and airloads correlation efforts are planned for the XV-15/ATBs, the AH-1G Cobra, and the UH-60 Phase II program to ensure that inaccuracies are identified and comprehensive rotorcraft analysis codes are improved and reflected in the advanced high-speed tiltrotor blade optimization effort.

J. J. Totah, J. F. Madden III
Rotorcraft Technology Branch
Ames Research Center
(415) 604-4126

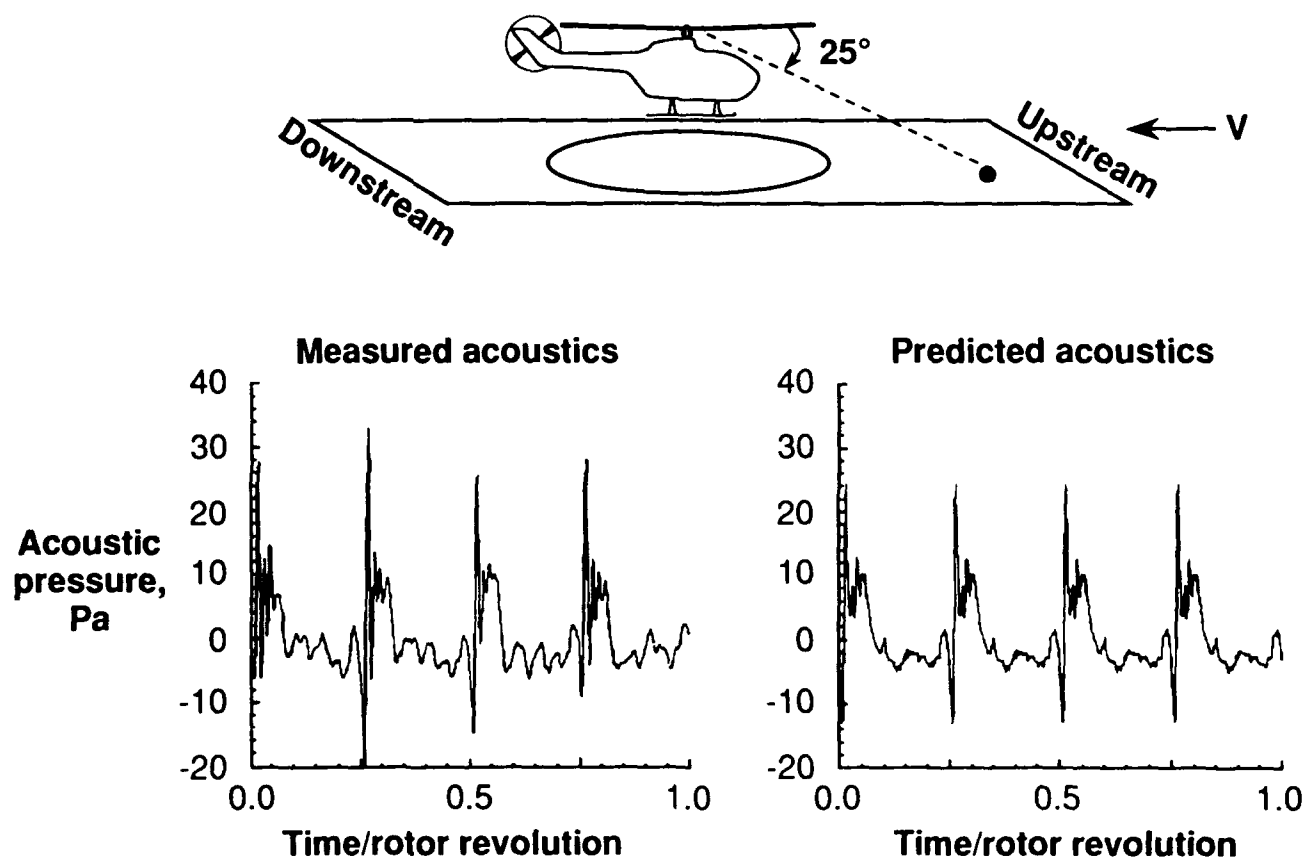


Figure 6-9. Comparison of Measured and Predicted Acoustic Signal for a Model Helicopter at a Strong Blade-Vortex Interaction Noise Condition

6-9 Blade-Vortex Interaction Noise Prediction Validation

Objective. To understand rotorcraft noise source mechanisms and to develop and validate noise prediction codes, specifically to validate a Langley-developed noise prediction code for blade-vortex interaction (BVI) noise using measured rotor blade surface pressures.

Approach. Far-field noise and blade pressure data obtained from a model rotor test were employed to validate the rotor noise prediction code, WOPWOP, for BVI noise. The test was a cooperative effort between Sikorsky Aircraft, the United Technologies Research Center (UTRC), NASA Langley and Ames Research Centers, and the U.S. Army Aeroflightdynamics Directorate. The model rotor was a 1/6 scale, 4-bladed, swept-tip design. The rotor blades were instrumented on both the upper and lower surfaces with 176 recess-mounted pressure transducers. This large number of transducers, combined with a high data digitization rate, resulted in a high resolution aerodynamic database. The blade pressure resolution was sufficient to capture short time events, such as BVI. Noise predictions were made using the measured blade pressures as input into the noise prediction code WOPWOP. The predicted noise time histories were then compared with the measured time histories.

Accomplishments. Measured and predicted acoustic time histories have been compared for a number of rotor operating conditions and measurement locations. A comparison between predicted and measured results for a BVI case at a moderate flight speed of 85 knots is presented in the figure. The top figure illustrates the microphone position under the flight path, and the lower figures show the measured and predicted acoustic results. The results are presented for one-rotor period and clearly show the impulsive BVI noise from each of the four blades. The comparison is good, allowing for blade-to-

blade variability in the measured data. The major features of the measured data are fairly well reproduced in both shape and magnitude.

Significance. The rotor noise prediction code WOPWOP can predict BVI noise given accurate high resolution blade loads data as input. This is significant because noise predictions made with predicted blade loads have not been in good agreement with measured noise data. The recently obtained acoustic and blade pressure data will add immensely to the understanding and development of predictions for both rotor blade loads and acoustics.

Status/Plans. Noise predictions for a variety of operating conditions will be made and compared with measured data. In addition, noise predictions from predicted blade loads will be made and compared with measured results. The predicted and measured blade loads will be compared and deficiencies in the predicted blade loads will be identified. This will allow for the development of an improved blade loads prediction and thus a better noise prediction capability.

Casey L. Burley
Acoustics Division
Langley Research Center
(804) 864-3659

Rotor Disk Loading

10°
resolution



1°
resolution

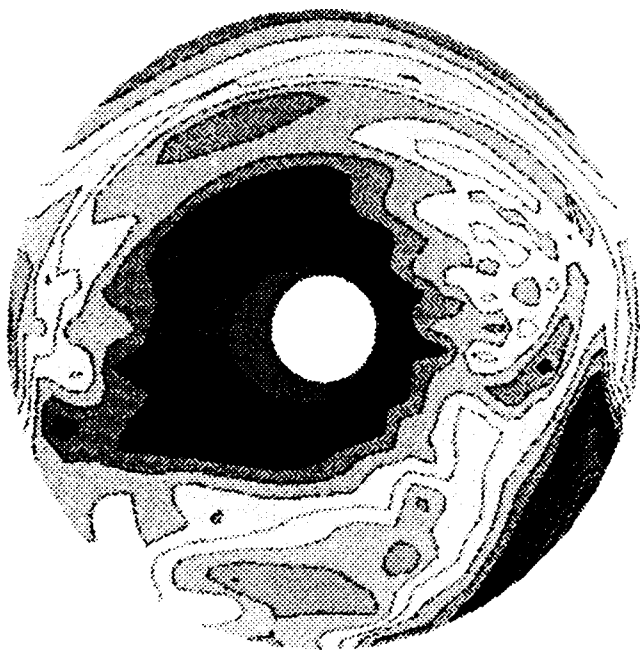


Figure 6-10. Comparison of Predicted Rotor Blade Loading for 10° Azimuthal Resolution and 1° Resolution

6-10 High Resolution Rotor Blade Loads for Blade-Vortex Interaction Noise Prediction

Objective. At present, the missing element in providing Langley with the first fully analytical prediction capability for helicopter main rotor noise is the specification of detailed blade loading. A study was undertaken to provide this detail, through a unique recoding and post-process modeling of the rotor performance code Comprehensive Analytical Model of Rotorcraft Aerodynamics and Dynamics (CAMRAD).

Approach. The accurate prediction of impulsive blade-vortex interaction (BVI) noise, as well as the prediction of low frequency loading noise when BVI occurs, requires accurate blade loading definition at azimuthal steps of 1° or less, as well as small radial blade increments. The well-known and often used performance code CAMRAD has sophisticated free-wake and aeroelastic blade modeling, but it has a 15° azimuthal resolution limitation. The approach taken to obtain a high resolution version of CAMRAD was to first increase the code resolution version of CAMRAD to the intrinsic limit (found to be 10° azimuth). Post-processing codes were developed to determine blade positions and tip vortex strengths and trajectories at very small incremental steps of 1° . At each incremental step, the induced velocities and blade sectional loadings were calculated.

Accomplishments. The CAMRAD code modifications and the post-processing code for the free wake and first order unsteady aerodynamics have been completed. An application of the code is shown in the figure, where the rotor disk loading, the lift encountered by the blades as they rotate, is plotted. Compared with the 10° resolution results, the 1° high-resolution results offer an order of magnitude increase in the level of detail and understanding of the blade-wake interactions. The loading reveals the tip vortex positions and the locations where they pass through the rotor disk. The high-resolution code has been

applied successfully in support of an experimental effort to reduce BVI noise through the use of higher harmonic control (HHC) of blade pitch. After incorporating HHC capability into the code, the effect of HHC on BVI noise levels was accurately predicted.

Significance. The effort has produced a more sophisticated and versatile prediction capability for the harmonic loading and impulsive BVI noise. The long experience of government and industry researchers in the use of CAMRAD for aerodynamic and aeroelastic calculations makes a high resolution version particularly attractive.

Status/Plans. Efforts are under way to complete the loads definition by installing a near wake model, as well as an advanced unsteady aerodynamics model. Detailed noise directivity predictions are to be obtained by using the high-resolution loading calculations in Langley's WOPWOP rotor noise code, and these will be compared with existing acoustic data sets. The code will continue to be applied in support of the noise reduction research on higher harmonic control.

Thomas F. Brooks
Acoustics Division
Langley Research Center
(804) 864-3634

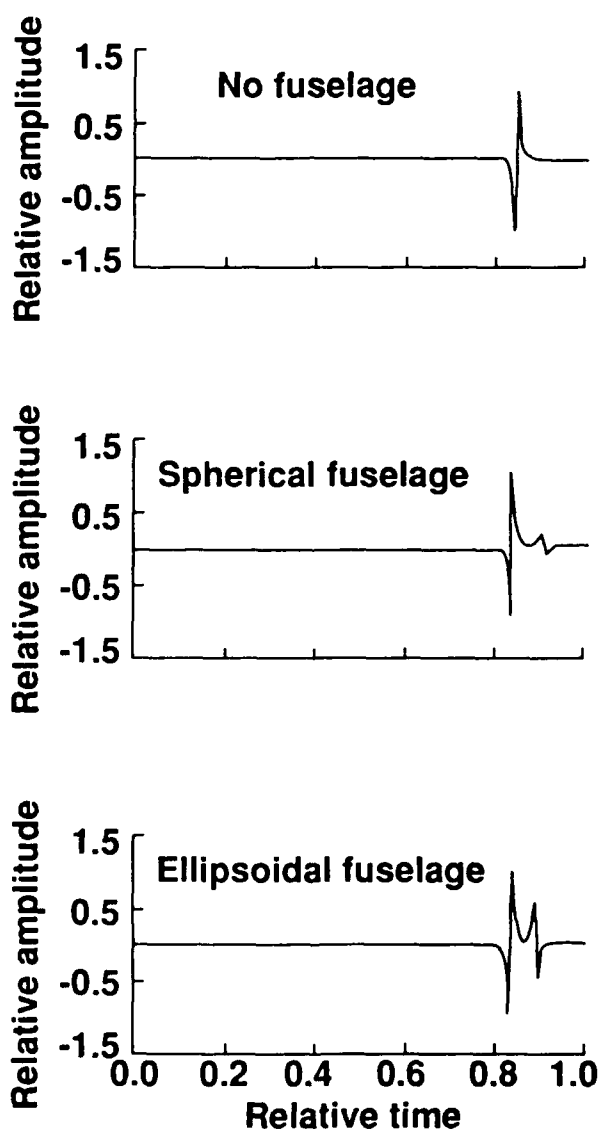
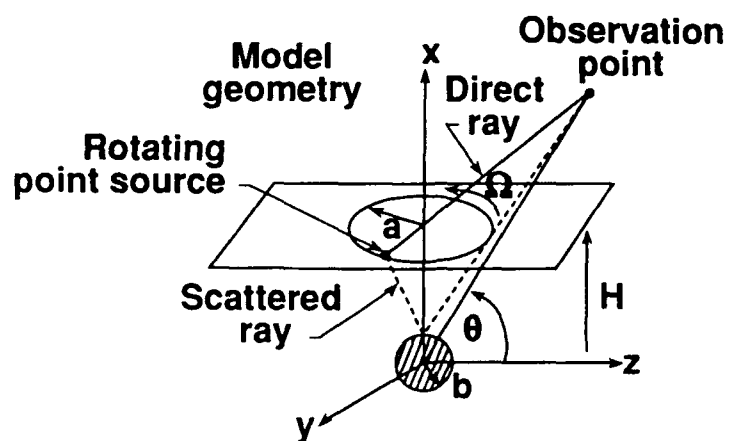


Figure 6-11. Predicted Effects of Fuselage Scattering of an Impulsive Rotor Noise Signal

6-11 Ray-Acoustics Approach to Fuselage Scattering of Rotor Noise

Objective. To predict the acoustic field of installed rotors and propellers. The specific objective of the present research is to develop a numerical method for the aircraft fuselage scattering of noise from a rotor.

Approach. A numerical implementation of ray acoustics theory in conjunction with a paraxial ray approximation is used to model the scattering of an impulsive noise source by a fuselage. This is a two-point ray tracing problem, where both the source position and observer location are known in space. This is modeled as a boundary value problem that requires an iterative solution, and is very expensive to solve computationally. In order to improve numerical efficiency, paraxial ray approximation (PRA) is used. This is developed from a Gaussian beam method (GBM), where Gaussian beams are high-frequency asymptotic time-harmonic solutions to the wave equation, and are concentrated close to rays. A GBM solution requires no iteration, but does involve a superposition of a large number of beams to compute the noise at a given observer location. The PRA evaluates the time-travel ray path and amplitudes both along the ray and in its vicinity. So a single ray can be used to obtain the solution at the observer, providing it passes sufficiently close to the observer position.

Accomplishments. An example of the fuselage scattering result is given in the figure for rotor impulsive noise source modeled as a point load rotating in a plane above the scattering body. The geometry of the model is shown in the figure. The point loading rotates at angular velocity Ω , on a disk of radius a , at a height H above the body. A spherical body of radius b is depicted in the figure. Numerical results are also shown in the figure for three different scattering bodies at an observer angle θ of 45° , $b/a=0.5$, $H/a=0.5$, and a source Mach number ($\Omega a/\text{speed of sound}$) of 0.7. The result for a free-field case, where

there is no fuselage, and a single impulse is seen. For the case of a sphere, the initial impulse is received cleanly, and is followed by a smaller, broader pulse due to scattering from the sphere. Where the sphere is replaced by an ellipsoid, a larger amplitude scattered pulse is seen. These results are highly dependent on observer position in addition to the shape of the scattering body.

Significance. Acoustic scattering from wing and fuselage surfaces for full aircraft configurations is always a concern in experimental aeroacoustics. In addition, model supports, microphone struts, and other wind tunnel hardware can cause reflection and scattering problems. This technique can be used to help understand measured acoustic results, and especially to explain differences between measured results and theoretical predictions, as predictions usually do not include scattering surfaces.

Status/Plans. A "user-friendly" version of the numerical implementation of this theory is being developed. This will be a useful diagnostic tool to the experimental acoustician, who will be able to define the specific geometrical setup of a particular test.

Michael A. Marcolini
Acoustics Division
Langley Research Center
(804) 864-3629

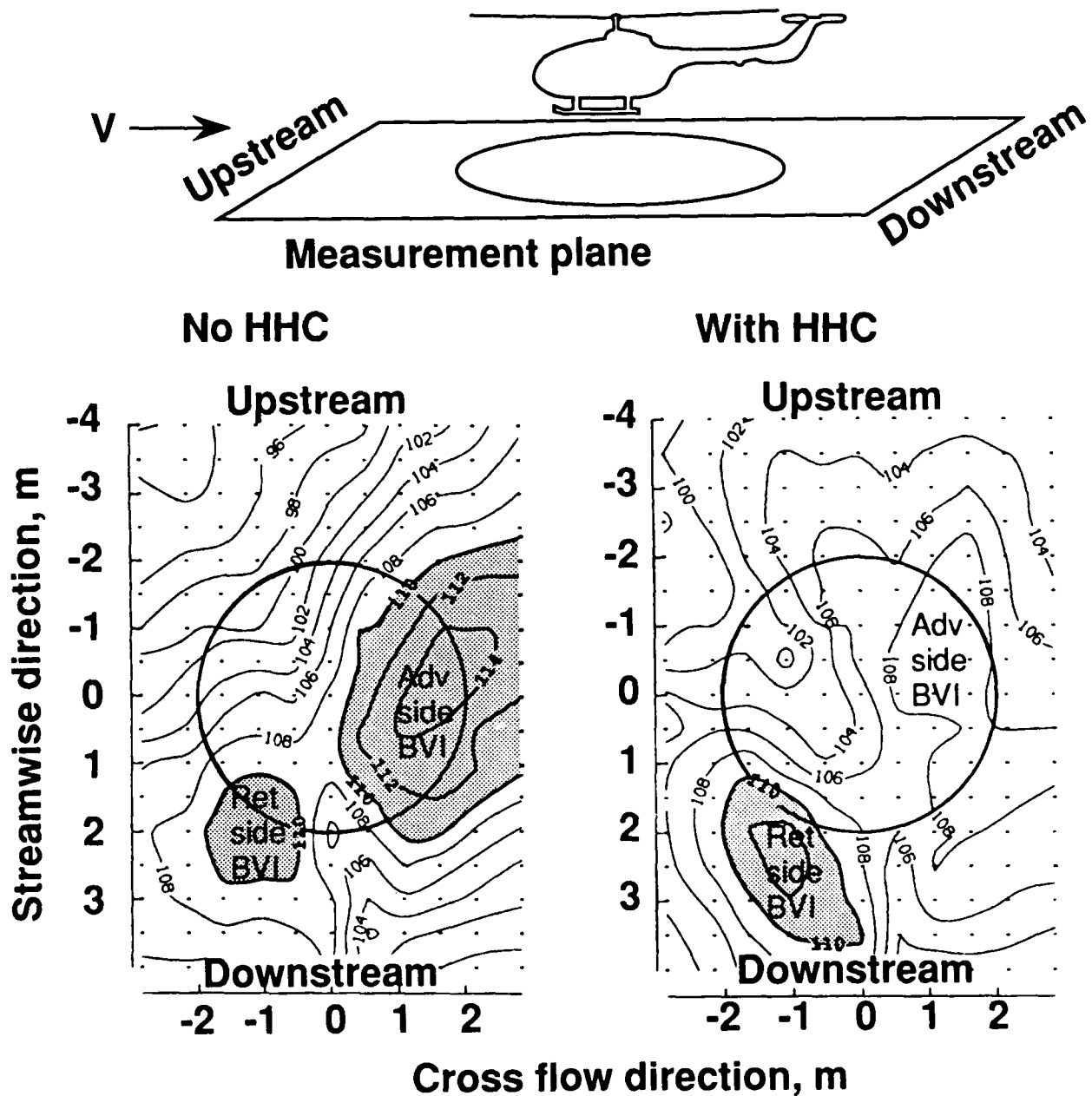


Figure 6-12. Comparison of Mid-Frequency Noise Contours for the BO-105 Rotor in Normal Flight and With Higher Harmonic Control

6-12 Rotor Impulsive Noise Reduction Using Higher Harmonic Control

Objective. Impulsive blade-vortex interaction (BVI) noise is one of the most objectionable types of helicopter noise. A previous rotor noise experiment in the Langley Transonic Dynamics Tunnel (TDT) proved that higher harmonic control (HHC) of blade pitch could reduce overall sound power. This experiment was undertaken to obtain the effect of HHC on the directivity of BVI noise.

Approach. The test, conducted in the anechoic German-Dutch Wind Tunnel (DNW), was a cooperative effort between NASA Langley, the German aerospace research establishment DLR, and the European helicopter companies MBB and Aerospatiale. A large database was acquired for a 40% scale model of the MBB BO-105 main rotor. Noise and vibration measurements were made for a range of operating conditions where higher harmonic blade pitch was superimposed on the normal collective and cyclic trim pitch. HHC control modes of 3 per rev (3P), 4P, and 5P at various amplitudes and phases were tested, as well as special mixed 3P/4P/5P modes. The noise was measured over a large measurement plane underneath the model rotor using a traversing in-flow microphone array.

Accomplishments. It was found that the BVI noise directivity could be significantly modified by using HHC. The figure presents BVI noise contour plots over the measurement plane for a particular descent flight condition, advance ratio of 0.15 and an equivalent descent angle of 6° , which is considered typical for full-scale helicopters. On the left, a baseline case is shown where HHC is not used. The levels given are mid-frequency values and represent the BVI portion of the total noise. The plot to the right is the noise contour for a particular HHC pitch schedule which causes a significant 6 dB reduction in the advancing side lobe levels, although the retreating side increases by 2 dB. The rela-

tive levels and directivity can be modified by changing the area of the rotor disk in which the HHC is employed.

Significance. This database is the first available on BVI noise radiation and directivity using HHC. The results support the key conclusion of the previous Langley test that HHC can be used to reduce BVI noise for descending flight conditions where BVI noise is most important. These results are doubly significant because of the two different rotor types used in the investigations. The present rotor is hingeless with dynamically scaled blades, while the rotor tested in the TDT was fully articulated with much stiffer blades.

Status/Plans. Analysis is continuing to establish more fully the BVI noise reduction benefits versus operational and HHC parameter variations. In addition, the vibration and low frequency noise data will be used to help establish the practicality of particular controls. The results will be compared with acoustic and vibratory predictions based on an improved high-resolution loading version of the CAMRAD rotor performance program currently under development at Langley.

Thomas F. Brooks
Acoustics Division
Langley Research Center
(804) 864-3634

JOINT ARMY BOEING RESEARCH PROGRAM

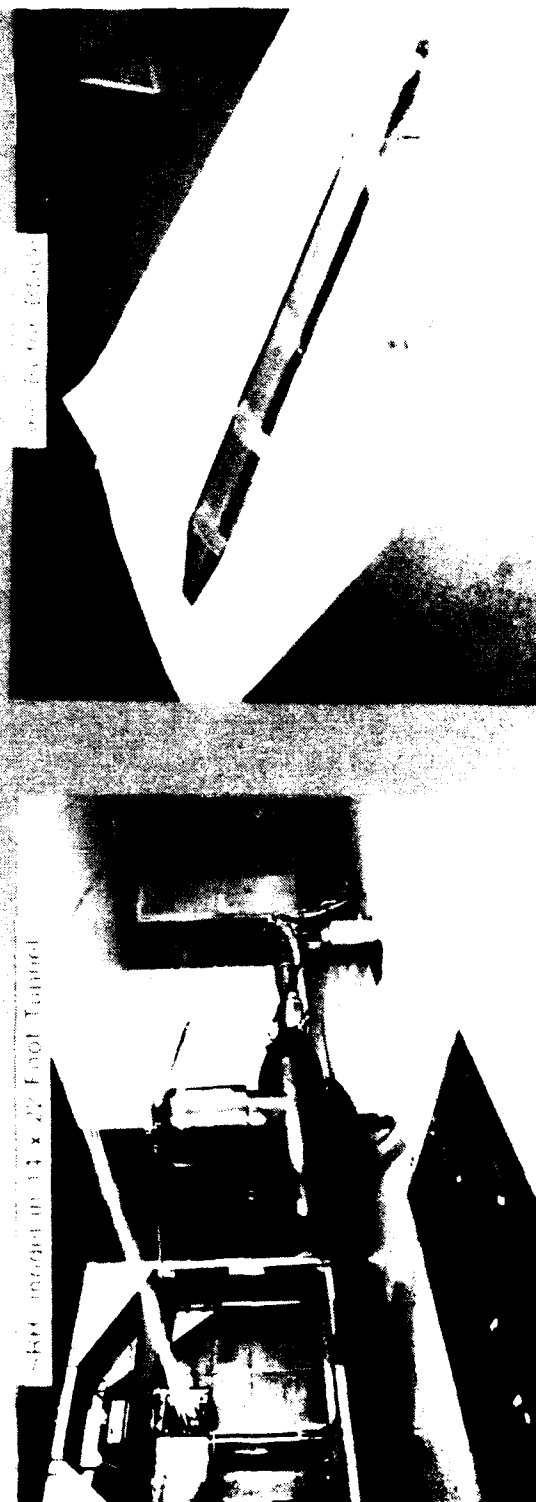


Figure 6-13. Joint Army/Boeing Research Program

6-13 Cooperative Army/NASA/Boeing Pressure-Instrumented Rotor Program

Objective. To (1) investigate the basic formation of the rotor wake directly behind the advancing blade, (2) validate a circulation box technique for measuring rotor loads, and (3) capture a blade-vortex interaction occurrence in the rotor wake.

Approach. A wind tunnel test was conducted in the 14- by 22-foot subsonic tunnel using the Boeing Single Rotor Helicopter (SRH) drive system, a pressure-instrumented model of the Boeing 360 rotor and a two-component laser velocimeter. Measurements of the dynamic blade surface pressures and the flow-field velocities were obtained for several flight conditions.

Accomplishments. Measurements of the blade surface pressures using the 66 transducers installed in the four rotor blades and velocity measurements using the laser were made for nine flight conditions ranging from high-speed forward flight to descent conditions. Velocity data were obtained for over 1600 flow-field measurement locations. In all cases, average pressure and velocity data as well as time-dependent data were acquired.

Significance. These data will be used to correlate surface pressure measurements with wake velocity measurements to determine the nature of the forcing function for rotor blade airloads. These data also provide a link between the acoustic measurements obtained in the German Dutch Wind Tunnel (DNW) and the flow-field phenomena which generates rotor noise. The data identifying the formation of the rotor tip vortex and wake will be used to improve analytical predictions of rotor wakes. The velocity data around the blade in a box will be used to validate the circulation measurement technique, and, if successful, will lead to the capability to mea-

sure blade loading without expensive and troublesome pressure transducers in the rotor blades.

Status/Plans. The pressure data are being digitized and reduced at Boeing Helicopters. The laser velocimeter data will be processed at Langley. A joint publication is anticipated next year. Correlation with analysis will be done both at Boeing with their proprietary B-65 code and at Langley using CAMRAD-JA with FPR coupling.

Susan L. Althoff
Subsonic Aerodynamics Branch
Langley Research Center
(804) 864-5059

Full- and Small-scale, $\mu = 0.20$, $C_T = 0.055$, $\alpha_B = 0^\circ$

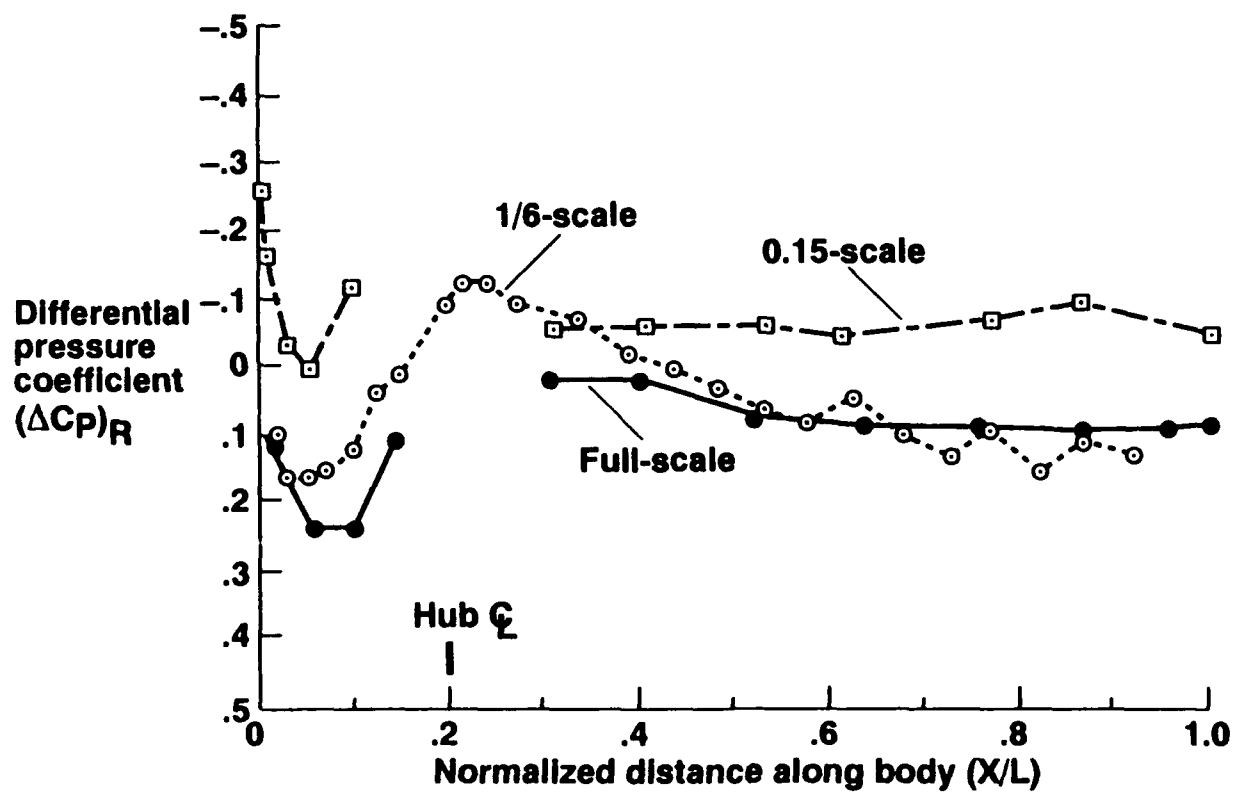


Figure 6-14. Effect of Rotor on Upper Surface Pressures

6-14 Rotor/Fuselage Aerodynamic Interactions Program

Objective. To quantify rotor/fuselage aerodynamic and acoustic interactions through wind tunnel testing and computation. The program results will assist in the design of rotorcraft systems by taking advantage of mutually beneficial aerodynamic interactions.

Approach. To achieve the program objective, a full-scale test of a Bell 412 rotor system with a simple axisymmetric fuselage was conducted in the 40- by 80-foot wind tunnel at Ames. Small-scale tests with similar fuselage shapes have been conducted in the past.

Accomplishments. Data from the 40- by 80-Foot Wind Tunnel test has been reduced and analyzed. A paper based on the test results was presented at the 1991 American Helicopter Society Forum.

Significance. Results from the wind tunnel test revealed that the magnitude of the aerodynamic interactions on the simple fuselage were small. The importance of rotor shaft and hub interactions was also shown. In addition, comparisons between full-scale and small-scale results demonstrated the importance of model configuration and installation differences. For example, the figure shows a comparison of the rotor effect on the upper surface pressures for full- and small-scale data. In the figure, $(\Delta C_p)_R$ represents the difference in pressure coefficient that is due to the rotor. The large differences between the full-scale and 1/6-scale results are attributed mainly to the lack of a rotor mast in the 1/6-scale test. The reason for the offset between the full-scale and 0.15-scale data is unclear, although potential causes include the unscaled hub and significantly different model mounting system used in the 0.15-scale test.

Status/Plans. Plans are to complete the documentation of the full-scale wind tunnel test results.

Thomas R. Norman and
Rotorcraft Aeromechanics Branch
Ames Research Center
(415) 604-6653

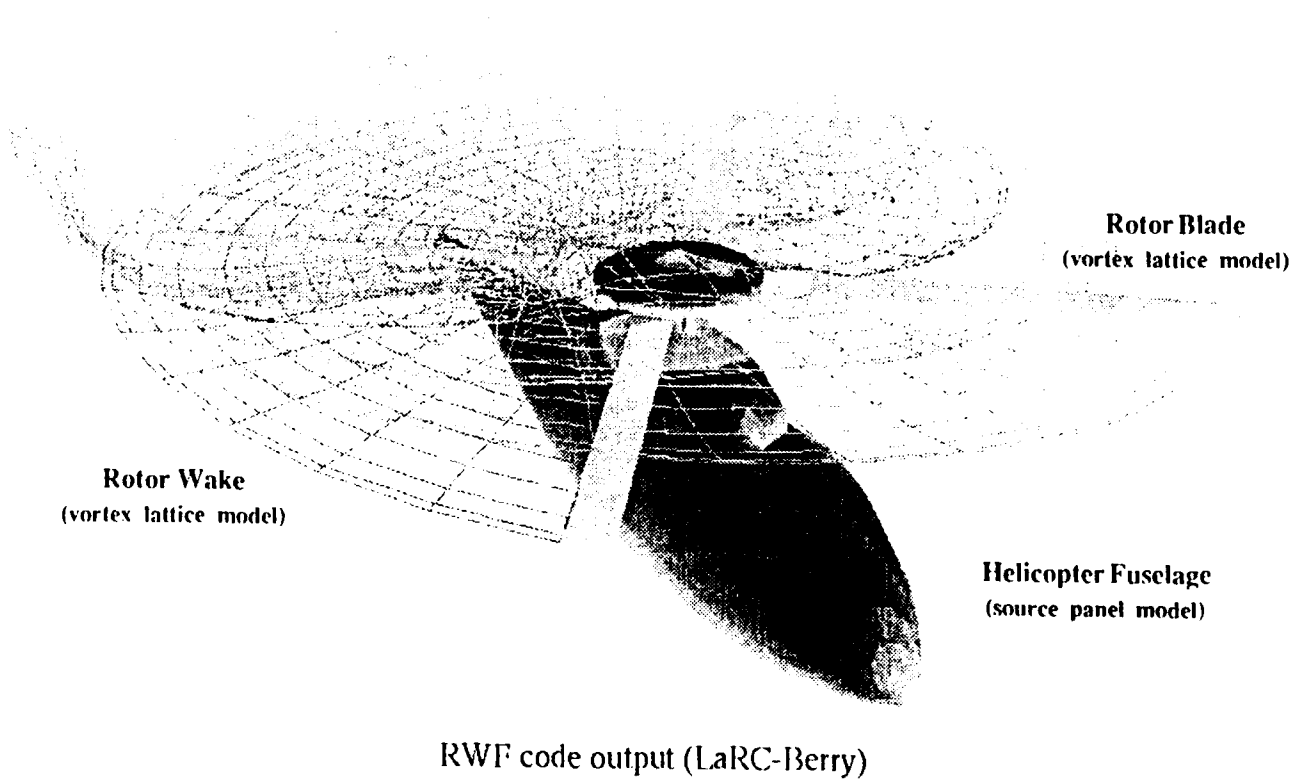


Figure 6-15. Rotor-Wake-Fuselage Code Development

6-15 Rotor-Wake-Fuselage Code Development

Objective. To predict the aerodynamic environment of a realistic helicopter configuration which accounts for the interaction of the rotor wake and the helicopter fuselage.

Approach. This program has been an in-house development effort. Existing code elements for computing the wake from a single rotor blade and the influence of a nonlifting source panel have been integrated into a code that computes the interacting flow field of multiple rotor blades with cyclic pitch, their shed wakes, and a nonlifting fuselage. The resulting computer code Rotor-Wake-Fuselage (RWF) has been under preliminary development since 1986.

Accomplishments. During FY 1991, preliminary copies of the implementing code (RWF) have been provided to two requesting U.S. helicopter companies. A version of the

code is under modification for production operation on the Langley Supercomputer Network System (SNS). The code is being used to assess fuselage effects on rotor inflow.

Significance. The computer code RWF is a valuable tool for investigating of realistic fuselage effects on helicopter configurations.

Status/Plans. After validation of the SNS production version of the RWF code, the code will be made available to interested U.S. users. A low level of continuing development is planned to respond to requirements of the target user community.

John D. Berry
Subsonic Aerodynamics Branch
Langley Research Center
(804) 864-5090

FOUR-BLADED BEARINGLESS ROTOR
CORRELATION WITH EXPERIMENT
4 DEG SHAFT ANGLE; ADV RATIO=0.23

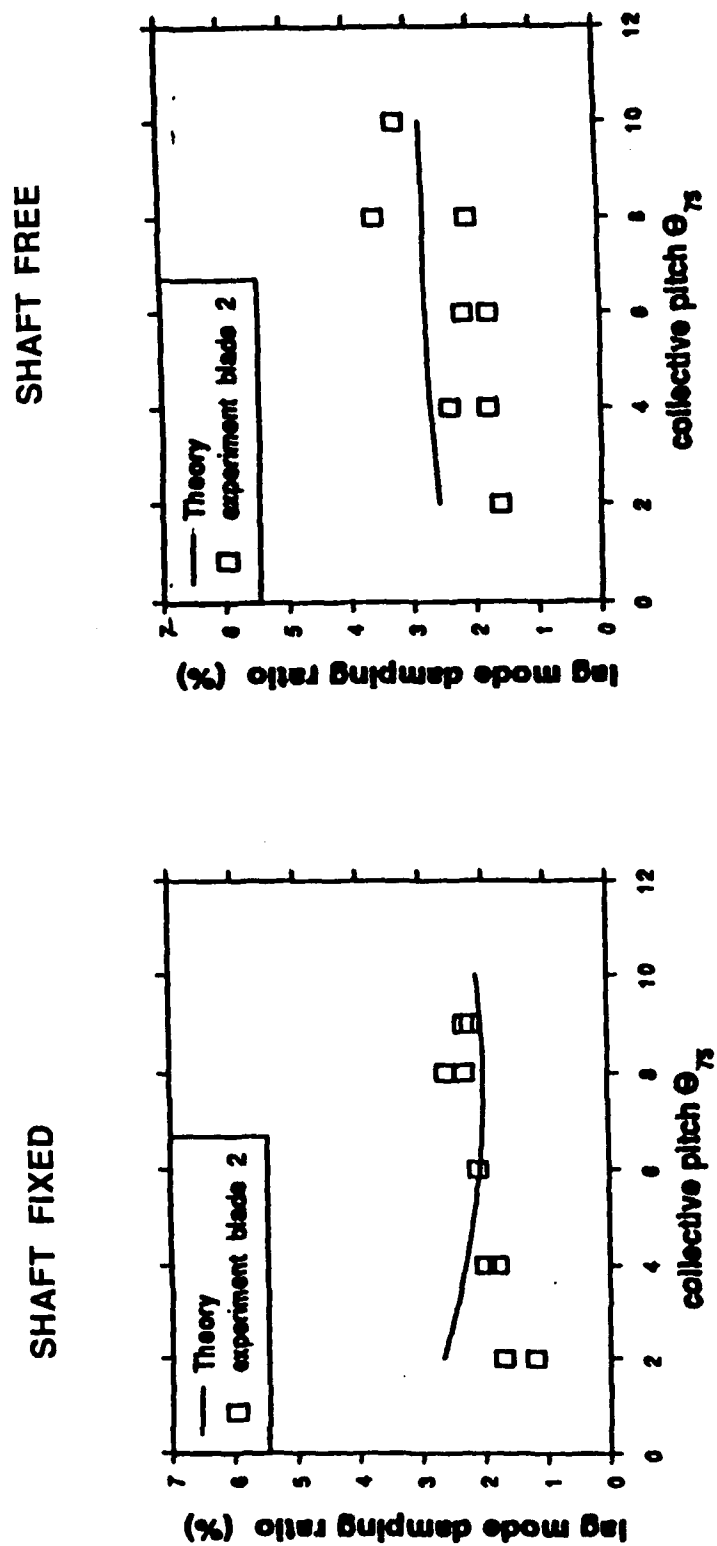


Figure 6-16. University of Maryland/Ames Research Center Bearingless Rotor Aeroelastic Analysis

6-16 Five-Bladed Bearingless Rotor Program

Objective. To document the performance, loads, and stability of five-bladed bearingless rotors, and to develop and validate comprehensive analyses to accurately predict and design new rotor configurations.

Approach. Testing of the McDonnell Douglas Helicopter Company (MDHC) Advanced Bearingless Rotor (MDAR) and the Sikorsky Five-Bladed Bearingless Main Rotor (SBMR) was conducted in the 40- by 80-foot wind tunnel through the flight envelope up to 200 knots. A comprehensive database on rotor performance, blade, flexbeam and torque tube loads, and aeroelastic stability was acquired. The results of these test programs will assist in the development and validation of the University of Maryland Advanced Rotorcraft Code (UMARC).

Accomplishments. A joint cooperative program was established for the MDAR tests. The first test was scheduled for the fourth quarter of CY 1991 in the 40 x 80 on the MDHC test stand. The second phase of the program with a pressure instrumented rotor has been initiated. A joint cooperative program was established with Sikorsky for testing of the SBMR in the 40 x 80 on the Rotor Test Apparatus in the second quarter of CY 1992. The UMARC Code has been documented and correlation is in progress for the SBMR stability data. The MDHC HARP rotor has been modeled and the MDAR modeling is awaiting data release from MDHC.

Significance. The correlation efforts with UMARC and experimental stability data have been encouraging. Correlation with the SBMR hover stability data has been good. Correlation with a four-bladed model scale bearingless

rotor wind tunnel test data for shaft fixed and shaft free (see figure) have shown good agreement.

Status/Plans. Wind tunnel test planning is continuing for both the MDAR and SBMR. Development and validation of UMARC continues as data becomes available.

Steve Jacklin
Rotorcraft Aeromechanics Branch
Ames Research Center
(415) 604-4567

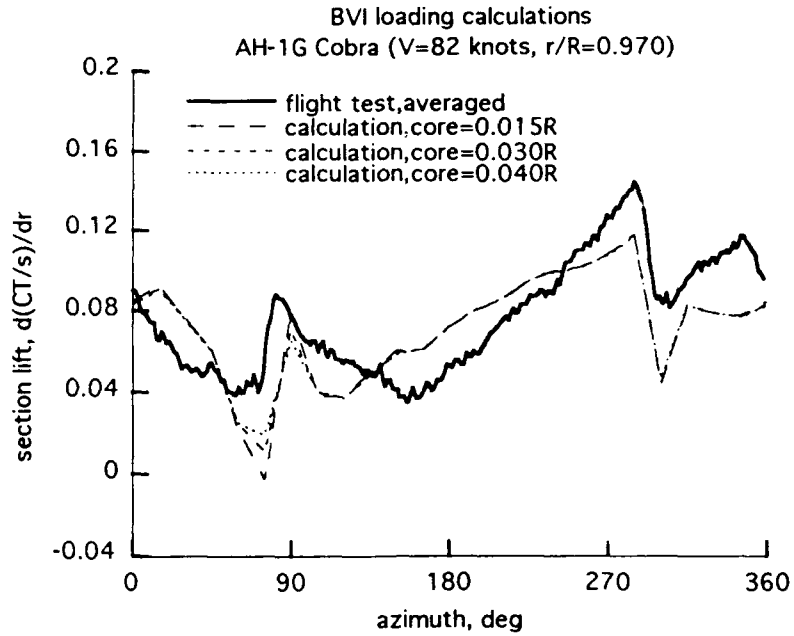


Figure A Correlation of CAMRAD/JA predicted section lift with measured section lift from AH-1G during BVI encounters.

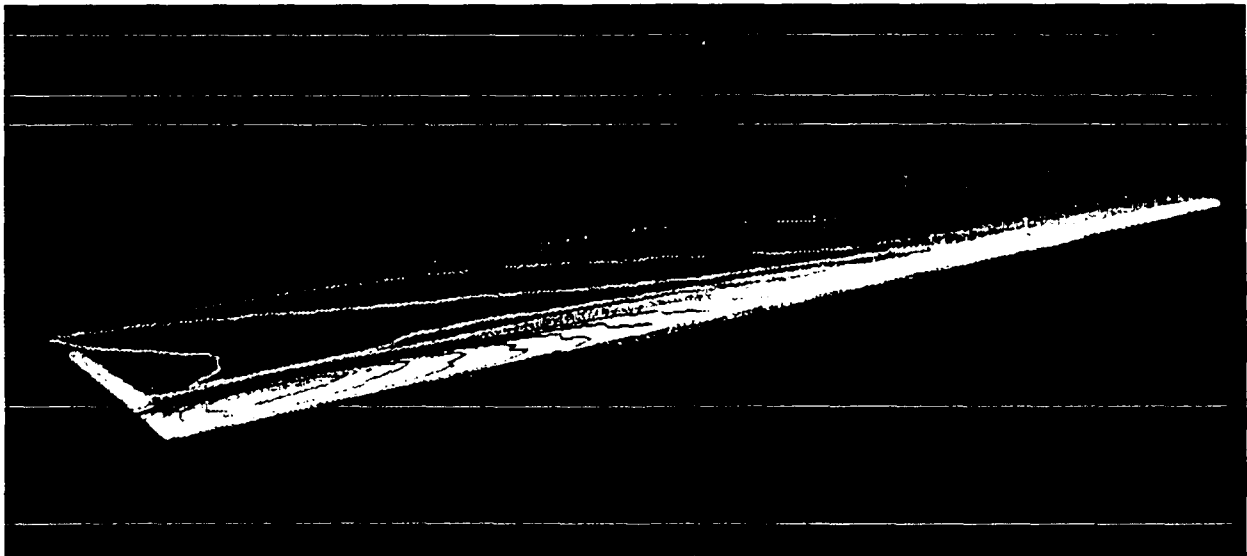


Figure B Calculated Mach contours for AH-1G blade at a high speed flight condition where transonic flow is encountered.

Figure 6-17. Rotor Airloads Correlation Using CFD/Lifting-Line Methods

6-17 Rotor Airloads Correlation Using CFD/Lifting-Line Methods

Objective. To assess the predicting capability of current state-of-the-art rotorcraft aerodynamic codes on modern rotors by comparing results with existing flight test data.

Approach. The comprehensive rotorcraft code, CAMRAD/JA, was used to model the aerodynamic and dynamics of the complete rotorcraft configuration. To obtain the detailed blade airloads, the Full Potential Rotor Code (FPR) was coupled with CAMRAD/JA in an iterative loop. The final solution was the predicted airloads on the rotor system which were then compared with flight measurements at different operating conditions.

Accomplishments. A detailed airloads correlation effort on an AH-1G Cobra helicopter has been completed. Computational methods were used to calculate the blade airloads and give insight into the nature of blade vortex interaction loads at low advance ratios. Figure A shows the correlation between calculated measured blade section lift during blade vortex interaction encounters. As shown in the figure, the section lift was calculated for several vortex core sizes. The effect was minimal for this case, implying the vortex did not pass near the blade. At high advance ratios, the same approach was used to predict the transonic compressibility effects that are present on the advancing side of the rotor disk. The use of computational fluid dynamics (CFD) allowed both a quantitative and qualitative analysis of the flow phenomena in a very efficient manner. Figure B shows predicted Mach contours at a high advance ratio where transonic flow is present. Also, computational fluid dynamics methods have been used to predict the rotor airloads on the UH-60 Blackhawk and to compare them with existing experimental data from the German-Dutch Wind Tunnel (DNW). This CFD model is being developed in preparation for Phase II of the UH-60 Airloads Program, currently under way at Ames.

Significance. The accurate prediction of rotor airloads is one of the biggest challenges in the field of theoretical aerodynamics and one which remains to be solved. Current rotorcraft aerodynamic codes make use of many approximations and assumptions that ultimately must be replaced by more accurate methods. To determine the validity of such methods and improve upon them, correlation work with experimental data is needed. Such improved codes will help in the design of better rotor systems.

Status/Plans. CFD methods are currently being used to model the UH-60 Blackhawk rotor system from hover to high advance ratios. Preliminary results have been compared with model wind tunnel data at different flight conditions. These methods will help in the prediction of rotor airloads during Phase II of the UH-60 Airloads Program.

Francisco J. Hernandez
Rotorcraft Technology Branch
Ames Research Center
(415) 604-1322

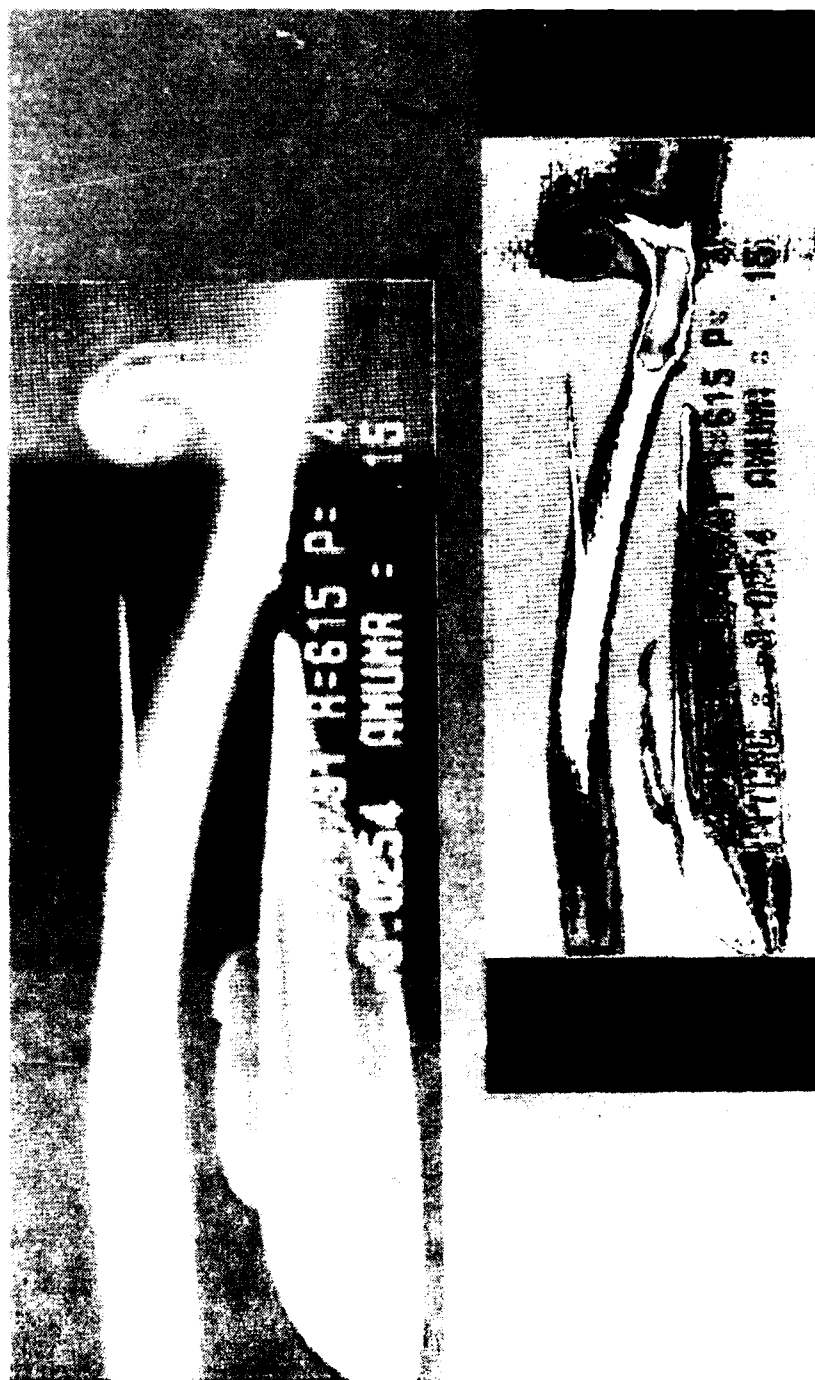


Figure 6-18. Roto Flow Field Investigation

6-18 Rotor Flow Field Investigation

Objective. To provide a comprehensive database documenting the velocity flow field generated by a thrusting helicopter rotor in forward flight. This database is intended to provide a means to validate the accuracy of the velocity and rotor load predictions of rotor computational methods.

Approach. A wind tunnel test was conducted in the 14- by 22-foot subsonic tunnel using the 2-Meter Rotor Test System and a two-component laser velocimeter to measure the velocity induced by the rotor above the plane of the rotor blade tips. Measurements were also made in two planes through the separated flow region behind the hub. A second laser was used to generate a light sheet to provide flow visualization of the vortex structure in the rotor wake.

Accomplishments. Measurements of the rotor-induced velocity were made at 180 locations in planes above the rotor blade tips at a height of 0.50 chord for an advance ratio (ratio of freestream velocity to rotor tip speed) of 0.23. Measurements with and without blades were made in the region of separated flow behind the rotor hub at 15 longitudinal stations, with 15 points at each station. In all cases, average velocity data as well as time-dependent data were acquired. Flow visualization studies were conducted for the rotor wake region above the rotor disk and downstream of the rotor for advance ratios of 0.15, 0.23, and 0.30.

Significance. The rotor inflow measurements, which were obtained during this test program, demonstrate the first production use of the newly developed Frequency Domain Processors (FDPs) for the laser velocimeter data acquisition system. The hub separation measurements provide the basis to define the extent of the separated flow behind the rotor hub for computational rotor-fuse-

lage interaction code validation. The flow visualization work provides the beginning of a visual database of the rotor vortex wake structure.

Status/Plans: The data obtained in this program will be used in-house for correlation with rotor performance codes and rotor-fuse-lage interaction codes. The flow visualization video data will be digitized and enhanced for further analysis by image processing software.

Susan L. Althoff, Joe W. Elliott
Subsonic Aerodynamics Branch
Langley Research Center
(804) 864-5059

Chapter 7

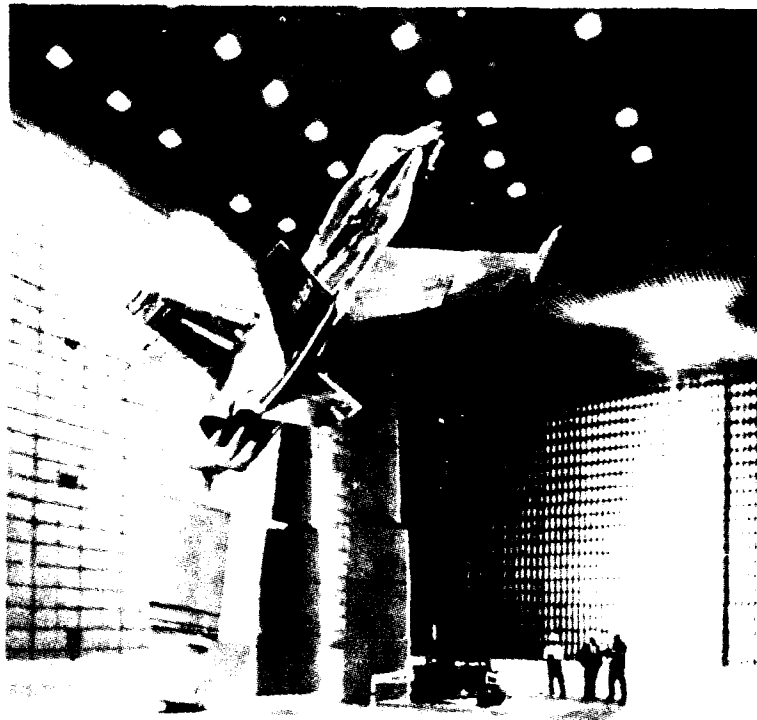
Fighter/Attack Aircraft

The objective of the Fighter/Attack Aircraft Program is to provide the required technologies for fighter/attack aircraft to achieve efficient, sustained supersonic cruise and maneuver performance; efficient store carriage and deployment at supersonic speeds; increased agility at subsonic speeds and acceptable handling qualities at extreme angles-of-attack; and short takeoff and vertical landing (STOVL) operation.

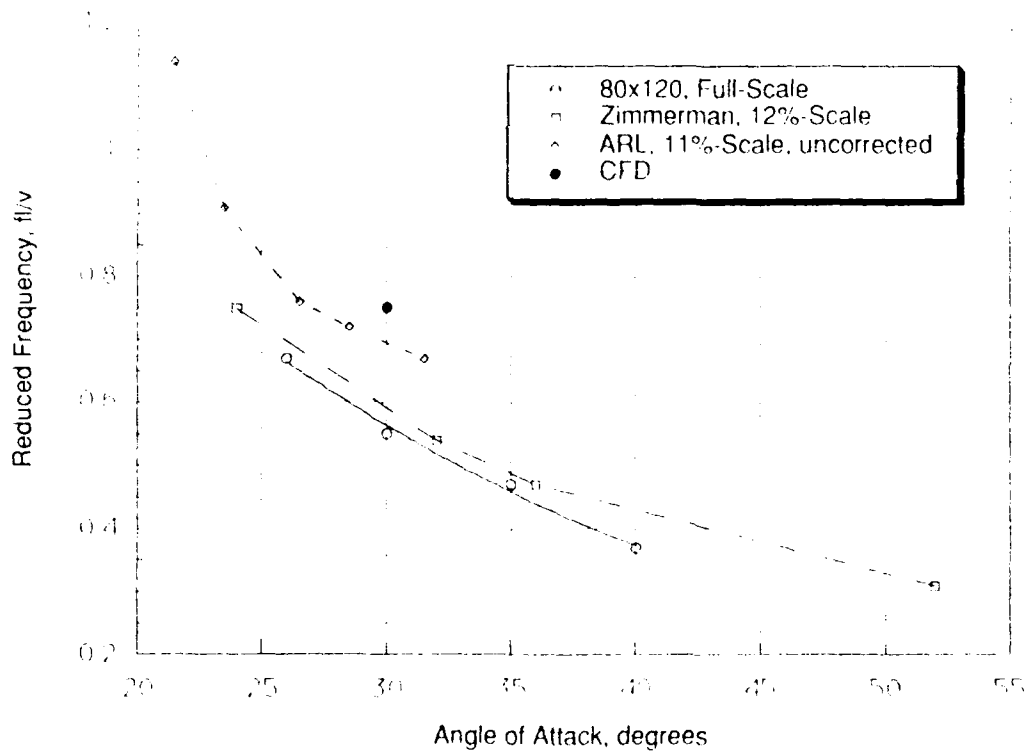
Improved prediction methods and/or experimental techniques are now available for high-lift aerodynamics, propulsion integration, weapon carriage, supersonic store cavity and separation aeroacoustics, integrated flight controls, and systems design for fighter/attack aircraft. Wind tunnel and piloted simulation studies have demonstrated the potential effectiveness of multiaxis thrust vectoring for propulsive control at extreme angles-of-attack. In addition, powered lift systems consistent with the operation of advanced STOVL aircraft have been identified, and configuration studies have been conducted to assess the impact of integrating these systems with supersonic airframe designs.

The Fighter/Attack Aircraft Program is focused on (1) CFD modeling and validation of cavity effects and near-field trajectory simulation for weapons launch during maneuver and modeling of 3-D flow fields for vehicles at high angles-of-attack with separated flow; (2) development of innovative propulsive and aerodynamic control systems concepts to provide increased vehicle control at angles-of-attack near and beyond maximum lift; (3) improved understanding of control requirements for control throughout the relevant flight envelope; (4) large-scale, ground-based testing of a STOVL fighter concept using ejector lift/vectored thrust to define critical transition aerodynamics; (5) studies of STOVL ground effects including inlet reingestion and ground erosion; and (6) integration studies to quantify the impact of emerging technologies and define the critical research areas for supersonic STOVL.

Program Manager: Benjamin Neumann
OAST/RF
Washington, DC 20546
(202) 453-2795



F/A-18 Aircraft



Comparison of small-scale and full-scale tail buffet frequency versus angle of attack. Experimental results are for fluctuating pressure measurements at a single point on the vertical tail while the CFD point is for the unsteady root bending moment on the tail.

Figure 7-1. Tail Buffet Frequency vs Angle-of-Attack

7-1 Full-Scale Test of F/A-18 at High Angles-of-Attack

Objective. To examine the aerodynamics of high angle-of-attack flight of fighter aircraft. Particular emphasis is placed on understanding the LEX-vortex (Leading Edge Extension) induced tail buffet and on developing a pneumatic forebody flow control concept for lateral control at high angle-of-attack. The test has also provided important data for computational fluid dynamics (CFD) validation and resolution of scaling issues, which have become apparent in comparing small-scale wind-tunnel data with flight results.

Approach. A retired Navy F/A-18A has been converted into a wind-tunnel model for testing in the 80- by 120-foot wind tunnel. The model is heavily instrumented to measure time-averaged forebody pressure distributions and the unsteady pressure distribution on one of the vertical tails. In addition, the nose of the aircraft has been modified with the addition of jet-type and slot-type blowing for flow control at very high angle-of-attack.

Accomplishments. Preliminary data from the wind-tunnel tests matched very well with flight data for overall forces and moments as well as for the radome and forebody pressure distributions. The unsteady vertical tail pressure data will be used to address wind tunnel scaling issues, to identify flow structures and dominant frequencies in the burst vortex, and to validate CFD analyses. Preliminary analysis of these data indicates that the frequency content of the fin pressure measured in the full-scale wind-tunnel test is close to that observed in several small-scale experiments. Similar pressure measurements are not yet available from the flight experiment.

The pneumatic forebody flow control has been shown to be effective for practical blowing slot lengths and blowing rates. At a given angle-of-attack, the yawing moment is linear over a wide range of blowing mass flow coefficient. At a 50° angle-of-attack, the pneumatic sys-

tem can provide more yawing moment than a full rudder deflection does at low angles-of-attack.

Significance. The pressure distributions measured on the full-scale model will provide a rich source of CFD validation data, which will help to improve the accuracy of 3-D Navier-Stokes computations. Current CFD efforts are ongoing to compute the unsteady burst-vortex induced pressures on the F-18 tail. The wind tunnel measurements will also be used in the development and validation of CFD for unsteady flows.

It has been demonstrated that pneumatic forebody flow control can generate control yawing moments of sufficient magnitude to provide directional control at extreme angles-of-attack where rudder control is no longer effective. These full-scale data are critical in order to define the planned flight experiment of pneumatic forebody flow control system on the High Alpha Research Vehicle, HARV.

Status/Plans. A second wind-tunnel test will be conducted in 1992 to optimize the forebody flow control system in preparation for flight testing, extend the surface pressure database to include the wings for use in CFD validation and correlation with flight, and to refine the measurement of unsteady pressures on the vertical tails of the aircraft.

James C. Ross
Fixed-Wing Aerodynamics Branch
Ames Research Center
(415) 604-6722



Figure 7-2. Tail Buffet Research

7-2 Tail Buffet Research

Objective. To study the effects of vortical flow fields on tail buffeting of modern high-performance aircraft, and explore methods of reducing buffet levels while maintaining the favorable effects of vortex flow on the high angle-of-attack aerodynamic characteristics.

Approach. A cooperative program was established between NASA, the Navy, and McDonnell Aircraft Company to conduct low-speed wind tunnel tests on a 0.16-scale F/A-18 model with dynamically scaled and instrumented vertical tails. This research provided data on the unsteady aerodynamic loadings and surface pressures of the tails. Changes to the configuration aimed at modifying the vortical flow field were tested to investigate the effect on both buffeting response levels on the tails and the overall aerodynamic characteristics of the configuration. Additional tests were conducted to obtain detailed aerodynamic information on the impact of the modifications.

Accomplishments. Testing in the Langley 30- by 60-foot tunnel provided a large database of dynamic response characteristics of the vertical tails and steady-state total force and moment data for several configurations. Correlation of measured tail buffet levels with previous, limited industry testing of the baseline F/A-18 configuration was very good. The study showed that repositioning and/or weakening of the primary vortex system can reduce tail buffet levels but can also have a large impact on the overall lift and stability characteristics. In addition, substantial amounts of tail buffeting were seen due to fuselage and wing wake flow, in the absence of a vortex system. Follow-on aerodynamic-only testing indicated that many of the stability effects were caused by changes in interactions between the vortex system and tail surfaces.

Significance. The results of this test indicate that relatively minor changes in an

aircraft's configuration can have a significant impact on its tail buffet characteristics. Thus, consideration of tail buffeting should be addressed early in the design stage of an aircraft, when configuration changes are still possible. Two issues to consider are: (1) regions of stalled or separated wake flow can be a major contributor to tail buffet; and (2) aerodynamic/stability impact can be due more to interactions of the vortex flow field with other aircraft surfaces than to changes in the vortex flow field itself.

Also, successful correlation with previous data using scaling parameters suggests that the same approach may be used to develop wind tunnel-to-flight scaling methods.

Status/Plans. Follow-on investigations of various innovative concepts to alleviate tail buffeting are planned. Correlation of results with research programs of other organizations is planned through a workshop on tail buffet research in August, 1991, for Aeronautics Technology Technical Panel HTP-5 members of The Technical Coordination Program. Results from current and future wind tunnel tests will be correlated with airplane flight test data for development and validation of scaling methods.

Gautam H. Shah
Flight Dynamics Branch
Langley Research Center
(804) 864-1163

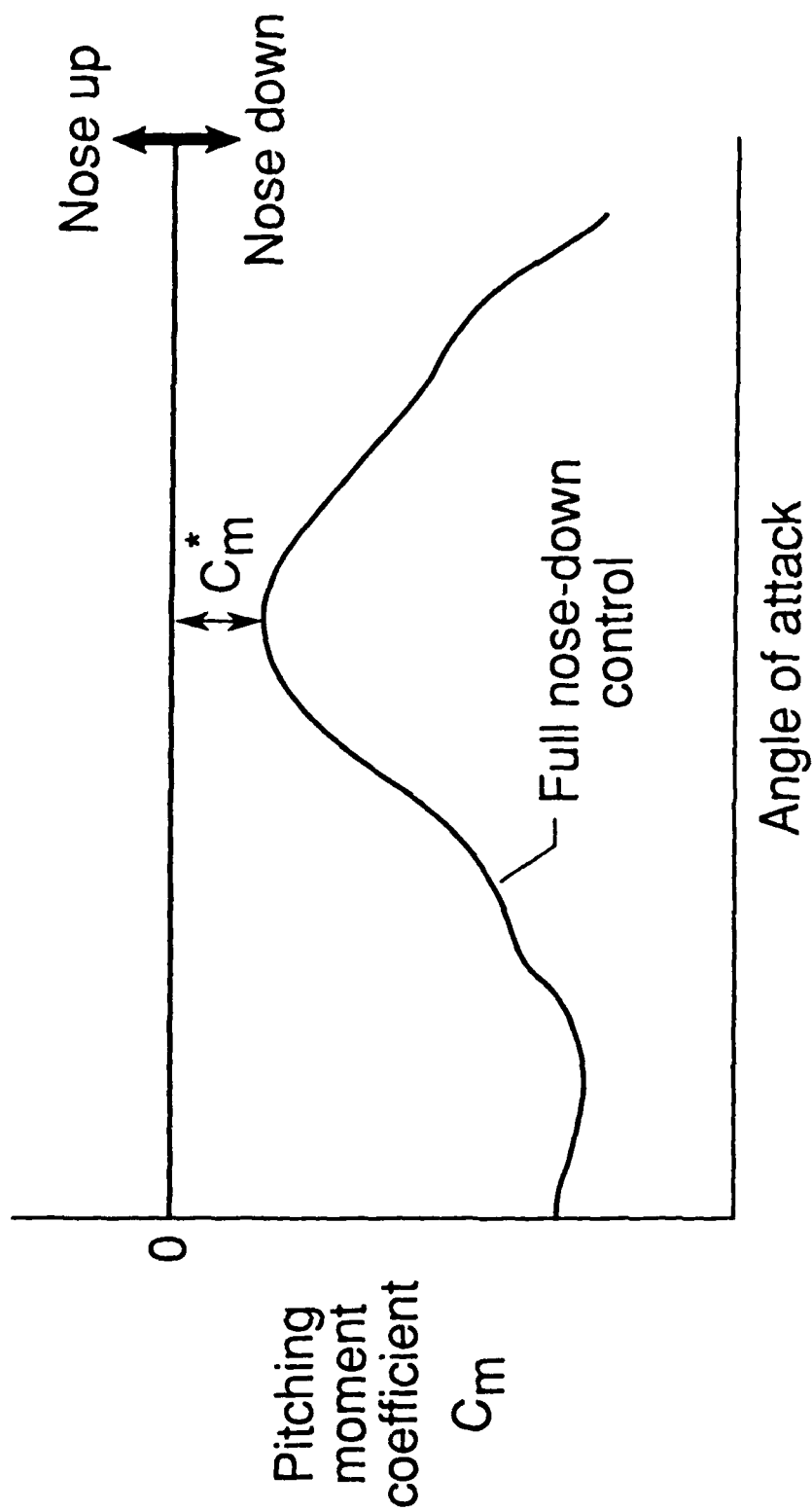


Figure 7-3. Typical Nose-Down Control Capability Characteristics for Relaxed Stability Combat Aircraft

7-3 Development of High-Angle-of-Attack Nose-Down Pitch Control Requirements for Relaxed Static Stability Combat Aircraft

Objective. To develop high-angle-of-attack nose-down control requirements that can be used as design guidelines early in the development cycle of advanced combat aircraft incorporating relaxed static stability in pitch.

Approach. A cooperative program was established between NASA and the U.S. Navy to perform the research. A systematic piloted simulation study was conducted on the Langley Differential Maneuvering Simulator to develop and assess candidate guidelines. The simulation process involved specific assessment maneuvers and pilot rating approaches developed for this application. A key element of the investigation was a parametric study involving systematic variations of critical parameters affecting nose-down control capability, particularly the minimum level available at high angles-of-attack (C_m^* , see accompanying figure). Extensive involvement of Navy researchers and pilots permitted acceleration of the research process.

Accomplishments. A comprehensive database of piloted simulation results was generated to enable the assessment and development of potential guidelines. The results were based on analysis of flight motions and pilot comments and ratings obtained during the parametric study. These results show a strong correlation of pilot rating to the airplane short-term pitch acceleration and pitch rate buildup in response to nose-down commands applied at high-angle-of-attack conditions. Using these data, candidate design guidelines and flight demonstration requirements were defined. Additional simulation tests were conducted to verify that these design guidelines could be used to predict pilot opinion of the aircraft response.

Significance. The use of relaxed static stability in pitch for performance enhancement is a key design approach for advanced combat aircraft. Successful application of this con-

cept requires design guidelines for defining high-angle-of-attack nose-down control requirements early in the development process. The output from this study is being used by the Navy to define these requirements for design and flight testing of the F-18 E/F. The Air Force is also interested in this study, both in terms of potential application to Advanced Tactical Fighter and for development of handbook criteria.

Status/Plans. A preliminary set of guidelines and flight demonstration requirements has been developed based on the results obtained to date. Simulation tests will be conducted to verify that the design guidelines are valid for complex maneuvering and to prepare for full-scale flight tests. A limited flight evaluation/validation program on a test F-18 airplane will be conducted by the Navy in September 1991. Detailed flight testing of proposed guidelines using the NASA High Alpha Research Vehicle (HARV) is planned.

Marilyn E. Ogburn, John V. Foster
Flight Dynamics Branch
Langley Research Center
(804)864-1136

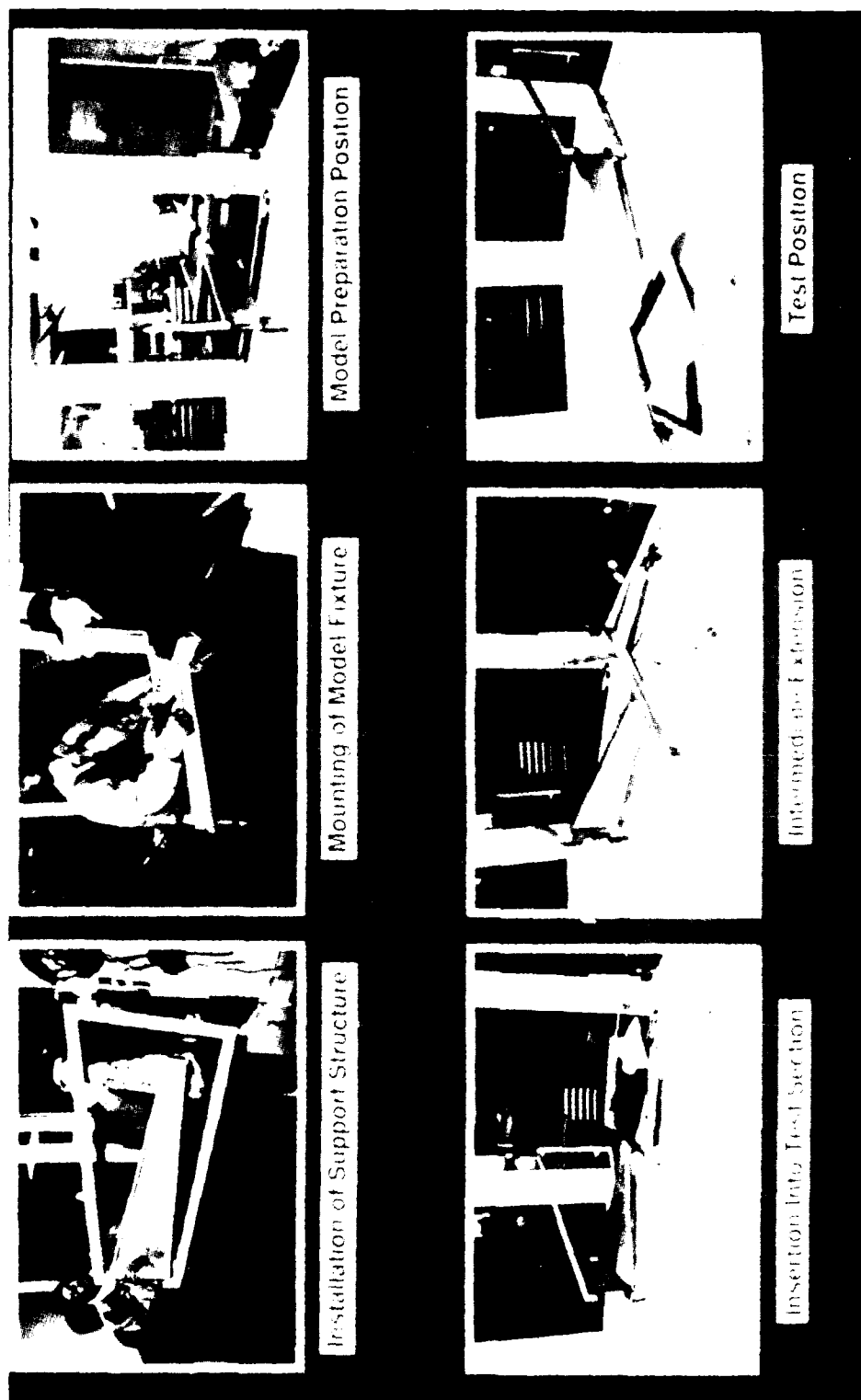


Figure 7-4. Investigation of the Tumbling Phenomenon in Aerodynamic Configurations

7-4 Investigation of the Tumbling Phenomenon in Aerodynamic Configurations

Objective. To determine the effect of plan-form geometry and mass distribution on the tumbling characteristics of wings.

Approach. Static and dynamic force tests were conducted in the 30- by 60-foot tunnel and free-tumbling tests were performed in the 20-foot Vertical Spin Tunnel using a series of generic wing models. Each set consists of twelve models with four different leading-edge sweep angles and three different trailing-edge sweep angles. Aerodynamic data through 360° angle-of-attack was used to develop a three-degree-of-freedom simulation for calculating tumbling behavior.

Free-tumbling tests were conducted over a range of center-of-gravity and inertial conditions. A free-to-pitch apparatus is being developed and instrumented to enable continuous rotation testing of a dynamically scaled model for single degree-of-freedom analysis.

Accomplishments. Free-tumbling results have shown that higher aspect ratio wings generally have a tumble/no tumble boundary at a more positive static margin than lower aspect ratio wings. This boundary can be shifted forward for the low-aspect ratio wings by changing the mass distribution. Initial results of the simulation show tumbling behaviors similar to those observed in free-tumbling tests.

Significance. As fighter design trends drive toward more tumble-susceptible configurations, the information generated from this research will provide design guidelines to assist in configuration development.

Status/Plans. The aerodynamic database will be completed. The instrumentation system for the free-to-pitch apparatus is nearly complete. Analysis of the free-tumbling results is continuing and the tumble simulation is being refined.

Raymond D. Whipple
Flight Dynamics Branch
Langley Research Center
(804) 864-1194



Figure 7-5. F-106 Vortex Flap Flight Experiment

7-5 F-106 Vortex Flap Flight Experiment

Objective. To demonstrate the feasibility of the vortex flap concept in a free-flight environment to characterize the wing flow field and to provide a database for sharp leading-edge wings to be used for calibration of design and analysis tools.

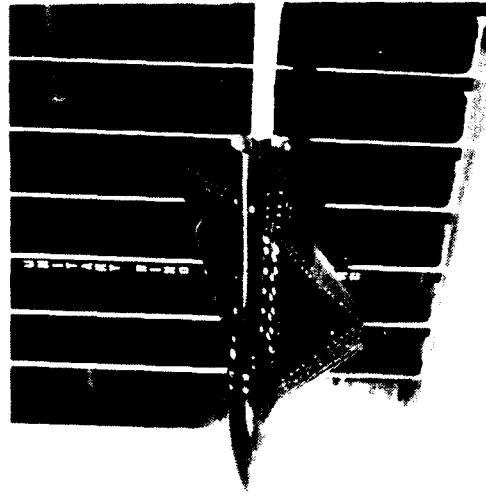
Approach. An F-106B aircraft was modified by the addition of wedge-shaped, leading-edge flaps to the existing wing. The wing flow field was characterized using surface pressure measurements and flow visualization data obtained through the use of flow cones, surface oil flows, and a light sheet/flow seeding system. A limited evaluation of the handling qualities and performance of the modified aircraft relative to the baseline aircraft was conducted.

Accomplishments. Flight activities for the modified aircraft with the vortex flap at 30° and 40° deflections have been completed. Aircraft performance data, detailed wing surface pressure measurements, and surface flow visualization were obtained at subsonic and transonic test conditions. Light-sheet and flow-seeding systems were installed to visualize the off-body flow and provided significant additional details of the wing flow-field characteristics at subsonic test conditions. The accompanying photograph shows the F-106 aircraft in flight with the vortex flap deflected 40° and a coating of oil defining surface flow patterns on the flap and wing upper surfaces.

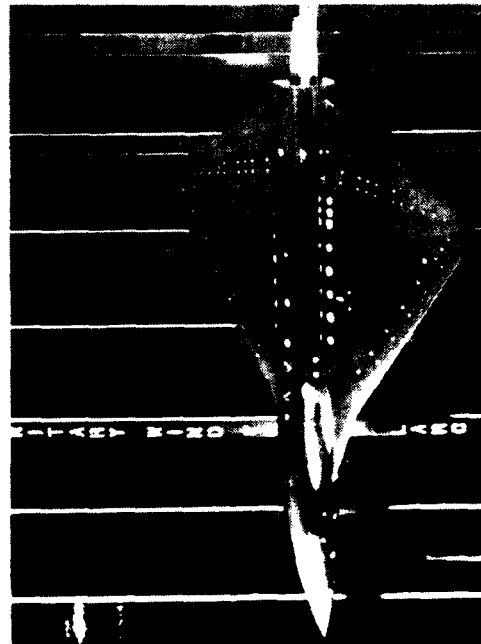
Significance. Flight testing has demonstrated the performance enhancement potential of the vortex flap and provided considerable insight concerning its flow field and loading distribution characteristics.

Status/Plans. Testing of the aircraft was completed in April 1991. Analysis and publication of the test results are continuing.

James B. Hallissy,
W. Elliott Schoonover, Jr., John E. Lamar
Applied Aerodynamics Division
Langley Research Center
(804) 864-2865



Cambered wing



Flat wing

Figure 7-6. Generic Fighter Models Installed in the Unitary Plan Wind Tunnel

7-6 Wing Camber Effects on Flap Effectiveness at Supersonic Speeds

Objective. To evaluate camber effects on leading- and trailing-edge flap effectiveness at supersonic speeds.

Approach. A cooperative program was established between NASA and General Dynamics to perform the research. Cambered and uncambered wing models were built with the same planform and flap geometry. The wing was designed to meet a broad spectrum of performance goals including efficient trimmed supersonic cruise performance and maneuver capability. The effects of camber on the flap performance were then studied through a comparison of force and moment measurements on both wings. The models were tested across the range from 1.6 to 2.16 in test section I of the Unitary Plan Wind Tunnel. The wings were tested with leading-edge flap deflections of -4° , -2° , 0° , 5° , 10° , and 15° and trailing-edge flap deflections of -30° , -20° , -10° , 0° , and 10° .

Accomplishments. The experimental results show that leading-edge flap deflections of up to 5° reduced drag at high lift on the flat wing. Small negative leading-edge flap deflections reduced drag on the cambered wing at low lift. Trailing-edge flap effectiveness decreased with increasing negative flap deflection. Wing camber had little effect on trailing-edge flap effectiveness.

Significance. This study shows that leading-edge flap deflections, which are customarily used at subsonic speeds, can be used to obtain drag reduction benefits at supersonic speeds. The drag produced by wing camber at supersonic speeds can also be reduced by negative deflections of leading-edge flaps. The study also showed that wing camber has a negligible effect on the trim-producing trailing-edge flap effectiveness at supersonic speeds.

Status/Plans. The study has been completed, and results are being documented in a formal NASA publication.

Gloria Hernandez
Applied Aerodynamics Division
Langley Research Center
(804) 864-5572

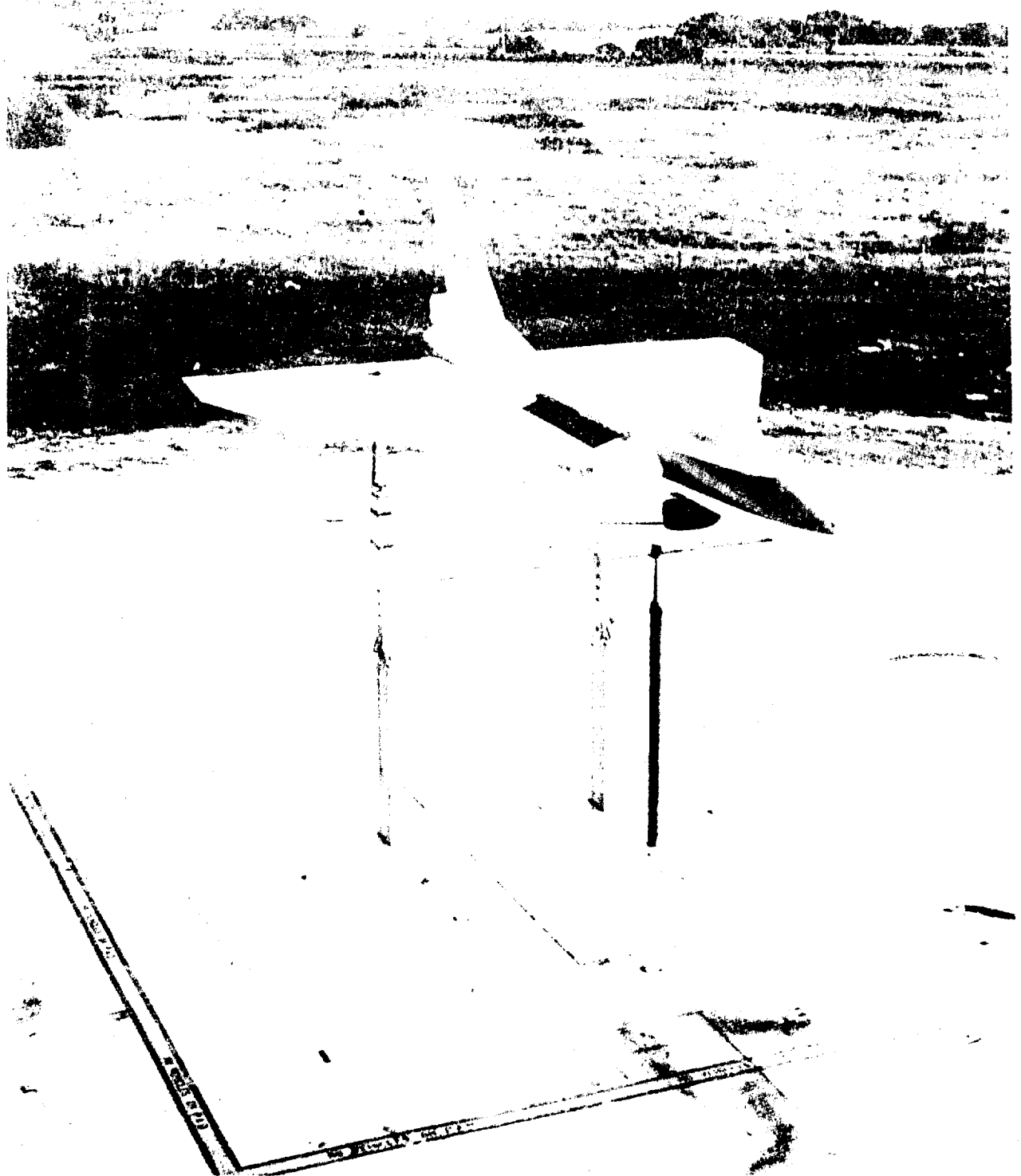


Figure 7-7. Outdoor Static Tests of the Full-Scale Ejector-Lift/Vectored-Thrust STOVL E-7A Configuration

7-7 Outdoor Static Tests of the Full-Scale Ejector-Lift/ Vectored-Thrust STOVL E-7A Configuration

Objective. To test the full-scale STOVL E-7A model at Ames Outdoor Aerodynamic Research Facility (OARF) to measure the thrust of the lifting ejectors and vectoring ventral nozzle of the vehicle. The tests will also reveal the interactions of the plumes from the lifting jets beneath the vehicle as they impinge upon the ground. The E-7A research program is part of a joint technology development program involving Boeing Canada's De Havilland Division and NASA Ames Research Center. The E-7A configuration emerged from a General Dynamics design study of ejector-lift concepts.

Approach. Static thrust calibrations of the propulsion system in the STOVL E-7A model were performed in the test sections of the Ames 40- by 80- and 80- by 120-foot wind tunnels as part of the forward-flight tests of the model. The static test of the model at the OARF will yield more accurate measurements of static thrust because jet-induced recirculation flow patterns in the wind tunnel tests due to the presence of tunnel wall boundaries will not be a factor. The two wind tunnel tests have provided low- and high-speed aerodynamic data. The outdoor test will complete the database on the full-scale model by providing static thrust calibrations. The E-7A model has been mounted approximately 25 feet above ground at the OARF.

Accomplishments. Static tests of the E-7A model are complete. The measured thrust augmentation ratio of the lifting ejectors is approximately 1.6. The augmentation ratio is defined as the net ejector thrust divided by the thrust of the primary nozzles. This value is close to that measured in the test section of the 80- by 120-foot wind tunnel. Changes in the shape of the base of the fuselage between the ejector systems were shown to have an

effect on the performance of the thrust-augmenting ejectors. Laser light sheet, smoke, and infrared flow visualization techniques have revealed that the hot ventral nozzle jet penetrates forward in a thin layer beneath the lower energy ejector jets.

Significance. Designers of ejector-lift/vectored-thrust STOVL configurations have been working under the assumption that an ejector thrust augmentation of 1.6 was achievable at full-scale. The level of ejector performance and forward-flight transition performance during the Ames E-7A tests demonstrates the viability of supersonic STOVL concepts which employ lifting ejectors.

Status/Plans. The lateral/directional performance of the E-7A model in hover mode is scheduled to be tested at low speeds and high yaw angles in the 80- by 120-foot wind tunnel beginning in June of 1992.

Tim Naumowicz, Brian E. Smith
National Full-Scale Aerodynamics Complex
Ames Research Center
(415) 604-6674

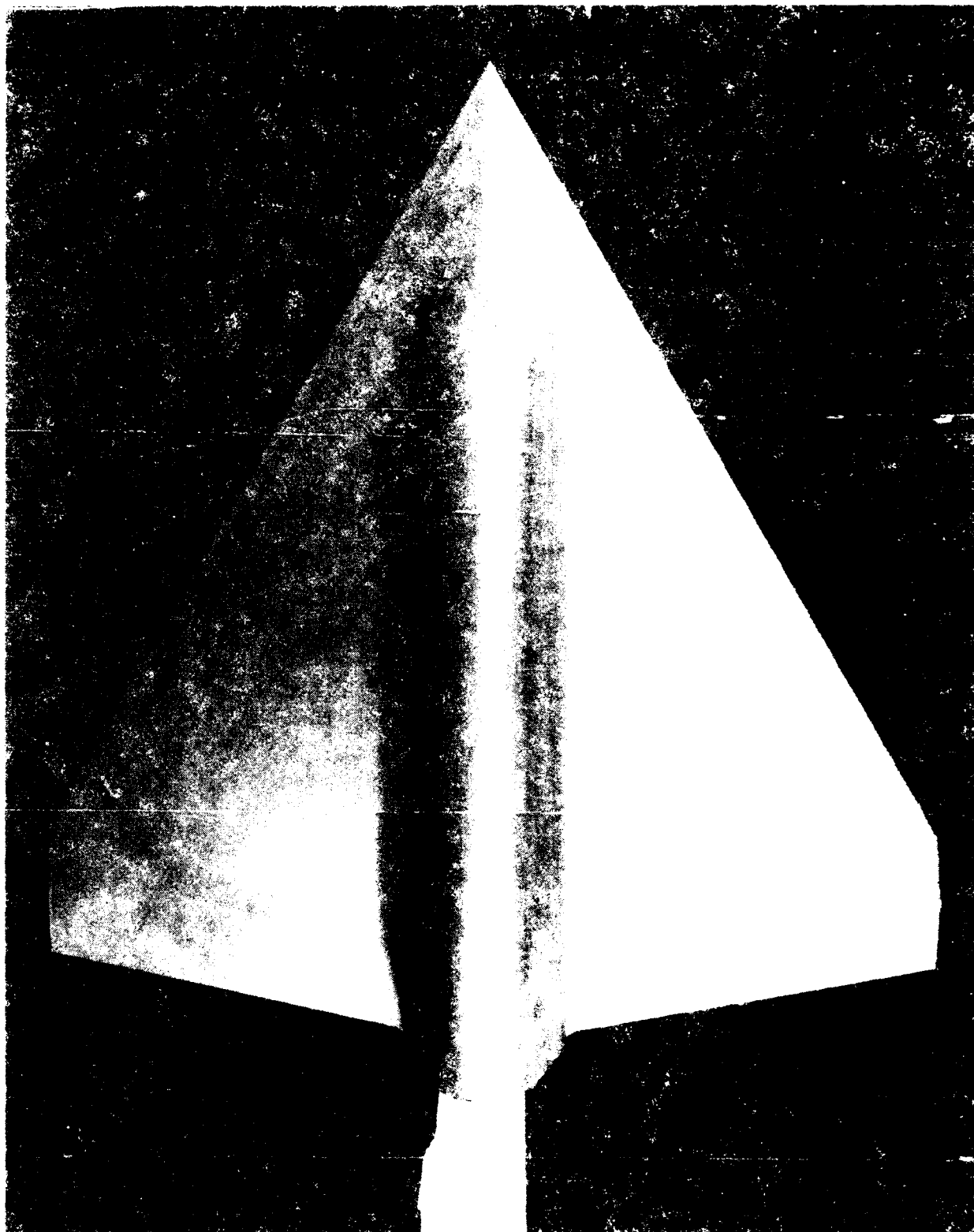


Figure 7-8. Volume of Oil in the Field of View of the Camera. The Volume of Oil in the Field of View of the Camera.

7-8 Validation of Out-of-Ground Effect Prediction Capability for Powered Lift Aircraft

Objective. To evaluate the capability of computational fluid dynamics (CFD) to predict the critical flow features for a Short Take-Off Vertical Landing (STOVL) aircraft configuration through comparison of computed results with the measurements of a companion experiment designed for CFD validation.

Approach. Previous simulations of critical powered lift flow components such as a jet in crossflow, which isolates the lift jet/aerodynamic interaction during transitional flight, showed favorable agreement with experiment. To extend the application of the F3D code, a simplified but representative STOVL aircraft configuration was selected for testing and simulation. The model geometry, a Delta wing (E-7A) planform with two jets located in a blended fuselage, minimizes the geometric modeling complexity while retaining the important physics of the lift jet/aerodynamic interaction. The unsteady Reynolds-averaged Navier-Stokes equations applied on patched or overlapped grids will be used for the computations.

Accomplishments. The transitional flight characteristics of the STOVL aircraft configuration were measured in the NASA Ames 7-by 10-foot wind tunnel. The results include forces and moments, steady and unsteady surface pressures, and jet pressures and temperatures. Measurements of the flow were also made in the tunnel test section upstream and downstream of the model and at the jet exits to provide boundary conditions for the computations. Flow visualization and total pressure measurements in the jet plumes provide a description of the three-dimensional jet efflux flow field.

Computational emphasis has been placed on establishing the numerical modeling requirements for the propulsive flow field. Previous thin-layer Navier-Stokes computations using F3D for a jet in crossflow indicated that the

computed vortices are less diffuse than in the experiment, and the jet wake region is not adequately simulated. By retaining viscous terms in all three directions, quantitative agreement with experiment has been improved. This modification is incorporated into the STOVL model simulation.

Significance. A comprehensive and well-documented set of measurements is provided for CFD validation comparisons.

Status/Plans. Computational grids are being developed for the STOVL model geometry. Computations (out-of-ground effects) will be completed and compared with experiment. Flow field measurements in and out of ground effects will be made using laser velocimetry.

Karlin R. Roth
Fixed Wing Aerodynamics Branch
Ames Research Center
(415) 604-6678

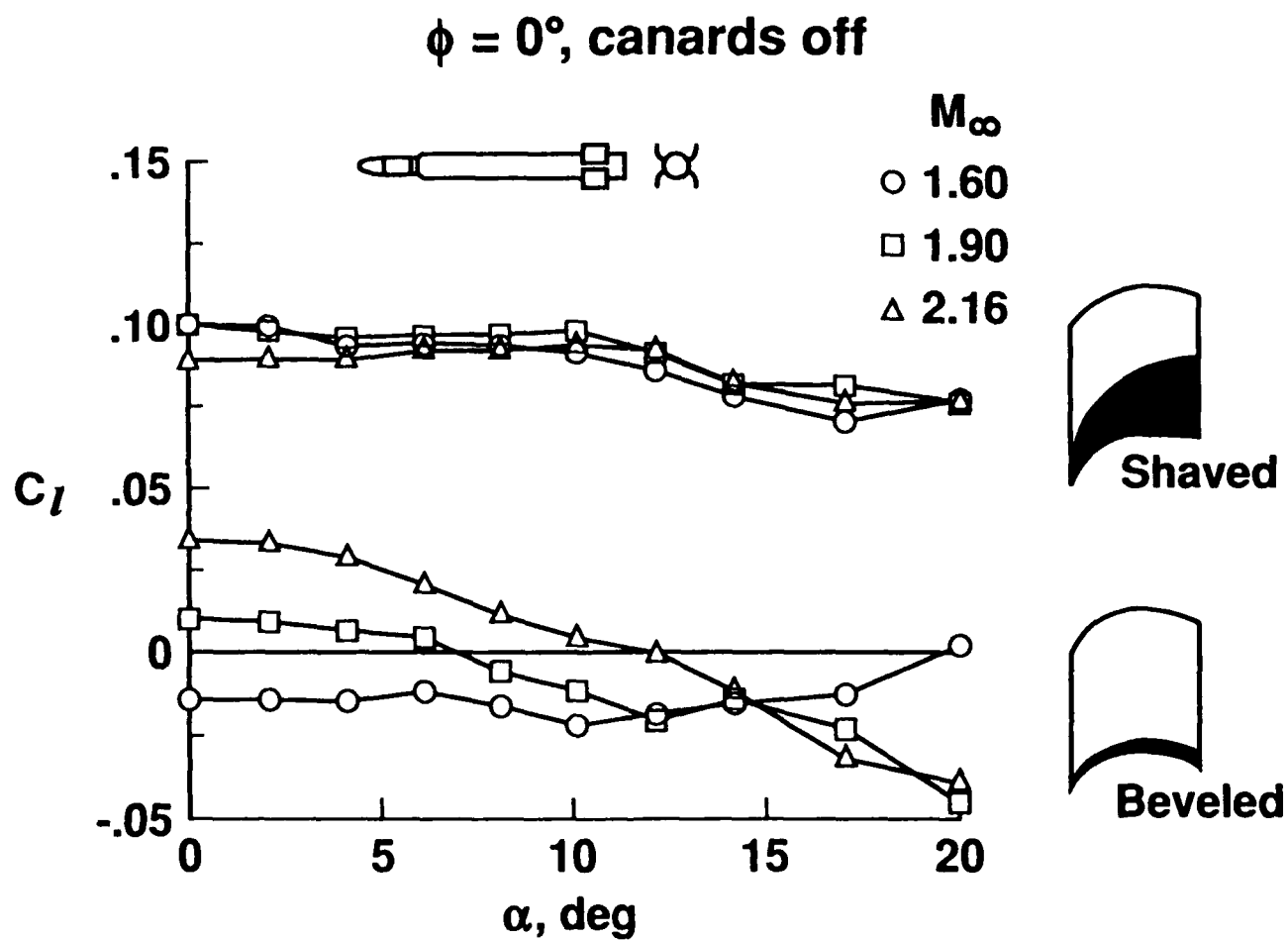


Figure 7-9. Effect of Tail Fin Shaving

7-9 Comparison of Shaved and Beveled Fins for Rolling Missile Applications

Objective. To investigate the effectiveness of shallow shaving along the leading and trailing edges of wrap-around missile fins for producing roll on the configuration.

Approach. An experimental investigation was conducted to investigate the aerodynamics of a tube-launched air-to-surface tactical missile configuration that employs planar canards and wrap-around tail fins arranged in opposing pairs. Fin shaping in the form of shallow shaving along the leading and trailing edges of the tail fins was investigated as a candidate for producing the rolling motion on this configuration that is needed for controllability. A second set of fins having a more conventional 45° bevel along the tail fin leading edges was investigated for comparison. Force and moment tests on this concept were conducted in the low Mach number test section of the Langley Unitary Plan Wind Tunnel at Mach 1.60, 1.90, and 2.16 at angles-of-attack up to 20° and roll angles up to 90° .

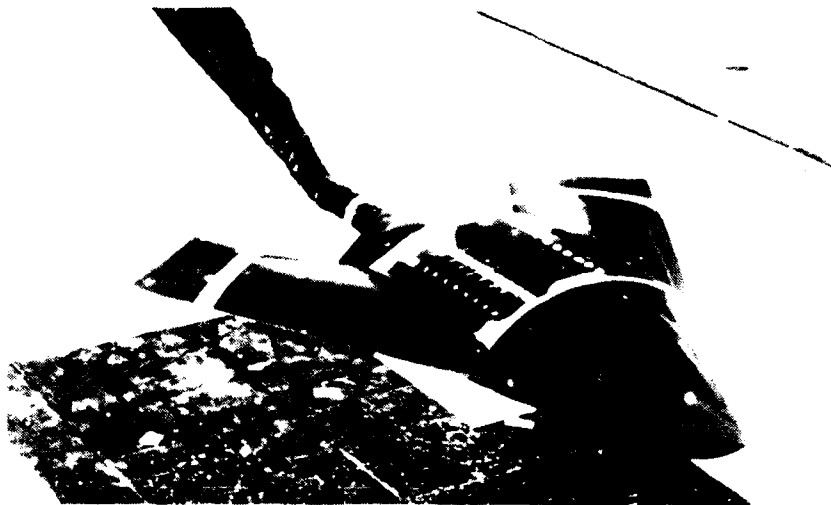
Accomplishments. To be most effective, the rolling moments on this configuration should be constant over the anticipated flight conditions. The results of this experiment show that the shaved fins were much more effective than the beveled fins in producing these favorable rolling moment characteristics. As shown in the figure, the shaved fins produced significantly larger rolling moments, and these moments were essentially invariant with both Mach number and angle-of-attack. The beveled fins, however, produced large variations with both parameters, in some cases even producing negative rolling moments.

Significance. Shallow shaving of the leading and trailing edges of fins has been shown to be an effective roll-producing technique for missile configurations that require rolling motion for controllability.

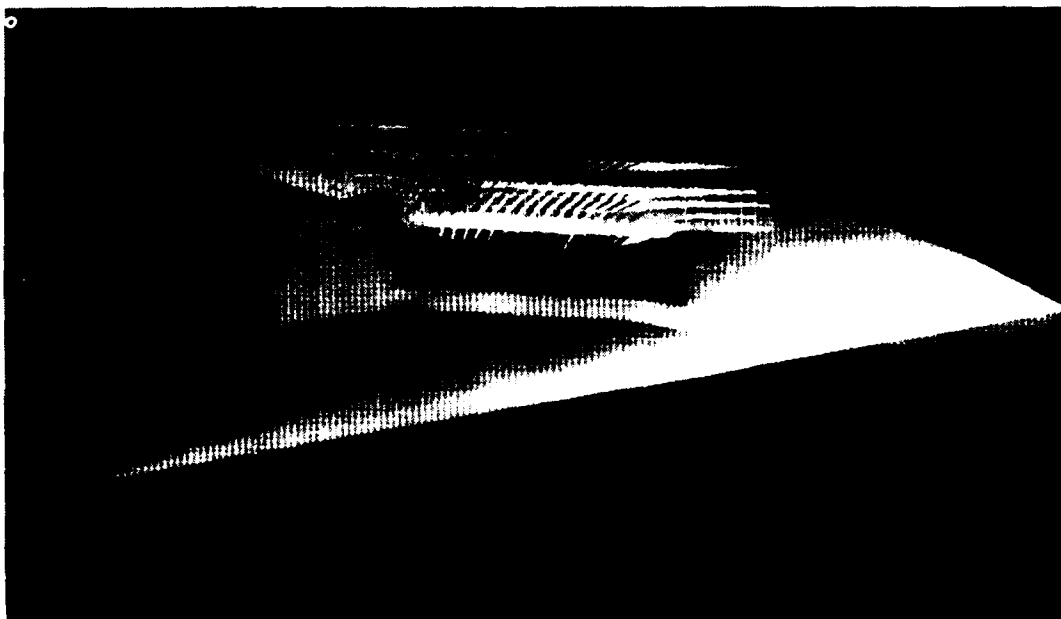
Status/Plans. Supersonic tests on this concept have been completed. Analysis of the data is continuing, and the results will be published in a NASA report. Subsonic/transonic tests of this concept may be performed.

Jerry M. Allen
Applied Aerodynamics Division
Langley Research Center
(804) 864-5592

Advanced VTOL Configuration



Powered Model Installed in the 14- by 22- Foot Subsonic Tunnel
for Ground Effects Testing



Augmentor Inlet Flow Field Velocity Vectors

Figure 7-10. STOL/STOVL Concepts for High-Performance Aircraft

7-10 STOL/STOVL Concepts for High-Performance Aircraft

Objective. To provide advanced aerodynamic technology and advanced concepts applicable to STOL/STOVL operations of current and future high-performance aircraft.

Approach. Through experimental and analytical studies, using powered models in both the Subsonic Basic Research Tunnel (SBRT) and the 14- by 22-Foot Subsonic Tunnel (14-by 22-FST), key problems were examined and promising solution concepts for providing STOL/STOVL capabilities for advanced aircraft were identified. The SBRT and 14- by 22-FST provide a unique combination of resources for the study of takeoff and landing aerodynamics in and out of ground effect.

Accomplishments. In FY 1991, two major tests were conducted in the 14- by 22-FST and the SBRT, which were made operational with a moving belt ground plane and data system. A detailed investigation of augmentor performance, ground effects, stability and control, and a Laser Velocimetry (LV) map of the augmentor inlet flow field was completed on an advanced VTOL concept shown in the accompanying figure. A study of the effects of high nozzle pressure ratio (NPR) exhaust flows; nozzle type, location, and number; various wing planforms; and moving belt ground plane on the aerodynamics of a generic VTOL configuration shown in the figure was also completed. The SBRT was used to assess the effect of a moving belt ground plane on the development of the ground vortex flow field from a single vertical jet in a cross flow.

Significance. These three experimental investigations have yielded the following significant results: (1) A method of venting the lower and upper surfaces to equalize pressure, which minimized the pitch-up tendency typical of configurations during transition, was demonstrated using the advanced VTOL configuration. (2) Comparisons of the computational and LV measured augmentor inlet

flow fields show very good agreement. (3) The data from the generic VTOL test and the isolated jet tests in SBRT are under analysis. Preliminary analysis of the effect of the moving belt ground plane on the ground vortex flow field, both in 14- by 22-FST and SBRT, show good agreement with results obtained using a moving jet in the Vortex Research Facility (VRF). These results indicate significant changes in the extent of the ground vortex when the exhaust flow penetrated against the freestream (belt on or moving jet) or against the wall boundary layer (belt off).

Status/Plans. The results of the ground vortex investigations will be analyzed to determine the effects of wing location, nozzle arrangements, and pressure ratio on configuration aerodynamics in and out of ground effect. A detailed quantitative determination of the actual extent of the ground vortex will be made and compared with the VRF moving model results. The SBRT will be completed with a model support system to allow model testing and an LV system for flow measurements.

John W. Paulson, Jr. (804) 864-5071
Guy T. Kemmerly (804) 864-5070
Kevin J. Kjerstad (804) 864-5022
Subsonic Aerodynamics Branch
Applied Aerodynamics Division
Langley Research Center

THIN-LAYER NAVIER-STOKES COMPUTATIONS

$M = 0.90$ $Re = 1.52$ million

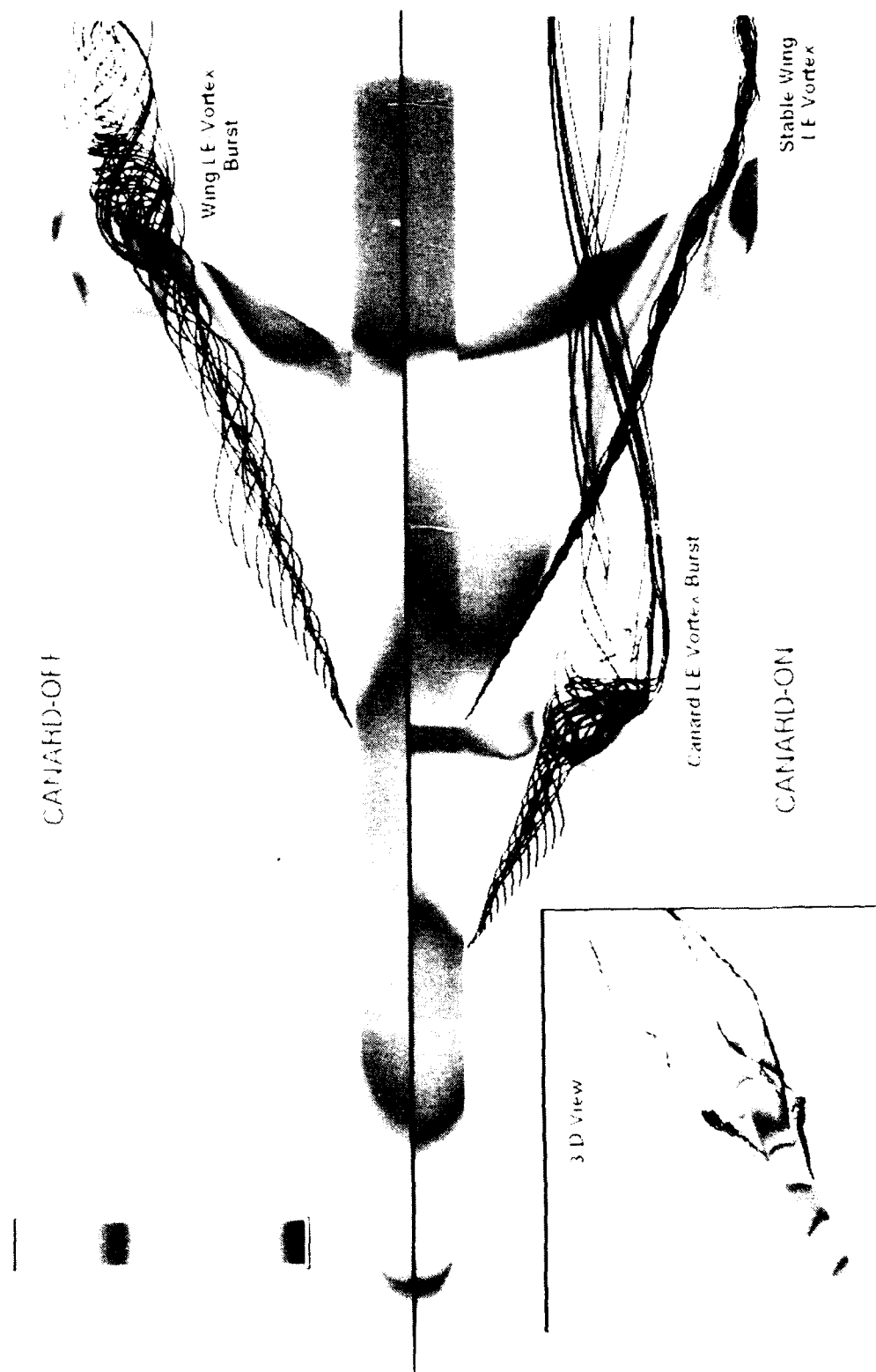


Figure 7-11. Effect of Canard on Wing-Body Aerodynamics

7-11 Effect of a Close-Coupled Canard on Wing-Body Aerodynamics

Objective. To accurately simulate the aerodynamics of a canard-wing-body configuration and investigate the characteristics of the canard-wing vortex interaction and breakdown.

Approach. Using an extension of the Transonic Navier-Stokes (TNS) code, Reynolds-averaged thin-layer Navier-Stokes equations were solved for the flow about a canard-wing-body configuration. Flow was considered fully turbulent and turbulence effects were modeled using the Baldwin-Lomax algebraic eddy viscosity model. The surface and flow-field grids were generated using the S3D code and the 3DGRAPE elliptic solver, respectively. A grid refinement study was performed and the total number of grid points ranges from 250,000 to over 1.7 million.

Accomplishments. Computations were made at a transonic Mach number of 0.90, angles-of-attack from 0° to 12° , and a Reynolds number based on mean aerodynamic wing chord of 1.52 million. Very good agreement of computed wing surface pressures and integrated forces (e.g., lift, pitching moments, and drag) with experimental measurements has been obtained and indicates that the computed results are accurate. The accompanying figure illustrates the effect of the canard at a 12° angle-of-attack. Specifically, the effect of the canard on the characteristics of wing vortex breakdown was noted. A side-by-side comparison of the canard-on and canard-off cases showed that the wing exhibits a stable vortex in the presence of the canard. This result indicates the potential of the canard to delay wing vortex breakdown and has been previously observed in numerous experimental studies.

The surface pressure map also shows the significant influence of the canard on the body aerodynamics.

Significance. Utilizing canards for enhanced aircraft performance requires a thorough understanding of the associated complex aerodynamics. Accurately predicting the nonlinear effects of the canard, including the canard-wing vortex interaction and wing vortex breakdown characteristics, improves the applicability of computational fluid dynamics towards the design and optimization of canard-configured aircraft.

Status/Plans. The effects of canard deflection, positioning, and size on wing-body aerodynamics are currently under investigation. A study of unsteady canard motion with applications towards aircraft control and maneuverability is planned.

Eugene L. Tu
Applied Computational Fluids Branch
Ames Research Center
(415) 604-4486

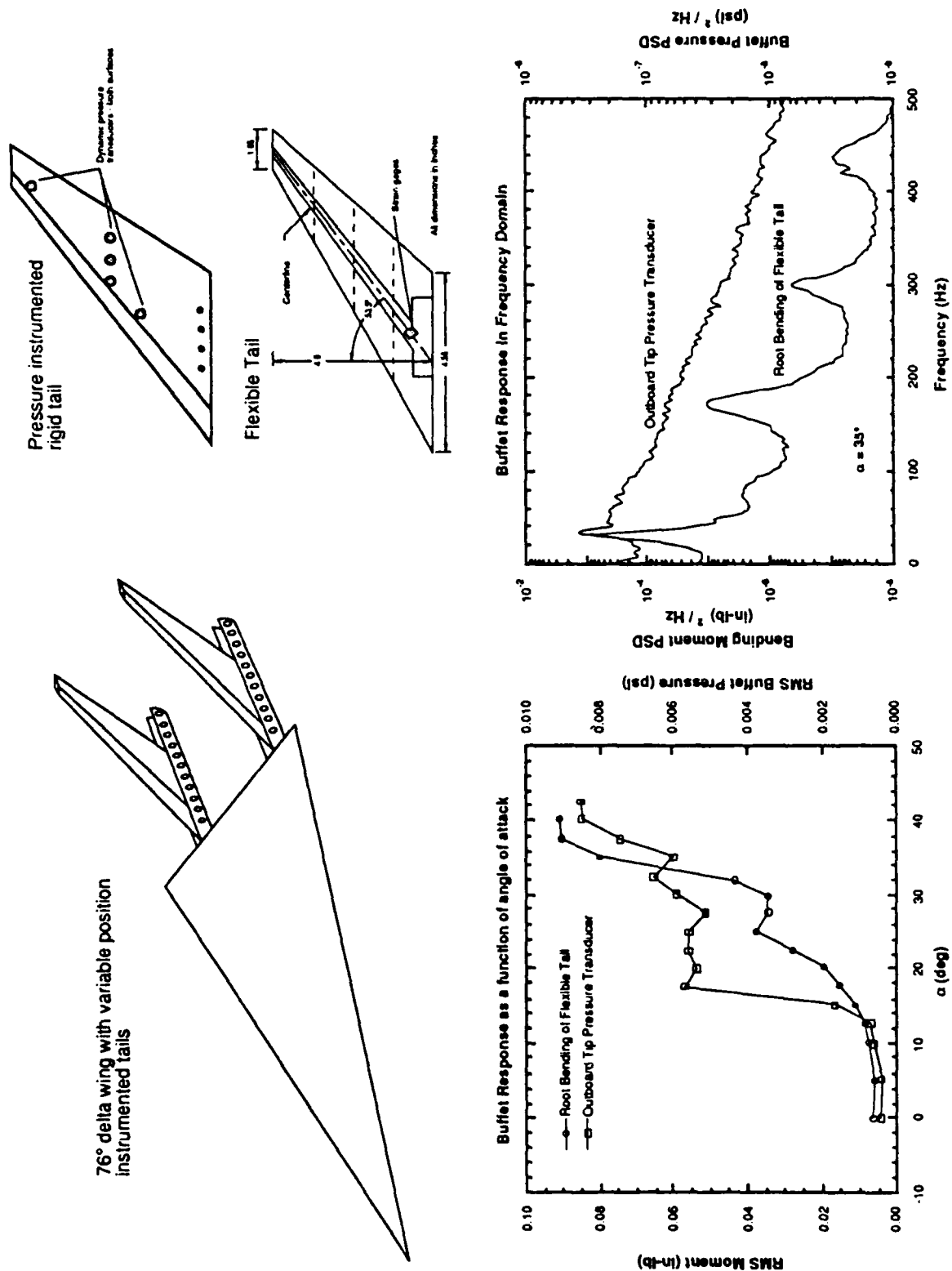


Figure 7-12. Fundamental Research in Vortex Interactions

7-12 Fundamental Research in Vortex Interactions

Objective. To develop a fundamental understanding of the vortex-fin (tail buffet) interaction process.

Approach. A cooperative program has been established between Langley Research Center and McDonnell Aircraft Company to study the fundamental physics in the vortex-fin interaction process. This program highlights a multidisciplinary investigation of the vortex-fin phenomenon, which will couple both experimental and computational researchers from the aerodynamics and structural dynamics communities. Instead of working with a complex configuration, a fundamental program using a geometrically simple 76° delta wing with two instrumented tails was developed. This simple configuration still captures all of the pertinent physics of the problem. The data obtained in the Langley Basic Aerodynamic Research Tunnel (BART) will include detailed measurements of flow field and surface parameters. Ten unsteady surface pressure transducers were installed on a rigid tail, and root bending and torsion responses were obtained from strain gages installed on a dynamically scaled flexible tail. Flow-field measurements included three-component laser velocimetry (LV).

Accomplishments. The testing for this multiphase experiment began in February 1991. A parametric study has been completed using laser light sheet flow visualization, force and moment measurements, and flexible tail response with the tails in nine positions (three chordwise and three spanwise locations). The results from the parametric study were used to select two tail positions to study in extensive detail with LV and unsteady surface pressure measurements. The figure shows some of the details of the model construction and a sample of the data. The dynamic responses, indicated by the root-mean-square (RMS) values of tail bending and buffet pressure, increase dramatically when the vortex

breakdown moves ahead of the tails in the lower left of the figure. The power spectral densities (PSD) are shown on the right. Several of the buffet pressures peak near the frequency of the first bending mode.

Significance. This fundamental program is an important topic to the high-performance military aircraft manufacturers because of the problem of structural fatigue caused by vortex-fin interaction on aircraft empennages. This test will broaden the database needed to validate the tail buffet laws currently being developed. This is the first experiment to correlate the unsteady off-body flow-field characteristics, i.e., velocity fluctuations, with the fin surface pressures.

Status/Plans. The unsteady surface pressure measurements are currently being acquired through the same angle-of-attack sweeps. The acquisition of the flow-field mean and fluctuating velocities is scheduled to begin in December 1991.

Anthony E. Washburn
Fluid Mechanics Division
Langley Research Center
(804) 864-1290

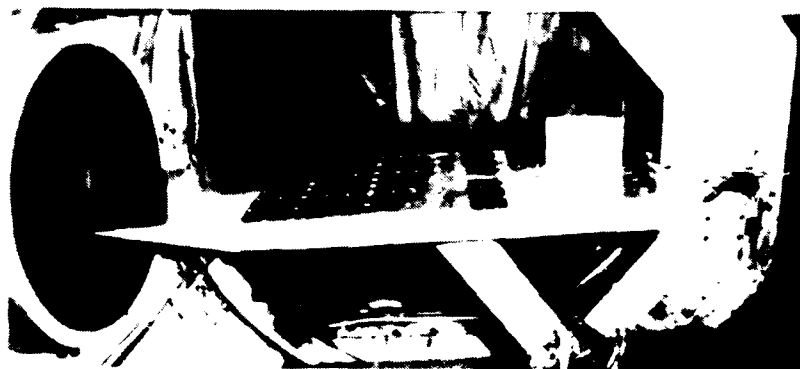
Chapter 8

Hypersonic Aerodynamics

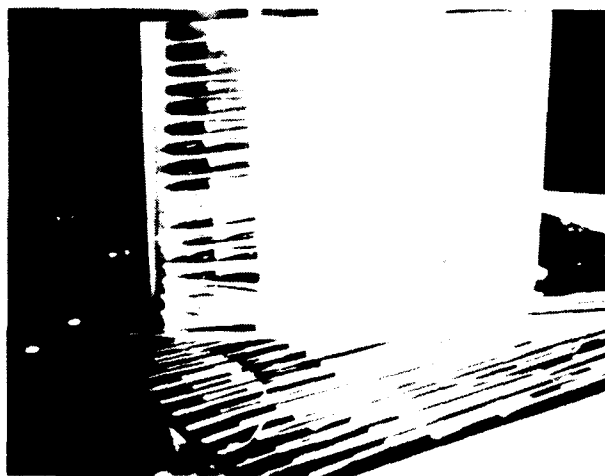
The Generic Hypersonics Aerodynamics program exists to institute a fundamental, permanent base of technological superiority in hypersonic aero/aerothermodynamics and to provide NASA with the long-term capability to achieve the goals of future NASA/DoD/DOE hypersonic vehicle research and development programs. It focuses on increasing the understanding of hypersonic aero/aerothermodynamics phenomena associated with slender, air-breathing hypersonic vehicles that use highly integrated airframe/propulsion systems and increasing the capability to experimentally and computationally simulate and analyze these phenomena. The program emphasizes both enabling and enhancing technologies related to hypersonic flight such as numerical simulation of turbulence and boundary layer transition, real-gas effects, rarefaction effects, shock/boundary layer interactions, and validation of computational methods. It explores flight research opportunities for technology areas that cannot be adequately addressed by computational methods or ground facilities. A major objective of the program is to structure cost-effective partnerships with industry which will enhance the rapid and efficient transfer of research results into the design and development of aerospace vehicles. University participation involves sponsored research and a refocusing and rededication of the aeronautics/astronautics curricula to hypersonics.

Program Manager: Jim Moss
OAST/RF
Washington, DC 20546
(202) 453-2820

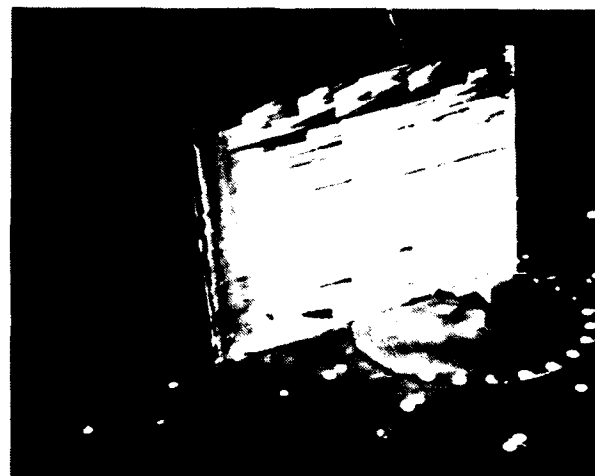
(a) $\delta = 2^\circ$ $Re_\delta = 9 \times 10^5$ Shock Generator Angles 5° - 15°



Test Model



Flow Field (a)



Flow Field (b)

Figure 8-1. Hypersonic Shock-Wave Boundary Layer Interaction

8-1 Experimental Study of Hypersonic Shock-Wave/Turbulent-Boundary Layer Interaction Flows

Objective. To provide accurate new hypersonic data for turbulence modeling and code validation.

Approach. Design, construct, and test a series of simple geometries that create three-dimensional (3-D) hypersonic shock-wave/turbulent-boundary layer interaction flows in the Ames 3.5-Foot Hypersonic Wind Tunnel.

Accomplishments. A new testbed was constructed for the 3.5-foot wind tunnel which enables one to test a series of 2-D and 3-D flow fields of varying complexity. The first test series was successfully completed. The test geometry consisted of a single sharp fin whose shock-wave interacts with a turbulent boundary layer. Test conditions were Mach number 8.2, Reynolds number $Re = 9 \times 10^6$ and fin angles from 5° to 15° . The measurements included surface flow direction, pressure and heat transfer, as well as detailed Pitot pressure and yaw angle surveys of the flow fields.

Significance. These new data represent the first 3-D hypersonic shock-wave/boundary layer interaction data suitable for turbulence modeling and code validation.

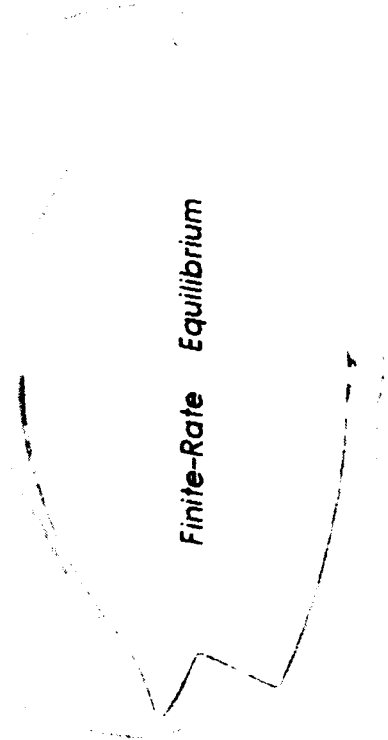
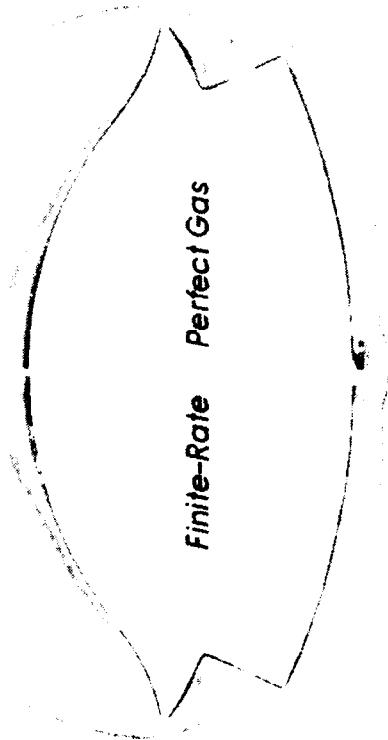
Status/Plans. More complex flow fields will be investigated with two fins and/or compression ramps, which will begin to look like hypersonic inlets.

C. C. Horstman, Marvin Kussoy
Fluid Dynamics Division
Ames Research Center
(415) 604-5950

GENERIC OPTION II -- FLOW-FIELD AT THE INLET PLANE ($x/L = 0.75$)

Mach 16.0 $Re_L = 7.2 \times 10^6$ $\alpha = 0^\circ$

TEMPERATURE CONTOURS



LOWER CENTERLINE PROFILES

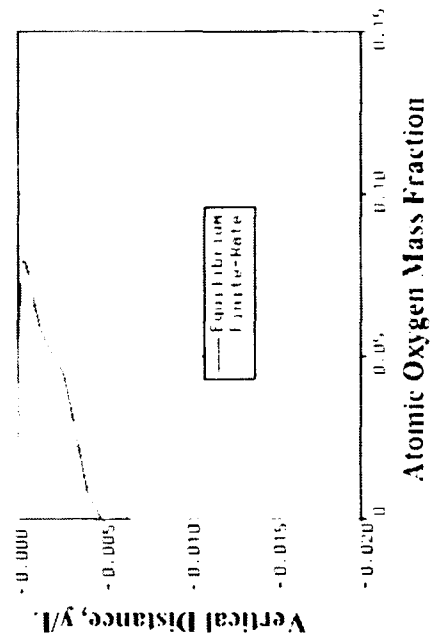
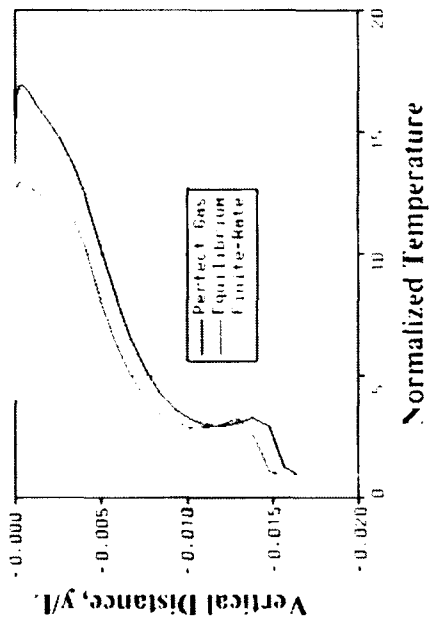


Figure 8-2. Numerical Performance Estimates for a Generic Hypersonic Forebody

8-2 Numerical Performance Estimates for a Generic Hypersonic Forebody

Objective. To examine the effects of nose bluntness and real-gas models on the computed flow physics and integrated performance parameters of a generic hypersonic forebody operating at NASP-like flight conditions.

Approach. The flow over the McDonnell Douglas Generic Option #2 36-inch blended-wing-body was computed for Mach 16 flow at an altitude of 125,000 ft. The parabolized Navier-Stokes solver, UPS, was employed with each of three available gas models: (1) perfect gas, $g = 1.4$, (2) equilibrium air, and (3) finite-rate air. Initial conditions for the space-marching calculations were provided by the time-dependent Navier-Stokes solver, TUFF, which possesses the same real-gas capabilities as UPS. Bluntness effects were studied at wind tunnel conditions (Mach 11.4, $Re_L = 2.904 \times 10^7$).

Accomplishments. Solutions were obtained for sharp- and blunt-nosed versions of the Generic Option vehicle under wind tunnel conditions, assuming a perfect gas. At zero incidence, the effect of bluntness was observed to be most significant along the lower centerline because of the accumulation of entropy-layer fluid into a viscous core along this line. The magnitude of the bluntness effect on centerline pressure and heat transfer distributions predicted by the computations generally agrees well with experimental data.

Real-gas effects were studied for the Mach 16 flight conditions by computing forebody flow fields using each of the three available gas models in the UPS and TUFF codes. A limited investigation of chemistry coupling and grid effects was also performed. These parameters were studied to evaluate their effect on the lower centerline flow physics and integrated performance measures such as lift, drag, and inlet mass flux. Integrated inlet

performance measures were generally more sensitive to real-gas effects than forebody performance measures such as lift, drag, and pitching moment.

Significance. The bluntness study provided confidence in the ability of the present CFD codes to predict surface pressures accurately at high Mach numbers for relatively complex configurations. Confident heat transfer prediction remains elusive because of grid sensitivity and boundary layer transition uncertainties. The high energy results give an indication of the level of importance of real-gas effects at NASP-like cruise conditions on both forebody flow-field physics and integrated performance parameters.

Status/Plans: The Option 2 geometry will be employed again to address issues involved in chemistry modeling such as loose vs. tight coupling and conservative vs. nonconservative form of the species equations.

Scott Lawrence
Applied Computational Fluids Branch
Ames Research Center
(415) 604-4050

Mach 15
 $\alpha = 0$ deg

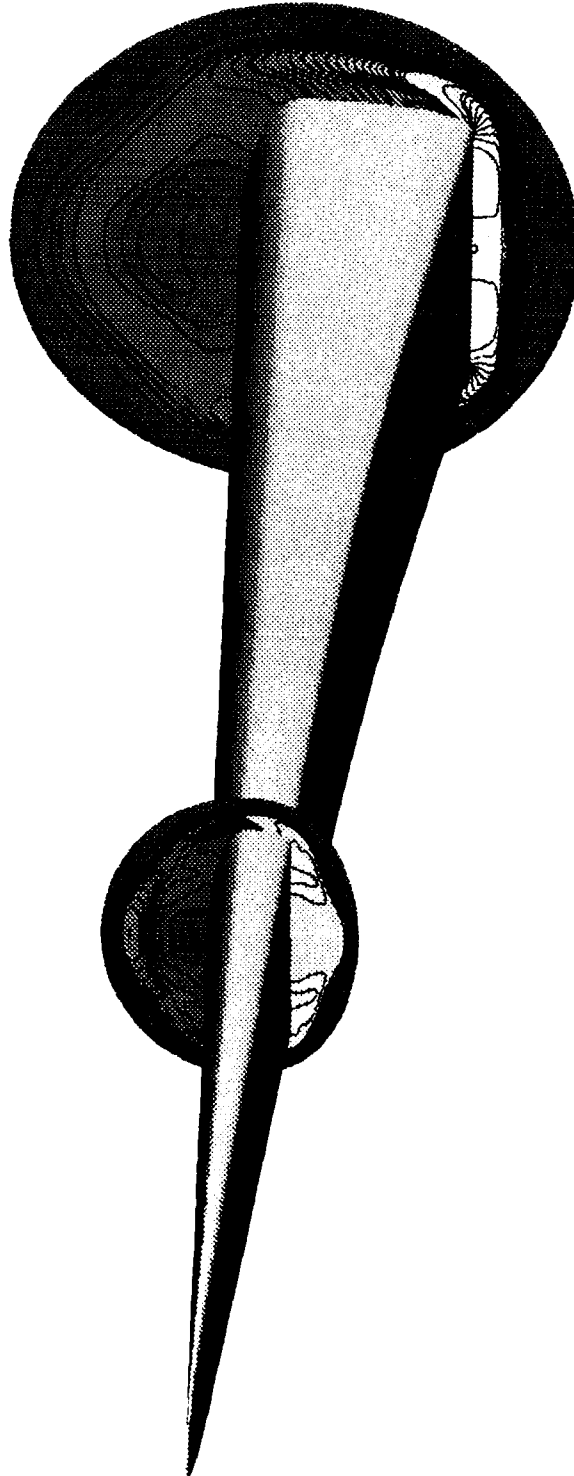


Figure 8-3. Forebody Pressure Contours

8-3 Calculation of Forebody Flow Field for a Candidate Aero-Space Plane Configuration

Objective. To demonstrate the application of the Langley Aerothermodynamic Upwind Relaxation Algorithm (LAURA) code to compute the flow over the forebody of a candidate Aero-Space Plane configuration, and to investigate flow-field anomalies predicted with another state-of-the-art flow-field code and to compare the results.

Approach. The LAURA code solves the time-dependent, thin-layer Navier-Stokes equations using a point-implicit scheme to converge the numerical solution. A two-block grid was used to calculate the blunted nose region and the downstream portion of the forebody in sequential steps. For comparison purposes, the flow-field grids used in this work were identical to those used by the other computational methods. The calculation was performed for flight conditions at Mach 15 and laminar, perfect gas flow was assumed.

Accomplishments. A converged solution over the Aero-Space Plane configuration was obtained which yielded complete flow-field quantities and surface properties (i.e., heating and pressure) for study. Computations were performed on the NAS Cray-2 computer and required approximately 22 hours of CPU time. Surface properties and the nature of the flow field at the engine inlet (forebody end) have been examined and comparisons with the other computational results have been made.

Significance. Results show that the LAURA code is capable of flow-field calculations for this type of configuration and is able to provide needed information about flow-field quality and surface heating. For example, the

calculation shows pockets of inflow and outflow on the lower surface and a buildup of the viscous boundary layer along the lower centerline. Also, anomalies in profiles of the total enthalpy at the engine inlet face, which were predicted in the other computational results, were not confirmed by the present calculation.

Status/Plans. Efforts are ongoing to resolve the anomalies in total enthalpy profiles. Knowledge gained in the present work will be applied in a forthcoming experimental/computational study in support of the National Aero-Space Plane program.

Richard A. Thompson
Aerothermodynamics Branch
Langley Research Center
(804) 864-4367

Computational/Experimental Investigation M = 10 air



PARAMETER STUDY

- Re
- CH
- Cool location

- First benchmark Mach 10 inlet study
- CFD used to design experiment
- Excellent CFD/experiment agreement

Figure 8-4. Computational/Experimental Parametric Study of 3-D Scramjet Inlets at Mach 10

8-4 Computational/Experimental Parametric Study of 3-D Scramjet Inlets at Mach 10

Objective. To calibrate current computational fluid dynamics (CFD) computer codes for hypersonic forebody/inlet flows using experimental data from the Generic Option #2 program.

Approach. Numerical simulation of three-dimensional hypersonic flow past a forebody/inlet configuration is performed using a state-of-the-art family of upwind methodology CFD computer codes, CFL3DE and CFL3D. Numerical results, including surface pressure and heat transfer along the forebody and inside the inlet, are compared with experimental data for the same configuration and freestream conditions.

Accomplishments. The forebody/inlet calculation has been completed. The computed forebody pressures and heat transfer exhibit reasonably good agreement with the experimental data as does the computed results in the inlet. In some regions of the inlet, the agreement is quite good considering the complex nature of the flow. In other regions, the agreement is poor indicating deficiencies in the numerical modeling.

Significance. The results demonstrate the ability of this family of CFD computer codes to predict forebody pressures and heat transfer rates with reasonably good accuracy. The results in the inlet are encouraging, but also indicate areas of needed improvement in the numerical modeling of internal flows. In particular, the turbulence modeling needs to be improved.

Status/Plans. Comparisons of the computed results and experimental data will be sent to the Generic Option #2 report authors for their comments and to learn of any update in the experimental data. After their response, the results will be documented in a NASP publication. Also, new turbulence models, better suited to internal flows, will be incorporated into this family of CFD computer codes.

Arthur D. Dilley, George F. Switzer,
William M. Eppard
Langley Research Center
(804) 864-2288

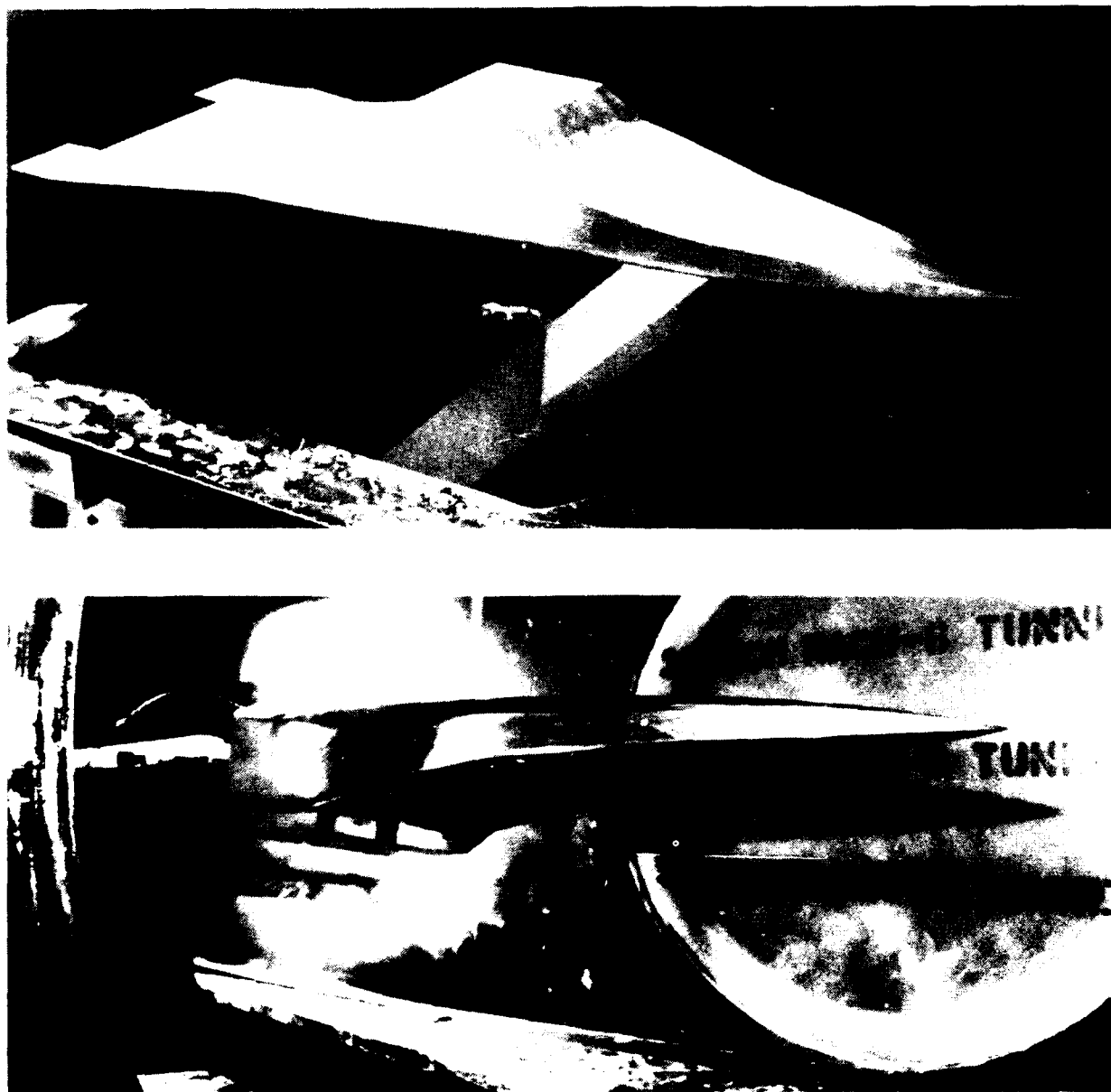


Figure 8-5. Technique for Hypersonic Powered Tests of Airbreathing Configurations

8-5 Technique for Hypersonic Powered Tests of Airbreathing Configurations

Objective. To experimentally evaluate an unproven technique of using metric model parts to conduct simulated exhaust powered tests of an airbreathing vehicle in a hypersonic wind tunnel.

Approach. The method required separate tests of two identically scaled models. The external surface force/moment contributions from the nose to the engine cowl trailing edge were determined from tests of the sting mounted, unpowered forebody model that was fully metric. The aftbody external surface force/moment contributions from the cowl trailing edge rearward were determined from tests of an entire model that had a metric aftbody. This entire model was supported by a strut mounted to the forebody and had a closed inlet and a metric aftbody. The scramjet exhaust was simulated by using a 70/30 (percent mole fraction) mixture of tetrafluoromethane and argon.

Accomplishments. Both models were tested in the Langley 20-Inch Mach 6 Wind Tunnel at a Reynolds number of $1.0 \times 10^6/\text{ft}$. The appropriate forebody and aftbody force accounting procedures for this metric model parts technique were developed and demonstrated. In addition, facility operating issues related to conducting exhaust simulation powered testing with a metric aftbody model were examined. Also, the powered metric aftbody model was configured with various wing incidence angles (-1.5° , -3.0° , -4.5°) and elevon deflection angles (0° , $\pm 10^\circ$, and $\pm 20^\circ$) to examine the trim characteristics with simulated exhaust.

Significance. This test program produced the first hypersonic powered force/moment data on a National Aero-Space Plane-type configuration. The results of this effort have shown that (1) the effect of the exhaust plume on the measured forebody forces/moments is negligible; (2) the internal inlet contribution to the forebody drag is less than 10%; and (3) the interference effect on the measured aftbody forces/moments as a result of the forebody strut mount is negligible.

Status/Plans. Additional tests of the powered TTD model in the 20-Inch Mach 6 Wind Tunnel are planned to investigate the use of air, as opposed to the tetrafluoromethane/argon mixture, as a simulated exhaust gas. This effort is part of Government Work Package 5 in support of the National Aero-Space Plane Program

David W. Witte
Applied Aerodynamics Division
Langley Research Center
(804) 864-5589

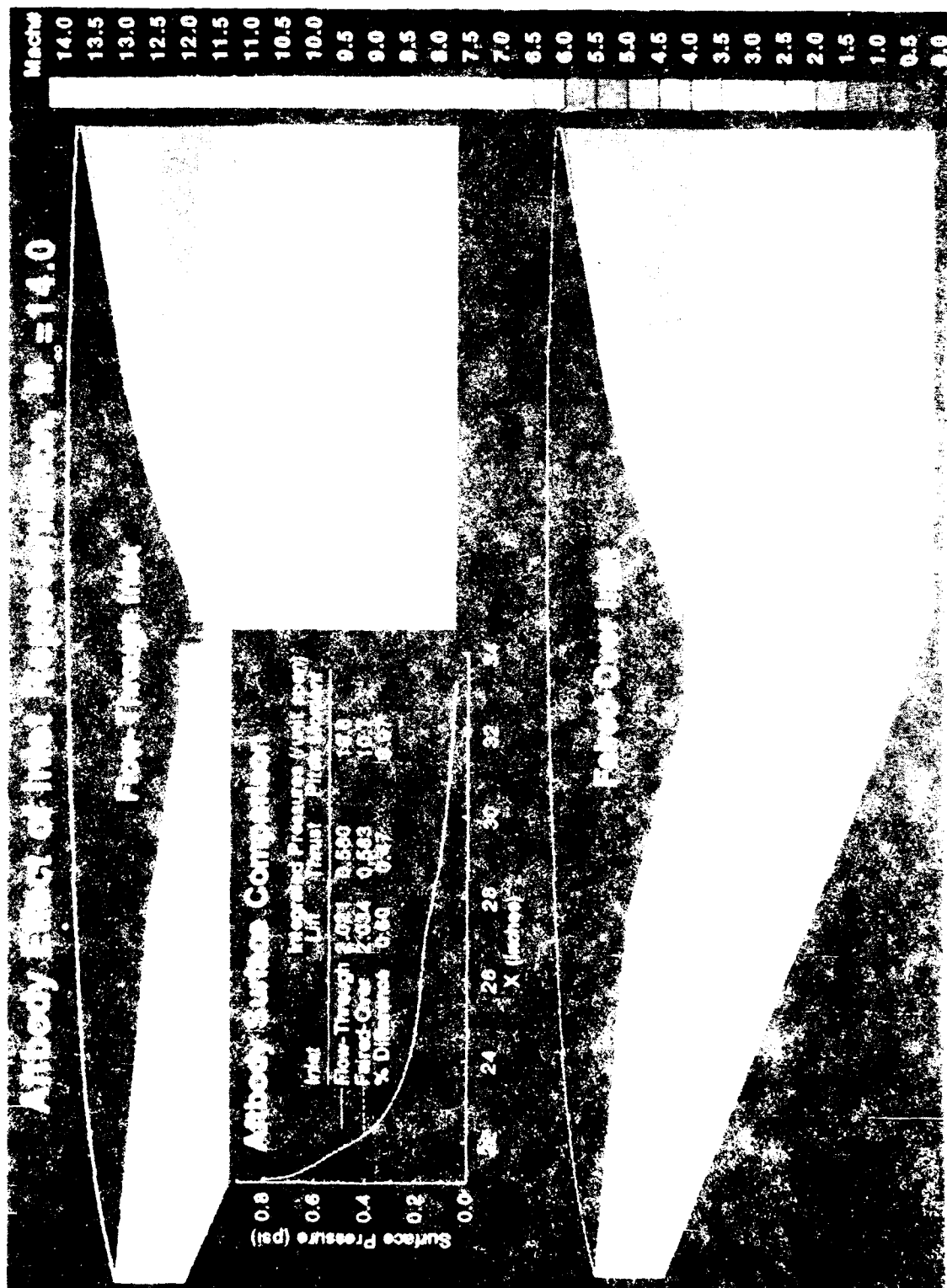


Figure 8-6. Airbody Effect of Inlet Representation

8-6 Effect of Inlet Representation on Powered Hypersonic Aftbody Flows

Objective. To assess the aftbody performance of a powered hypersonic airbreather (PHA) model by computationally examining the effects of a flow-through inlet and a faired-over inlet at a variety of freestream conditions.

Approach. One method for obtaining powered effects on PHA concepts is to fair over the inlet and then route alternate gases through the combustor section to simulate the combustion products. However, the fairing alters the external flow field and possibly affects the aftbody local flow field and surface pressures. The effect of the fairing was studied using the General Aerodynamic Simulation Program (GASP) to analyze two PHA configurations. The flow-through inlet model provided the necessary inlet geometry to simulate the flow associated with the cowl leading edge. The faired-over inlet model eliminated all cowl leading-edge effects by covering the inlet, resulting in a simple expansion over the cowl.

Accomplishments. Two-dimensional CFD simulations were performed on the two configurations at various freestream conditions, including Mach numbers 3.0 to 14.0 at $Re_\infty = 2.0 \times 10^6/\text{ft.}$ and Reynolds numbers 0.5 to $7.0 \times 10^6/\text{ft.}$ at $M_\infty = 6.0$. These conditions yielded static nozzle pressure ratio (SNPR) values from 12 to 256 because of the different freestream pressures. The internal conditions were identical for all solutions, namely $M = 1.0$ at the nozzle throat with a jet total pressure of 30 psi.

Comparison of Mach number contours for the two inlet representations is shown in the figure for the conditions at $M_\infty = 14.0$ and $Re_\infty = 2.0 \times 10^6/\text{ft.}$ Significant differences can be seen in the flow fields near the cowl for the two configurations. The cowl leading edge on the flow-through inlet creates a shock followed by a moderate expansion of the flow and then a recompression between this expansion region

and the cowl. For the faired-over inlet, there is only an expansion. Also, the size of the boundary layer on the flow-through inlet case is significantly smaller because it develops only from the cowl leading edge instead of on the entire forebody. In the aftbody region, the flows are quite similar, including the location of the cowl trailing-edge shock, the shear layer, and the weak compression within the shear layer. The line plot compares aftbody surface pressures and integrated force and moment components for the two PHA configurations at this freestream condition. The result is that the difference in integrated aftbody pressures due to different representations is less than 1%. This comparison remained consistent for the entire set of freestream conditions that were simulated.

Significance. Within the scope of this investigation, two-dimensional CFD results indicate that there is no significant effect on powered aftbody performance due to fairing over the inlet compared to a flow-through inlet. Flow-field differences exist for the two inlet representations, but they are isolated to the flow region near the cowl and appear to have minimal impact on aftbody surface pressures.

Status/Plans. There is a need to extend the CFD solutions to three-dimensional to account for 3-D relief effects as well as proper expansion of the plume onto the entire span of the aftbody and any wing or control surfaces that may be subject to influence by the exhaust flow.

Lawrence D. Huebner
Applied Aerodynamics Division
Langley Research Center
(804) 864-5583

2D GASP PNS TURBULENT SOLUTION VS. EXPERIMENT

Pitot pressure

50% Argon, 50% Freon - 12 jet: SNPR = 26.1

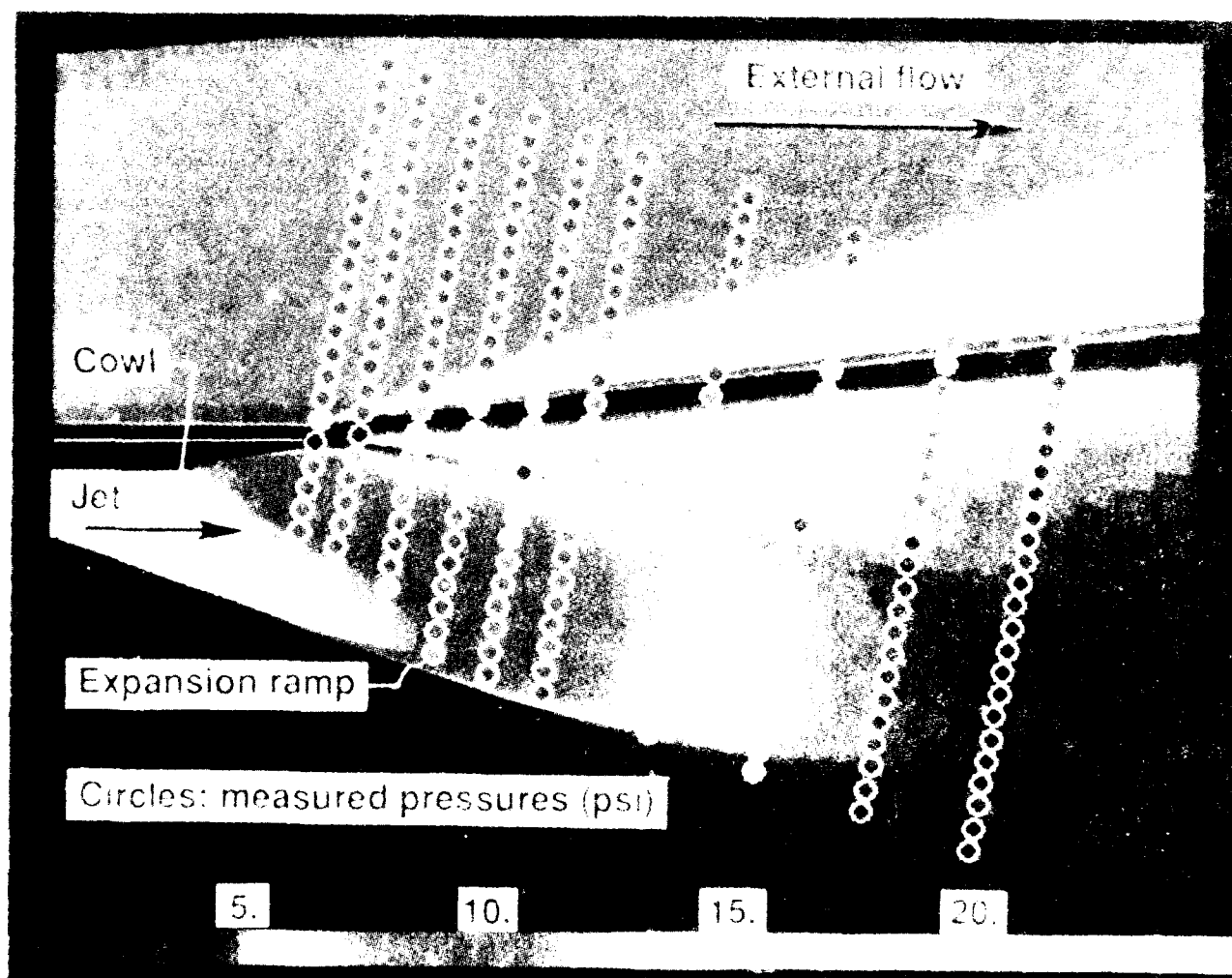


Figure 8-7. 2-D GASP PNS Turbulent Solution vs Experiment

8-7 Generic Scramjet Nozzle/Aftbody Studies

Objective. To determine optimum numerical algorithms and codes for analyzing diffusive multiple-species, hypersonic 3D flow fields, including comparisons with appropriate experimental data. The goal is to develop procedures for the analysis and design of generic hypersonic aftbody geometries.

Approach. Several Euler/Navier-Stokes codes, employing a variety of numerical algorithms, were exercised to analyze flow about a powered generic scramjet nozzle/aftbody model. The calculated results were compared with measured surface (static) and flow-field (pitot) pressures for several single- and multiple-species flows.

Accomplishments. Flow-field pitot pressures were measured about a powered Generic Scramjet Nozzle/Aftbody (GSNA) model in the Langley 20-Inch Mach 6 Wind Tunnel. The GSNA has been modeled using computational fluid dynamics (CFD) codes ranging from a 2-D Euler (inviscid) code to 3-D Navier-Stokes (viscous) codes. An explicit Parabolized Navier-Stokes (PNS) code with multiple gaseous species capability was modified to allow solid wall boundary conditions internal to the grid to define a cowl separating a jet flow from a freestream flow. Calculations in Euler mode were made to determine the accuracy obtainable with inviscid calculations. Results from both 2-D and 3-D calculations were compared with the experimental data. The implicit, multiple-zone General Aerodynamic Simulation Program (GASP) code was similarly exercised and shown to be more robust than the explicit code for high nozzle pressure ratios. The jet fluid was modeled as air (perfect gas), a mixture of nitrogen and oxygen, and two mixtures of argon and Freon to simulate the ratio of specific heats of actual hot scramjet exhaust gases. GASP 2-D PNS calculations, including turbulence modeling (as shown in the figure), showed improved agreement with experiment over Euler solutions, both in terms

of surface pressures and flow-field details around the cowl trailing edge. A 3-D explicit, elliptic full Navier-Stokes code was modified to accept block-structured grids and two multiple-species, half-span nozzle calculations were performed.

Significance. Proposed hypersonic vehicles will operate in flight regimes beyond the accessibility of ground-based facilities. The ability to numerically analyze and design scramjet/aftbody components for such vehicles is crucial for efficient, interdisciplinary propulsion/airframe integration.

Status/Plans. A NASA Technical Paper has been written documenting the flow-field pressure measurement experiment (to be released) and an AIAA paper documenting the CFD results and data comparisons (surface and flow field) has been published. A full 3-D hypersonic vehicle will be numerically modeled with powered scramjet exhaust flow simulation and comparisons made between the CFD results and ongoing wind tunnel measurements. In addition, the GASP code will be coupled with an iterative design/optimization code to permit automated design of scramjet aftbody geometries for optimum lift and thrust constrained by pitching moment requirements.

Kenneth E. Tatum, William J. Monta
Applied Aerodynamics Division
Langley Research Center
(804) 864-5587

PEMACH-Computed Pressure Distributions and Exp. Data Comparisons

Generic Option #2 Inlet Model

$M_\infty = 12.00$ $\alpha = 0$

Centerline Shock Structure

Bottom Surface

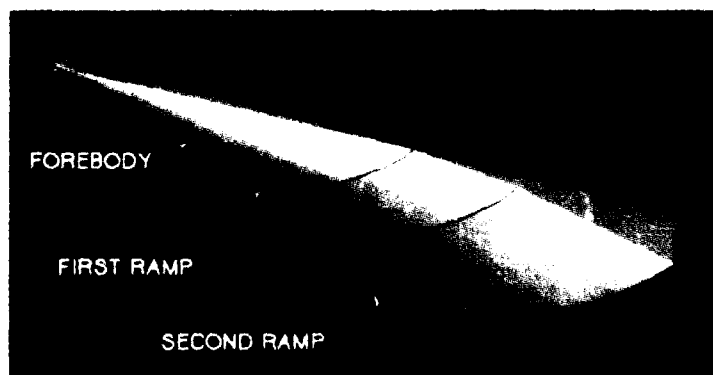


Figure 8-8. PEMACH - Computed Pressure Distributions and Experimental Data Comparisons

8-8 Advanced Aero-Propulsion Performance Design Tool (PEMACH)

Objective. To improve the current capability to rapidly predict local pressure and thermal loads on hypersonic conceptual designs for structural analysis and stability and control analysis.

Approach. An engineering technique based on the method of characteristics (MOC) was chosen as a starting point for this study, which began last year. Although this particular technique was originally developed for applications to supersonic wings and conical shapes, it has shown very good agreement with experimental and flight data up to a Mach number of 4. The method is being adapted to complete hypersonic configurations and results compared with experimental data, Navier-Stokes (NS) calculations, and engineering methods currently in use.

Accomplishments. The code, PEMACH, (a Practical Engineering Method for Aero-propulsion Characteristics at Hypersonic Mach Numbers) can now solve the flow over the fuselage and wings, including capture of engine mass flow, in a quasi-3-D fashion at hypersonic Mach numbers. The code includes solution capabilities for either sharp or blunt leading and trailing edges, and for completely arbitrary planform.

Part of the method development was calibration to experimental results, as illustrated in the figure. The illustrated comparison used the experimental results from the National Aero-Space Plane (NASP) Generic Option #2 3-D forebody-inlet model. Excellent agreement with wall pressures, both on and off centerline, and shock locations are illustrated in the figure. Comparison with CFD solutions verify accurate prediction of mass capture, and comparisons with unpowered aerodynamic test results from the NASP Test Technique Demonstrator (TTD) model verify accurate prediction of $C_m \alpha$ over a large variation in angle-of-attack.

Significance. This capability brings the ability to quickly predict configuration loads suitable for structural, thermal, and stability and control analysis.

Status/Plans. A preliminary version of PEMACH has been released and is currently being used for aerodynamic (lift, drag, moments) analysis and design of hypersonic vehicles. Work is continuing to efficiently model the inlet and nozzle flows, to fully couple the boundary layer to the 3-D effects, and include boundary layer transition prediction.

Suresh H. Goradia,
VIGYAN Associates

Abel O. Torres, Charles R. McClinton
Hypersonic Technology Office
Langley Research Center
(804) 864-6253



Figure 8-9. Wing Glove for Pegasus Crossflow Transition Experiment

8-9 Wing Glove for Pegasus Crossflow Transition Experiment

Objective. To design and fabricate a wing glove that provides a smooth non-ablating test surface for the measurement of hypersonic 3-D crossflow boundary layer transition.

Approach. Ablation products from the current thermal protection system on the Pegasus delta wing will interfere with sensitive aerodynamic measurements like boundary layer transition. To minimize this interference, an aerodynamically shaped glove with a smooth nonablating surface was installed on the existing wing. A ceramic glove fairing was used to provide a smooth transition between the wing and glove surface. All of the flight instrumentation was contained within the glove so that the integration with Pegasus was simply a cable connection.

Accomplishments. A prototype wing glove was fabricated to identify and demonstrate concepts for meeting the requirements of the crossflow transition experiment. The glove consists of a copper skin attached to the ceramic blanket known as TABI (Tailorable Advanced Blanket Insulation). Since the aerothermodynamic heating at hypersonic speeds is substantial, a copper skin was chosen to quickly conduct heat away from the leading edge and therefore reduce the thermal gradient and stresses. TABI both supports the copper skin and insulates it from the composite wing. Recent work with the rigid ceramic insulation known as TUF1 (Tough Uni-Piece Fibrous Insulation) shows good progress toward fabrication of the ceramic glove fairing.

Significance. Based on this work, a FX-0 glove will be fabricated and flown on the Pegasus flight, scheduled for June 1992. This FX-0 glove is the first of three gloves planned for this hypersonic flight research program. The goal of FX-0 is to validate the glove concept for measuring crossflow transition on a swept delta wing at hypersonic speed. Future gloves will be optimized for making more precise measurements of this phenomena.

Status/Plans. Further work is required to finalize the fairing design and glove assembly. Fabrication of the FX-0 glove and its fairing is scheduled to begin January 1992.

Paul Kolodziej
Thermal Protection Materials Branch
Ames Research Center
(415) 604-5377

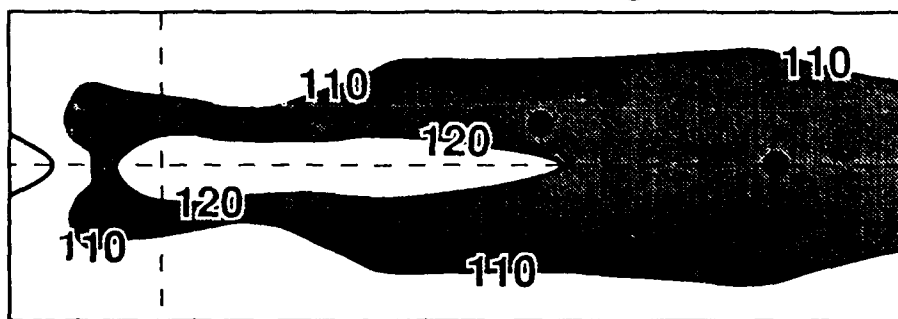
Chapter 9

Aeroacoustics Research and Technology

Aeroacoustics is concerned with the fundamental understanding, prediction, and control of noise and acoustic loads produced by the motion of fluids and bodies moving through the atmosphere. To achieve this objective, research is being conducted in three main areas: 1) Computational Aeroacoustics – establish CFD methodology as a discipline for acoustics technology development focusing on computational models of high-speed flow noise and shock/vortex interactions. 2) Supersonic Jets/Loads – understand/predict/reduce noise and acoustic loads generated by high-speed aircraft and, in particular, establish innovative concepts for supersonic jet noise suppression and develop a detailed acoustics loads database on airframe structures. 3) Long Range Propagation – model atmospheric propagation effects supported by fundamental verification/validation experiments.

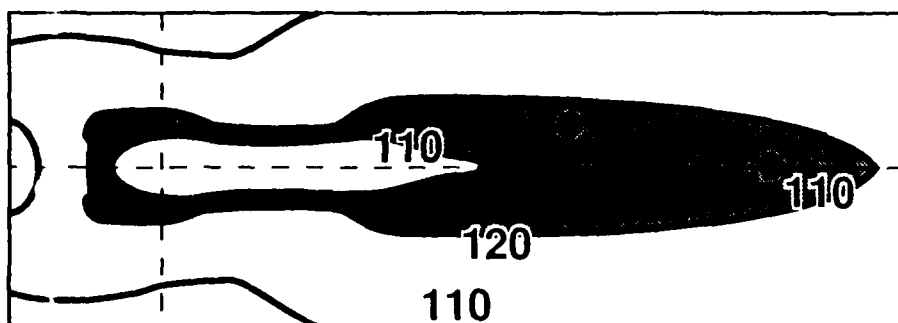
Program Manager: Benjamin Neumann
OAST/RF
Washington, DC 20546
(202) 453-2795

100% thrust, standard lift configuration



**Sideline 116.3
Centerline 116.3**

80% thrust, 30% lift increase



**Sideline 112.3
Centerline 112.3**

Figure 9-1. Contours of Effective Perceived Noise Levels (EPNdB) for Standard Takeoff and Reduced Thrust/Increased Lift Takeoff for a Jet Aircraft

9-1 Jet Noise Predictions for Reduced Thrust Takeoff Study

Objective. To demonstrate the use of the Aircraft Noise Prediction Program (ANOPP) to evaluate the effects of reduced jet thrust on community noise levels. Reduced jet thrust levels at takeoff increase the required distance on the runway (ground roll) before lift-off. To compensate for the increased ground roll, several levels of increased lift were included in the study.

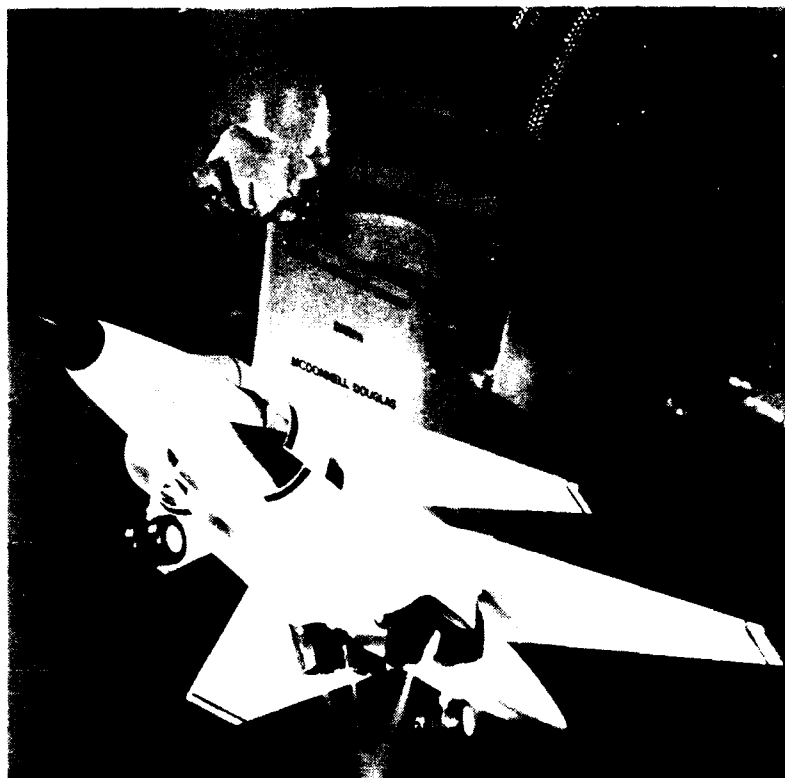
Approach. Predictions were made using the ANOPP dual stream coannular jet noise module for the AST-205-1 aircraft powered by GE21/J11B14A scaled engines. A power setting of 100% thrust and a standard lift configuration were used as a baseline for this study. Power settings varied from 100% to 80% maximum thrust, while lift was increased in increments of 15% to a maximum of 60%. An angular rotation rate of 3° per second and a constant climb angle of 8° were used. Effective Perceived Noise Level (EPNL) values were calculated at the FAA prescribed noise measuring points. Noise levels were also calculated on a 1-by-6 mile grid of 65 observer positions, with each observer located 4 feet above the ground. Noise contours were generated from these observer positions.

Accomplishments. Contours for both the baseline case and the 80% thrust/30% increased lift case are shown in the figure. The reduced thrust case decreases the necessary ground roll distance by 646 feet and lowers the sideline EPNL level by 4 EPNdB from the maximum thrust baseline case. Although the centerline noise level is not of major concern, it too benefits by 4 EPNdB from the reduction in thrust and increase in lift. Additionally, as the figure shows, reducing thrust and increasing lift alter the shapes of the contours. As thrust is decreased and lift is increased, the contours tend to shorten in length and become more compact.

Significance. The use of the ANOPP prediction code shows that reduced thrust takeoff procedures can be beneficial. Sideline noise levels are of greatest concern during takeoff. Since the FAA sideline noise measurement point location depends on the point of lift-off, only a slight benefit can be derived from increasing the amount of lift while keeping thrust at a maximum. The key to reducing jet noise lies in thrust reduction.

Status/Plans. It has been shown that reduced thrust, used in conjunction with increased lift to compensate for increased runway distance, can reduce Effective Perceived Noise levels at the sideline and centerline FAA noise measurement locations. Better jet noise prediction modules being designed for ANOPP will allow the noise impact from a high-speed civil transport (HSCT) aircraft on community noise to be evaluated.

Robert A. Golub
Acoustics Division
Langley Research Center
(804) 864-5281



Effect of temperature on OASPL

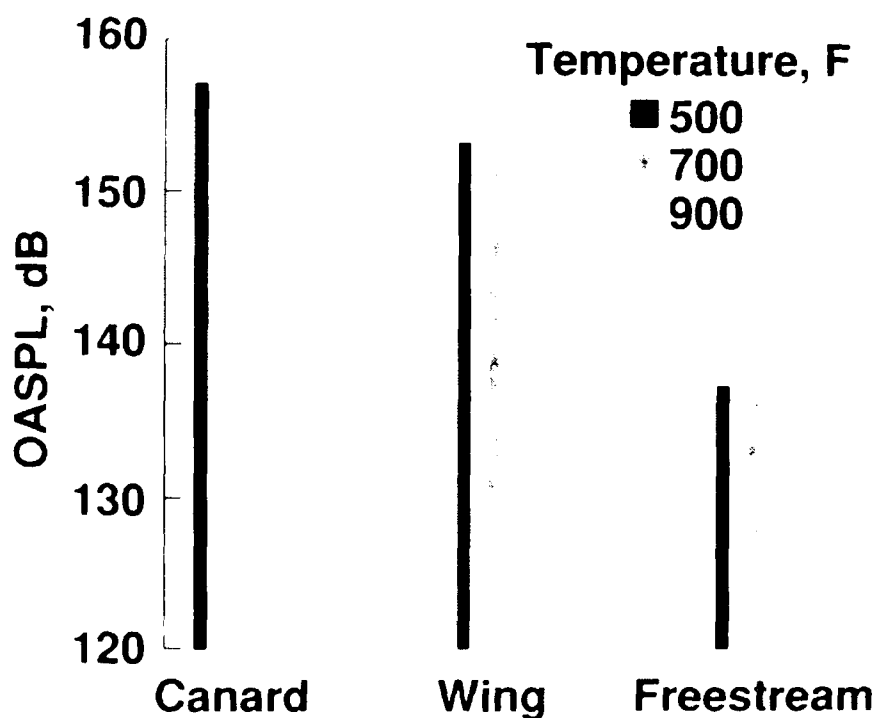


Figure 9-2. Scale Model of McAir 279-3C Installed for Hot-Gas Ingestion Testing (top); Effect of Jet Temperature on Measured Overall Sound Pressure Levels Measured at Three Levels on the Model (bottom)

9-2 ASTOVL Acoustic Loads Test

Objective. To characterize the acoustics and dynamic structural loading of an advanced short takeoff/vertical landing (ASTOVL) aircraft operating in ground effect and at elevated jet exit temperatures. This research was part of a Lewis/Langley cooperative program, complementary to in-house research aimed at improving the understanding of the impingement acoustics of multiple heated jets.

Approach. A 9.2% scale model of the McAir 279-3C aircraft was tested in the Lewis 9- by 15-Foot Low-Speed Wind Tunnel. The model (see accompanying figure) was built to evaluate the hot gas ingestion (HGI) characteristics of the design at temperatures up to 1000° F, at nozzle pressure ratios (NPR) of 4. The model geometry parameters varied included forward nozzle splay angle (from 12° inward to 18° outward) and Lift Improvement Device (LID) configuration (on, off). Acoustic data were obtained from a linear array of five freestream microphones located parallel to the model centerline. Model dynamic loads were measured with eight watercooled dynamic pressure transducers located on the underside of the canard, wing, and aft fuselage.

Accomplishments. Data were taken for over 700 combinations of model geometry and test conditions. The data shown illustrate the minimal effect of jet temperature on the noise level (OASPL) as measured on the canard, the wing, and in the freestream, while the jets were operating at the design condition. As shown by the data, levels up to 160 dB were observed on the canard (which was closer to the nozzles than the wing) and up to 140 dB in the freestream. At other conditions, levels as high as 180 dB with discrete tones 160 dB in amplitude were measured. Tones were generated at a wide variety of conditions (model height, nozzle pressure ratios, jet temperatures) and geometries. Both free-jet tones

and impingement tones were observed, and their frequencies were well predicted by current jet noise theories.

Significance. Acoustic loads on ASTOVL configurations can potentially attain sufficiently high levels to cause structural failure. No satisfactory theory exists that can predict the acoustics of multiple heated non-axisymmetric jets operating in ground effect in an off-design condition. The acquired data will be valuable in understanding both the fundamental physics of jet-impingement and the configuration issues in ASTOVL aircraft acoustics.

Status/Plans. This test served as Phase II of Lewis' hot gas ingestion work with this design. Additional acoustic testing is planned for Phase III, including the placement of transducers on the underside of the fuselage between the nozzles. This will allow for the investigation of the dynamics of fountain impingement on the model, and the propagation of noise from the fountain to the farfield.

L. Kerry Mitchell
Acoustics Division
Langley Research Center
(804) 864-3625

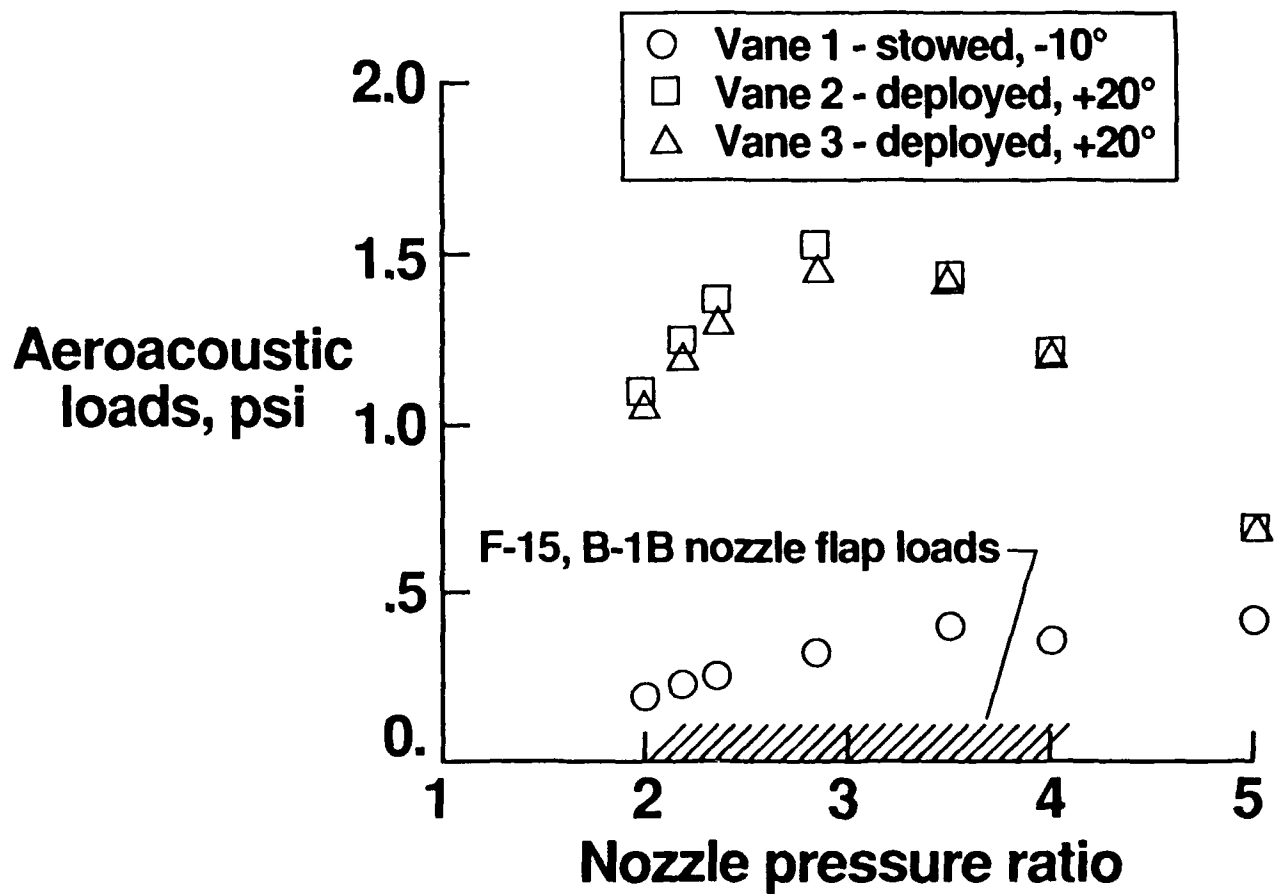


Figure 9-3. Aeroacoustic Loads on Thrust Vectoring Vanes of a Model F-18 High Alpha Research Vehicle (HARV)

9-3 Aeroacoustic Loads on F-18 High Alpha Research Vehicle (HARV)

Objective. To provide a benchmark database on the nearfield acoustic loads generated by supersonic jet plumes of high-performance aircraft. High aeroacoustic load levels due to twin jet resonance have caused component failures on F-15 and B-1B aircraft. A model and full-scale static study was conducted to evaluate aeroacoustic loads associated with the thrust vectoring control system (TVCS) of the F-18 High Alpha Research Vehicle (HARV).

Approach. A 7.4% aft-end model of the F-18 HARV/TVCS was designed, constructed, and instrumented with water-cooled dynamic pressure sensors to measure aeroacoustic loads on the three thrust vectoring vanes. Dynamic loads were measured on the model for vane angles from stowed (-10°) to fully deployed ($+20^\circ$). Only military power nozzles were studied with nozzle pressure ratios ranging from 2 to 5 and jet total temperatures from 104° to 680°F . In a parallel effort, researchers at NASA Ames/Dryden measured the near-field acoustic characteristics of the F-18 HARV with TVCS installed on the twin F-404 engines and on an unmodified F-18. The divergent nozzle flaps on the F-404 engines were removed on the F-18 HARV, leaving essentially convergent nozzles. Near-field sensors were positioned near the aircraft in a similar fashion to one used in the model scale study.

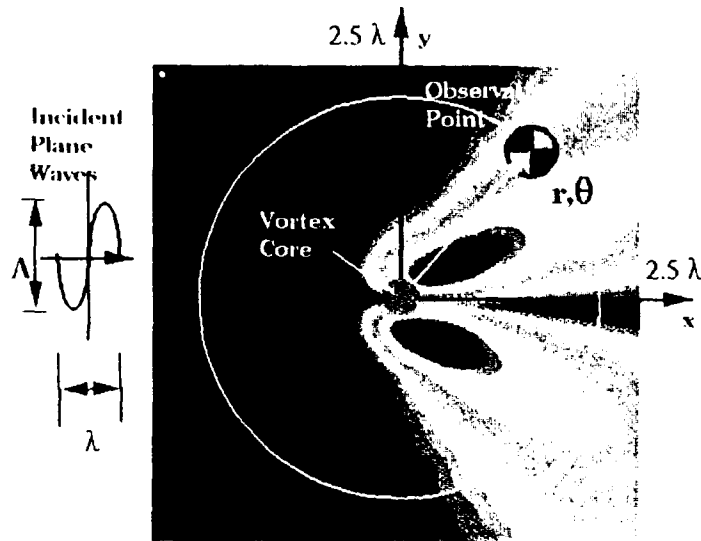
Accomplishments. Overall dynamic pressure loads varied considerably with vane angle position and nozzle pressure ratio, as shown in the figure. The peak pressure value of 1.5 psi at a nozzle pressure ratio of 2.8, recorded for thrusting vanes at 20° , translates to an estimated full-scale dynamic force load on a vane of between 300 and 400 lbs. Stowed vanes (-10°) experience much smaller dynamic loads, 0.4 psi rms. At higher pressure ratios, the initial spread rate of the jet is less, and less jet/vane interaction occurs. These levels are significantly higher than previously re-

corded on previous F-15 and B-1B outer divergent flap studies. The F-15 and B-1B loads were dominated by a twinjet resonance mechanism, which is absent in the present research when the vanes are fully deployed. Ground tests of a full scale F-18 HARV at Dryden also confirmed high levels of near-field loads. The removal of the divergent nozzle flaps on the baseline F-18 to accommodate the TVCS resulted in a convergent nozzle configuration. Convergent nozzles produce significantly greater shock noise. At the maximum afterburner power setting, a condition not tested in the model study, an intense tone was present in the near-field spectrum. This tone lies near the predicted frequency for twin supersonic plume resonance—a phenomenon known to contribute to the high acoustic loads for the convergent nozzle configuration.

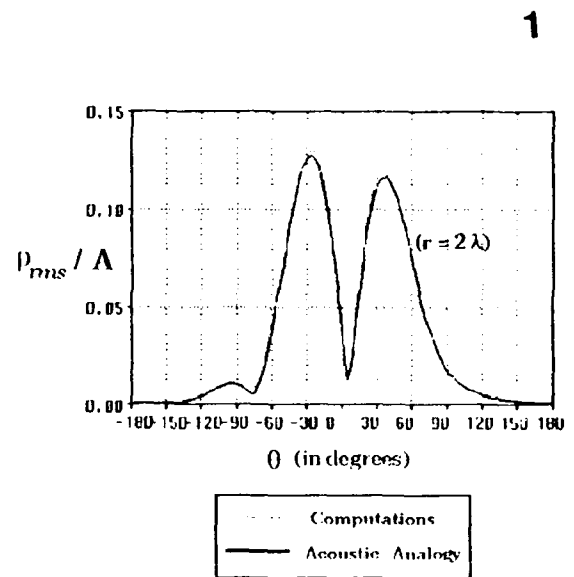
Significance. The database obtained in the present research effort provides structural design guidelines for future application of a TVCS. The removal of the engine nozzle flaps and installation of the TVCS confirms prior predictions that significant increases in plume shock noise will interact with the aircraft structure, which could possibly reduce the expected life cycle for components on the F-18 aircraft.

Status/Plans. The results of research will be reported with NASA Ames/Dryden.

John M. Seiner
Acoustics Division
Langley Research Center
(804) 864-6276

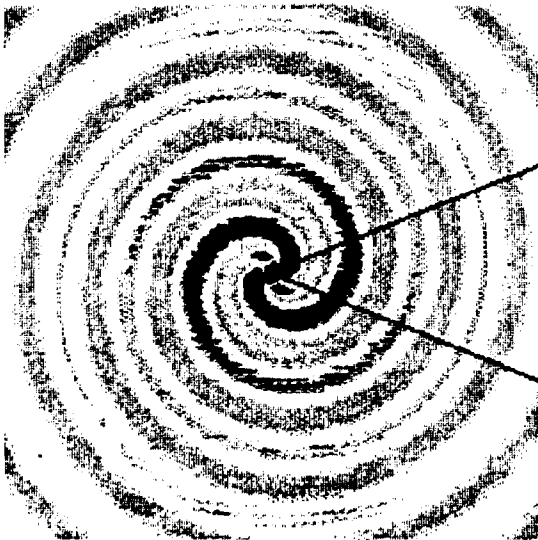


Iso-Contours of the Root Mean Square Density of the Scattered Waves



Comparison with Acoustic Analogy at the Observation Point

Far Field Pressure Fluctuations



Near Field Vorticity

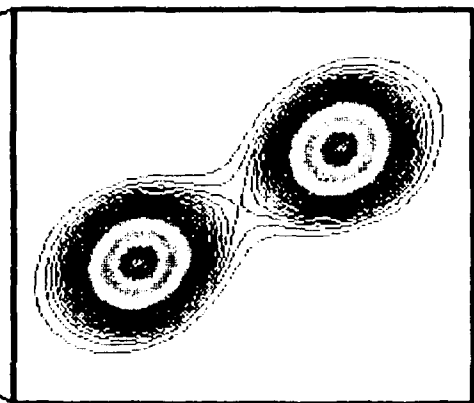


Figure 9-4. Direct Computation of Aerodynamic Sound Generation. Figure 1: Scattering of Plane Sound Waves by a Compressible Vortex; Figure 2: Sound Generated by Co-Rotating Vortices

9-4 Direct Computation of Aerodynamic Sound Generation

Objective. The prediction of the far-field sound produced by a turbulent flow requires a detailed knowledge of acoustic source terms. In many theories these terms are crudely approximated, based on empirical correlations. Computation of both the acoustic sources and far-field sound using the unsteady Navier-Stokes equations allows the physics of the sound generation process to be studied directly. Such a knowledge will allow direct validation of aeroacoustic theories and help develop noise control strategies.

Approach. The Navier-Stokes equations are solved numerically. The infinite domain is truncated and newly developed obliquely nonreflecting boundary conditions are employed at the computational boundaries.

Accomplishments. To address the feasibility and accuracy of direct computation of aerodynamic sound generation, several model problems have been considered, including: the scattering of sound waves by a two-dimensional (2-D) compressible vortex, and sound generation by a 2-D co-rotating vortex pair. Figure 1 shows (1) the amplitude of the acoustic field generated by the interaction of incident planar waves with the 2-D compressible viscous vortex, and (2) a comparison of scattering amplitude directly measured in the computations, with a theoretical prediction based on an acoustic analogy. Their agreement verifies the accurate representation of the acoustic sources by the numerics: discretization does not act as a significant source of sound in the computations. Figure 2 shows a preliminary computation of the far-field pressure fluctuations of the sound field, which is generated by a co-rotating vortex pair, and vorticity contours in the vicinity of the vortex pair.

Significance. Successful simulation of the simple test problems mentioned above, including excellent agreement with theories and experiments, shows that accurate direct computation of fluid flow with sound sources and far-field sound, whose energy is 10 orders of magnitude smaller than the flow energy, is feasible.

Status/Plans. The codes developed will be used to compute the sound generation in two and three dimensional turbulent shear flows.

Sanjiva K. Lele
Department of Aeronautics and Astronautics
Stanford, University
(415) 723-7721

Parviz Moin
Ames Research Center
(415) 604-5127

Tim Colonius, Brian E. Mitchell
Department of Mechanical Engineering
Stanford, University
(415) 723-9602

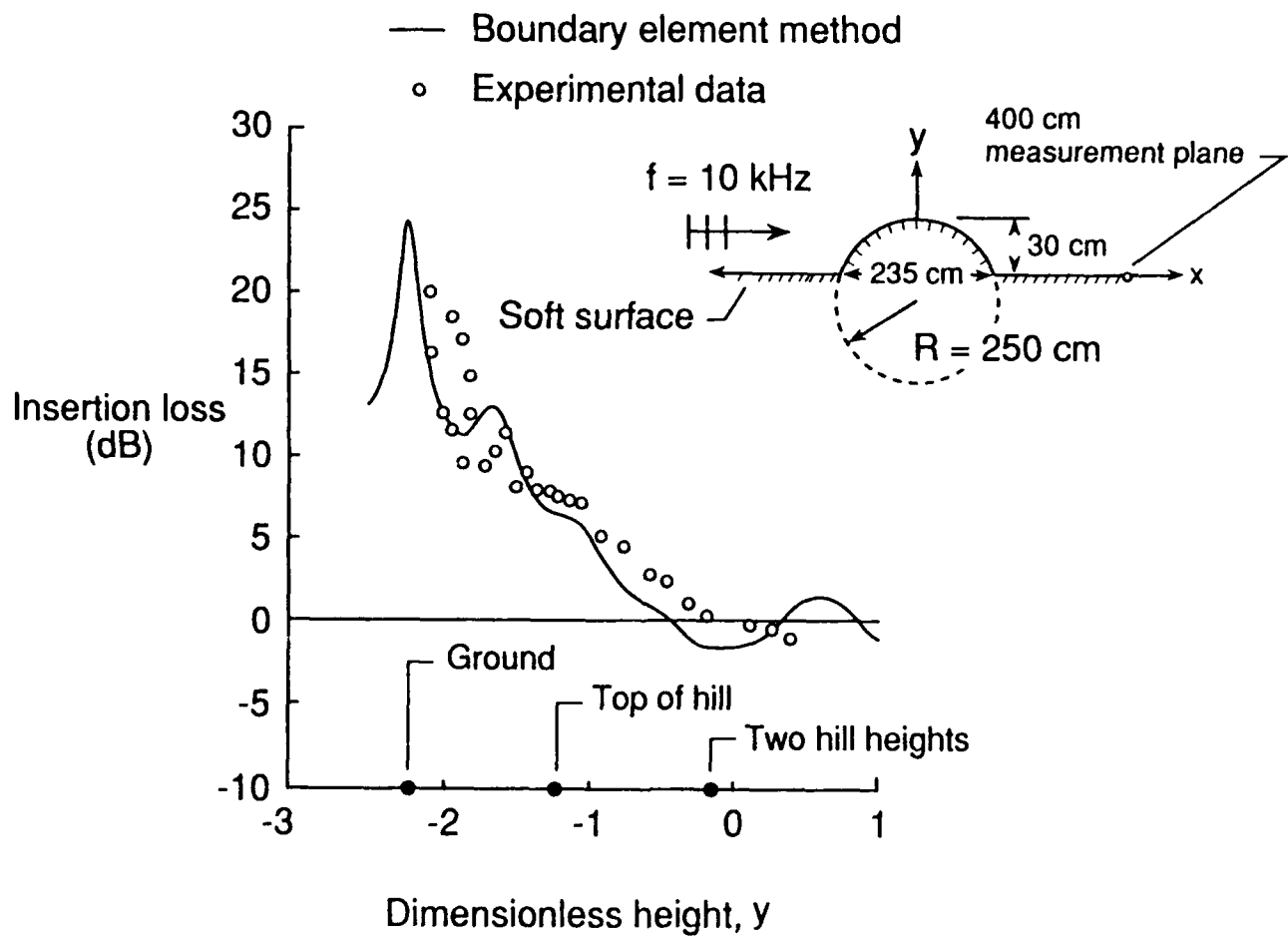


Figure 9-5. Comparison of Boundary Element Method with Experimental Results

9-5 Computational Model for Long-Range Acoustic Propagation

Objective. To develop a method capable of predicting the collective influence of the important physical features of long-range propagation.

Approach. Two-dimensional sound propagation over an arbitrarily shaped ridge situated on a locally reacting infinite boundary in a homogeneous medium is treated using the Boundary Element Method. The discretization procedure provides a set of linear algebraic equations which are solved for the unknowns over the boundary surface of the obstacle. The solution of the boundary unknowns is used to compute the sound field at any point of interest in the domain.

Accomplishments. A computational method capable of studying long-range propagation was developed. An effective scheme to reduce computational time and storage while retaining reasonable solution accuracy using cubic isoparametric elements, approximate polynomials, and asymptotic expansions of the Hankel function was implemented. An out-of-core equation solver for the large, fully populated unsymmetric algebraic equations produced by the Boundary Element Method was developed, and computed results compared with measured data.

Significance. This research has shown that the Boundary Element Method can be used to study long-range propagation. Several innovations have made it possible to apply the method to frequencies and distances never before possible with numerical methods. Results also show that the method compares well with measured results.

Status/Plans. The method will be used to help analyze data from field experiments.

Willie R. Watson
Applied Acoustics Branch
Langley Research Center
(804) 864-5290

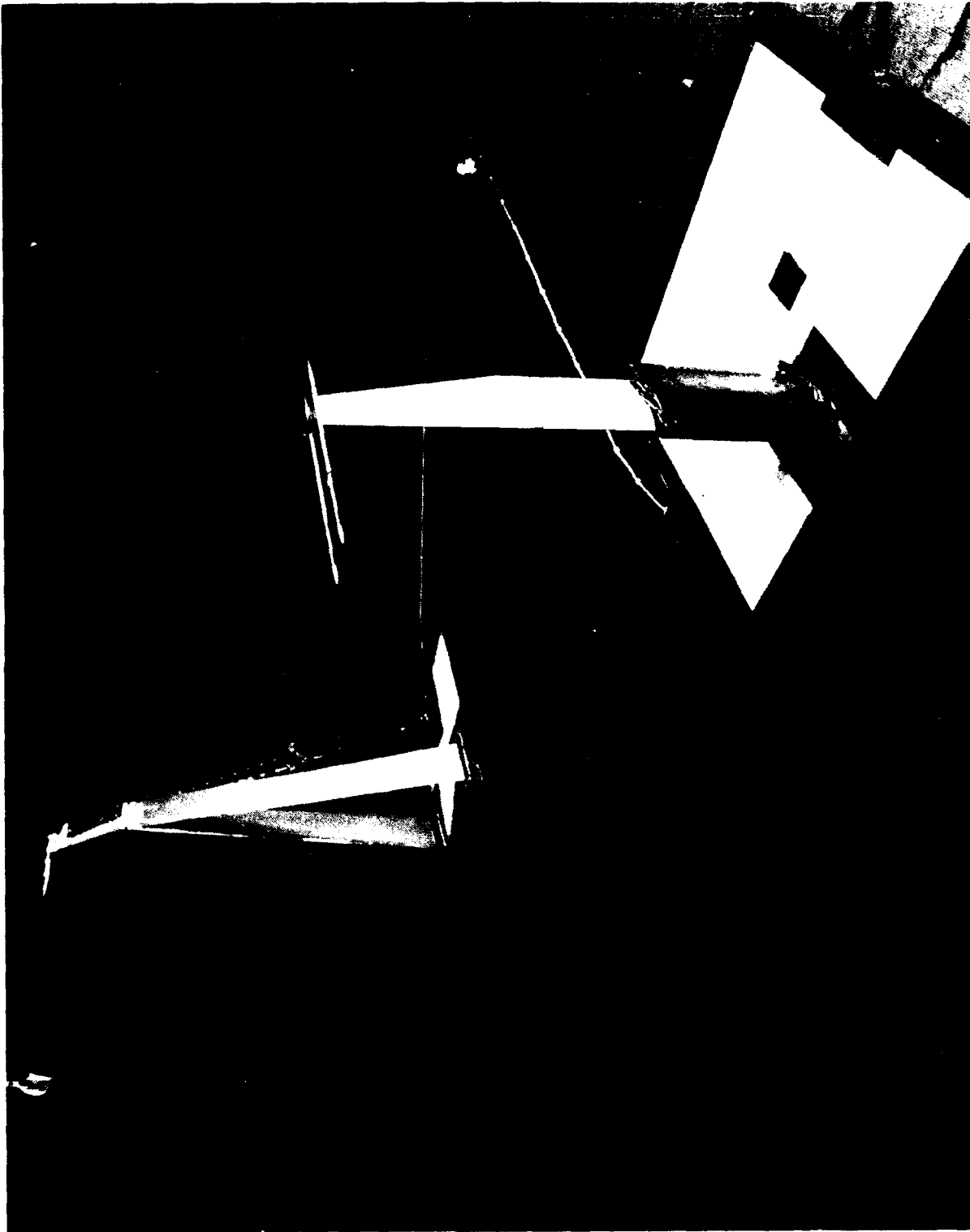


Figure 9-6. Quiet Struts and Sensors for Wind Tunnel Acoustic Studies

9-6 Quiet Struts and Sensors for Wind Tunnel Acoustic Studies

Objective. To develop the technology and design methodology for quiet struts and sensors to be used in subsonic airflow: primarily closed-return wind tunnels.

Approach. Computational fluid dynamics (CFD) will be used to analyze flow fields around struts and junctions so as to identify low-drag configurations, which should thereby have low levels of self noise. Selected shapes and mounting configurations will be tested in the Ames 7- by 10-foot wind tunnel. Acoustic sensors will be tested with nose cones designed to generate low levels of wind-induced noise. Investigations will be made of signal processing methods for combining signals from microphone pairs such that uncorrelated (wind) noise will be attenuated.

Accomplishments. A 40 x 80 wind tunnel test of special acoustic sensors developed by Northrop Corporation has shown that nose cones shaped like Pitot probes round noses, and with the sensor openings several probe diameters downstream from the nose shoulder, generate 6 dB to 10 dB less wind noise than do the commercial microphones with nose cones used at Ames. Further reductions in turbulence-induced noise were achieved by summing the signals from two sensors in the same probe or by summing signals from two sensors in adjacent probes. Uncorrelated sound was thereby cancelled.

CFD simulations have identified several strut/brace junctions that have well-behaved flow fields and are potentially quiet components for microphone struts. A wide range of important geometric parameters have been identified for aeroacoustic testing in the 7- by 10-foot tunnel.

Significance. Improved acoustic sensors and support struts will result in significantly lower background noise in closed-return wind tunnels, without any modification to the facility as long as wind noise is the dominant noise source, as it is in the 40- by 80-foot tunnel. This is equivalent to adding expensive screens to the circuit for turbulence control. The quality of acoustic data acquired from low-noise Advanced Ducted Propellers, HSR jet suppressors, and similar devices will be significantly improved.

Status/Plans. Quiet struts have been designed for testing in the 7- by 10- foot wind tunnel. Fabrication of the struts and associated hardware will commence in the near future. Discussions concerning future cooperative research on sensor development with Northrop Corporation are being planned.

Paul T. Soderman
Fixed-Wing Aerodynamics Branch
Ames Research Center
(415) 604-6675

Chapter 10

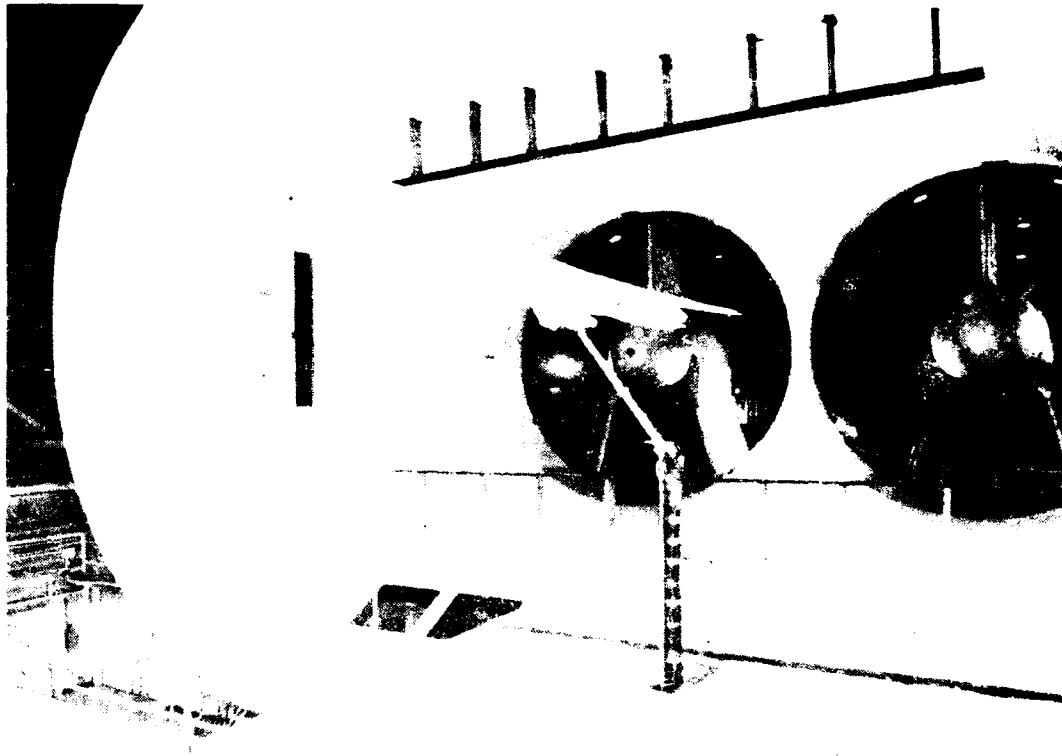
High-Speed Research

The High-Speed Research Program seeks to provide the technology answers for an environmentally safe design of a supersonic transport. In aerodynamics the technologies focus on efficiencies needed to provide a low noise configuration, both in climb out and cruise. The specific objectives of the program are to provide enabling technologies for supersonic transports to achieve in a practical configuration: acceptable overland sonic booms, efficient second stage climb-out for low noise, and supersonic laminar flow control for peak cruise efficiency. The laminar flow control will significantly reduce the aircraft gross weight, hence the noise signatures. The sonic boom element will be evaluated in FY 1992 to determine whether the promise of low boom is great enough to continue research.

There is a great body of data from the previous supersonic cruise research program that ended in the early 1980s. However, prediction methods, optimization techniques, and experimental testing have improved for complex configurations. In addition, new ideas for high lift devices and subsonic laminar flow control are now candidates for investigation for supersonic configurations. These developments have given hope that supersonic aircraft efficiencies can be improved to help the environmental and economic realities of the coming age. Based upon systems studies these efficiencies translate into goals for lift-to-drag ratios of 10 in climb, 15 in transonic cruise, and 10 in supersonic cruise.

The High-Speed Research Program is focused on (1) CFD modeling and validation of aeroacoustic analysis including measurement techniques and atmospheric modeling; (2) development of innovative high lift devices to provide increased lift-to-drag ratios on climb out; (3) design, wind tunnel test and analysis of low sonic boom configurations; (4) large-scale flight evaluation of supersonic laminar flow control including design codes for transition prediction, and the practical installation of suction systems.

Program Manager: Benjamin Neumann
OAST/RF
Washington, DC 20546
(202) 453-2795



0.045 Scale AST-105 High Speed Civil Transport Model
30- by 60-Foot Tunnel

Complete Configuration, LEF=30 deg, TEF=20 deg, $Q=7.0$ psf
Fineness Ratio (FR) measured ahead of wing apex/fuselage juncture

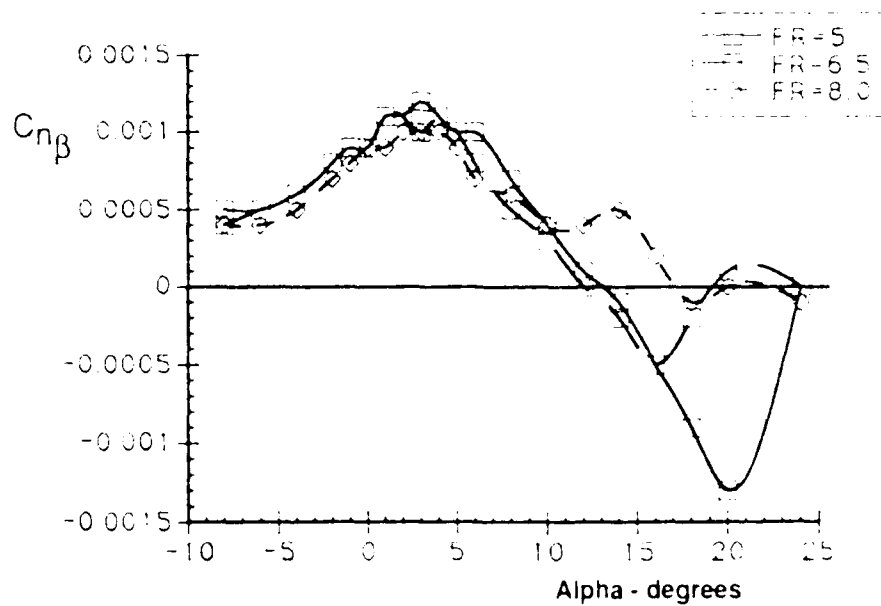


Figure 10-1. Effect of Forebody Length on Directional Stability

10-1 Effect of Fuselage Forebody Fineness Ratio on HSCT High-Lift Directional Stability

Objective. To determine the effect of increased forebody fineness ratio (length/diameter) on the directional stability characteristics of high-speed civil transport (HSCT) configurations under high-lift conditions.

Approach. An existing model, representative of current HSCT designs and having a forebody fineness ratio of 5.0, was modified to permit testing with alternate forebodies having fineness ratios of 6.5 and 8.0. Tests were conducted in the 30- by 60-foot tunnel to identify potential vehicle integration effects which may possibly limit the utility of HSCT high-lift concepts.

Accomplishments. Results of the investigation showed only minor effects of forebody fineness ratio on configuration directional stability for the angle-of-attack range corresponding to normal low-speed operating conditions. For higher angles-of-attack, increasing fineness ratio was found to have a positive stabilizing effect on directional stability.

Significance. Projected advances in HSCT high-lift system effectiveness will permit significant reductions in vehicle wing size. Since the fuselage is sized by passenger/volume requirements (which will remain unchanged)

reductions in wing area result in corresponding increases in relative fuselage forebody length and consequently increases in forebody fineness ratio. Previous experience with military vehicles has indicated that high-fineness ratio forebodies can significantly affect vehicle directional stability characteristics.

These results indicate that advances in HSCT high-lift systems may be used to accomplish reduction in wing size without adversely affecting directional stability characteristics.

Status/Plans. No future work is planned in this area.

E. Richard White
Flight Dynamics Branch
Langley Research Center
(804)864-1147

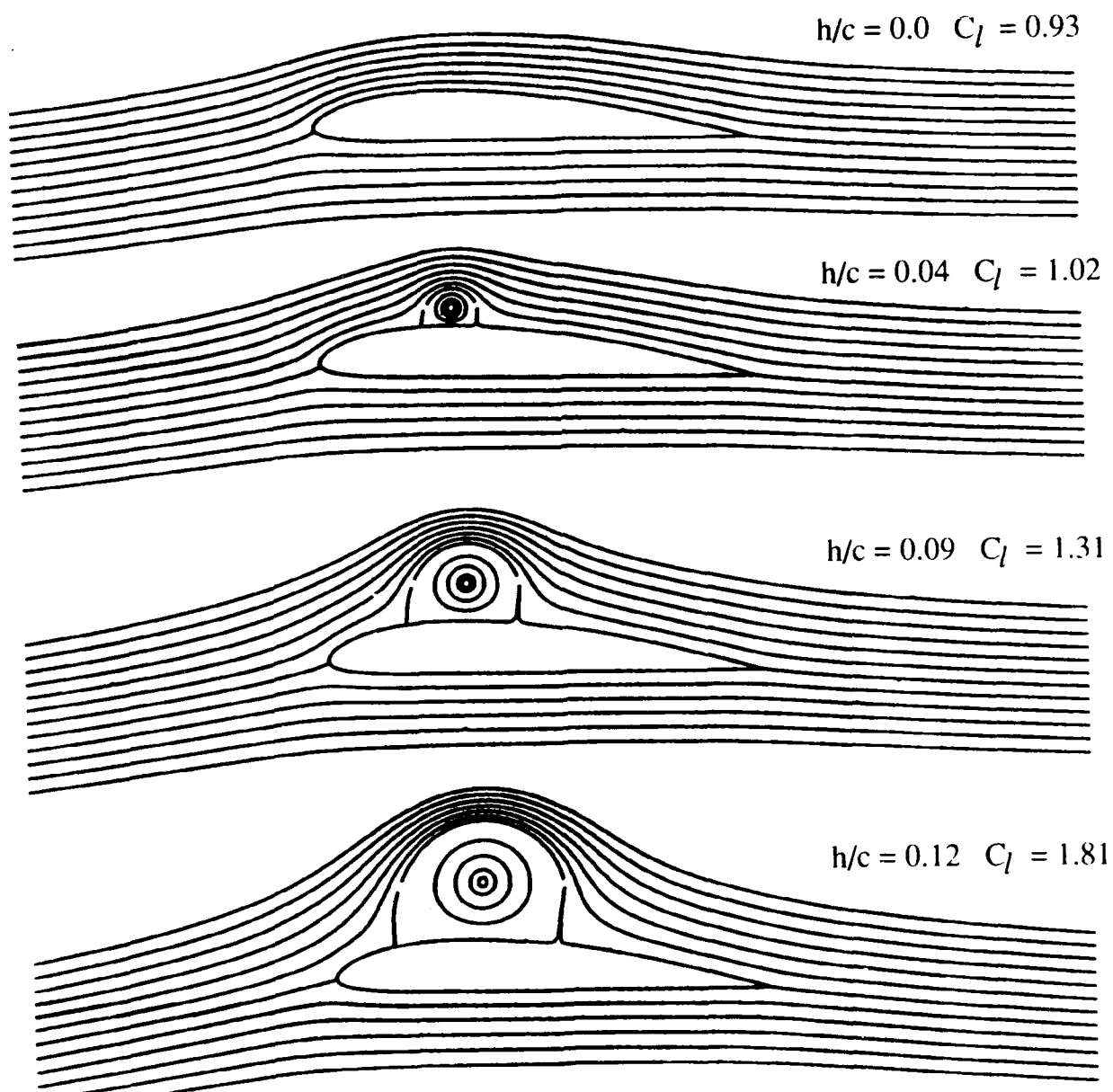


Figure 10-2. Computed Streamlines for Various Fence Heights on a NACA 4412 Airfoil

10-2 High-Lift Systems Research for HSCT Application

Objective. To develop advanced high-lift systems that will help reduce the community noise impact and contribute to the economic success of new high-speed civil transport aircraft.

Approach. A combined computational and experimental program is being pursued. Based on limited small-scale testing, theoretical and computational analyses, and a literature search for suitable high-lift devices, the trapped vortex was selected as the most promising technology.

Accomplishments. Potential flow analyses have demonstrated the stability conditions required for trapping a vortex on a wing. The need for two fences to trap a vortex with very little suction at the vortex core was a significant discovery. Preliminary water-channel and wind-tunnel tests have shown the effectiveness of the two-fence configuration for simple geometries. These results also validated the computations. Additional Navier-Stokes computations have shown that the vortex trapping process is not sensitive to Reynolds number.

Cooperative wind tunnel tests were performed with Boeing Commercial Airplane Company at the University of Washington Aeronautical Laboratory. These tests showed that for a representative high-speed civil transport model, a double-fence configuration generated a tighter vortex than did a single-fence.

Significance. The theoretical and water channel results are very encouraging. A practical system based on the trapped vortex should eliminate the need for complex leading and trailing edge flaps, while providing sufficiently high lift coefficients to allow safe, controllable landings. This concept can generate significant lift coefficients at low angles-of-attack, reducing the tail strike problem at takeoff and touchdown. Reducing the lift-off angle-of-attack by 4° saves at least 2500 pounds in landing-gear weight. In addition to lower landing gear weight, the wing area required for takeoff is reduced. Overall, a significant aircraft weight savings can be achieved which will result in lower engine thrust requirements and safer, quieter operation.

Status/Plans. The computational studies have shown the trapped vortex to be a viable technique for generating high-lift at low angles-of-attack. A small-scale test is under way in the Ames 7- by 10-foot wind tunnel which will define the effect that various geometric parameters (fence spacing and height, etc.) have on the vortex trapping process. These results will be applied immediately in another cooperative test of the Boeing low-speed model at the Ames 7- by 10- foot wind tunnel.

James C. Ross
Fixed-Wing Aerodynamics Branch
Ames Research Center
(415) 604-6722

HIGH-SPEED RESEARCH PROGRAM

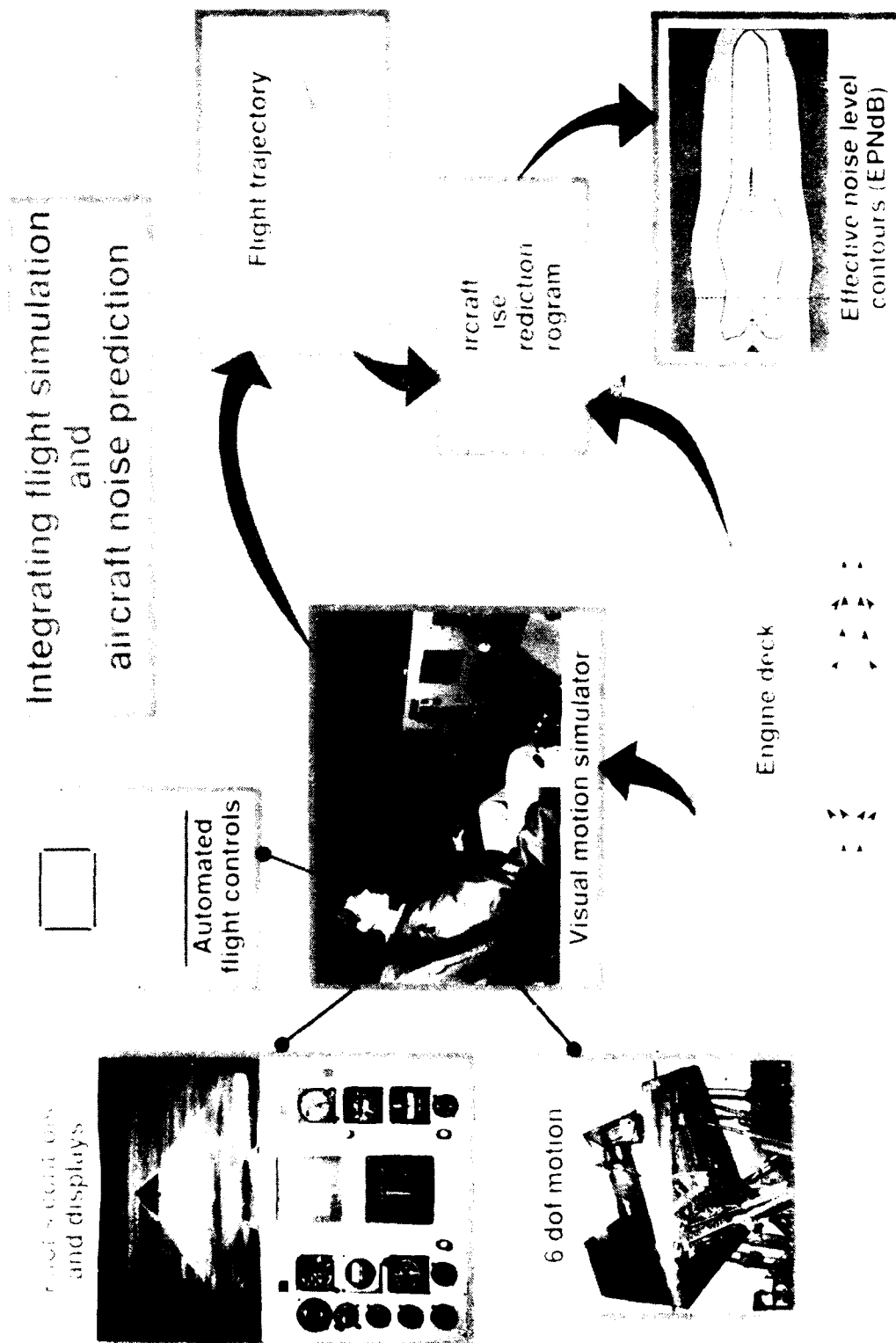


Figure 10-3. Integration of the VMS and ANOPP for High-Speed Civil Transport (HSCT) Community Noise Prediction

10-3 Integration of Flight Simulation With Aircraft Noise Prediction

Objective. To provide a tool to evaluate the effects of high-lift aerodynamics and aircraft operating procedures upon high-speed civil transport (HSCT) community noise.

Approach. The approach combines the flight simulation capabilities of the Langley Visual Motion Simulator (VMS) and the noise prediction capabilities of the Aircraft Noise Prediction Program (ANOPP) to predict ground contours for HSCT community noise evaluation. The VMS is a ground-based flight motion simulator with six degrees-of-freedom. It features a variable atmosphere model and computer-generated out-the-window visual scenery. It has an advanced transport-type cockpit equipped with a full complement of aircraft flight and engine-thrust controls as well as flight instrumentation displays. Aerodynamic control forces on the sidestick controller and rudder pedals are provided by a hydraulic system coupled to an analog computer. The simulator provides the pilot with realistic variable-feel characteristics of aircraft stiffness, damping, coulomb friction, breakout forces, and inertia. The ANOPP code consists of dedicated noise prediction modules for jet powered aircraft. This prediction program requires a detailed description of the aircraft position and engine operating conditions as a function of time. With the flight trajectories and engine propulsion requirements provided from the VMS, ANOPP is capable of predicting the ground contours of the noise levels associated with simulated takeoff, landing, or level flight. The accompanying figure conceptualizes the relationship between the two software-based prediction systems.

Accomplishments. In the initial evaluation study, the VMS has been reprogrammed to simulate the NASA designed AST-105 aircraft. This aircraft has a cruise Mach number of 2.6, carries 273 passengers, and has a range of 4500 nautical miles. It is powered by four

Pratt & Whitney VSCE-516 engines. The complete set of aerodynamic and propulsion data available for this supersonic aircraft provides a validation for the simulator. The ANOPP code has had upgrades performed to the flight dynamics, atmospheric absorption and jet mixing noise modules for better supersonic aircraft noise prediction. The VMS simulator has been operated for trial flights and the output has been utilized in the ANOPP code to predict contours.

Significance. A successful high-speed civil transport must be environmentally compatible. Advanced operating procedures, advanced propulsion systems, high-lift aerodynamic concepts, and acoustic suppression have all been proposed as techniques for community noise reduction. The effects of using these new technologies must be quantified to ensure that a proposed high-speed civil transport can meet acceptable community noise limits with minimum economic penalty.

Status/Plans. A baseline community noise evaluation of the AST-105 configuration will be completed to assess the impact of the advanced engines and advanced piloting procedures. The simulator and noise prediction code will be updated to simulate a more current proposed HSCT aircraft.

Robert A. Golub
Acoustics Division
Langley Research Center
(804) 864-5281



Blended wing-body configuration

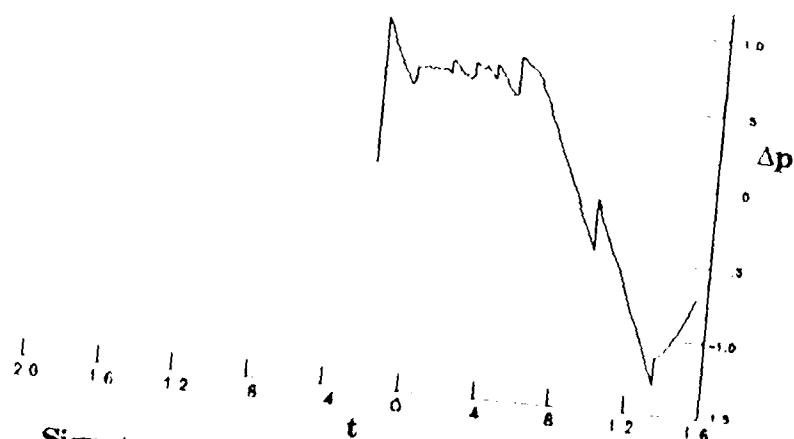
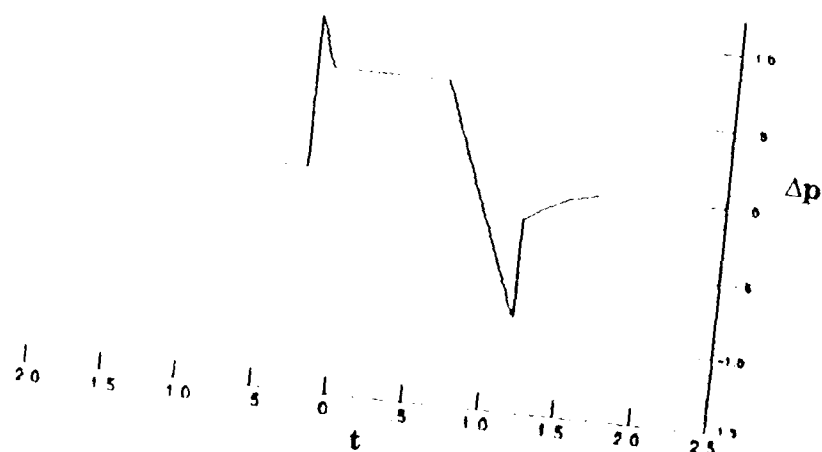


Figure 10-4. Computed Signature Results for Low Boom Configuration

10-4 Design System for Low Sonic Boom Configurations

Objective. To facilitate and accelerate the design and analysis of low sonic boom blended wing-body configurations.

Approach. Existing codes were modified so that all input and output geometry and array formats were compatible. New codes were written and incorporated as required. One new code automatically adjusts the thickness distribution to obtain the geometry required by low-boom constraints. Computerized lofting was incorporated to reduce drawing board work. Use of a blended wing-body concept eliminates the tedious problem of accounting for the wing-fuselage gap that occurs when they are treated as separate components. Graphics codes were incorporated for rapid display of relevant geometries and distributions.

Accomplishments. Some sample designs have been completed. Ground-level signature results for one case are shown in the accompanying figure.

Significance. High-speed civil transport (HSCT) milestones for assessment of the sonic boom problem can be met more easily if model design can be accelerated. Configurations with acceptable sonic boom characteristics would open the possibility of overland supersonic flight.

Status/Plans. Experience in the use of the system is being gained. Some minor tailoring of the codes occurs as a result of this experience.

Raymond L. Barger, Mary S. Adams
Fluid Mechanics Division
Langley Research Center
(804) 864-2315

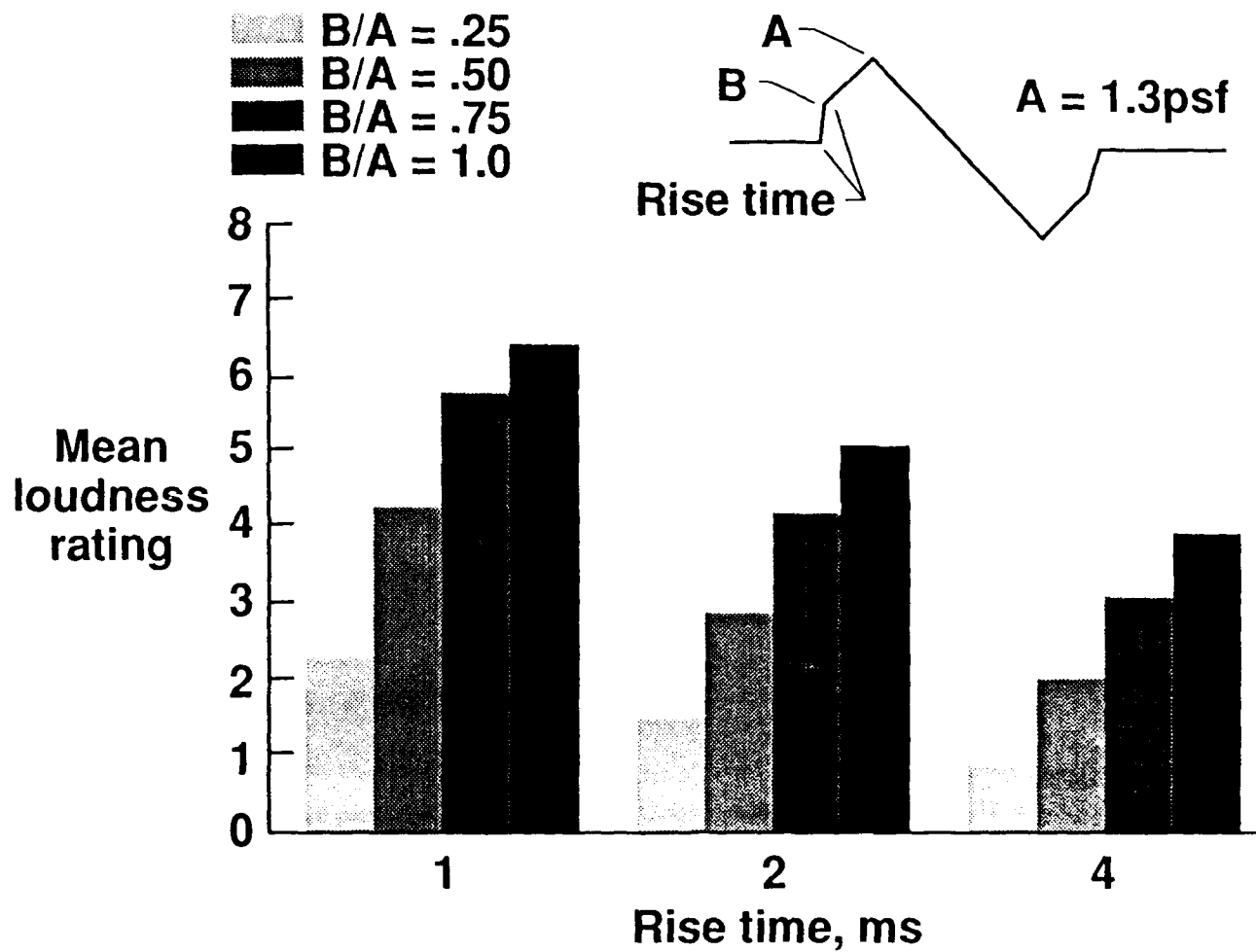


Figure 10-5. Benefit of Boom Shaping

10-5 Sonic Boom Shaping For Reduced Loudness

Objective. To quantify the effects of sonic boom signature shaping on subjective judgments of boom loudness.

Approach. A new Langley Research Center sonic boom simulator was used to obtain subjective loudness judgments from a group of local residents of a wide range of candidate boom shapes. The shapes were front-shock minimized and covered a range of initial to peak overpressures (0.25 to 1.00), initial rise times (1 to 4 msec), and secondary rise times (20 to 50 msec). Duration for all booms was held constant at 300 msec.

Accomplishments. Subjective loudness ratings were obtained for the range of shapes shown at the top of the figure. These shapes were characterized by an initial rapid rise to an intermediate overpressure (level B) followed by a more gradual rise to peak overpressure (level A). The mean loudness ratings, as a function of initial rise time for four ratios of intermediate to peak overpressure, are shown in the bottom figure. These data show that loudness, for constant peak overpressure, decreased with increasing rise time and, for a specific rise time, increased with intermediate to peak pressure ratio.

Significance. These results indicate that significant reductions in boom loudness can be achieved by detailed shaping of the boom signatures. They also provide data that can be used in the selection of a preferred boom shape.

Status/Plans. Future studies will introduce a "house filter" into the boom simulation process in order to assess indoor effects. Asymmetrical boom signatures will also be investigated to determine whether asymmetry may provide additional reductions in perceived loudness.

Jack D. Leatherwood
Acoustics Division
Langley Research Center
(804) 864-3591

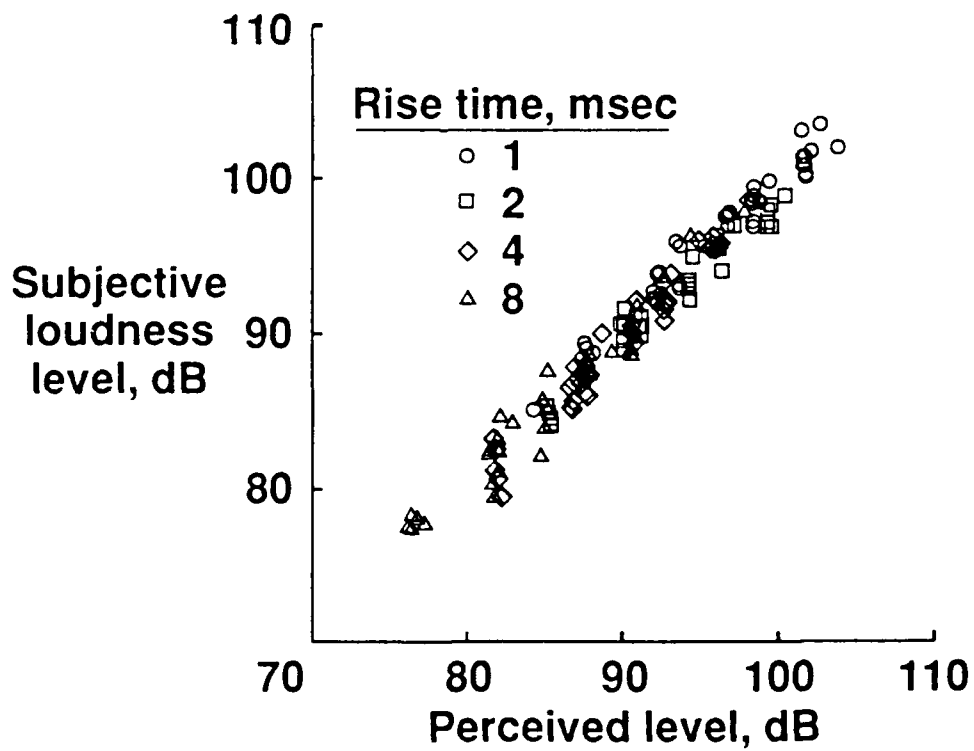
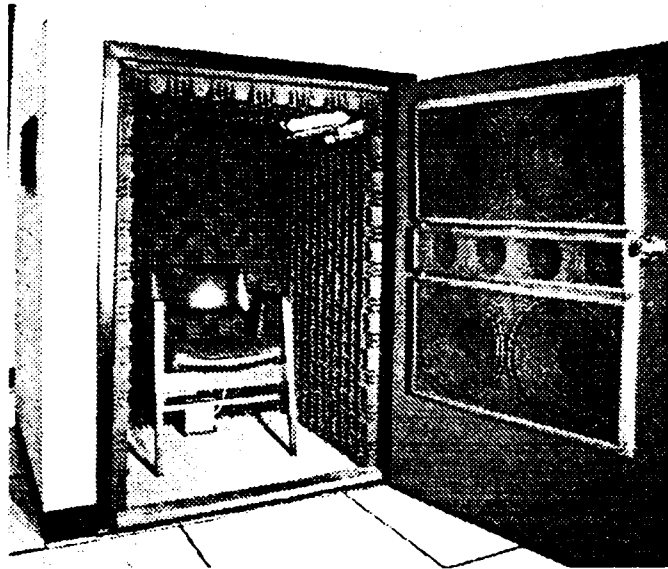


Figure 10-6. (1) Sonic Boom Simulator (L-90-5755); (2) Subjective Loudness of Sonic Booms as a Function of Perceived Level (PL).

10-6 Prediction of Subjective Response to Sonic Booms

Objective. A noise metric that adequately predicts the subjective loudness of sonic booms that have different physical characteristics is needed for the assessment of sonic boom signatures predicted for candidate high-speed transport configurations. To address this need, the sonic boom simulator shown in the upper figure was developed to study subjective response to sonic booms. This investigation was aimed at assessing the effects on subjective loudness of the overall duration, rise time, overpressure, and wave shape of sonic booms.

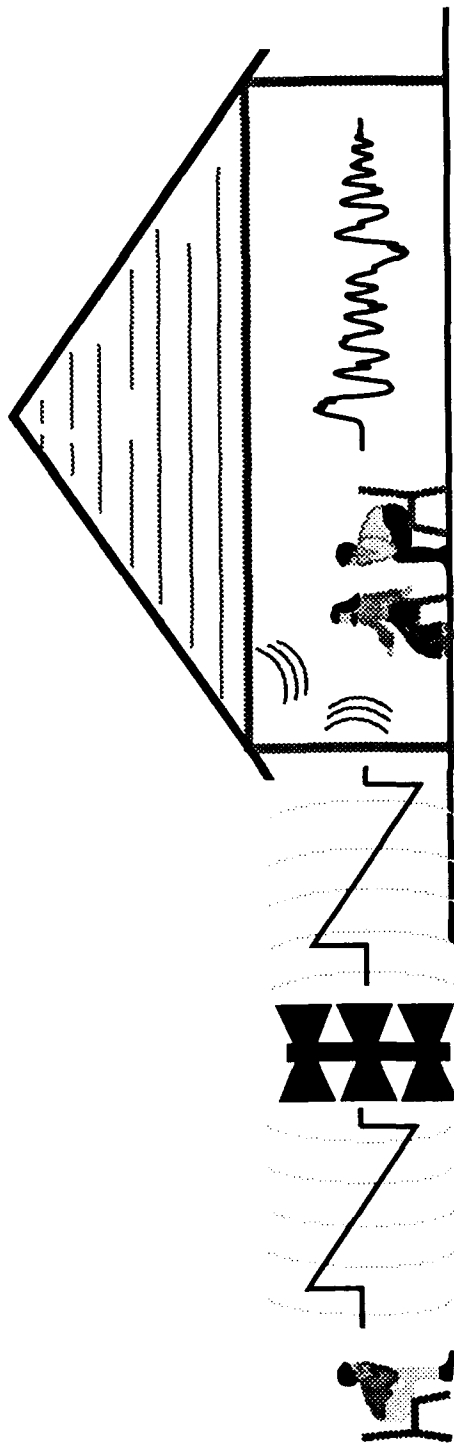
Approach. Loudness judgments of selected sonic boom signatures were obtained from 36 test subjects using the method of numerical category scaling. Each test subject judged the loudness of each of 150 simulated sonic booms on a scale from 0 to 10. The set of 150 sonic booms represented different combinations of overall duration, rise time, overpressure, and wave shape. Overall duration ranged from 25 to 425 msec with rise times of 1, 2, 4, and 8 msec. These ranges of overall duration and rise time easily encompass the values predicted for high-speed civil transports. The overpressures for the different wave shapes, N-wave and "minimized," varied from approximately 0.6 to 1.6 psf. The loudness judgments were averaged across test subjects and converted into decibel-like subjective loudness levels for each of the 150 sonic booms.

Accomplishments. Analyses of several different noise metrics indicated that perceived level (PL) was the best predictor of subjective response to sonic booms. The lower figure shows the subjective loudness levels plotted against PL for each of the four rise times. Perceived level adequately accounted for the effects of rise time, overpressure, and wave shape. However, a small effect of duration on subjective response (~1 dB) over the very wide duration range considered was found, which is not accounted for by PL.

Significance. The results of this study indicate that a noise metric exists that effectively predicts the subjective response to sonic booms as heard outdoors. Thus, a validated method is available for comparative assessment of the subjective acceptability of sonic boom signatures predicted for candidate high-speed transport configurations.

Status/Plans. The sonic boom simulator will continue to support efforts to develop a high-speed transport having sonic boom signatures that permit overland supersonic flight. Relative acceptability of various proposed "minimized" signatures will be investigated in future studies.

David A. McCurdy
Acoustics Division
Langley Research Center
(804) 864-3596



- Special low frequency acoustic drivers developed; 3Hz - 30Hz, 30Hz - 300Hz
- Real house to create indoor acoustic effects
 - High frequency attenuation
 - Rattles and vibration
 - Room reverberation
- Planned research
 - Indoor/outdoor annoyance; July - August, 1991
 - Comparison with other noise sources; July - August, 1991
 - Building response; January - March, 1992

Figure 10-7. Indoor/Outdoor Sonic Boom Simulation Facility

10-7 Indoor/Outdoor Sonic Boom Simulation Facility

Objective. To determine an acceptable level of sonic boom exposure for a high-speed civil transport, human response to booms heard both indoors and outdoors is to be examined. The first step in this study is the development of a suitable sonic boom simulator.

Approach. A simulator is required which can provide realistic sonic boom signatures at the facade of a typical residential structure. Since the frequency content of sonic booms extends to very low frequencies, conventional loudspeaker arrangements are unable to generate realistic sonic boom waveforms. The Georgia Tech Research Institute (GTRI) was given the task to design and fabricate an array of acoustic drivers that could cover the frequency range from 3 Hz to 4 kHz, and generate an N-wave having an amplitude of approximately 2 pounds per square foot.

Accomplishments. A sonic boom simulator has been designed that consists of 25 acoustic horns and loudspeakers. The custom-designed, very low frequency horns are servomotor driven and radiate sound over the range 3 Hz to 30 Hz. The other, conventional loudspeakers radiate sound from 30 Hz to 4 kHz. The loudspeakers are arranged in a vertical array adjacent to an uninhabited house located at the GTRI laboratory.

Significance. When fully operational, this

sonic boom simulation facility will provide the unique capability of exposing a house to realistic sonic boom waveforms. It is known that human response to sonic booms heard indoors is quite different from outdoor response. This is due to a variety of factors such as acoustic transmission loss and noise-induced vibration and rattle. This facility will enable a systematic investigation to be made of these indoor/outdoor differences.

Status/Plans. The simulator is currently operational and human response testing, both indoors and outdoors, will begin in fall 1991.

Kevin P. Shepherd
Acoustics Division
Langley Research Center
(804) 864-3583

Surveyed areas



● Objectives:

- Develop sonic boom response questionnaire
- Provide preliminary data on extent of sonic boom annoyance

● Sonic boom exposure:

- Long term SR-71, 0.5 to 1.0 psf, ~ 1 per week
- Exposure ceased 6 months prior to study

● Findings:

- Little to moderate annoyance
- Startle reaction frequently noted
- Vibration frequently noted, some damage attributed to sonic booms

Figure 10-8. Preliminary Sonic Boom Survey

10-8 Preliminary Sonic Boom Survey

Objective. To develop a response questionnaire for an extensive survey and to provide some data on the extent of annoyance to sonic booms in areas which have been exposed for many years to sonic booms with intensities comparable to those from proposed future supersonic civil transports.

Approach. The present study developed a questionnaire for subsequent and more extensive surveys through interviews in two communities that had experienced supersonic overflights of SR-71 airplanes for several years. It was estimated, based on analysis of USAF files of supersonic flight operations, that the SR-71 overflights occurred on average about once per week and produced sonic booms with peak overpressures of 0.5 to 1.0 psi, although exposures had ceased about 6 months prior to the survey. A total of 23 respondents living in the border area of Washington and Idaho and 22 respondents living in central Utah were interviewed during July 1990. Questions that addressed the following topics were included: terminology for sonic booms, extent of vibration, activity interference, links to previous surveys (e.g., Oklahoma City, 1964), startle reaction, and extent of annoyance with links to community annoyance by conventional aircraft noise.

Accomplishments. This effort has produced a draft questionnaire that appears to meet most of the goals established for this preliminary survey. In addition, the preliminary survey provides a number of findings related to the extent of annoyance from and perception of sonic booms in the survey areas. People were aware of sonic booms and on average gave ratings of "a little annoyed" to "moderately annoyed" and about equal to some other noise source. Almost all of the respondents reported that they had been startled by sonic booms and nearly half reported that their sleep had on occasion been disturbed. A high proportion of people reported that things vi-

brated, shook, or rattled during a boom. The most frequently mentioned items were the whole house, dishes, pictures, and knick-knacks. About one-quarter of the respondents associated sonic booms with damage to their house, although only eight people in the entire sample thought that sonic booms were an issue in their community.

Significance. This preliminary survey has provided information for final development of a questionnaire for a major sonic boom annoyance survey. In addition, the insight on the extent of annoyance due to long-term sonic boom exposure has provided valuable but statistically limited information as to whether people will accept sonic booms with intensity on the order of those predicted for future supersonic transports.

Status/Plans. A major survey of human annoyance is planned to be conducted in conjunction with a USAF investigation of the extent and prediction of sonic boom exposure in the Nellis Military Operating Area of southern Nevada. The NASA portion of this study will provide estimates of the relationship between sonic boom exposure and community response.

Kevin P. Shepherd
Acoustics Division
Langley Research Center
(804) 864-3583

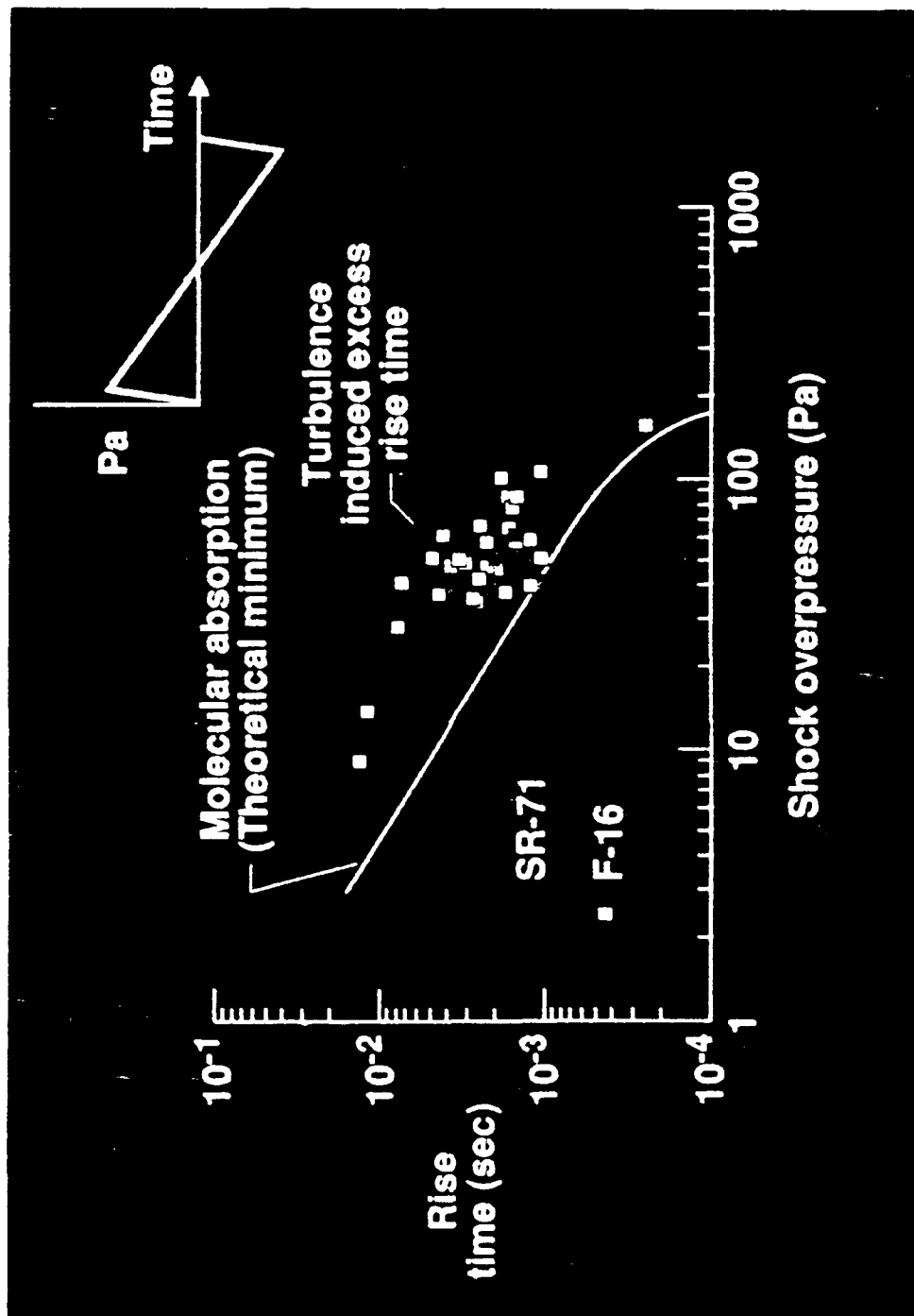


Figure 10-9. Sonic Boom Propagation - Effect of Atmosphere on Boom Shape

10-9 Minimum Sonic Boom Rise Time Determined by Absorption

Objective. To quantify the effects of atmospheric absorption and turbulence on sonic boom wave forms. This research is in support of the High-Speed Research Program, which is addressing the feasibility of supersonic flight over land.

Approach. Predictions of a recently developed theory describing the effects of molecular absorption and viscous dissipation on sonic boom rise times were compared with rise times determined from measured sonic boom signatures generated by F-16 and SR-71 aircraft. A total of 116 sonic boom signatures were analyzed in this study. The Mach number range was from a low of 1.14 to a high of 3.0. Flight altitudes varied between 3.84 km and 22.3 km, thus providing a wide range of peak overpressure, which is the variable of primary importance for predicting sonic boom rise time. This work was carried out by Dr. A. Pierce of Pennsylvania State University under a grant to consider atmospheric effects on sonic boom wave forms.

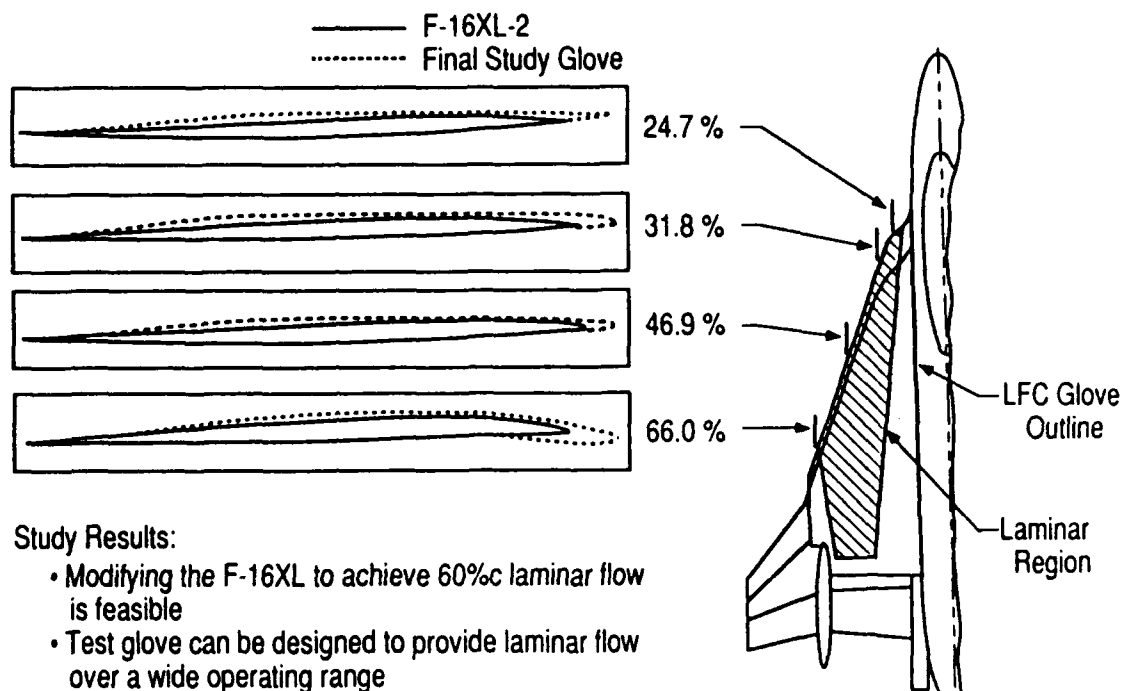
Accomplishments. The accompanying figure provides comparisons of two theoretical rise time curves as a function of shock overpressure, and rise times as determined from measured sonic booms. The comparisons show that the rise time predicted by the new theory is consistently less than that determined from the measured sonic boom signatures. Since atmospheric turbulence could not be controlled during the measurement period, and atmospheric turbulence is thought to be a major factor in sonic boom rise times, most of the difference is currently attributed to atmospheric turbulence. This is a tentative conclusion, however, as the two data points below the predicted curve on the right-hand figure attest to the possibility of exceptional cases.

Significance. The prediction of rise time provided by the new theory is considerably better than that given by previous theory which neglected molecular absorption. Further, the new theory provides a conservative estimate of sonic boom rise time.

Status/Plans. The new absorption theory will be integrated into currently available sonic boom prediction codes. Additional comparisons with other sonic boom databases are planned. Further work on atmospheric effects on sonic booms will concentrate on the development of the tools required to predict the effects of turbulence.

Gerry L. McAninch
Applied Acoustics Branch
Langley Research Center
(804)-864-5269

DAC F-16XL-2 SLFC DESIGN FEASIBILITY STUDY



Study Results:

- Modifying the F-16XL to achieve 60% c laminar flow is feasible
- Test glove can be designed to provide laminar flow over a wide operating range
- Aerodynamics, design integration are key challenges

F-16XL-1 ROCKWELL SUCTION GLOVE

Preliminary Transition Data

Outboard Active Glove

Mach = 1.4
 Alt = 50,000 ft
 Re/ft = 1.7 million

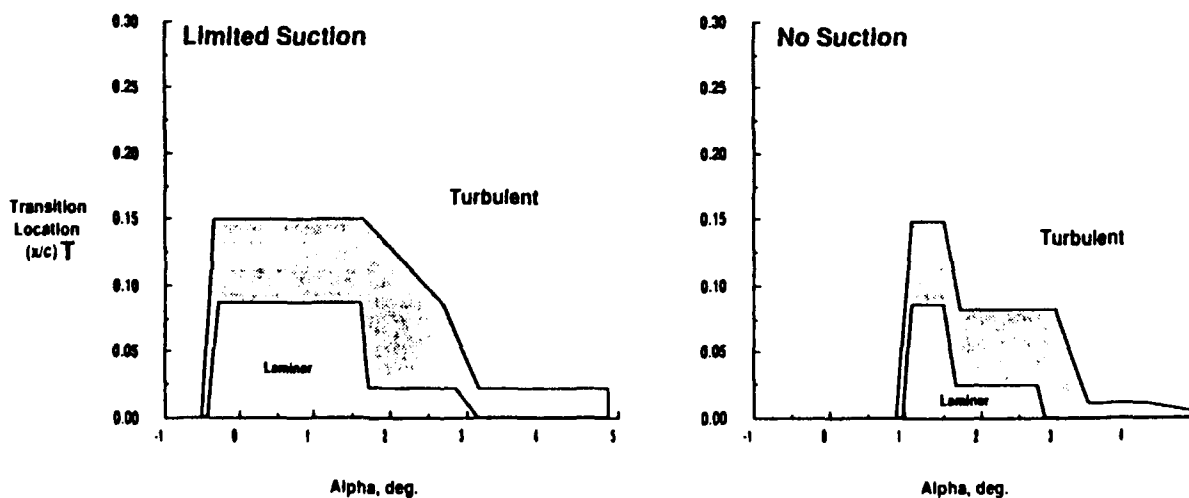


Figure 10-10. Supersonic Laminar Flow Control Program

10-10 Supersonic Laminar Flow Control Program

Objective. To develop and validate technology for practical, reliable, and maintainable supersonic laminar flow control concepts for future high-speed civil transports (HSCTs).

Approach. A balanced program involving NASA and industry has been structured to carry out the supersonic laminar flow control program. The program utilizes a mix of computational efforts, ground facility experiments, and flight testing. Advanced computational fluid dynamics (CFD) methods and boundary layer stability codes are being developed to guide the design and for code validation. Swept-wing model experiments are under way in low disturbance supersonic wind tunnels to provide data on leading-edge transition physics. Ongoing and planned precursor flight tests on the F-16XL-1 and -2 will obtain design criteria and code calibration data to reduce the risk for the suction panel tests on the F-16XL-2. Flight tests of suction panels in FY 1995 will achieve extensive laminar flow over a range of flight conditions and provide data for code validation and development of design methodologies.

Accomplishments. The RFP for the design, fabrication, and installation of suction panels and a suction system on the F-16XL-2 was released on July 29. Data from the Rockwell suction panel on the F-16XL-1 are being used to calibrate CFD codes. Laminar flow to about 8.6% chord was obtained in initial flights at $M=1.4$ and an altitude of 50,000 feet both with low suction and without suction. Recent flights have demonstrated laminar flow to about 25% chord with full suction for similar flight conditions. The F-16XL-2 supersonic laminar flow control feasibility study was completed. Technology studies with industry were initiated. A non-suction swept wing pressure model was tested in the LaRC low disturbance supersonic tunnel.

Significance. Industry is preparing proposals in response to the RFP. Data obtained from the F-16XL-1 flight tests are providing inputs for code calibration and transition prediction methodology, as well as improving our understanding of laminar flow/transition physics over a highly swept supersonic wing. Data from ground facility tests, to date, are verifying the design methods and will provide data for CFD calibration and comparison with flight tests. The F-16XL-2 feasibility study verified that achieving extensive laminar flow with a suction glove on the F-16XL-2 is feasible, but illustrated that special treatment of the wing/fuselage area would be required to achieve laminar flow while not producing stability and control problems.

Status/Plans. Award of the F-16XL-2 contract is anticipated for March 1992. Flight testing of the F-16XL-1 is scheduled for completion at the end of calendar year 1991. Precursor tests with the F-16XL-2 will be initiated in about March 1992.

Michael C. Fischer
Flight Applications Division
Langley Research Center
(804) 864-1921

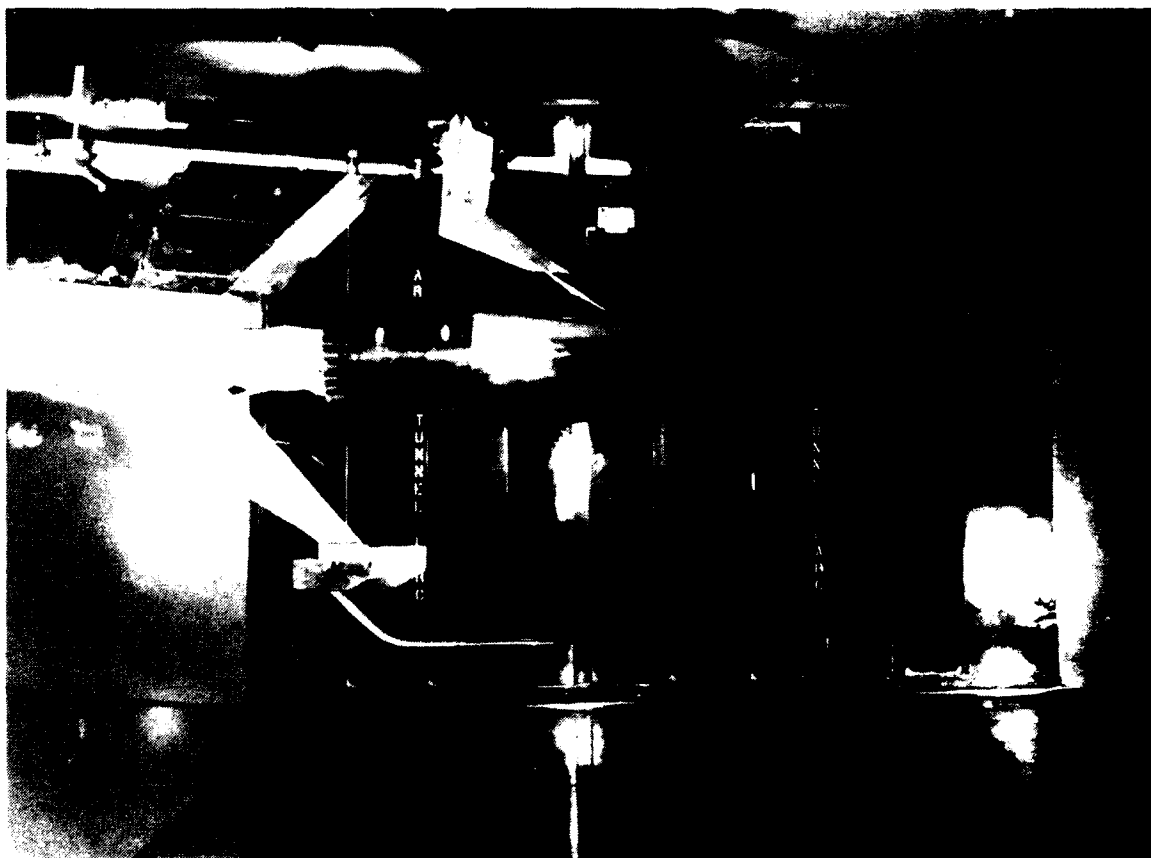


Figure 10-11. The AEDC 10-Degree Transition Cone

10-11 Flow Quality Study in the Unitary Plan Wind Tunnel

Objective. To determine the flow quality in the NASA Langley Unitary Plan Wind Tunnel (UPWT) based on measurement of cone transition Reynolds number.

Approach. The potential deterioration of the UPWT nozzle and test section wall surface finish over the past several years has led to a reevaluation of the tunnel flow quality using the Arnold Engineering Development Center (AEDC) 10° Transition Cone model. This model was last tested in the UPWT in 1974. The present study was conducted at the same Mach number and Reynolds number test conditions as the previous test as well as several additional Mach numbers concentrated in the region of interest for high-speed civil transport (HSCT) studies.

Accomplishments. The AEDC 10° Transition Cone model was tested in test section two of the UPWT at Mach numbers of 2.36, 2.86, 3.51, and 4.60 and over a Reynolds number range of 1.0×10^6 to 5.0×10^6 per foot. Generally the current levels of transition Reynolds number were slightly lower than those obtained in the 1974 tests. This reduction in transition Reynolds number may be a result of increased tunnel turbulence levels caused by deterioration of the nozzle/test section wall finish or perhaps other flow disturbance producing mechanisms (e.g., turning vane induced disturbances). However, the AEDC 10° Transition Cone model surface finish was found to have numerous imperfections and may have caused the relative reduction in transition Reynolds number.

Significance. The current emphasis on HSCT studies has reiterated the need to have well-defined wind tunnel flow quality levels. The AEDC 10° Transition Cone, which has been tested in numerous wind tunnels around the world, provides a common reference to compare flow quality between facilities. The present results indicate the effects of potential deteriorations in the UPWT flow quality and/or the test model surface finish.

Status/Plans. Requests have been made to AEDC to permit Langley Research Center to refinish the surface of the AEDC 10° Transition Cone. Once refinished the model will be retested in the UPWT.

Jeffrey D. Flamm
Applied Aerodynamics Division
Langley Research Center
(804) 864-5955

Chapter 11

Aerothermodynamics Research and Technology

The Aerothermodynamics Research and Technology program focuses on advancing both our understanding of and ability to address the issues associated with high-temperature gas effects as they impact the aerodynamic and heating environments encountered by vehicles and spacecraft for both Earth and planetary missions. The problems of high Mach number flight throughout the continuum, transitional, and free molecular flow regimes are of primary importance to the program. For the Earth-to-Orbit (ETO) vehicles, which encounter Mach numbers as great as 25, a significant amount of dissociation and chemical nonequilibrium exists at the high altitudes (i.e., above 50 km). Also, because many ETO vehicle concepts must return to Earth for landing, the relationship between high-speed aerothermodynamic efficiency and low-speed flight performance must be investigated for each configuration. For more energetic missions that may involve probes or aeroassist space transfer vehicles (ASTVs), flight Mach numbers as large as 50 are encountered, and ionization, radiation, and thermochemical nonequilibrium can be significant to the vehicle designs.

The Aerothermodynamics R&T program addresses the issues through emphasized research in four primary areas: computational tool development; experimental research and computational validation; facilities research and development; and configuration assessment. The computational tools developed include not only computational fluid dynamics methods but also computational chemistry methods which provide a unique ability to calculate high-temperature gas properties. The vehicle synthesis engineering tools developed are becoming industry standards for preliminary design and analysis. Application of aerothermodynamics technology to vehicle designs will result in reduced flight environment uncertainty, optimized configurations, and improved performance margins.

Program Manager: Jim Moss
OAST/RF
Washington, DC 20546
(202) 453-2820

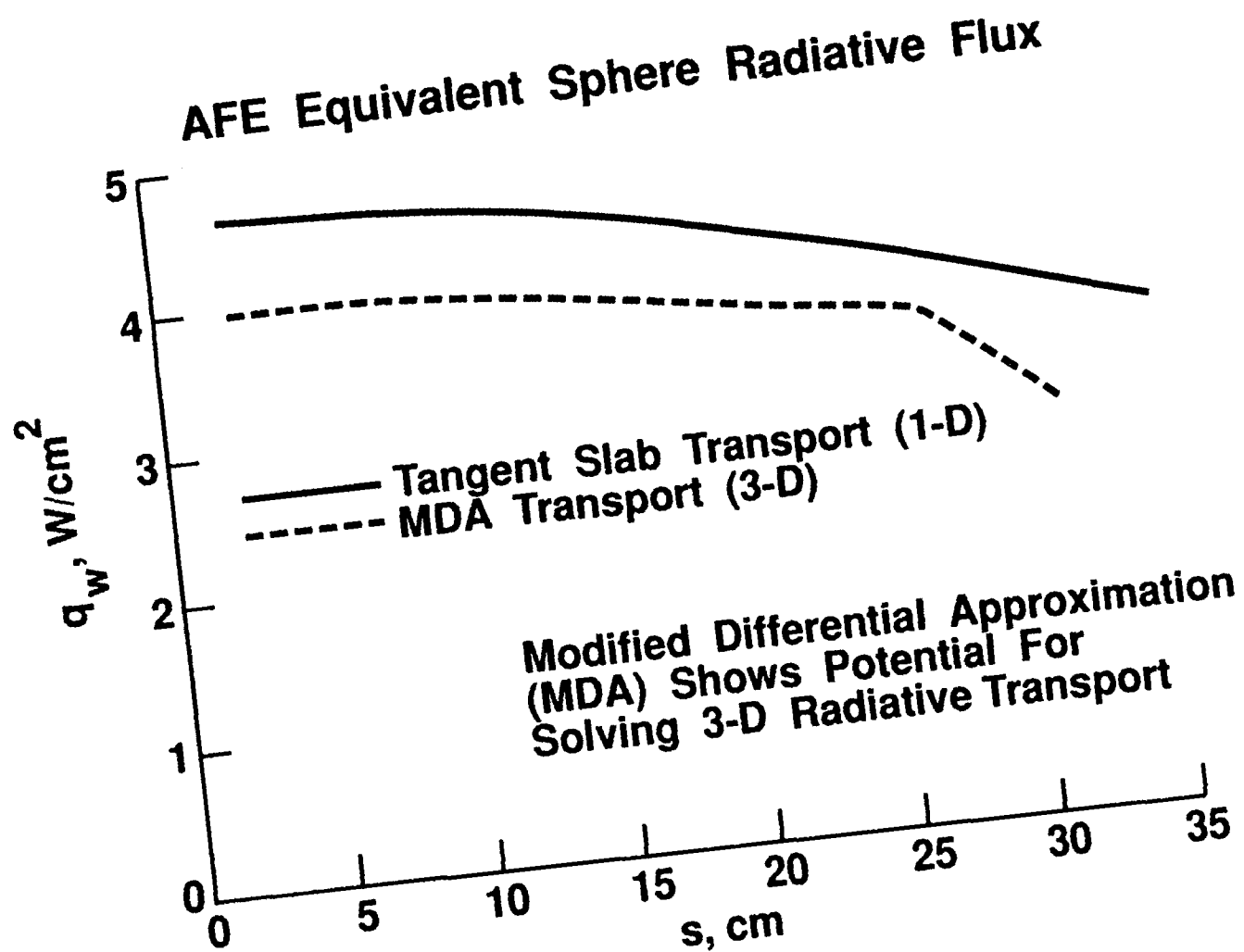


Figure 11-1. Advancement in Radiative Transport

11-1 Advancements in Radiation Transport

Objective. To develop improved methods to predict radiative heating over three-dimensional configurations in thermochemical nonequilibrium flows.

Approach. A radiation transport code was developed that minimizes the spectral array required for adequate resolution of the radiative flux. Techniques were defined to optimize the coupling of the radiative transport to a flow-field code. A method was developed to efficiently account for 3-D radiation effects over complex configurations.

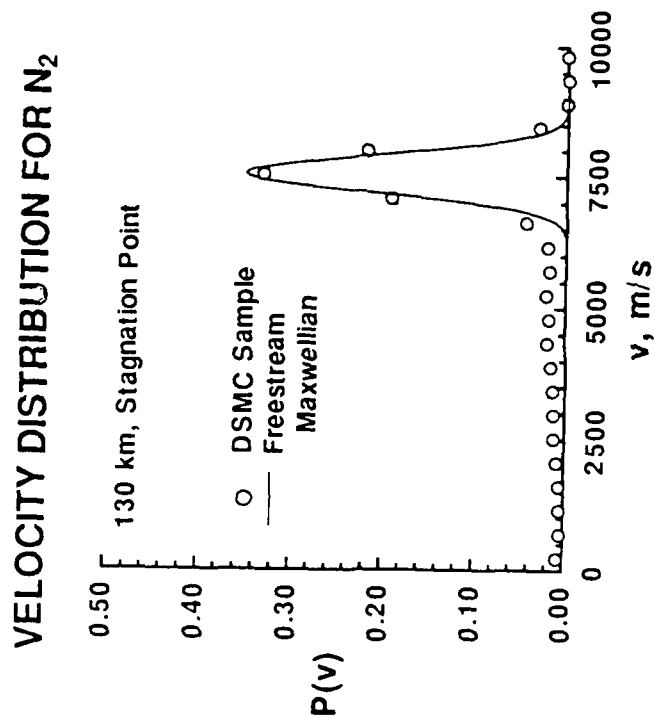
Accomplishments. A nonequilibrium radiative heating prediction method, the Langley Optimized Radiative Nonequilibrium (LORAN) code has been developed. Numerical studies have been performed to determine the minimum spectral points required for adequate predictions of the radiative flux. The results have been compared with ground-based and flight measurements, and with the detailed Park NEQAIR code, with good agreement. Initial studies have demonstrated the feasibility of using the LORAN code coupled with the flow-field code LAURA. A Modified Differential Approximation (MDA) method has been adopted for 3-D radiative transport, and has been applied successfully for axisymmetric, blunt-body cases.

Significance. High-temperature radiative transport at equilibrium conditions over axisymmetric blunt bodies at zero angle-of-attack with the one-dimensional tangent-slab approximation is reasonably advanced over earlier studies on Earth entries and the work on the Pioneer Venus and Project Galileo probes. However, for aerobraking applications, the radiative transport is expected to be at thermochemical nonequilibrium conditions over complex 3-D configurations at non-zero angles-of-attack. Current advancements in the development of the nonequilibrium LORAN code, coupled to the LAURA flow field,

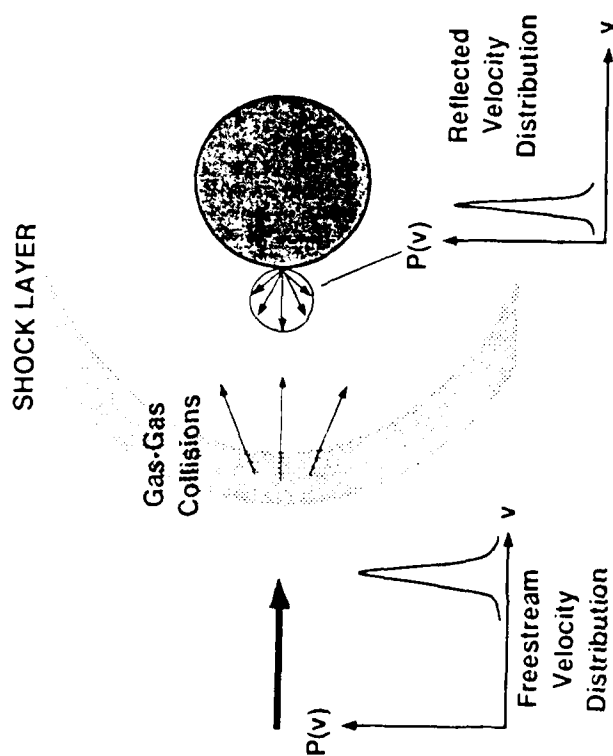
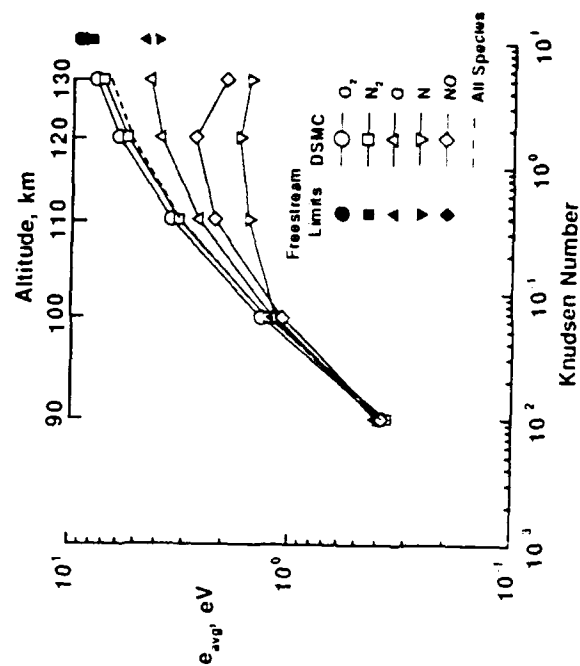
and the development of the 3-D MDA code are an excellent start to predicting and interpreting Aero-Assist Flight Experiment results, and in the application to aerobrakes in the Space Exploration Initiative.

Status/Plans. Efforts are continuing to improve the accuracy and efficiency of the recently developed 3-D radiative transport methods. The methods will be further demonstrated through applications at additional flow conditions and vehicle configurations.

Lin C. Hartung
Aerothermodynamics Branch
Langley Research Center
(804) 864-4371



AVERAGE ENERGY PER MOLECULE



VELOCITY DISTRIBUTION FOR N_2

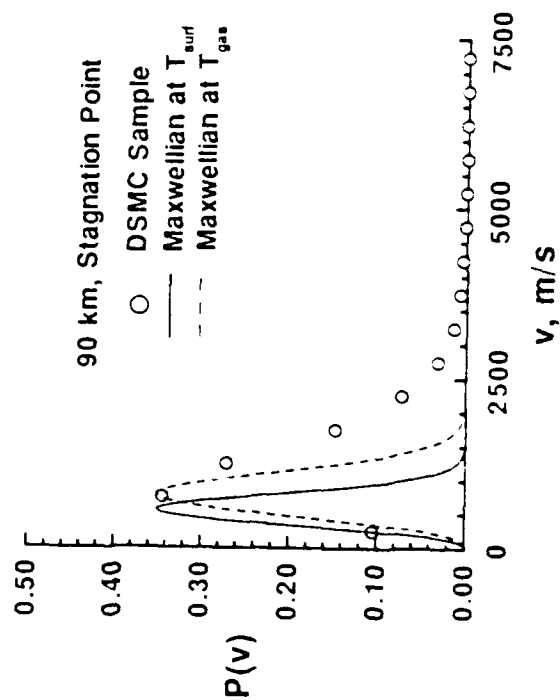


Figure 11-2. Energetics of Gas-Surface Interactions in Transitional Flows at Entry Velocities

11-2 Energetics of Gas-Surface Interactions in Transitional Flows at Entry Velocities

Objective. To provide fundamental information on the velocities and energies of molecules incident on a surface behind a shock layer in transitional flows at entry velocities and to provide data to support experiments on proposed tethered satellites.

Approach. The direct simulation Monte Carlo (DSMC) method was used to model the flow about a 1.6-m diameter sphere in the altitude range of 130 to 90 km for Earth entry at 7.5 km/s. Samples of the velocity and translational energy distributions were taken for gas molecules striking the surface at various points on the sphere and for each gas species.

Accomplishments. Velocity distributions were computed for each of five gas species at five different altitudes as a function of the circumferential location on the sphere. The computations required the sampling of more than one million molecules at each condition. The results will be published in AIAA Paper 91-1338.

Significance. Proposed experiments in transitional, entry flows will require sophisticated instrumentation to study the details of gas-surface interactions. These DSMC results show the wide range of incident velocities and energies that must be considered in designing such experiments. The results also demonstrate the high degree of translational nonequilibrium present behind the shock layer.

Status/Plans. Additional studies to fully characterize the translational velocity distributions throughout the flow field are planned for the purpose of evaluating possible means of coupling DSMC and Navier-Stokes solution methods.

Richard G. Wilmoth, James N. Moss
Aerothermodynamics Branch
Langley Research Center
(804) 864-4367

Virendra K. Dogra
Vigyan Research Associates
(804) 864-2957

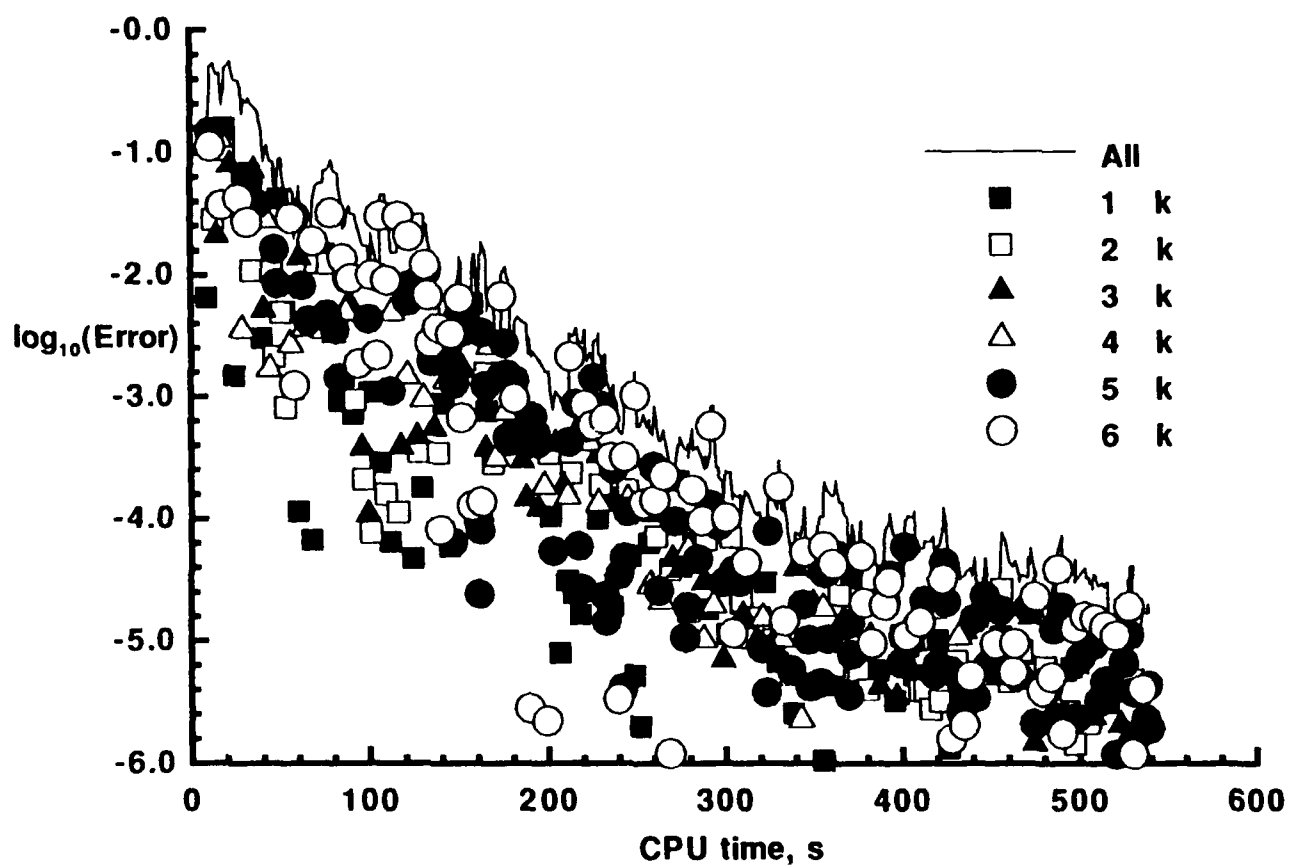


Figure 11-3. Convergence History: Six Tasks Adapting Partition Boundaries

11-3 Asynchronous Macrotasked Relaxation Strategies for the Solution of Viscous Hypersonic Flows

Objective. To exploit parallel, multitasking capabilities of CRAY-class supercomputers to improve efficiency of numerical simulations of viscous, hypersonic flows in thermochemical nonequilibrium.

Approach. An upwind-biased, point-implicit relaxation of the governing equations was implemented. Relaxation factors were independently defined for the viscous and inviscid contributions to the solution. Computational work was divided into several, independently executed tasks through partitioning of the computational domain using CRAY macrotasking. The point-implicit relaxation, which limits the computational stencil, in combination with the appropriate relaxation factors eliminated the need for synchronized communication between the tasks for steady flow problems.

Accomplishments. Solutions for hypersonic flows over aerobrakes, including the wake flow, have been obtained using as many as eight tasks executing asynchronously. Sacrificing synchronization on coarse grain machines has shown no adverse effects on total CPU time required to obtain a solution, and reduces turnaround time for a given job. Adaptive partitioning provides further, moderate improvement in required CPU time by moving partition boundaries to concentrate task activity in areas where the contribution to the solution error is the highest. The accompanying figure shows the convergence history for each of six tasks applied simultaneously and asynchronously to the solution of hypersonic, reacting flow over an aerobrake. The pattern is somewhat chaotic, because of the lack of synchronization and moving partition boundaries, but the overall trend is decreasing by approximately a factor of six times faster in turnaround time than a single task application.

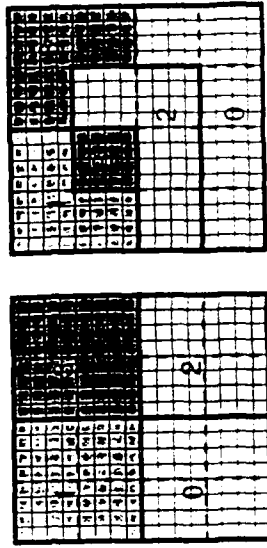
Significance. Simulations of moderately complex entry vehicles (i.e., HL-20, aerobrake-payload assemblies) have large memory requirements, sometimes requiring dedicated use of a supercomputer. The present asynchronous, macrotasking strategy enables complete utilization of all processors in the dedicated mode with speedup proportional to the number of processors for coarse grain machines like the Cray-2. Furthermore, while a single Cray Y-MP does not have sufficient memory to execute these simulations, networking several such machines to provide even faster turnaround is theoretically possible.

Status/Plans. These strategies will be applied to STS and HL-20 flow-field simulations.

Peter A. Gnoffo
Aerothermodynamics Branch
Langley Research Center
(804) 864-4380

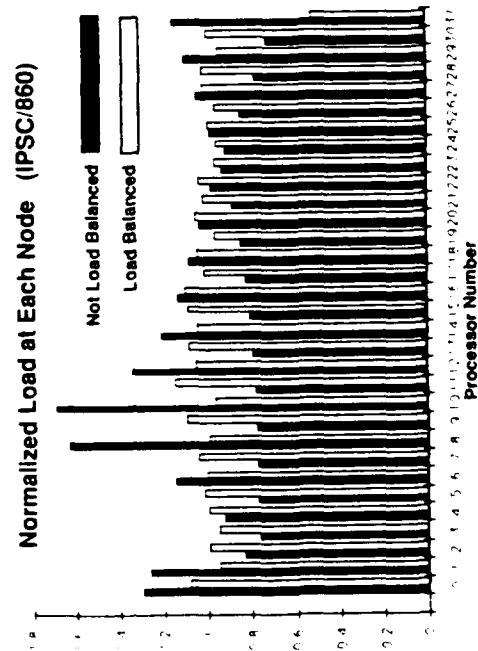
DOMAIN DECOMPOSITION

- Several sub-domains assigned to each CPU
- Sub-domains of fixed size and shape
- Load balancing done infrequently



- o Parallelization through dynamic domain decomposition.
- o Linear speedup over full range of number of processors.
- o Vectorizable algorithms used at each node.

EFFECT OF DYNAMIC LOAD BALANCING



PERFORMANCE ON THE iPSC/860 COMPARED TO CRAY

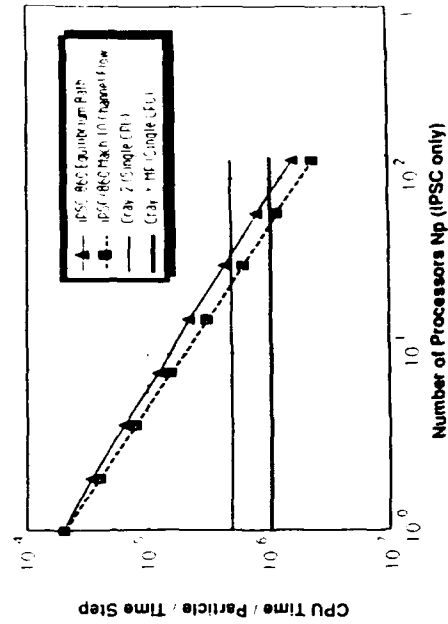


Figure 11-4. Particle Simulation in a Multiprocessor Environment

11-4 Particle Simulation in a Multiprocessor Environment

Objective. To develop a particle simulation code that is portable to a wide class of vector and multiprocessor supercomputers and capable of addressing large-scale rarefied flow problems.

Approach. Direct particle simulation methods model flows as a collection of discrete particles that interact with each other and with boundaries through collisions. The collision-selection rule used is highly compatible with the requirements for vectorization. These methods have been implemented on the 128 processor Intel iPSC/860, and a dynamic domain decomposition is utilized to distribute the simulation across processors and to balance the load.

Accomplishments. A new code has been developed that can take advantage of medium-grain parallelism through a domain decomposition while retaining the vector compatibility of previous codes. This provides a capability to examine three-dimensional flow problems involving gas mixtures in thermochemical non-equilibrium. The code is portable over a wide class of Multiple Instruction Multiple Data (MIMD) machine architectures. Speedup as additional processors are devoted to the simulation remains linear to the full 128 processors of the iPSC/860 tested to date.

Significance. With continuing interest in hypersonic flight, a need exists for a computational capability to predict the aerodynamic and thermal environment found around vehicles such as the National Aero-space Plane (NASP) or the Aero-Assist Flight Experiment (AFE). Because of the difficulties in applying the continuum equations to the very low-density hypersonic regimes these vehicles will encounter, application of direct particle simulation methods is an appropriate consideration. The numerical efficiency of this ap-

proach and the scalability to large numbers of processors enables larger-scale applications of direct particle simulations than previously possible.

Status/Plans. The current version of the developed particle simulation code will port to several parallel MIMD and vector machine architectures. Grid adaption techniques will be employed to increase resolution in areas of the flow having larger gradients. More advanced models for thermal and chemical relaxation, now under development, will be incorporated in the current code.

Jeffrey D. McDonald
Eloret Institute
Aerothermodynamics Branch
Ames Research Center
(415) 604-1140

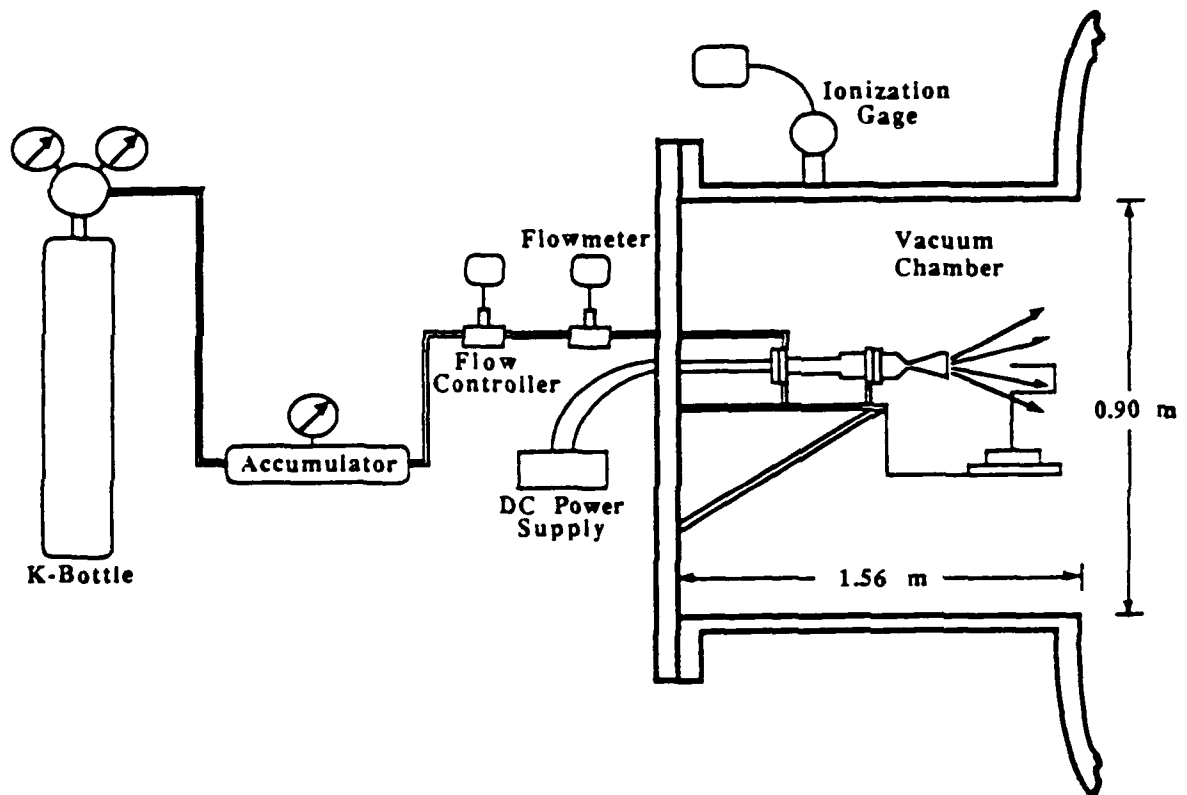
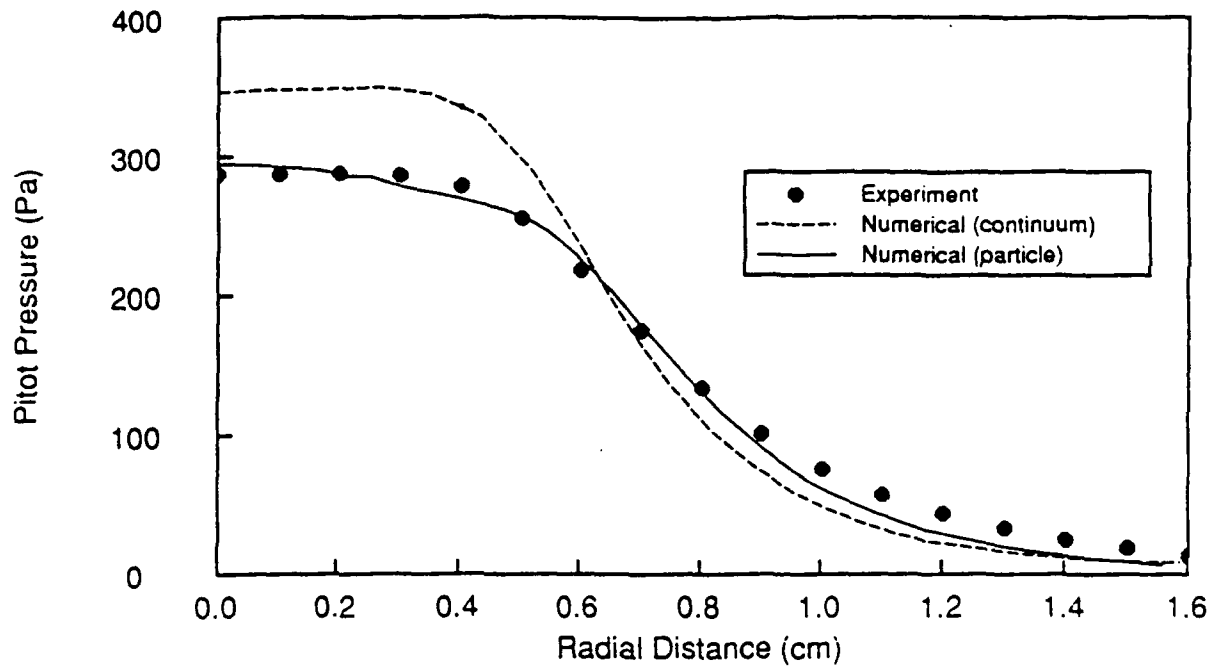


Figure 11-5. Experimental and Numerical Analyses of Small Rockets (Transverse Pitot Pressure Profiles at Nozzle Exit)

11-5 Numerical and Experimental Analyses of Small Rocket Flows

Objective. To provide experimental and numerical data for accurate prediction of rarefied flow of small, low-thrust rockets used for control of spacecraft.

Approach. Expansion of diatomic nitrogen through a low thrust rocket was considered. A small nozzle flow provided conditions that pass from continuum to rarefied. To assess rarefaction effects, the nozzle flow was computed with both a traditional continuum CFD technique and a stochastic particle simulation method. The plume was also calculated with the particle method. The computations were compared with new experimental data for Pitot pressure and flow angle.

Accomplishments. Comparison of pitot pressure at the nozzle exit reveals that the particle method predictions agree very well with the experimental data, whereas the continuum solutions overpredict the pressure by 25%. The particle method solutions continue to agree with experimental data further out into the expansion plume. The numerical efficiency of the particle method has been improved substantially by restructuring the algorithms to suit the architecture of vector supercomputers. A typical run of the particle method code required 3 CPU hours and 24 Mwords of central memory on a Cray Y-MP.

Significance. The differences in the continuum and particle method solutions will increase as the plume expands. The present study reveals that significant errors will be incurred through the prediction of such flows with continuum CFD. To obtain accurate solutions of small plumes, and hence accurate assessment of the interaction between the plume and the spacecraft, it is necessary to employ the particle simulation technique.

Status/Plans. The particle method computations will be extended further in the transverse direction and into the backflow region behind the rocket. Furthermore, solutions will be generated through the same nozzle for the expansion of argon for comparison with additional experimental measurements.

Iain D. Boyd
Eloret Institute
Aerothermodynamics Branch
Ames Research Center
(415) 604-4907

Paul F. Penko
Lewis Research Center
(216) 433-2404

35° Ramp, $\rho_\infty = 10.72 \times 10^{-6} \text{ kg/m}^3$
 $M_\infty = 24.26$, $\lambda_\infty = 0.230 \text{ mm}$, $T_w = 394.2 \text{ K}$

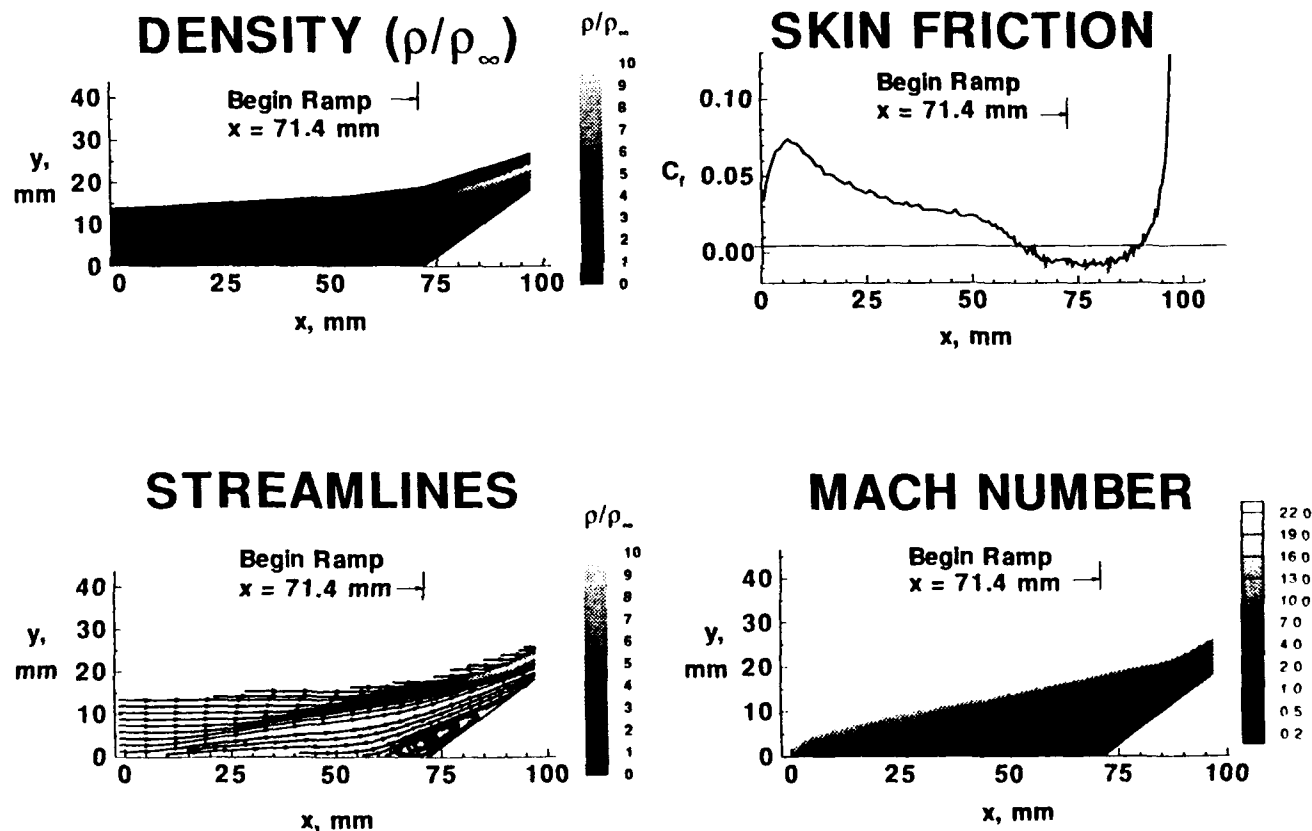


Figure 11-6. Hypersonic Rarefied Flow About a Compression Corner

11-6 Hypersonic Rarefied Flow About a Compression Corner

Objective. To numerically simulate the phenomena of shock/boundary layer interactions and compare the numerical results with the experimentally measured data obtained in the DLR wind tunnels at Gottingen, Germany.

Approach. The focus is on the merged-layer interactions that occur for hypersonic ($M_\infty \approx 20$) nitrogen flow over a two-dimensional model consisting of a flat plate followed by a compression ramp. The ramp corner is located 71.4 mm from the plate leading edge, and ramp angles of 0° , 15° , 25° , and 35° are considered. Freestream Reynolds number based on model length ranges from 6,000 to 39,000. The calculations are made with a 2-D version of the direct simulation Monte Carlo (DSMC) method.

Accomplishments. Calculations have been made for four test conditions using the DSMC method. Results of these calculations have been compared with various experimental measurements to provide both quantitative and qualitative comparisons. The experimental and computational findings agree on the combination of flow conditions and ramp angles necessary to produce separation.

Significance. The capability to accurately calculate the phenomena associated with shock/boundary layer interactions is critical for the design of future space transportation vehicles. The present study gives added confidence in the ability of the DSMC method to simulate such flows for hypersonic rarefied conditions.

Status/Plans. Results of the study have been published in AIAA Paper 91-1313.

James N. Moss, Joseph M. Price
Aerothermodynamics Branch
Langley Research Center
(804) 864-4379

Ch.-H. Chun
DLR Institute for Experimental
Fluid Mechanics
Gottingen, Germany

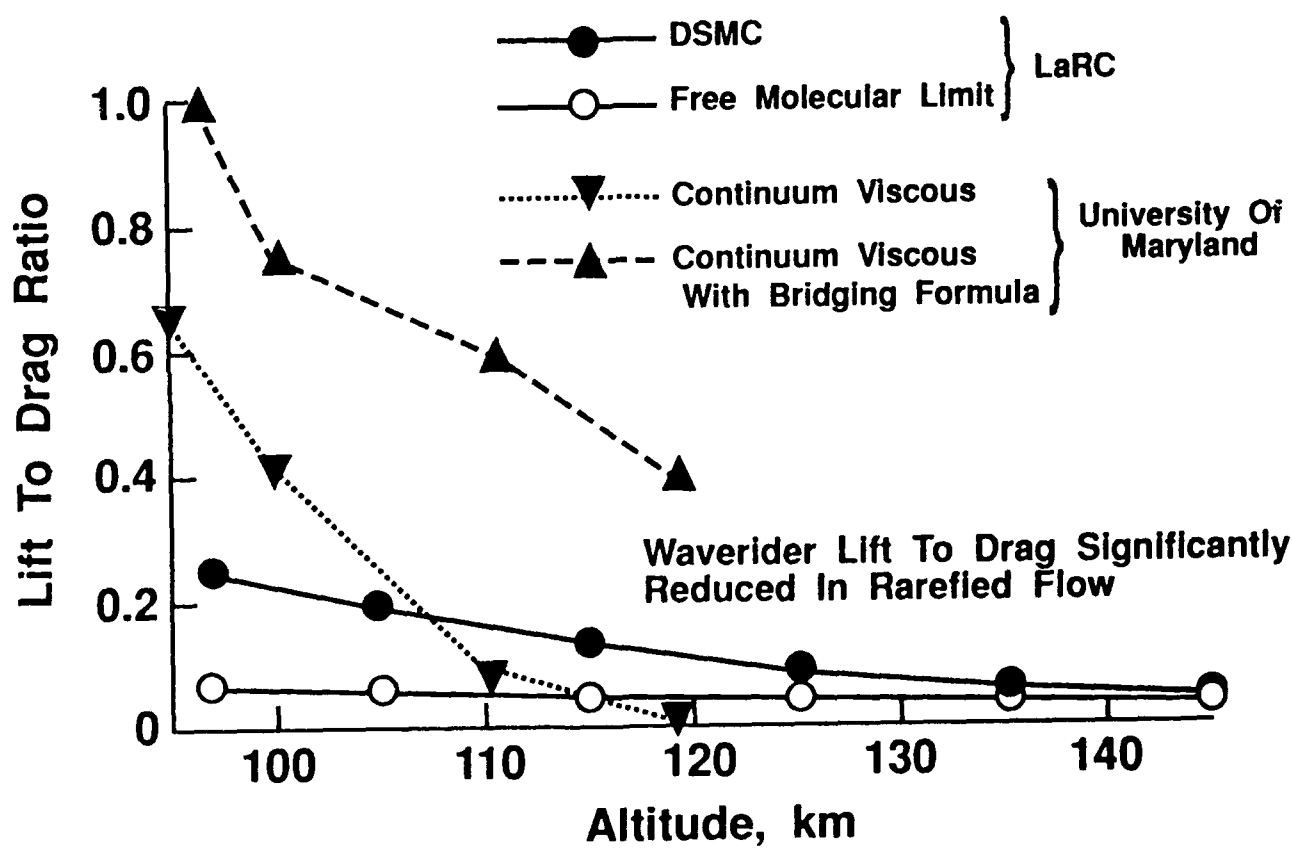


Figure 11-7. Rarefied Flow Regime Hypersonic Waverider Configuration, Mach No. 25

11-7 Advancement in Developing an Efficient 3-D DSMC Code

Objective. To significantly improve our present capability to calculate rarefied flows over complex configurations at low altitudes.

Approach. The capability of a new direct simulation Monte Carlo (DSMC) code, denoted as F3, was further developed, demonstrated, and validated and flow fields were simulated in the rarefied flow regime about complex configurations in three dimensions.

Accomplishments. Significant code improvements have been made in the areas of surface definition and grid generation for code setup, graphical displays for diagnosis procedures, and post-processing and analyzing results, and in data compressing techniques to reduce memory size. F3 was used to simulate the flow field over a delta wing at angles-of-attack from 0° to 30° for a Mach 20 flow at a Knudsen number of 0.016. The aerodynamic coefficients were in excellent agreement with ground-based experimental data, thus providing partial validation of the code. Solutions had been obtained over a hypersonic waverider configuration proposed by the University of Maryland that was optimized for Mach 25 at an altitude of 90 km. Also, solutions were obtained using an approximate bridging technique to correct for rarefied flow effects at higher altitudes. Finally, solutions were obtained with the current F3 DSMC code at altitudes from 97 to 145 km. The F3 lift-to-drag ratios were much lower than those predicted by the University of Maryland.

Significance. The computational efficiency, code setup procedures, and memory management of the F3 code are far superior to our earlier 3-D DSMC code, with no loss in accuracy. Our present simulation for the delta wing with the F3 code was set up in a few days and required 1 to 2 days on a 32-bit workstation as contrasted with several months to setup and one Cray CPU day with the earlier code. The present results with the F3 code show that the high values of lift-to-drag predicted for a waverider concept are significantly reduced at high-altitude, rarefied flow conditions.

Status/Plans. Future improvements to the code will include adaptive gridding, a variable inner mesh resolution, improved memory management, and optimization for vector and parallel computing. Code will be demonstrated for selected 3-D configurations.

Didier F. G. Rault
Aerothermodynamics Branch
Langley Research Center
(804) 864-4388



Mach = 7.4, $\alpha = 40^\circ$

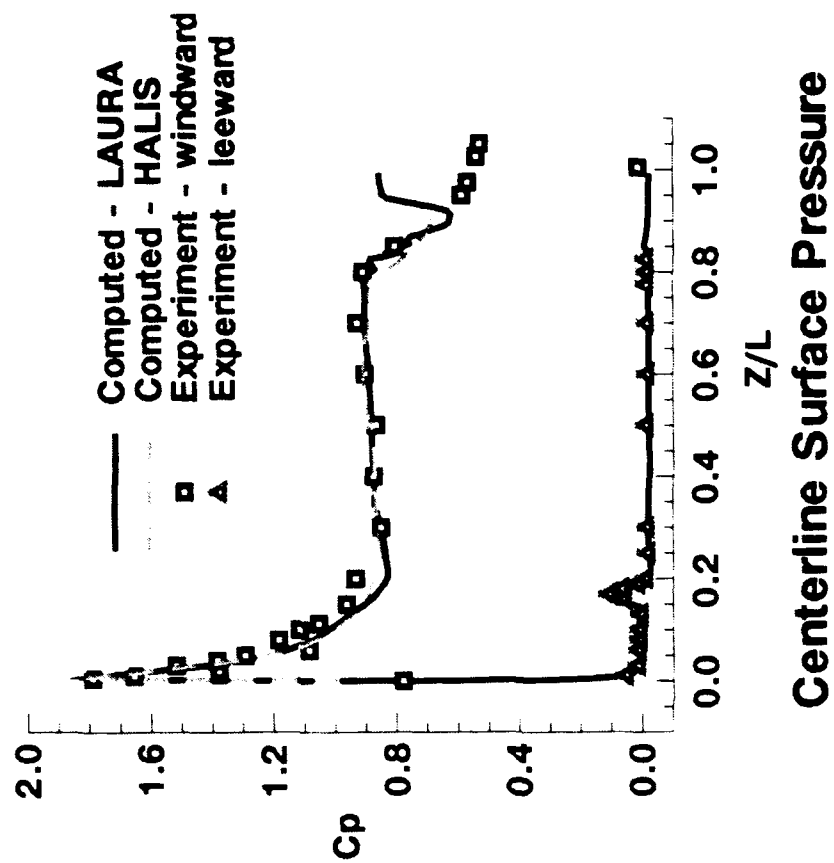


Figure 11-8. Shuttle Orbiter Pressure

11-8 Flow-Field Computations for Shuttle Orbiter

Objective. To obtain flow-field solutions for the shuttle orbiter adequate for comparison with the flight data from the Shuttle Infrared Leaside Temperature Sensor (SILTS) experiment.

Approach. Improved gridding techniques were used to define the surface and volume grids. The Langley Aerothermodynamic Upwind Relaxation Algorithm (LAURA) code was used to obtain the flow-field solutions.

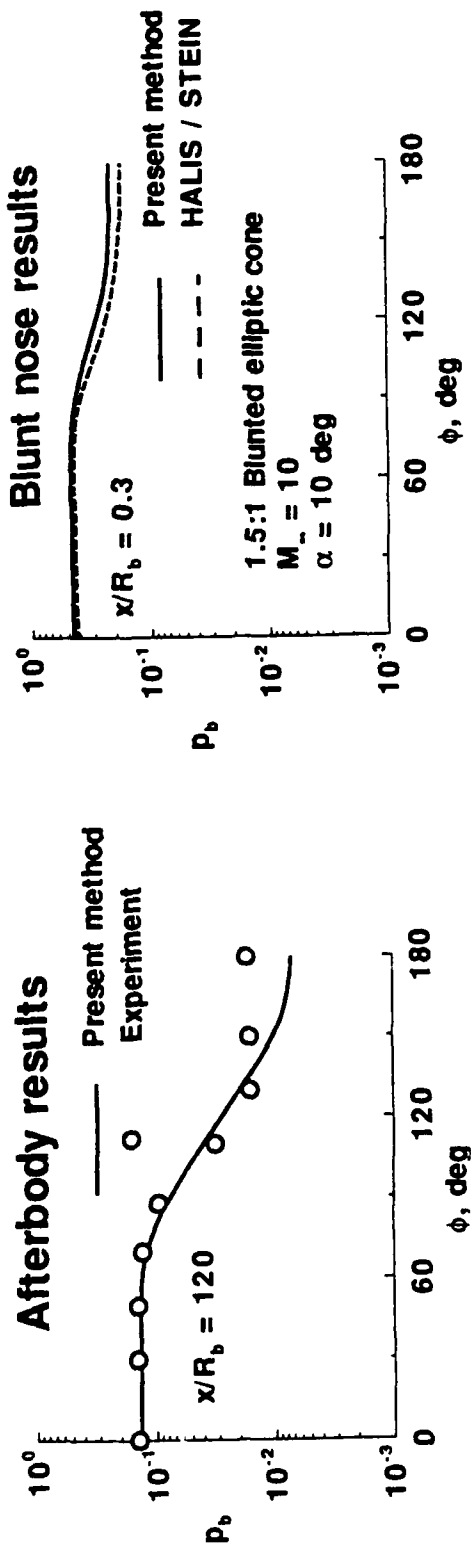
Accomplishments. A grid and flow-field solution has been obtained for inviscid flow at a 40° angle-of-attack for Mach 7.4 flow, a wind tunnel case. The computed surface pressures are in excellent agreement with the experimental data on both the windward and leeward surfaces. The results identified a small region of non-smooth grid surface near the aft end of the vehicle. This small grid problem has been resolved, and a grid for a viscous solution has been completed.

Significance. The first computational solution has been obtained for the complete orbiter configuration at a hypersonic flow condition. The analysis of the results for the wind tunnel case provides confidence that the grid technique and the LAURA code can provide excellent results; thus, we can proceed with more computer-intensive cases and analyze viscous flow with nonequilibrium chemistry at actual shuttle flight conditions. This solution also adds significantly to our database of computational results for complex configurations such as the HL-20, National Aero-Space Plane, and the Aero-Assist Flight Experiment vehicle.

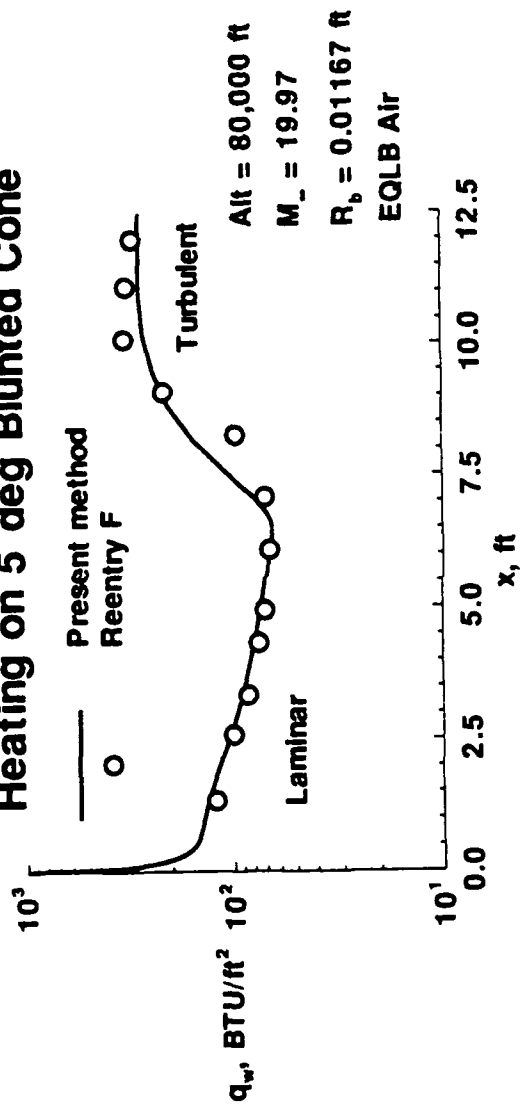
Status/Plans. Viscous flow solutions with non equilibrium chemistry will be obtained at actual shuttle flight conditions. The computational results will be compared with SILTS flight data and data from the Developmental Flight Instrumentation flights.

William L. Kleb, K. James Weilmuenster
Aerothermodynamics Branch
Langley Research Center
(804) 864-4364

Inviscid Comparisons on Blunted Elliptic Cone



Heating on 5 deg Blunted Cone



Figures 11-9. Approximate Flow Field and Heating Analysis

11-9 Approximate Heating Analysis

Objective. To develop rapid but reliable approximate flow-field analysis capability for application in conceptual design studies and preliminary aerothermal design.

Approach. Boundary layer techniques were incorporated in a versatile inviscid method for heat-transfer predictions over 3-D surfaces at various angles-of-attack.

Accomplishments. An inviscid method has been developed incorporating the normal pressure approximation of Maslen. The method has been demonstrated to yield rapid but reliable inviscid solutions over axisymmetric and 3-D surfaces at angle-of-attack. The code requires 10 seconds of computer time on a workstation to obtain a solution over a 3-D blunt nose. Boundary layer approximations have been included for axisymmetric vehicles at angle-of-attack for (1) perfect gas and equilibrium chemistry and (2) laminar and turbulent heating calculations.

Significance. Successful demonstration of the approximate flow-field technique for 3-D configurations will significantly advance the useability of engineering methods. The analysis would provide the aerothermal community with a unique approximate method for computing the heating rates over 3-D blunt noses needed in thermal design studies. Currently, more detailed methods require many hours of computation.

Status/Plans. The boundary layer methods are presently being included in the inviscid method for application to 3-D vehicles. Comparison of results will be made with a detailed Navier-Stokes method.

Christopher J. Riley
Aerothermodynamic Branch
Langley Research Center
(804) 864-4387

$$M_\infty = 6 \quad Re_\infty = 2 \times 10^6 / m \quad \alpha = 30^\circ$$

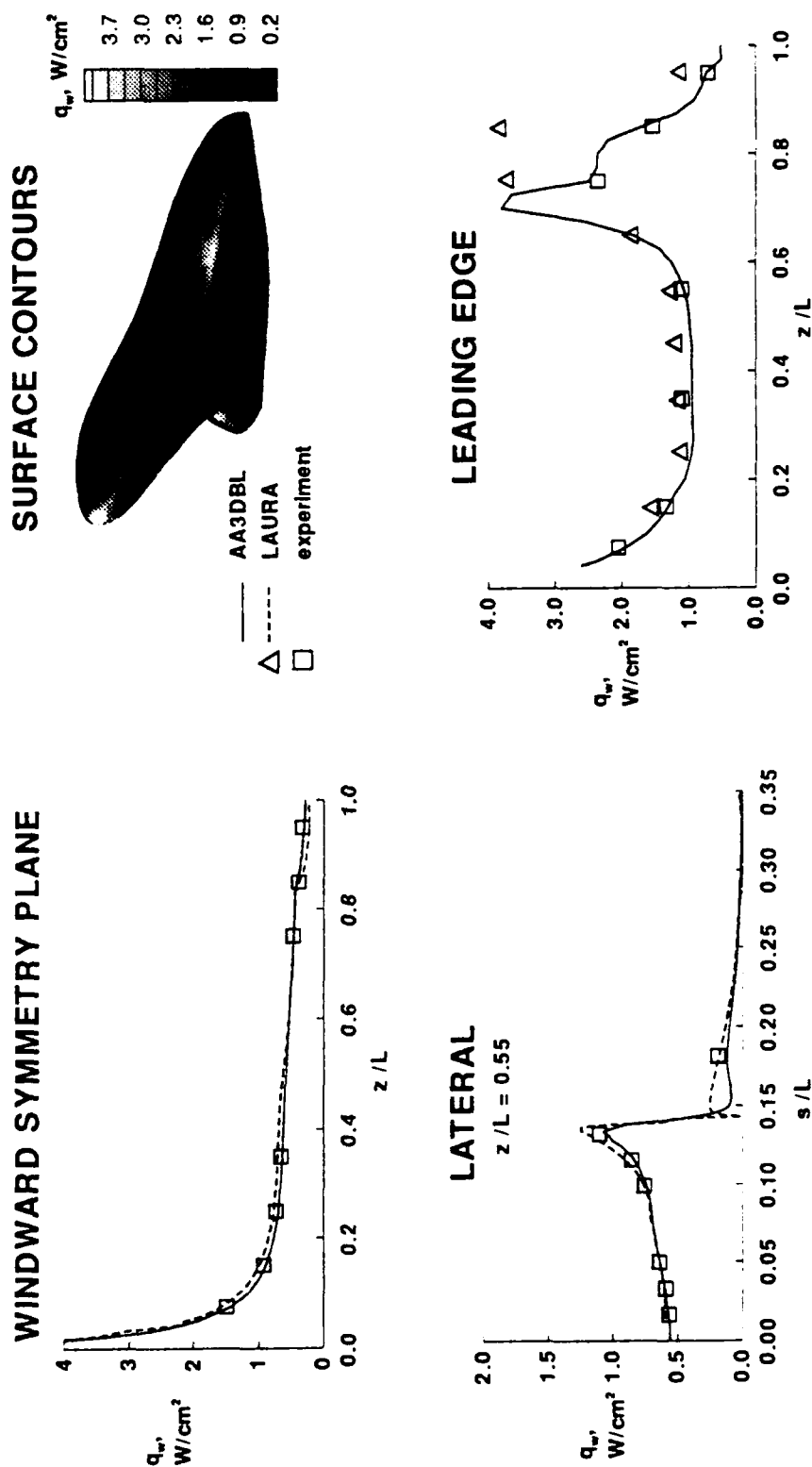


Figure 11-10. Heating on Modified Shuttle Orbiter

11-10 Comparison of Heating Rate Calculations with Experimental Data on a Modified Shuttle Orbiter at Mach 6

Objective. To provide detailed information on the ability of an "engineering code" based on combined inviscid and boundary theory AA3DBL/HALIS (Axisymmetric Analog for Three-Dimensional Boundary Layer/High Alpha Inviscid Solution) and a "benchmark" Navier-Stokes code LAURA (Langley Aerothermodynamic Upwind Relaxation Algorithm) to predict heating rates from the windward symmetry plane and in the vicinity of wing leading edges on winged vehicles at large angles-of-attack.

Approach. Heating rate calculations from AA3DBL/HALIS and LAURA were compared with experimental data obtained at Mach 6 on a modified Shuttle Orbiter model. This is the first step in a process designed to validate the codes for application to winged vehicles in the flight environment.

Accomplishments. Comparisons have been made at 30° and 40° angle-of-attack for conditions where the flow over the model was completely laminar. Both codes compare well with the experimental data along the wind-

ward symmetry plane, in a circumferential direction around the model, and in the high heating region along the fuselage or wing leading edge.

Significance. These results give confidence that both AA3DBL/HALIS and LAURA can be used to predict more accurately the heating environment of future entry vehicles and should lead to less conservatism in design. In addition, since AA3DBL/HALIS require only 1% of the time required for similar LAURA calculations, it should be very useful for performing parametric studies.

Status/Plans. AA3DBL/HALIS and LAURA will be compared with wind tunnel data at other flow conditions and with available flight data.

H. Harris Hamilton II, Francis A. Greene,
K. James Weilmuenster
Aerothermodynamics Branch
Langley Research Center
(804) 864-4365

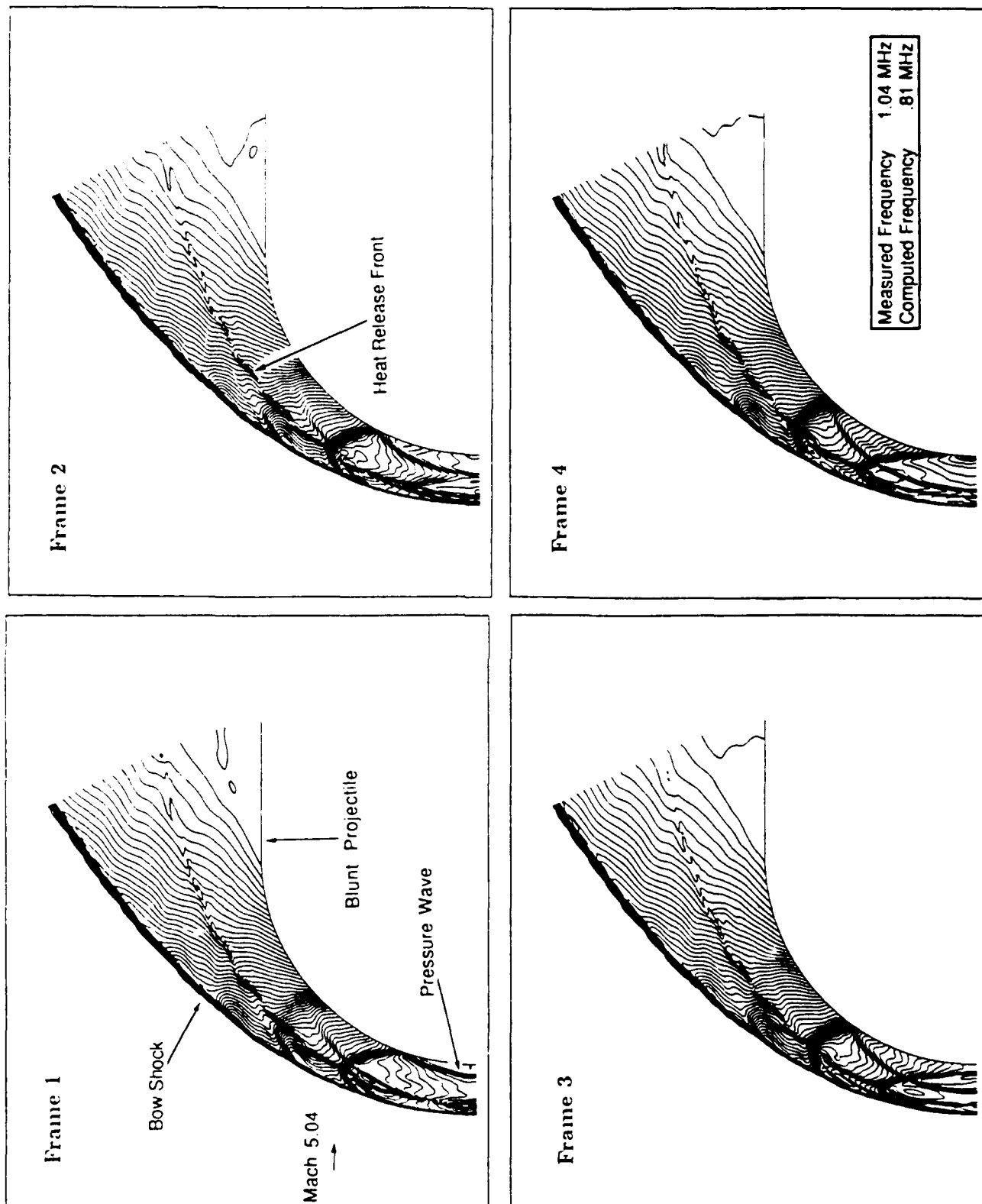


Figure 11-11.Computed Meridional Pressure Contours from Mach 5.04 Flow of Premixed Hydrogen-Air over a Blunt Body Using a 181x127 Grid (4 Frames of an Oscillation Cycle).

11-11 Numerical Simulation of Unsteady Shock-Induced Combustion

Objective. To develop a computational method that will lead to the simulation and understanding of the unsteady shock-induced combustion observed in ballistic range experiments.

Approach. Ballistic range experiments produce a periodic, unsteady flow when a blunt projectile is fired supersonically into a premixed hydrogen-air mixture (Frame 1 in the figure). This unsteady behavior is caused by the combustion of the mixture, which has been heated by the bow shock in front of the projectile. Observations show that the heat release due to combustion does not occur immediately behind the bow shock but is delayed by the finite rate of the chemical reactions in the high-speed flow. The region between the shock and the heat release is called the induction zone. There is little or no heat release in this zone, but the concentrations of chemical species important for ignition increase exponentially. Previous work has shown that the chemistry in the induction zone must be modeled accurately to simulate these flows. The grid spacing requirements for sufficient accuracy are so stringent that simulating these unsteady flows has not been feasible. A transformation of the species continuity equations has been found to reduce grid requirements and make such simulations practical. This transformation is compatible with current numerical methods.

Accomplishments. This work represents the first known numerical simulation to incorporate a detailed chemical reaction model capable of simulating the unsteady shock-induced combustion phenomenon seen in ballistic range experiments (Frames 2 and 3). A new formulation of the species continuity equations has been developed and incorporated in a proven numerical scheme. This new formu-

lation increases the accuracy of numerical calculations in flows with exponentially varying species concentrations.

Significance. The physical mechanism causing unsteady combustion in supersonic ballistic range experiments is now better understood. This will lead to improved simulations of combustion processes for hypersonic systems.

Status/Plans: The current formulation will be applied to other problems in which shock-induced combustion or ignition is important. Examples are flows in shock-tunnels or ram-accelerators. Application of this work to other types of flows with exponentially changing species concentrations, such as ionization processes, may also be valuable.

Gregory J. Wilson, Myles A. Sussman
Aerothermodynamics Branch
Ames Research Center
(415) 604-4228

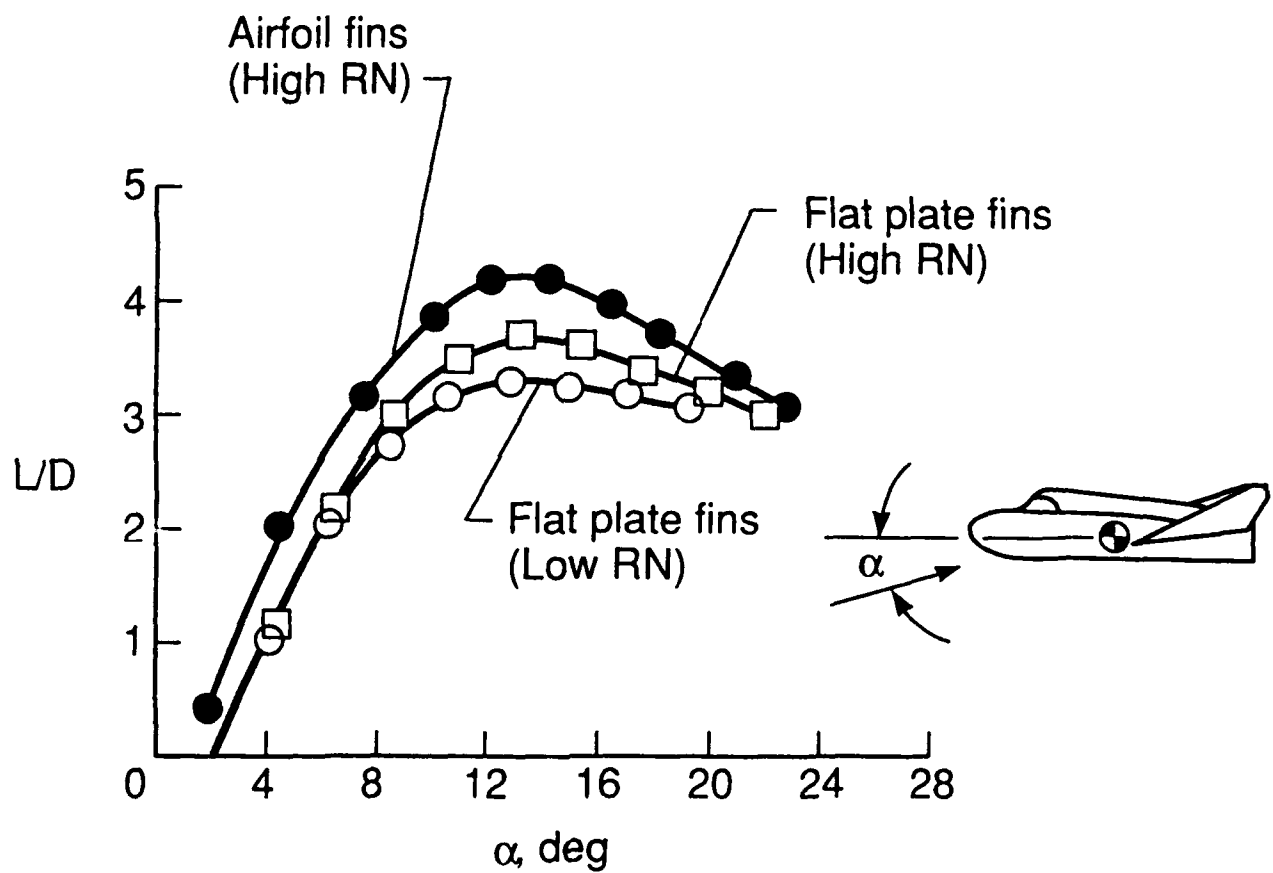


Figure 11-12. Subsonic L/D Improvements of HL-20

11-12 Aerodynamic/Aerothermodynamic Characteristics of HL-20/HL-20 A/B Lifting Body Configurations

Objective. To experimentally determine aerodynamic/aerothermodynamic characteristics of an HL-20 lifting body configuration at hypersonic to subsonic flow conditions (i. e., entry to landing), and to evolve optimum lifting body configurations from aerodynamic perspective via modification of aerolines and control surfaces.

Approach. Force and moment measurements were performed on the HL-20 configuration at subsonic (Low-Turbulence Pressure Tunnel [LTPT], 7- by 10-ft. Tunnel), transonic (Calspan Transonic Tunnel, 8-foot Transonic Tunnel), supersonic Unitary Plan Wind Tunnel [UPWT], and hypersonic flow conditions (HFC) to determine the effects of compressibility and viscosity and to simulate real-gas effects. Thermal mappings and flow visualizations were performed at hypersonic conditions to determine aerothermodynamic characteristics. HL-20 aerolines, including control surfaces, were modified to enhance aerodynamic performance with no sacrifice in aerothermodynamic performance.

Accomplishments. HL-20, HL-20A series (four different configurations having a stream-lined upper surface including canopy, windward surface chamber, and reduced base area) configurations were tested extensively at subsonic, supersonic, and hypersonic conditions. Tests of the HL-20B series (second iteration; flat-like upper surface and wings faired into body) and HL-20/Titan 4 ascent configuration were initiated in the MSFC 14-inch tunnel.

Significance. Unprecedented ground-based data have been established for HL-20/HL-20A lifting body configurations, clearly surpassing previous phase A studies. Aerodynamic characteristics were determined from Mach 20 to 0.1 (entry to landing). Aerodynamic performance of HL-20 at subsonic speeds has improved significantly via modification of the wing from cylinder-slab to airfoil

(lift-to-drag ratio increased approximately 20%); at subsonic conditions, the effect of Reynolds number vanished for values in excess of 8 million per foot in the LTPT. Aerodynamic performance of HL-20s free of real-gas effects primarily because of flat windward surface (unlike the shuttle orbiter, which experienced significant real-gas effects on pitching moment). The HL-20A concept provides improved subsonic aerodynamic performance, but must reenter at high incidence to match lift/drag (i.e., cross range) of the HL-20 and the will experience significantly higher heating in the nose region as a result of streamlining of the nose.

Status/Plans. We plan to complete wind tunnel testing of HL-20, HL-20A, and HL-20B concepts; reduce and analyze data; and disseminate results. Will initiate CFD code calibration study at hypersonic conditions for HL-20 configuration.

Bernard Spencer, Jr., George M. Ware, N.
Ronald Merski
Experimental Hypersonics Branch
Langley Research Center
(804) 864-5245

Chapter 12

Aerobraking

Aerobraking can provide a substantial increase in payload or decrease in initial mission mass for missions that require a trajectory deceleration in the vicinity of an atmosphere-bearing planet. The objective of the Aerobraking Technology program is to develop and validate key supporting technologies which allow the effective use of aerobraking for manned lunar missions, robotic and manned round trip missions to Mars, and other planetary exploration missions. The term aerobraking in this context includes 1) capture into a planetary orbit, 2) reduction of orbit altitude, 3) direct entry from a hyperbolic trajectory, and 4) entry from orbit. The key supporting technologies include aerothermodynamic modeling; high temperature thermal protection systems; adaptive guidance, navigation, and control; and lightweight structures that minimize or eliminate in-space construction and/or assembly. Aerobraking systems are strongly affected by each of these supporting technologies. System analysis that addresses missions, vehicle concepts, and operations is used to integrate the discipline areas, to assess technology requirements and trades, and to ensure that system requirements are satisfied.

Program Manager: Jim Moss
OAST/RF
Washington, DC 20546
(202) 453-2820

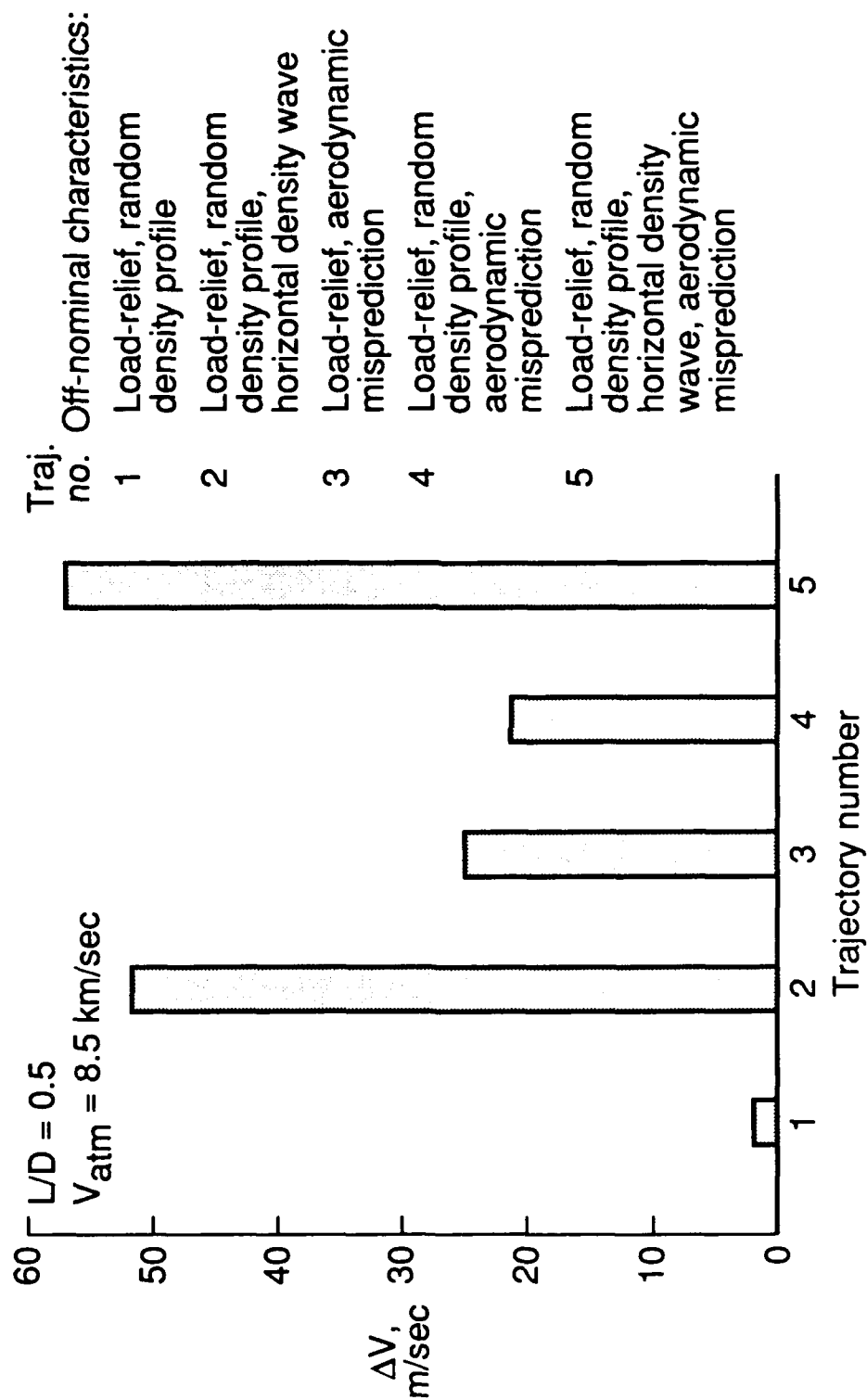


Figure 12-1. Additional Post-Aerocapture ΔV Requirements Resulting From Multiple Off-Nominal Effects

12-1 Effect of Atmospheric and Aerodynamic Uncertainties on Manned-Mars Aerobrake Feasibility

Objective. To develop a state-of-the-art Mars aerobraking guidance algorithm capable of managing off-nominal atmospheric and aerodynamic conditions.

Approach. A predictor-corrector guidance algorithm with deceleration feedback was developed and implemented into a three-degree-of-freedom simulation to assess the impact of uncertainties in the Mars atmospheric density profile and vehicle aerodynamics on mission feasibility. Additionally, because the mission is manned, a load-relief capability was incorporated such that the maximum sensed deceleration did not exceed 5 g's (1 g is the acceleration of a body at rest on the Earth's surface).

Accomplishment. The predictor-corrector algorithm has demonstrated the capability to accurately guide a Mars aerobraking vehicle through a wide range of off-nominal conditions (while providing load-relief) to the proper exit orbit. The off-nominal conditions simulated include errors in the atmospheric density profile (both vertical and horizontal structure) as well as a mispredicted trim angle-of-attack. The figure shows the amount of additional ΔV required to insert the vehicle into the proper parking orbit as a result of various combinations of off-nominal effects. The cases illustrated in this figure are representative of several worst-case scenarios; however, in each case, the mission was completed successfully. Note that a contingency ΔV budget on the order of the nominal ΔV (75 m/sec) would be more than adequate to account for post-aerocapture orbital trim after atmospheric flight through an off-nominal environment. In comparison to the Mars departure propulsive requirements (on the order of 2-3 km/sec), this is a relatively minor increase in the

total ΔV budget. The algorithm was also used in support of the Mars Atmospheric Knowledge Working Group (MAKWG) to help characterize the significance of off-nominal atmospheric conditions.

Significance. With the use of an adaptive guidance algorithm, atmospheric and aerodynamic uncertainties can be adequately managed and do not pose mission failure concerns that would preclude the use of aerobraking in a manned Mars mission.

Status/Plans. The results of this study have been documented in AIAA Papers 91-0058 and 91-2873 as well as the final report of the MAKWG. Further refinement of this analysis includes incorporation of the algorithm into a six-degree-of-freedom Monte Carlo simulation to better understand the coupled effect of various off-nominal conditions and identify the vehicle control implications.

R. D. Braun, R. W. Powell
Vehicle Analysis Branch
Langley Research Center
(804) 864-4507

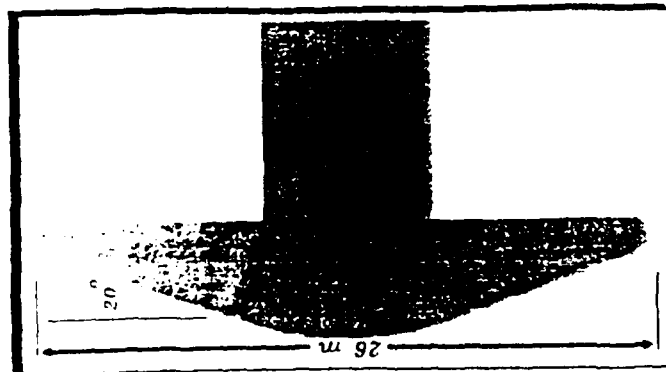


Fig. 1a Manned vehicle geometry

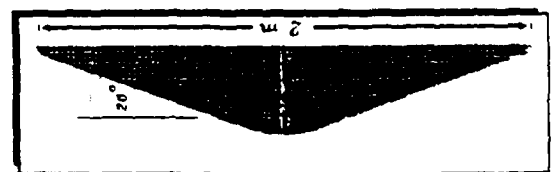


Fig. 2a MESUR probe geometry

MANNED VEHICLE

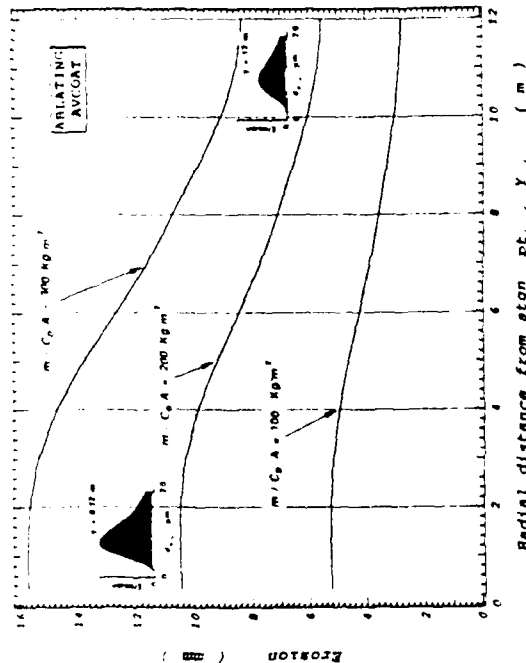


Fig. 1b Surface erosion on an ablating AVCOAT heatshield

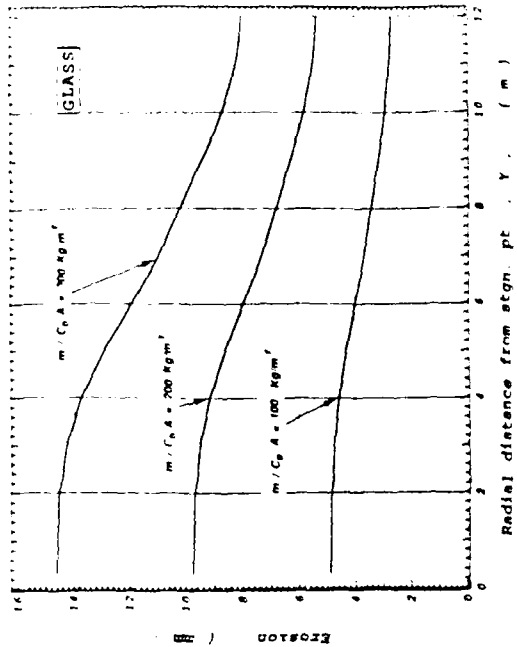


Fig. 1c Surface erosion on a glass heatshield

MESUR PROBE

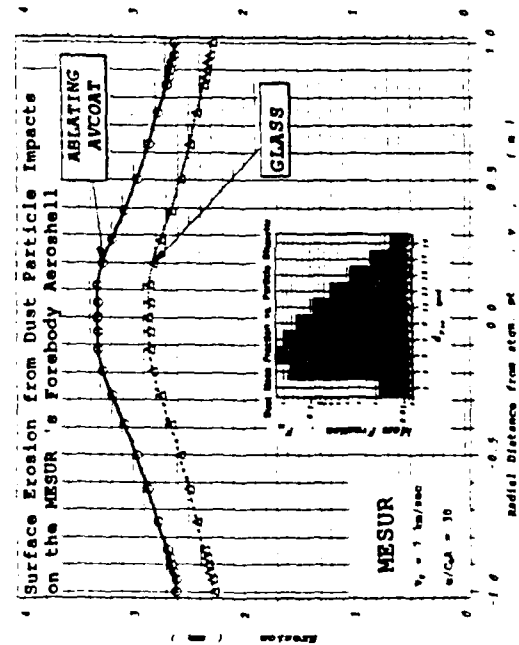


Fig. 2b Surface erosion on glass and ablating AVCOAT heat shields for $V_e = 7$ km/sec and $m/C_p A = 30$ kg/m²

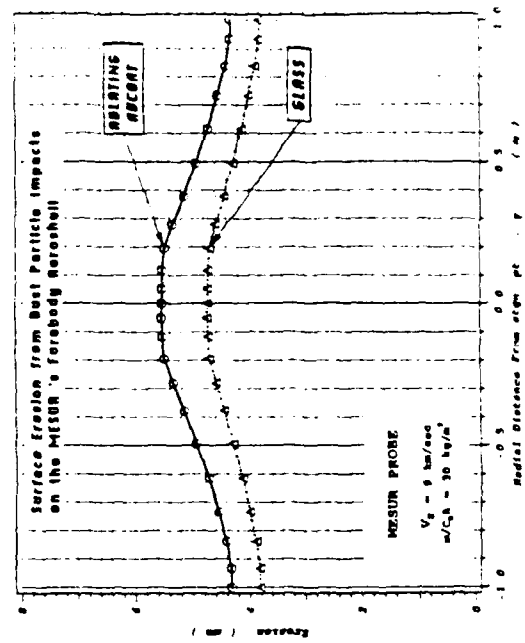


Fig. 2c Surface erosion on glass and ablating AVCOAT heat shields for $V_e = 9$ km/sec and $m/C_p A = 30$ kg/m²

Figure 12-2. Heat Shield Erosion in a Dusty Martian Atmosphere

12-2 Heat Shield Erosion in a Dusty Martian Atmosphere

Objective. To determine the extent of heat shield erosion from dust particle impacts that occur on a large, blunt aerobrake configuration during aerocapture maneuvers at Mars and the Mars Environmental Survey probes entering the atmosphere along ballistic flight paths.

Approach. An explicit Navier-Stokes code was used to compute the flow field about the vehicle shapes shown in Figures 1a and 2a. Calculations using a particle size distribution ranging from 1 to 19 μm were made. The paths, deceleration, heating, and sublimation of silicate (SiO_2) dust spherules which enter the forebody shock-layer at various locations were calculated and traced to surface impact. Two heat shield materials were considered: a glass surface that is representative of Shuttle ceramic tiles and a low-density ablator, AVCOAT, that was used on the Apollo capsule.

Accomplishments. The dustless flow field was computed at a number of points along several entry trajectories for the manned vehicle and the MESUR probe. Subsequently, dust particles were introduced into the shock layer and their trajectories were traced. The approximate surface erosion is shown in Figures 1b and 1c for the manned vehicle as a function of radial distance from the stagnation point. For a vehicle with $m/\text{CDA} = 200 \text{ kg/m}^2$, over 9 mm of glass can be destroyed, while for ablating AVCOAT the erosion exceeds 10 mm in the stagnation region.

This research was extended to examine the heat shield erosion caused by atmospheric dust for small, unmanned, probes entering the Martian atmosphere along ballistic flight paths. Heat shield erosion, energy and fre-

quency of particle impacts were calculated at several points along atmospheric trajectories with entry velocities of 7 and 9 km/sec and vehicles with ballistic coefficients of 30 (see Figures. 2b, 2c) and 40 kg/m^2 .

Significance. The presently available erosion results for the manned vehicle indicate that the design of the heat shield can be significantly affected by atmospheric dust. For example, it appears that glass-coated tiles are unsuitable heat shield materials for high-speed Mars entries unless coated with a protective material. For AVCOAT, the TPS mass may have to be increased by 25% to 29%, or about 1% of the vehicle mass, for entry at 8.6 km/sec. For the MESUR probe the results clearly show that the surface insulation glassy tile, which has a 0.35 mm glass coating, requires a protective layer of TUF1 (matrix of silica and alumina fibers). For the AVCOAT ablator, the heat shield mass must be increased by about 30% to account for erosion during or shortly after a dust storm. Therefore, the vehicle's heat shield must be designed to account for dust particle impact damage.

Status/Plans. The previous research will be extended to implement a coupled flow model to assess gas-solid chemical coupling and examine the effect of micron-sized particles on the vehicle heat shield for different insulation materials. The latest results will be reported at the AIAA Aerospace Science Meeting in January 1992.

Periklis Papadopoulos, Michael Tauber
Aerothermodynamics Branch
Ames Research Center
(415) 604-1146

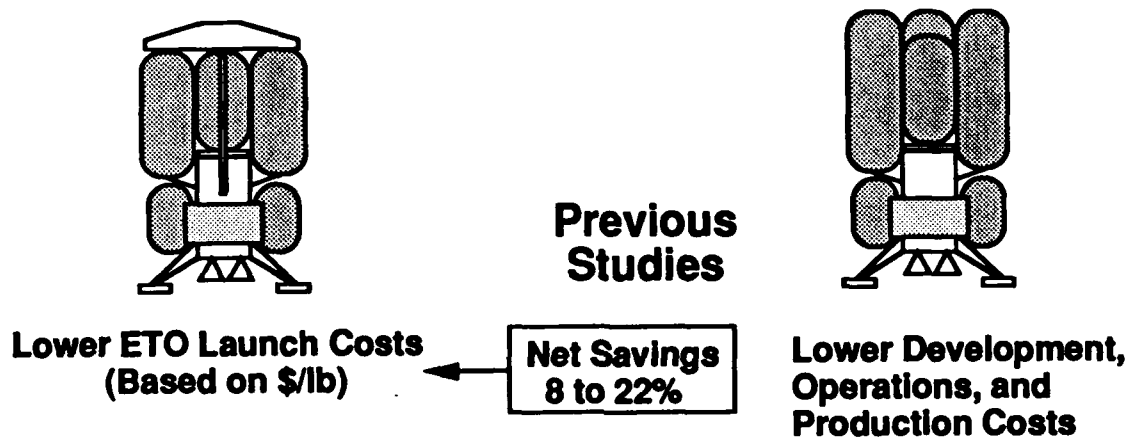


Figure 12-3. Aerobraked Lunar Transfer Vehicle (LTV) Cost and Operations Study

12-3 Aerobraked Lunar Transfer Vehicle Cost and Operations Study

Objectives. To use cost and risk analyses to compare all-propulsive versus aerobraked concepts for a lunar transfer vehicle (LTV) and to use resultant cost and risk knowledge to define technology development roadmaps.

Approach. Develop life cycle cost (LCC) models with sufficient depth of detail in all phases of LTV operations and in technology development programs to capture differences between aerobraked and all-propulsive LTV concepts. Use risk analysis to identify critical technology test requirements and risk-reducing design changes.

Accomplishments. Relative life cycle cost estimates show a 7%-10% (inside uncertainty band) cost advantage for an aerobraked LTV when compared with an all-propulsive concept based on the 90-Day Report Option 5 lunar mission (25 years, one mission per year, originating in low-Earth orbit). Cost savings stem from reduced Earth-to-orbit launch costs, reduced lunar orbit propellant boiloff, reduced gravity losses, and fewer on-orbit operations tasks (marginal advantage; assumes three-piece erectable aerobrake). Cost increases stem from Design Development Test & Evaluation (DDT&E) programs, aeropass software production and maintenance, and mission operations. Test and production facilities and space station (or free flyer) support facilities have been considered. Cost and risk analysis results have led to several design modifications (relative to the baselined MSFC concept), and technology development programs have been defined (for costing purposes) in major discipline areas.

Significance. Viability of the aerobrake for the lunar mission has been examined in terms of life cycle costs. To date, estimates had shown that the mass savings from aerobrakes were significant, but the question remained whether resources invested into aerobrake development programs exceeded these savings. After in-depth estimates of major aerobrake DDT&E and operations issues, aerobrake options have been shown to be competitive with all-propulsive approaches for the lunar missions. New, larger launch vehicles or fewer missions could alter the results.

Status/Plans. Additional analysis and costing studies will address single-use ablator designs and aerobrake disposal, and identification of lunar aerobrake development spinoffs for future Mars missions will be made.

Lawrence F. Rowell
Space Systems Division
Langley Research Center
(804) 864-44502

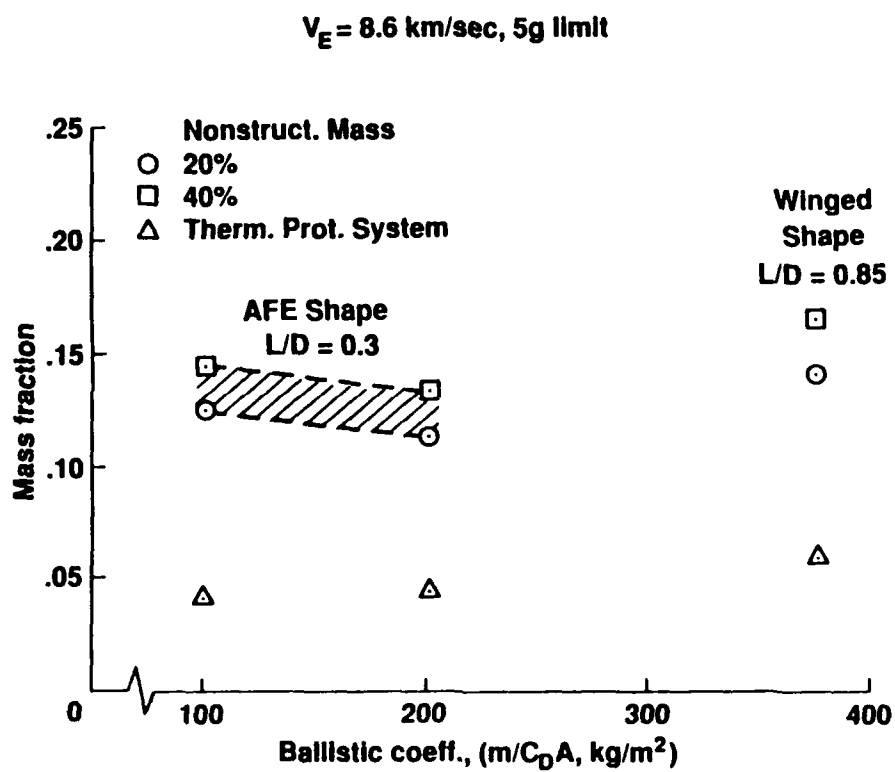


Figure 12-4. Mass Fraction of Aerobrakes for Manned Mars Mission

12-4 Aerobrake Design Studies for Manned Mars Missions

Objective. To systematically access the impact of aerobrake 4D and ballistic coefficient on aerobrake mass fraction and mission trajectory and verify the advantages of using aerobrakes over using chemical propellants for Mars entry.

Approach. The vehicles' mass fractions that must be devoted to the aerobrakes, including the heat shields, have been computed for a high-speed manned Mars entry of 8.6 km/sec and with an Earth 5 g deceleration limit. Blunt, low lift-drag ratio (L/D), configurations with ballistic coefficients ($m/C_D A$) of 100 and 200 kg/m² were studied. In addition, a delta-winged vehicle, with a L/D of 0.85 and a ballistic coefficient of 375 kg/m², was studied. The convective and equilibrium radiative heating and the pressures were computed at selected body locations for the Martian atmospheric gases along the overshoot and undershoot trajectories. Both insulative, heat shields and ablators were considered. Polyimide/graphite (PI/Gr) primary structural members were assumed for structural analyses. However, the basic shell structure consisted of an aluminum honeycomb sandwich core between PI/Gr face sheets; the shell was stiffened by I-beam frames. Multi-variable optimization was used to minimize the structural weights.

Accomplishments. After adding heat shielding and optimizing the structure, the aerobrakes' mass fractions (defined as heat shield plus aerobrake mass divided by the vehicle's total mass at entry) varied from about 15% to 13% for ballistic coefficients of 100 and 200 kg/m², respectively, for the blunt shapes and was slightly under 17% for the winged vehicle (see figure). The higher mass fraction for the winged-vehicle resulted from its much higher ballistic coefficient which created more intense heating and a higher mass fraction for thermal protection. However, the increase in L/D from 0.3 to 0.85 for the winged vehicle nearly doubles the entry

flightpath angle corridor width and provides an order of magnitude increase in cross-range capability during descent from orbit. Also, the winged vehicle can be launched into Earth orbit fully assembled. The blunt shapes will probably have to be assembled in orbit, which is complex and potentially hazardous.

Significance. The aerobrakes' mass fractions range from less than to slightly over the 15% value that is considered to make aerobraking indisputably superior to chemical propulsive braking. In fact, using the best current chemical propellants yielded a propulsion system mass fraction that exceeded the aerobrakes' values by factors of 4 to 5.

Future Plans. The results of the study were reported at an AIAA meeting. In addition, the analysis procedures that were developed will be applied to minimize the aerobrake masses for the unmanned probe/landers being studied for the Mars Environmental Survey (MESUR) missions.

M. Tauber, M. Chargin, W. Henline,
K. R. Hamm, Jr., H. Miura
Ames Research Center
(415) 604-6086

A. Chiu and L. Yang
Sterling Software
Palo Alto, CA

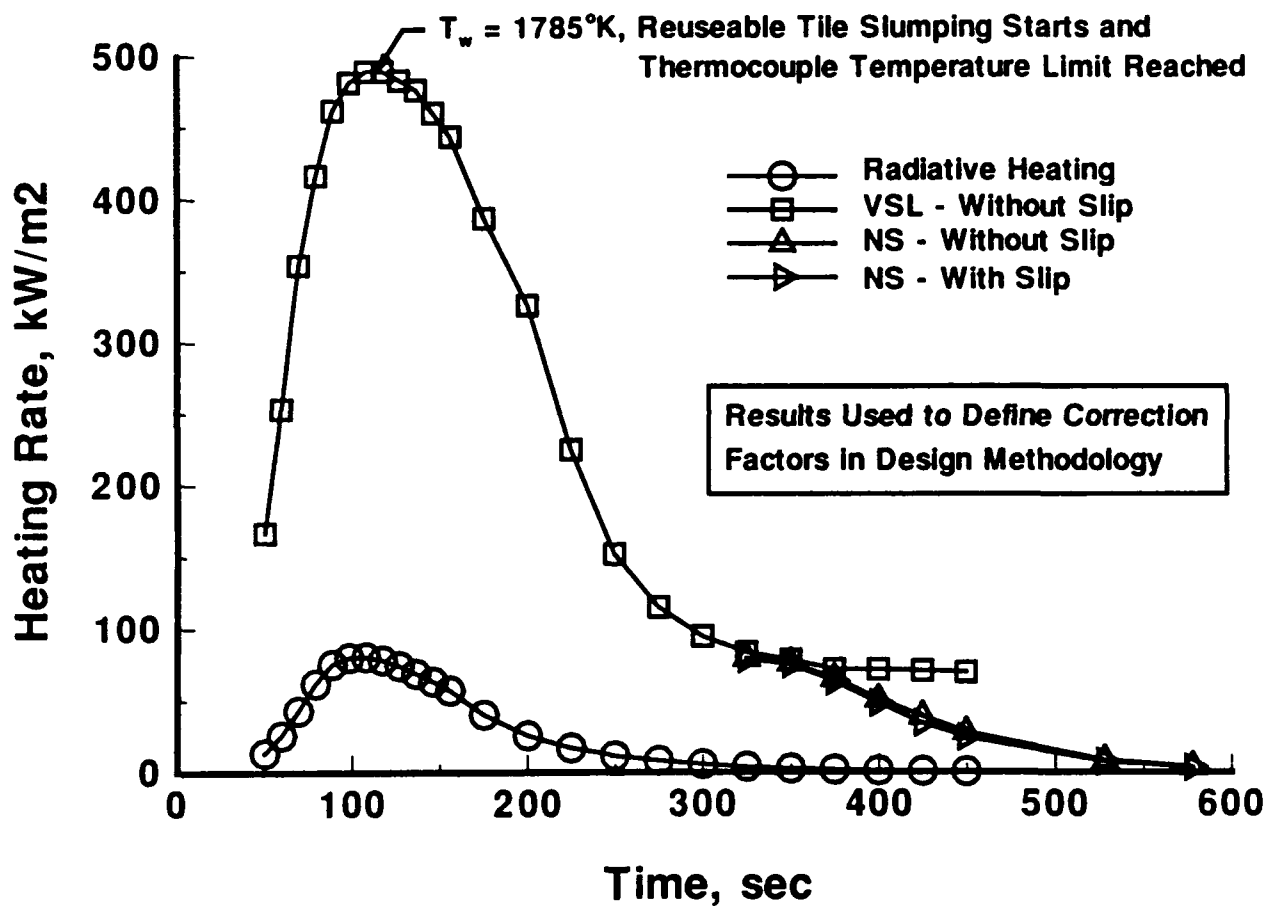


Figure 12-5. Stagnation Point Heating Rate on AFE

12-5 Heating Rates for Aeroassist Flight Experiment

Objective. To define the heating rates and flow-field characteristics over the Aeroassist Flight Experiment (AFE) vehicle for the purpose of vehicle design, experiments' design, and scientific pre-flight predictions.

Approach. The convective and radiative heating rates and the flow-field characteristics were calculated with several different computational codes at flight conditions from currently considered trajectories.

Accomplishments. The stagnation-point heating rates have been calculated at flight conditions along the current trajectory. The heating rates over the complete vehicle, forebody and afterbody, have been calculated at two flight conditions - time of peak heating and beginning of prime data period. The calculations are based on the best estimate of physical input data and also consider uncertainties in critical values such as catalytic wall coefficients and variations in radiation methods. The results have been supplied to key organizations within the AFE project. The results are being used in the heat shield design and in the design of the experiments. The stagnation-point heating rates are used to define correction factors to the heating method used in the heat shield design, and the heating rates over the complete configuration are used as anchor points in the design process.

Significance. The heating rates, supplied by Langley, are based on the best techniques available, and are the most complete data set of accurate calculations. The AFE project has relied heavily on these results and our assessment of the heating environment in the vehicle design. Our results have shown that the heating environment for the current trajectory yield heat shield surface temperatures that are near the limit of the tile material. Any changes to the trajectory that result in increased heating rates could seriously jeopardize the survival of several experiments and acquisition of quality data.

Status/Plans. The plan is to remain continuously involved in the calculation and assessment of the heating for the AFE. The impact in uncertainties of several critical parameters on the heating rates is being assessed.

H. Harris Hamilton II
Aerothermodynamics Branch
Langley Research Center
(804) 864-4365

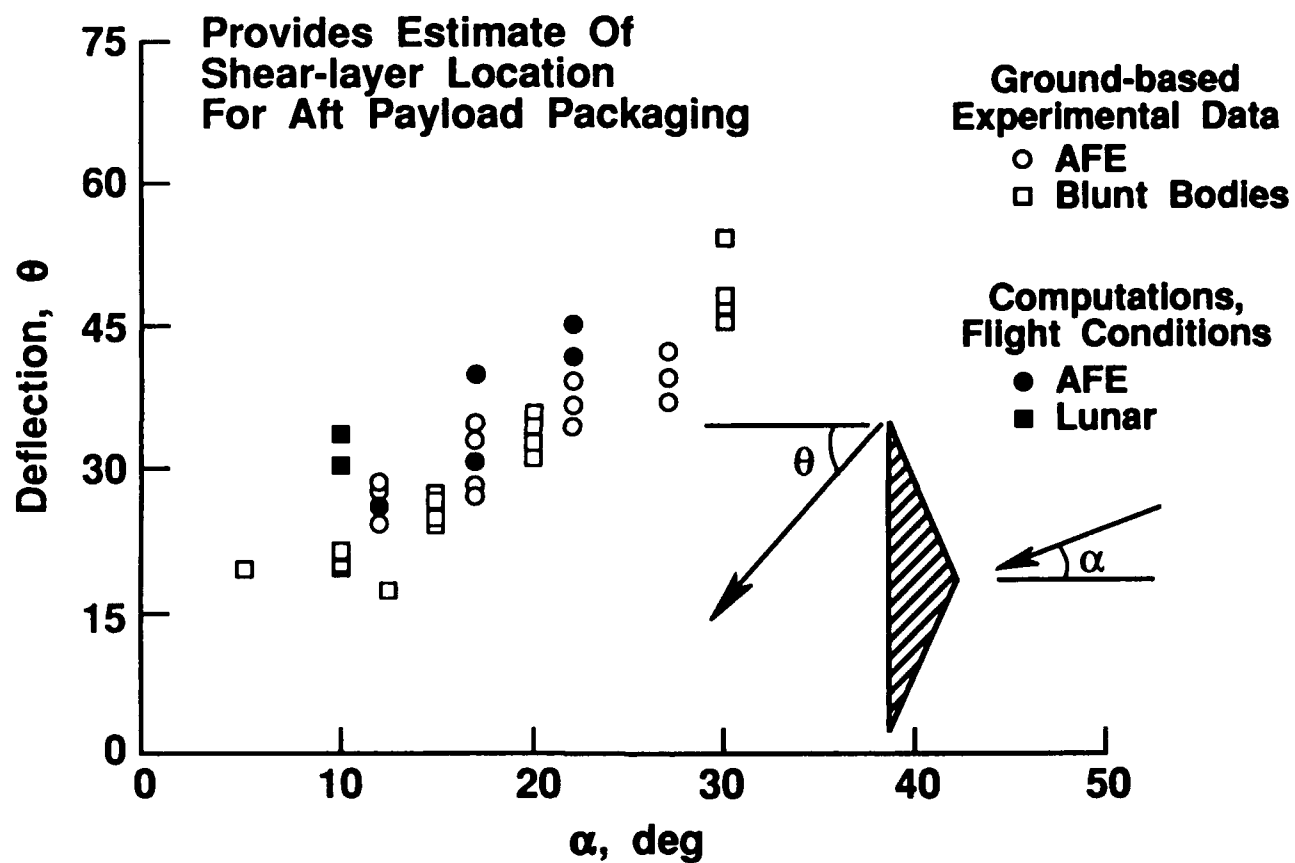


Figure 12-6. Wake Flows for Aerobrakes Shear-Layer Deflection Angles

12-6 Wake Flows for Aerobrakes

Objective. To numerically simulate the near wake flow-field behind aerobrakes, with emphasis on defining wake closure and shear layer impingement heating on payloads.

Approach. The simulations were implemented with the Langley Aerothermodynamic Upwind Relaxation Algorithm (LAURA), appropriate for solving viscous, hypersonic flows in thermochemical nonequilibrium. Three aerobrake configurations, the Aeroassist Flight Experiment (AFE) vehicle, and a blunted, 70° cone with two different shoulder radii (Lunar configuration), were studied. Angle-of-attack and altitude (Reynolds number) variations at typical flight conditions are included in the study.

Accomplishments. Shear-layer deflection angles have been recorded for a matrix of trajectory points and vehicle configurations. A near-linear trend in shear-layer deflection angles is evident in ground-based experimental data and the current simulations at flight condition; however, the flight simulations show somewhat larger deflections possibly resulting from gas chemistry effects. Shear-layer impingement on the AFE can cause localized hot spots on the afterbody on the order of 1 W/cm², more than a factor of ten larger than ambient heating on the surrounding afterbody surface. Enhanced viscous effects at high altitude will delay shear-layer separation. This delay can cause peak impingement heating on the afterbody to occur earlier in the trajectory than peak, stagnation-point heating.

Significance. The positioning of a payload behind an aerobrake is defined by two criteria: vehicle center-of-gravity constraints and minimization of aerothermodynamic loads. The present study addresses the second criterion. It is the first computational investigation of flight conditions that calculates boundaries for payload packaging and the magnitudes of impingement heating levels if those boundaries are breached. Current results can be used as estimates in system studies for payload packaging.

Status/Plans. More comprehensive grid refinement studies and solution adaptive grid techniques will be applied to reduce uncertainties associated with truncation error. Other configurations, vehicle sizes, and flight conditions may be considered.

Peter A. Gnoffo
Aerothermodynamics Branch
Langley Research Center
(804) 864-4380

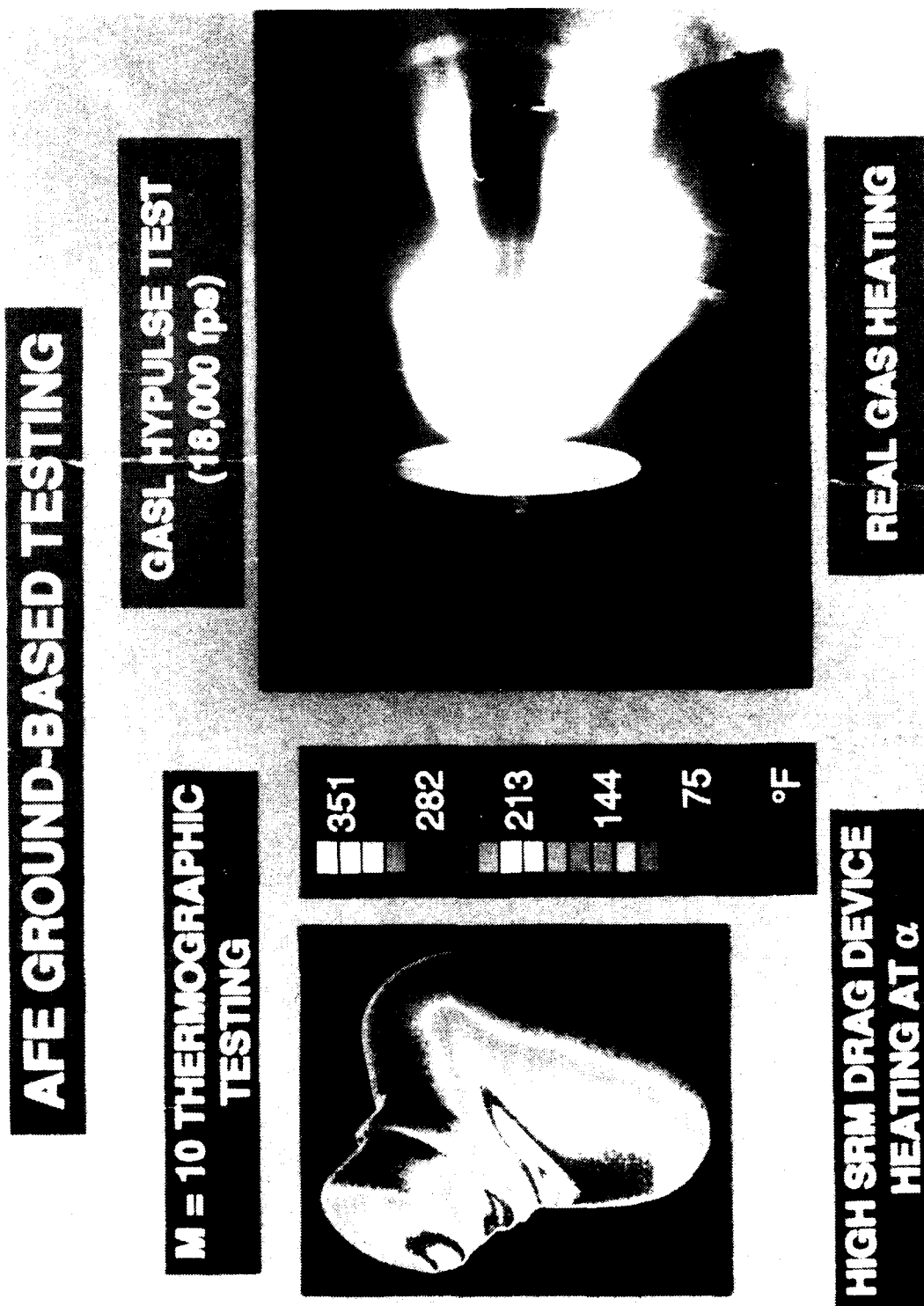


Figure 12-7. Aeroassist Flight Experiment Ground-Based Testing

12-7 Aeroassist Flight Experiment Ground-Based Testing

Objective. To experimentally determine/assess: (1) lateral stability characteristics of Aeroassist Flight Experiment (AFE) configuration; (2) aerothermodynamic characteristics of solid rocket motor (SRM) ballute (balloon parachute) drag device; (3) high enthalpy, dissociated real-gas heating distributions on forebody; and (4) aerodynamic/aerothermodynamic characteristics at higher Mach numbers (viscous interaction parameter).

Approach. The following were performed: (1) force and moment tests at Mach 6 and 10 in air and Mach 6 in CF₄ (density ratio range from 5.3 to 12) over range of sideslip angle to determine lateral stability characteristics; (2) thermal mappings at Mach 10 via thermographic phosphor technique to examine heating characteristics on SRM-ballute device proposed to control entry trajectory of SRM; (3) convective heat transfer measurements in Australian National University (ANU) shock tunnel (T3) and General Applied Science Laboratory (GASL) expansion tube (Hypulse); and (4) force and moment and surface pressure and heat transfer tests at Mach 12 and 14 in Wright Laboratory Hypersonic Wind Tunnel (WLHWT).

Accomplishments. Lateral stability tests (requested by Johnson Space Center) were performed in a timely manner and data were immediately disseminated. Over 60 tests were performed in ANU T3 on two different scale models. Following calibration of Hypulse by the Experimental Hypersonics Branch researchers, tests were performed in air, helium, and CO₂ at velocities between 16,000 and 21,000 ft. per second. Force and moment tests were completed and pressure heat transfer tests were initiated in the Wright Laboratory HWT.

Significance. The AFE vehicle is laterally stable and subject data have been entered into the flight book (CFD codes presently are unable to provide critical data on lateral stability). Shock/shock interaction occurs on the SRM-ballute configuration at incidence resulting in regions of extremely high heating on the ballute surface. These data reveal probable failure of the ballute device during entry because of this interaction. Preliminary comparison of air and helium data in Hypulse reveals no significant effect of real-gas on heating distribution, thus no impact on present Thermal Protection System design nor trajectory. Preliminary analysis of aerodynamic characteristics at Mach 14 in air reveal negligible effects of compressibility for the AFE configuration.

Status/Plans. CFD code (LAURA) will be exercised to compare predicted and measured heating characteristics on SRM-ballute. We plan to initiate reduction/analysis of data obtained in the ANU T3, complete analysis of GASL Hypulse data, and complete testing in the WLHWT.

John R. Micol, Scott A. Berry,
Michael DiFulvio, Charles M. Hackett
Experimental Hypersonics Branch
Langley Research Center
(804) 864-5250

